CANADIAN BASELINE PROGRAM

Summary of Progress to 1998

An overview of the measurements underway in the Canadian Baseline Program, and results to date

Acknowledgements

The credits for individual chapters in this report are shown under the chapter titles. However, the results presented here were only possible thanks to many years of work by an even larger number of individuals. The authors would like to especially acknowledge the contribution of Dr. Neil Trivett, now retired from AES, who led the Canadian Baseline program for over a decade and deserves much of the credit for the program as it is today.

The report was compiled by Ms. Manuela Racki of MD Engineering, 45 Memorial Avenue, Stoney Creek, Ontario, Canada, L8G 4C5.

Comments or inquiries concerning this report or requests for copies should be directed to:

Manager, Climate Research Program
Air Quality Research Branch
Atmospheric Environment Service, Environment Canada
4905 Dufferin Street, Toronto, Onatrio M3H 5T4

January 1999

Contents

FOREWORD

One of the fundamental questions that must be addressed in assessing the science of climate change is, how are the composition and properties of the atmosphere changing as a result of human influences, how do these changes compare to the natural forces of change, and how do we expect these changes to evolve in the future?

While water vapour and clouds are among the most important atmospheric constituents of climatic significance, and changes in their concentrations can have major influences on the radiative fluxes of both incoming sunlight and outgoing heat radiation, such changes are largely controlled by the response of the hydrological cycle to other forces upon the thermal properties of the climate system, and hence are not primary causes for change. Rather, the most significant atmospheric components that can be changed by both natural and human influences external to the climate system are other greenhouse gases, particularly carbon dioxide and methane, and aerosols.

Analyses of ice cores and current measurement programs which have accumulated a significantly long data set to permit trend analyses, indicate that humans have already radically altered the composition of the atmosphere and hence its radiative properties. Since the beginning of the industrial revolution some 200 years ago, concentrations of carbon dioxide have increased by about 27% above the pre-industrial background value of the last millenium (about 280 ppmv). Atmospheric methane concentrations show that pre-industrial levels have more than doubled during the past two centuries. Concentrations of other greenhouse gases have been rising slowly but steadily (e.g., nitrous oxide) or accumulating rapidly (e.g., chlorofluorocarbons, which have no significant natural sources). In some parts of the world, the concentration of tropospheric ozone has increased dramatically, with levels in the Northern Hemisphere today estimated to be about twice pre-industrial values. Concentrations of aerosols in some industrial regions have increased by a factor of 20 to 30 above background levels.

In other words, we have quite unintentionally started a long-term, global-scale geophysical experiment with the life-support system of this planet—an experiment that we do not control and, as yet, understand poorly.

The World Meteorological Organization's 1984-1993 long-term plan, presented at the WMO Ninth Congress, identified deficiencies in the special observational networks for background air pollution; in particular, carbon dioxide, ozone, aerosols and radiation. The WMO stressed the need for accurate measurements over long periods of time to document trends and project future pollutant loads in the atmosphere.

The Atmospheric Environment Service (AES) had been involved in a flask sampling program for carbon dioxide at Alert, on the northern tip of Ellesmere Island in the Canadian Arctic, and Sable Island, off the coast of Nova Scotia in the Atlantic Ocean, since 1975. In August 1986, Canada's efforts were upgraded substantially by the official opening of an observatory at Alert for continuous monitoring of background concentrations of trace gases and aerosols, by Mr. Howard Ferguson, the then Assistant Deputy Minister for the Atmospheric Environment Service. This event marked the end of several years of planning and co-ordination, and signified Environment Canada's commitment not only to Canada's environment, but also to that of the international community at large.

The opening of the observatory also marked the beginning of a new phase of continuous background atmospheric chemistry monitoring at the Atmospheric Environment Service. Alert is now an official WMO Global Atmospheric Watch (GAW) observatory (one of the some 20 observatories around the world, which also include Mauna Loa, South Pole and Cape Grim—see figure below). The measurement program at Alert has grown substantially since its relatively humble beginnings and now includes measurements by a number of international organizations as well as AES.

In December 1989, another observatory was opened in northern Ontario at Fraserdale—one of the few existing continental sites in the world where greenhouse gas concentrations are measured. Operations at Fraserdale were terminated in late 1996, but the measurement program there is currently being re-instituted.

The above two sites, along with the flask sampling programs at the two coastal sites (Sable Island, NS, and Estevan Point, BC), constitute Environment Canada's contribution to the international measurement effort in assessing the impact of human activities on global atmospheric chemistry. We are proud of our achievements to date, and look forward to decades of continued contributions to the global program.

Gordon McBean
Assistant Deputy Minister
Atmospheric Environment Service

WORLD METEOROLOGICAL ORGANIZATION

GLOBAL ATMOSPHERE WATCH

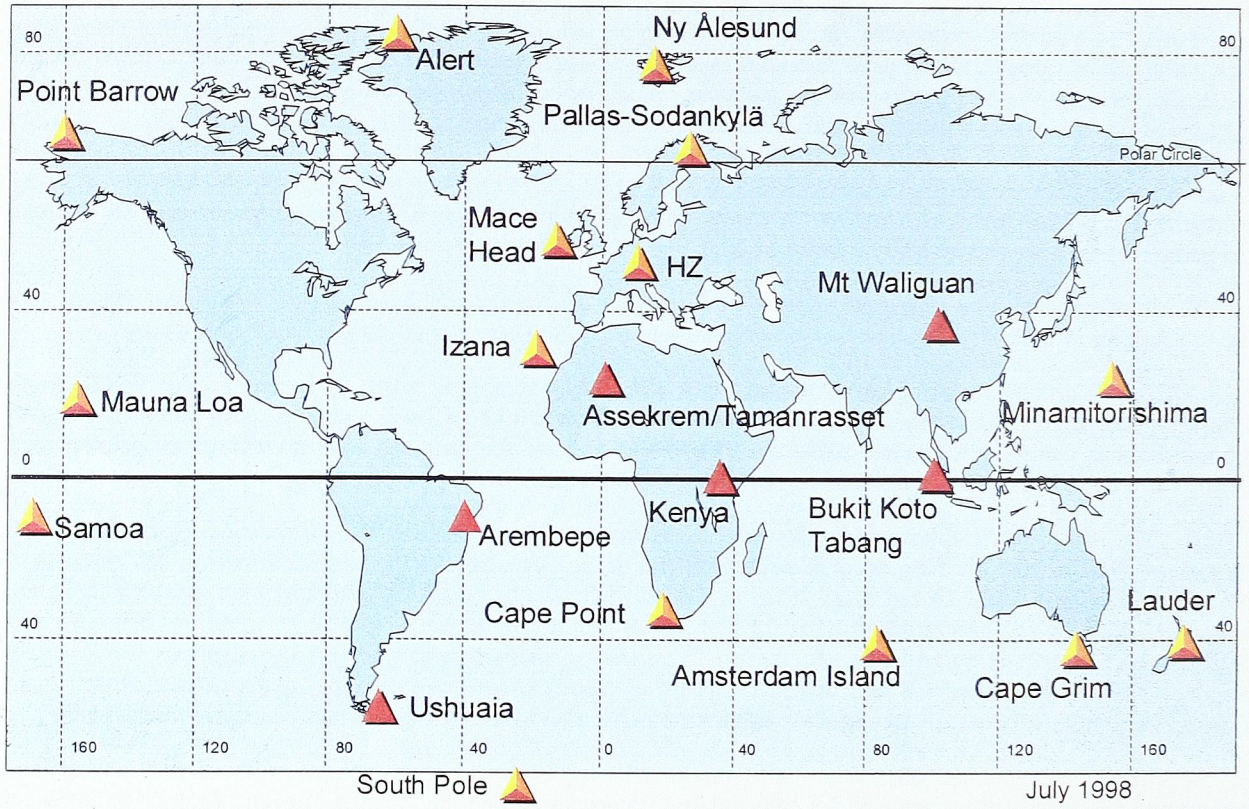

PREFACE

This is the first of a series of progress reports on the Canadian Baseline Program. Scientific results from the program have been presented in a number of peer-reviewed publications and at conferences. This report, however, is in response to a recommendation coming out of one of the two peer reviews of the program which have taken place since its inception (the first review was in 1991 and the second in 1997): namely, that the program establish a regular data reporting publication.

The Canadian Baseline Program began at Alert, NWT, with a simple flask sampling program for carbon dioxide in 1975. Over time, other measurements were established at Alert, and two coastal sites were added. The first of these – Sable Island, off the coast of Nova Scotia in the Atlantic Ocean – also dates from 1975. The other coastal site is currently Estevan Point, on the west coast of Vancouver Island, British Columbia, which in 1992 replaced the earlier Cape St. James site (in the Queen Charlotte Islands off Canada's west coast; implemented in 1982). In December 1989, another observatory was opened in northern Ontario at Fraserdale, as part of a major study of methane production along the coastal areas of Hudson Bay and James Bay, in Canada's wetlands. This station was closed in 1996 due to financial constraints, but is now (1998) being re-opened.

The measurements at the above-mentioned sites constitute Canada's contribution to the World Meteorological Organization's Global Atmosphere Watch (GAW) Program. The objective of the GAW program is to make available on-going background concentration measurements of selected atmospheric constituents and related physical parameters representative of all parts of the globe, and to promote scientific studies utilizing GAW measurements. The emphasis of the program is on developing a better understanding of the natural biogeochemical cycles and the impact of human activities on these cycles. The atmospheric monitoring activities included in the GAW program are research-oriented rather than routine, providing the scientific and policy-making communities with high quality data from which both communities can fulfill their requisite needs. Data measured under the program can be used to determine the impact of control strategies for specific components such as chlorofluorocarbons and carbon dioxide.

The major criterion for GAW baseline and regional sites is the absence of local and/or regional sources of air pollution. Measurement of the following components constitutes the minimum recommended monitoring program at a GAW observatory:

- greenhouse gases, such as carbon dioxide, methane, nitrous oxide, tropospheric ozone and chlorofluorocarbons;
- ozone: surface, total column, and vertical profile
- radiation and optical properties of the atmosphere including UV-B, turbidity, visibility, total aerosol loading and vertical profiles, and water vapour profiles
- chemical composition of precipitation
- reactive gas species such as oxides of sulphur and nitrogen
- particle number concentration including chemical composition and size fractionation
- selected heavy chlorinated hydrocarbons
- selected trace metals such as lead and cadmium
- stable and unstable isotopes such as ^{85}Kr, ^{222}Rn, ^{7}Be, ^{210}Pb, ^{14}C and ^{13}C in CO_2 and CH_4
- routine meteorological observations and air mass trajectories for each station

The observatory at Alert is an official WMO GAW baseline station. With the exception of a few of the minor components, Canada contributes data to the WMO's GAW program in all of the measurements listed above.

The purpose of this first report is to make available to the scientific community an overview of the type of measurements underway in the Canadian Baseline Program, and to convey some of the most important results. Where work has already been reported elsewhere, details are omitted (but references are included). In some cases, for example with the flask program, a considerable amount of detail is given on the technical procedures used, which is generally not appropriate for inclusion in a journal publication. Detailed descriptions of the measurement sites, and an analysis of the climatology at each site, are also found in the report.

Programs run by both Atmospheric Environment Service (AES) scientists, and scientific collaborators outside of AES, are included. There has been a great deal of scientific collaboration, particularly at the Alert GAW Observatory, and it is hoped that this report will give the reader a better appreciation of the importance of the measurements being carried out by cooperating groups, how the measurements fit into the global context, and how they are being used to resolve some of the major scientific questions of the day related to global warming.

The report is organized into the following sections:

1. Site Descriptions
2. Measurement Programs and Results
3. Measurement and Protocol Descriptions
4. Data Management
5. Cooperative Programs

Inquiries and/or comments should be addressed to:

Maris Lusis, Manager
Climate Research Program, Air Quality Research Branch
Atmospheric Environment Service
4905 Dufferin Street
Downsview, ON
M3H 5T4
(416) 739-4449

1. OBSERVATORY

1.1. ALERT

Douglas E.J. Worthy, Neil B.A. Trivett and Christian Blanchette

The Atmospheric Environment Service, as part of Canada's commitment to the World Meteorological Organization's Background Air Pollution Monitoring Network (BAPMoN), initiated the Canadian Baseline Program at Alert in 1975. (BAPMoN has since been renamed to Global Atmospheric Watch (GAW)). The major objectives of the Canadian Baseline Program at Alert have been to:

- obtain background concentrations of atmospheric constituents, their variability and possible long-term changes;
- monitor changes to the source/sink distributions of these trace species through long-term measurement of their ambient concentrations;
- evaluate the global transport of such materials into and out of Canadian ecosystems;
- determine the impact of reduction/control strategies for specific components;
- make available to the research community precise measurements of selected atmospheric constituents for representative Canadian ecosystems and, where applicable, other parts of the globe; and
- promote scientific studies utilizing baseline measurements.

The Canadian Baseline Program started with simple weekly flask measurements for carbon dioxide (refer to Section 2.1.2 for details). In 1986, the Alert GAW Observatory was built to permit the continuous measurement of carbon dioxide as well as other greenhouse gases, aerosols and meteorology. The observatory is the most northerly continuous monitoring observatory in the GAW network, and as such, is far removed from the major industrial regions of the Northern Hemisphere and, therefore, representative of the tropospheric air over the Arctic basin. Because of its extreme northern location, Alert is also a unique and important site for atmospheric studies of phenomena such as Arctic Haze, long-range transport of air pollutants and tropospheric ozone depletion.

The research activities at Alert are oriented at providing the scientific and policy communities with high quality data from which both communities can fulfill their requisite needs. A summary of the measurement programs at Alert is given in Table 1-1.

1.1.1. SITE DESCRIPTION

Alert is located at 82°27'N 62°31'W on the edge of the Lincoln Sea at the northeastern tip of Ellesmere Island in the Canadian Arctic (Figure 1.1).

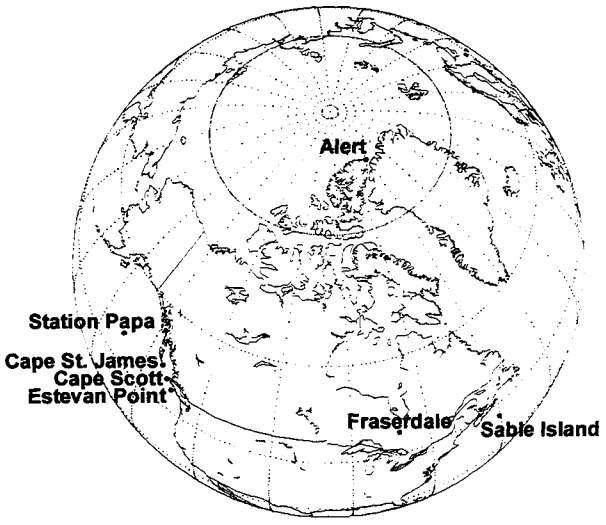

Figure 1.1 Map showing the location of the Alert GAW Observatory (82°27'N, 62°31'W). The location of the observatory at Fraserdale (49°53'N, 81°34'W) is also shown as well as the locations of the flask sampling sites. Sable Island and Estevan Point are operational flask sampling sites, whereas, Cape St. James, Station Papa and Cape Scott are discontinued flask sampling sites.

The terrain in the immediate area of Alert is steeply rolling, on the order of 100-150 m above sea level, with frequent deep ravines and high cliffs. The land is covered with snow for almost ten months of the year. During the summertime, however, the land is covered with a sparse covering of polar desert vegetation. Alert experiences 106 days of full darkness (October 30 to February 13), 153 days of 24-hour daylight (April 7 to September 7) and two 53-day transition periods with some diurnal cycle going from virtually total daylight to total darkness (and vice-versa) (see Figure 1.2). The mean annual temperature is -18° C and the monthly mean temperatures above freezing occur only in the months of July and August (see Figure 1.2). Generally, in the wintertime the Arctic is characterized by a persistent cold rather than an extreme cold (in mean daily minima) [*Maxwell, J.B.*, 1980].

Table 1-1. Measurement programs at Alert, NWT.

CONTINUOUS MEASUREMENTS			
Meteorology	**Agency**	**Level**	**Sampling Record**
Wind speed and direction	AES[1]	2 m, 5 m, 10 m, 20 m, 40 m	1985 - Present
Temperature	AES[1]	2 m, 5 m, 10 m, 20 m, 40 m	1985 - Present
Dew Point	AES[1]	2 m	1985 - Present
Pressure	AES[1]	200 m ASL	1985 - Present
Gases			
CO_2	AES[1]	10 m	1987 – Present
CH_4	AES[1]	10 m	1987 – Present
F-11, F-12 and F-113	AES[1]	10 m	1993 – Present
SF_6	AES[1]/CMDL[3]	10 m	1995 – Present
Nitrous Oxide	AES[1]/CMDL[3]	10 m	1995 – Present
CO	AES[1]	10 m	1998 – Present
Radon	AES[1]/UOH[2]	3 m	1989 – Present
O_3	AES[1]	3 m	1986 – Present
Atmospheric Mercury	AES[1]	5 m	1995 – Present
Peroxy Acetylnitrate (PAN)	AES[1]	3 m	1986 – Present
Aerosol			
Aitken Nuclei	AES[1]	10 m	1985 – 1997
Aerosol Scattering	AES[1]	10 m	1985 – 1997
Aerosol Soot	AES[1]	10 m	1989 – Present
Polyaromatic Hydrocarbons (PAH)	AES[1]	10 m	1993 – Present
FLASK MEASUREMENTS			
Compound Measured			
CO_2 and CH_4	CMDL[3]	0.5 L, 2.5 L	1985 – Present
CO_2	AES[1]	2.0 L	1975 – Present
CO_2, CH_4, N_2O, SF_6, ^{13}C and ^{18}O	AES[1]	2.0 L	1998 – Present
CO_2, ^{13}C and ^{18}O	SIO[4]	5.0 L	1984 – Present
CO_2, CO, CH_4, ^{13}C and ^{18}O	CSIRO[5]	5.0 L	1988 – Present
CO_2, ^{13}C and ^{14}C in CO_2	IOS[11]	5.0 L	1995 – Present
CO_2	MGO[7]	1.5 L	1992 – 1993
Oxygen to Nitrogen Ratio	SIO[4]	5.0 L	1989 – Present
Halocarbons	OGC[10]	2.0 L	1987 – 1992
Halocarbons	NIES[9]	5.0 L	1997 – Present
Halocarbons / Hydrocarbons	IFC[6]	1.0 L	1988 – 1996
F-11, F-12 and Nitrous Oxide	CMDL[3]	0.3 L	1988 – Present
OTHER PROGRAMS			
Compound Measured	**Agency**	**Methodology**	**Sampling Record**
Major Ions & Trace Elements	AES[1]	Hi-Volume Filter	1984 – Present
Snow Chemistry	AES[1]	CAPMoN Collector	1991 – 1996
Atmospheric Mercury	AES[1]	Filter Pack	1992 – Present
Toxics	AES[1]	Hi-Volume Filter	1992 – Present
^{14}C in CO_2	UOH[2]	NaOH Solution	1987 – Present
^{13}C and ^{14}C in CH_4	UOH[2]	Cryogenic Trapping	1990 – Present
CO, ^{17}O and ^{18}O in CO	MPI[8]	Cryogenic Trapping	1996 – Present

1 Atmospheric Environment Service, Downsview, Ontario, Canada
2 University of Heidelberg, Heidelberg, Germany
3 Climate Modelling and Diagnostics Laboratory, Boulder, Colorado, USA
4 Scripps Institute of Oceanography, San Diego, California, USA
5 Commonwealth Scientific and Industrial Research Organization, Melbourne, Australia
6 Institüt für Chemie, Julich, Germany
7 Main Geophysical Observatory, St. Petersburg, Russia
8 Max Planck Institute, Mainz, Germany
9 National Institute for Environmental Studies, Ibaraki, Japan
10 Oregon Graduate Centre, Oregon, USA
11 Institute for Ocean Sciences, Victoria, British Columbia, Canada

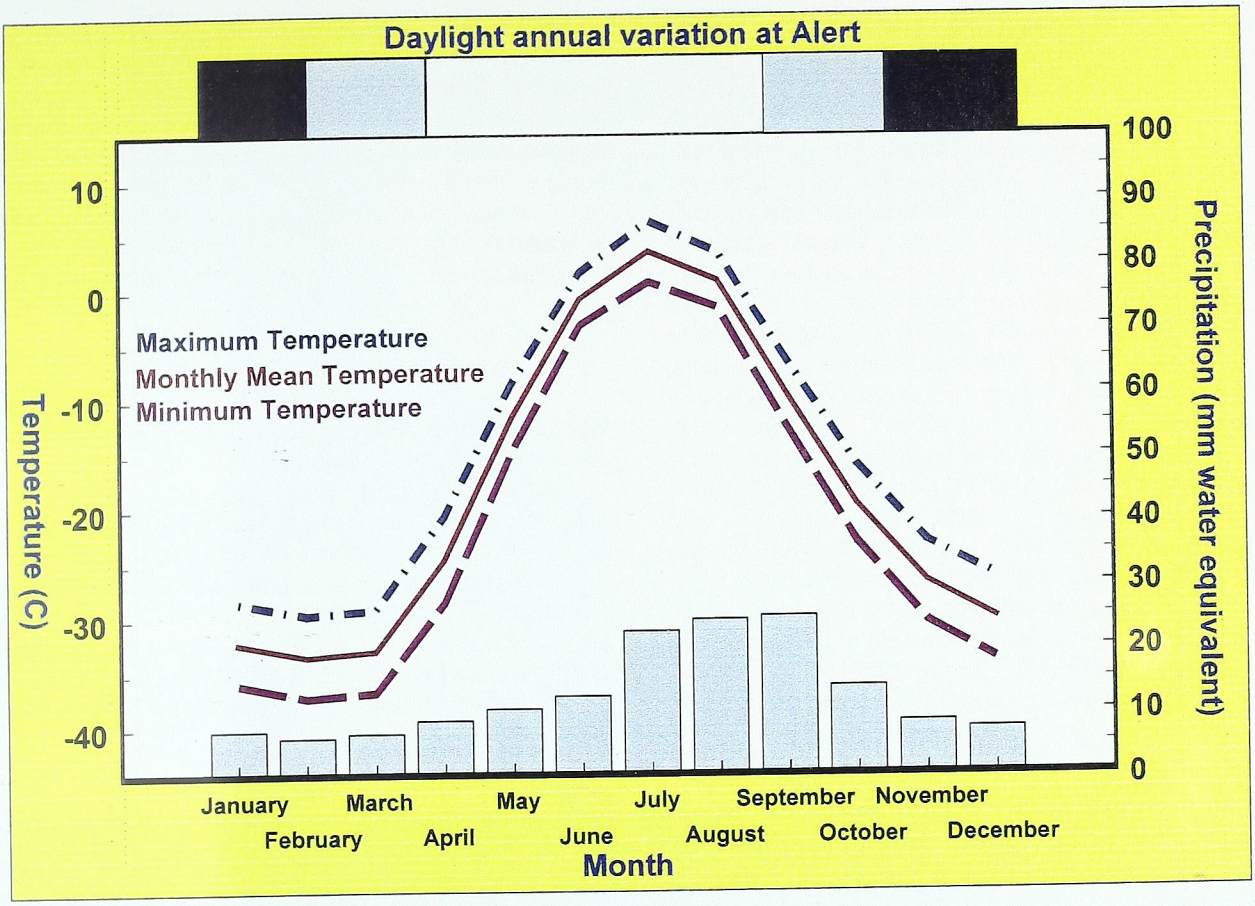

Figure 1.2 Monthly mean temperature, monthly mean minimum and maximum temperature, monthly mean precipitation in water equivalent, and variation in daylight over a 1-year cycle. The data were collected at the weather station at Alert between 1951 and 1995. The weather station is approximately 6 km NNE of the observatory. The top bar shows the periods of total darkness (black), twilight (gray) or 24-hour daylight (white).

The amplitude of the diurnal cycle of the hourly averaged temperature is relatively small with a maximum of about 3.5° C occurring during the transition periods of light and dark. The amplitude remains generally constant (around 0.2° C) during the wintertime and summertime. The day to day variability in the temperature is largest in the wintertime primarily due to changes in the Arctic temperature inversions and rapid transport of new Arctic air masses into the region.

Canadian Forces Station (CFS) Alert is located on a ridge on the western side of Alert Inlet (Figure 1.3), which is an extension of Dumbell Bay. The weather station is located at the southern edge of CFS Alert's main camp and somewhat below the ridge on which the camp is situated. The ridge does influence the meteorological observations made at the weather station, especially for wind speed and direction. The main camp is staffed with 100 to 200 military and civilian personnel. The Alert GAW Observatory is located on a plateau about 6 km SSW of the main camp. The plateau rises abruptly to an elevation of about 200 m (with local hills rising to 500 m). The plateau forms the northern edge of the Hazen Plateau, which continues to rise to the south, reaching a typical elevation of 1000 m and extending through the central part of northern Ellesmere Island. The southeastern edge of the Hazen Plateau is defined by the 7500 km^2 Agassiz Ice Cap, a permanent feature with a central elevation greater than 2000 m. Southwest of Alert is the rugged United States range, with peaks exceeding 2500 m. The Greenland coast is 60 km east of Alert.

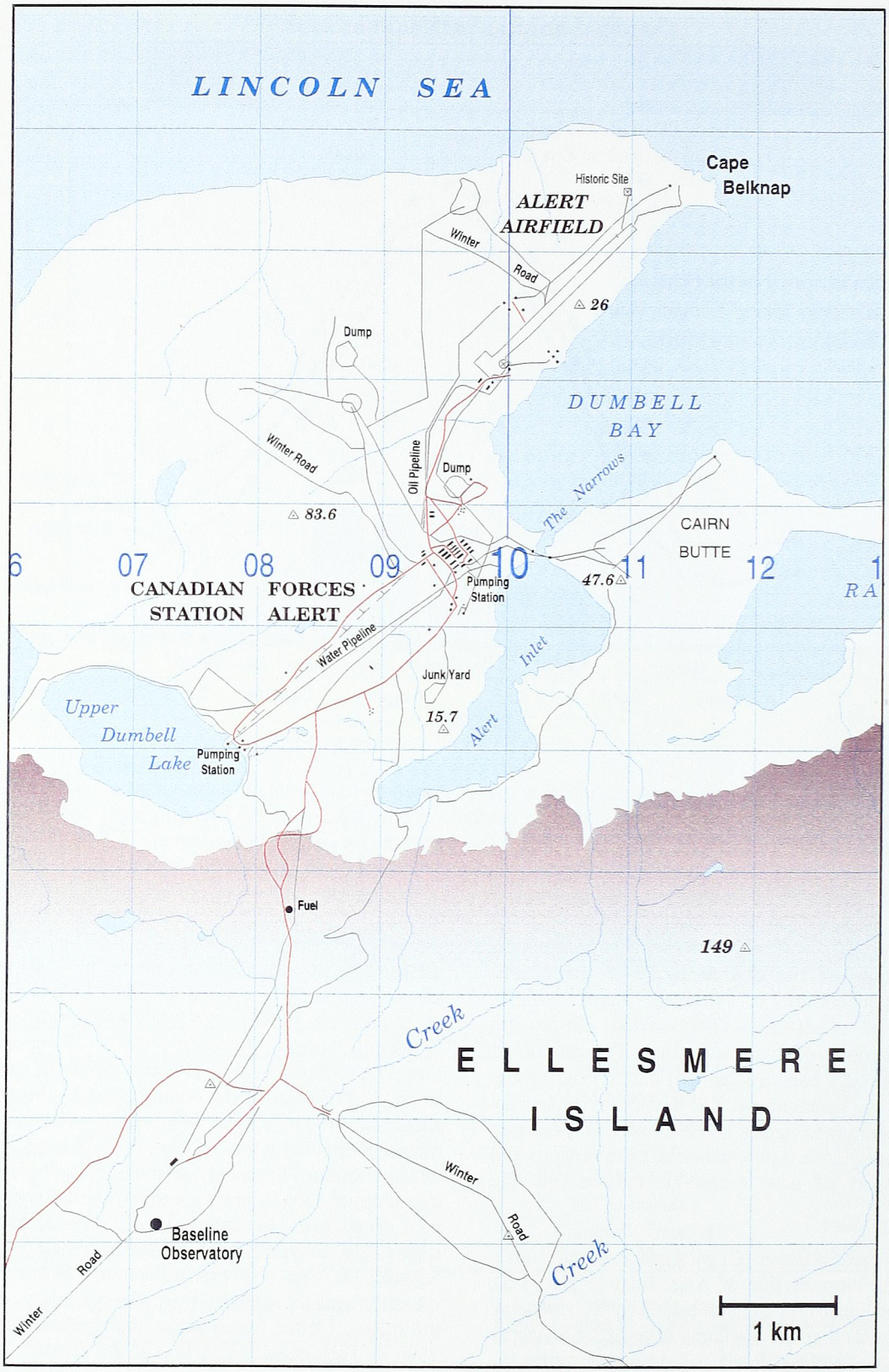

Figure 1.3 Location map of the observatory at Alert (labelled as "Baseline Observatory").

The Alert GAW Observatory is about 400 m^2 in size (Figure 1.4). The observatory has two laboratories that contain analytical instruments and equipment, a storage room, pump room and cylinder room, as well as a kitchen and sleeping facilities. A 20 m meteorological tower located 50 m WSW of the observatory is instrumented for wind measurements at the 5 m, 10 m and 20 m levels and temperature and humidity measurements at the 2 m level.

1.1.2. CLIMATOLOGY

Temperature inversions are prevalent in the Arctic and can be barriers for vertical mixing in the lower troposphere. Temperature inversions are present all year long but are more frequent and persistent during the wintertime. The inversions are mainly due to surface radiative cooling and can be associated with very cold surface temperatures [*Jackson*, 1960]. During the summertime, temperature inversions tend to be related to advection of warmer air over relatively cold air (such as the air over the ice pack) [*Maxwell*, 1980]. Typically, temperature gradients reach 10°/100m during the wintertime with depths ranging up to 2000 m, and 4-5°/100m during the summertime with depths ranging up to 300 m [*Maxwell*, 1980; *Raatz*, 1986]. Temperature inversions can de-couple lower tropospheric air from air above the inversion layer. This implies that air with similar origin can have a different chemical make-up especially during slow transport periods when dry depositions of pollutants from the surface layer can significantly alter concentrations [*Raatz*, 1986]. However, when transport is rapid and pollutants have been released in cold air, vertical mixing may be prevented between the source region and Alert. The former case is associated with cleaner air near the ground and larger concentrations of pollutants in layers above the inversion, while the latter case is associated with a reverse situation. Consequently, the breakup of temperature inversions, which could be related to modifications in the intensity of the circulation or the distribution of clouds [*Raatz*, 1986], can lead to the incursion of air with either larger [*Conway et al.*, 1989; *Hopper and Hart*, 1994] or lower [*Yuen et al.*, 1996] concentrations of pollutants.

Figure 1.4 Alert GAW Observatory.

Most of the air sampled at Alert is part of the Arctic air masses [*Maxwell*, 1980]. Arctic circulation is controlled by semi-permanent pressure systems. The summer climatology suggests that a dominant high pressure system centered around the North Pole reduces exchanges with lower latitudes. Winter climatology, as indicated by the mean winter surface pressure [*Maxwell*, 1980], shows the presence of four semi-permanent pressure systems that create the main transport pattern of air being transported from Asia and Europe to Alert. Synoptic scale weather patterns can occasionally lead to very fast transport (4-5 days) from Eurasia to Alert as can be seen from the trajectory analysis given below.

Five-day Lagrangian back-trajectories from January 1988 to December 1997 were calculated to evaluate the air parcel history at Alert. (The back-trajectories were calculated at end point heights corresponding to 1000, 925, 850 and 700 hPa pressure levels at 0000, 0600, 1200 and 1800 UTC.) The trajectory model used in the calculations was developed and described in *Olsen et al.*, [1978]. Six geographical sectors (see Figure 1.5) were used to define the major source regions. The results of the 5-day back-trajectory calculations were classified according to these six sectors. For each sector, the frequency distribution of the trajectory origins 1-day and 5-days back in time is shown. About 88% of the air parcels arriving at Alert originated 5 days earlier in sectors 1, 2, 3 and 6 (around 20% in each sector). Less than 15% of the trajectories had originated from sectors 4 and 5. The radial distance between Alert and the origin of the air parcel at the start of each trajectory five days earlier is characterized by the 25^{th}, 50^{th}, (median value), and 75^{th} percentile contours in Figure 1.5. The median distance travelled by air parcels originating in sector 3 (i.e., the "Siberian" sector) was about 2200 km. This distance was significantly greater than that of air parcels from the other sectors, which travelled less than 1000 km (within the Canadian Arctic Archipelago). More importantly, during the wintertime the median distance travelled by air parcels originating in sector 3 was about 3000 km. Rapid long-range transport of air masses was a characteristic feature of sector 3 especially in the wintertime when the air masses contained elevated concentrations of CO_2, black carbon, PAN and other pollutants [*Worthy et al.*, 1994]. Such episodes were responsible for the large variability observed in most of the trace gases monitored at Alert, including CO_2 and CH_4 [*Worthy et al.*, 1994; *Yuen et al.*, 1994].

The seasonal pattern in transport shows, more or less, a constant frequency all year long in air masses originating from Asia (with shorter distances travelled during the summer), an enhanced summer transport from North America and Europe and a reduced transport from Alaska and extreme East Asia. This pattern changes the characteristics of the air sampled at Alert over the year.

Local wind meteorological studies at Alert are difficult because the wind observations are significantly affected by topography. The prevailing winds at the observatory are SSE to WWS due to channeling by the mountainous regions of northern Ellesmere Island and Greenland. The seasonally stratified windrose plots are shown in Figure 1.6. Winds, for the most part, are usually very calm but there are periods when the wind can exceed 20 m s^{-1}. A more detailed meteorological summary can be found in *Hopper et al.* [1994].

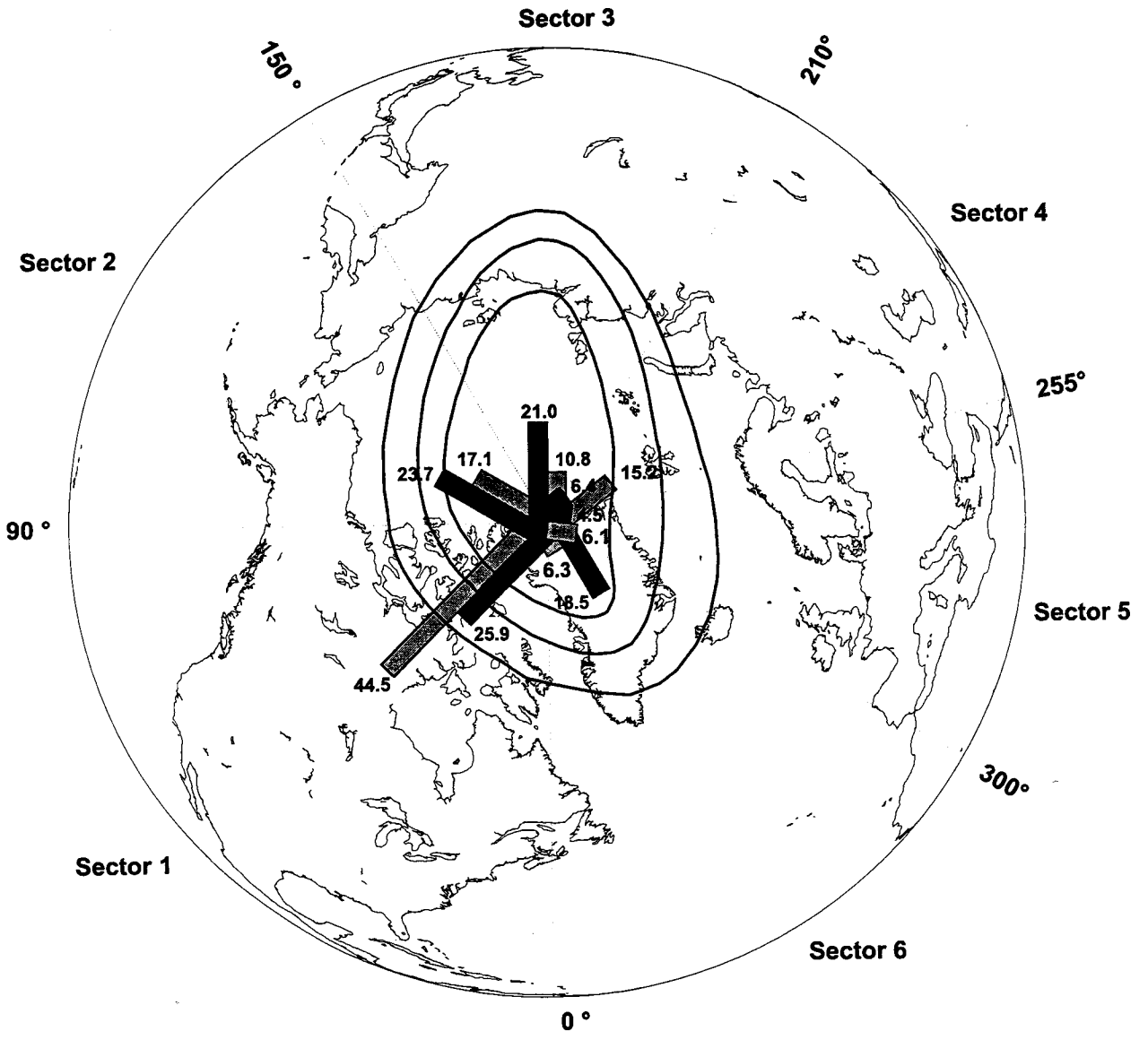

Figure 1.5 Alert trajectory sectors associated with different source regions. The trajectory end point sector classification scheme uses a transformed coordinate system with Alert defined as the center. The bars indicate the percent frequency of the occurrence of air parcel origin by sector for 1-day (grey bars) and 5-days (black bars) back in time for the period 1988-1997. Also included are contours of the lower quartile (25%), median (50%), and upper quartile (75%) distances travelled by 5-day back-trajectories.

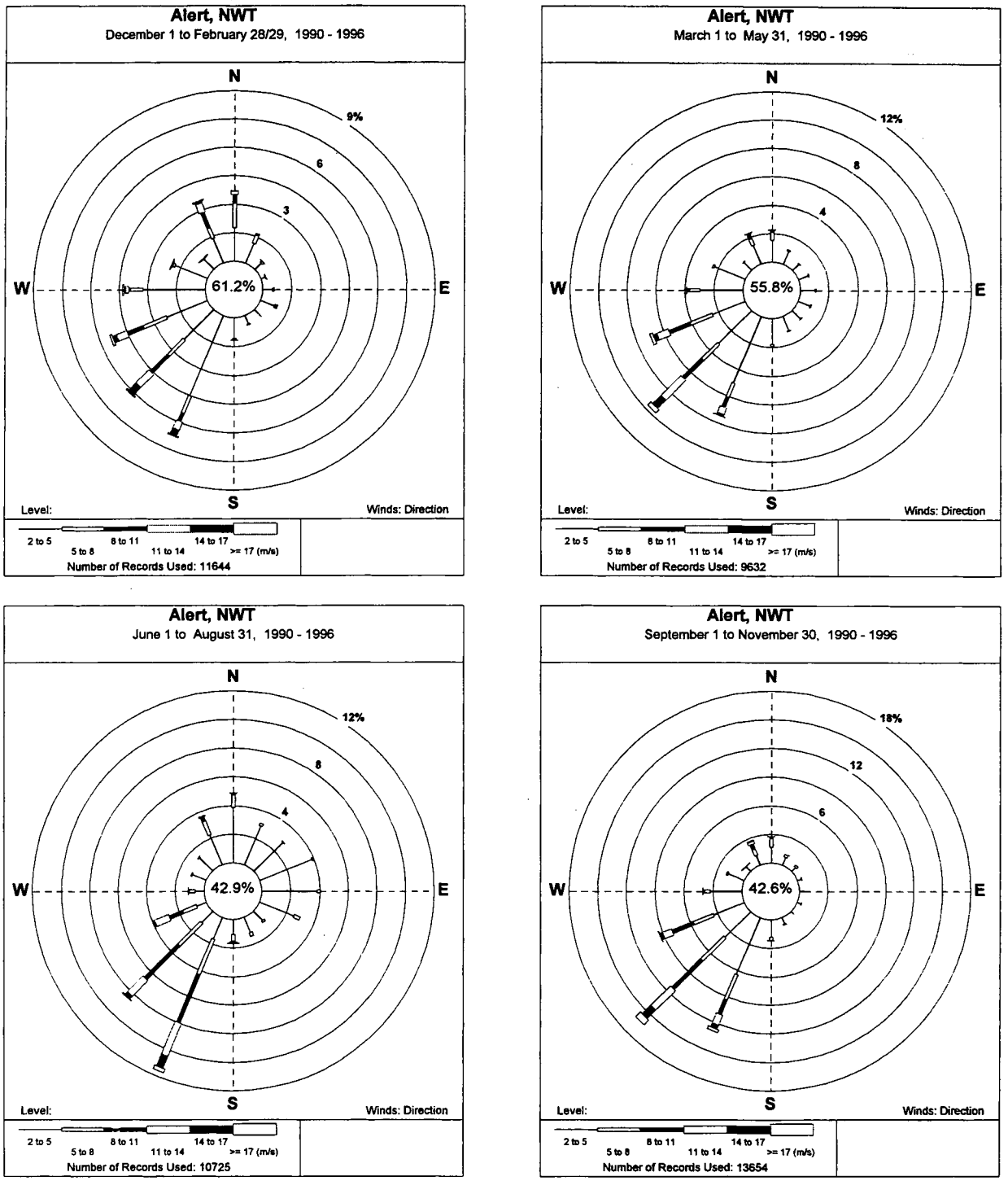

Figure 1.6 Seasonally stratified windrose plots for Alert.

1.2. FRASERDALE

Douglas E.J. Worthy and Neil B.A. Trivett

In December 1989, the Atmospheric Environment Service (AES) of Environment Canada established an observatory at Fraserdale, Ontario. The observatory is located 210 m above sea level on the southern perimeter of the Hudson Bay Lowland (HBL) (49°53'N, 81°34'W). The primary purpose of the observatory is to measure the annual and seasonal variation in CO_2 and CH_4 in the northern wetlands and boreal forest ecosystems. From these measurements scientists can estimate the uptake of carbon by the boreal forest and the release of CH_4 from the wetlands. The routine measurements carried out at the observatory are listed in Table 1-2. The observatory is shown in Figure 1.7.

Table 1-2. Routine measurements made at the Fraserdale observatory.

Parameter	Level
Wind speed and direction[1]	5 m, 10 m, 20 m and 40 m
Temperature[1]	5 m, 10 m, 20 m and 40 m
Humidity[1]	2 m
Pressure[1]	210 m ASL
Carbon dioxide[1]	40 m, 20 m and 10 m*
Methane[1]	40 m, 20 m and 10 m*
222Radon-daughters[2]	20 m and 10 m*
Ozone[1]	5 m
Black carbon[1]	10 m
Isotopes in methane[2]	Integrated sampling
Isotopes in methane[3]	Flask sampling

1 Atmospheric Environment Service, Downsview, Ontario, Canada
2 University of Heidelberg, Heidelberg, Germany,
3 University of Washington, Seattle, Washington, USA
*The first level indicated is the primary level with selected measurements at the other levels.

Figure 1.7 Fraserdale observatory.

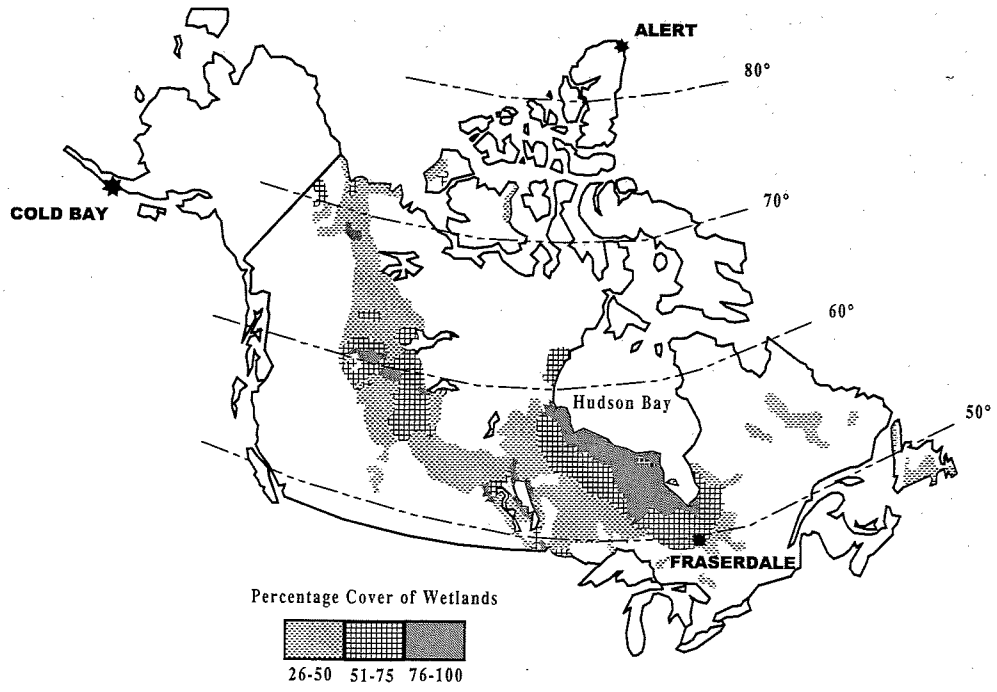

Figure 1.8 Map showing Fraserdale (49°53' N, 81°34'W), Alert (82°27' N, 62°31' W), Cold Bay (55°12' N, 162°43'W) and the estimated wetland coverage in Canada derived from results published in *Roulet and Ash* [1992] and *Mortsch* [1990]. The Hudson Bay Lowland is primarily the dark region between Fraserdale and the southern edge of Hudson Bay.

1.2.1. SITE DESCRIPTION

Fraserdale is in a region that has extensive wetland coverage (Figure 1.8). The observatory is located in a 1 km^2 clearing in the boreal forest at the edge of a reservoir formed by a hydroelectric generating dam on the Abitibi River at the head of the Abitibi Canyon. The terrain in the surrounding area is slightly rolling with extensive areas of impeded drainage. A mixture of black and white spruce, balsam fir, white birch, maple and quaking aspen trees surround the observatory. The nearest source of anthropogenic contamination is the living quarters of the generating station's maintenance staff located about 1 km northwest of the site. (The quarters are inhabited Monday to Thursday.)

The closest town to the south is Smooth Rock Falls (population 2,500) about 70 km from Fraserdale. The closest town to the north is Moosonee (population 1,500) about 200 km away. The closest major city, Timmins (population 50,000), is about 150 km south of Fraserdale.

The observatory consists of two trailers (4 m x 10 m each) connected in a "T" configuration. About 10 m southwest of the observatory is a 40 m high standard triangular tower equipped with instrumentation for meteorology and radon measurements [*Kuhlmann et al.*, 1997]. Three sampling lines (0.95 cm o.d. Dekoron®) are strung from the tower to the inside of the observatory. Two of the three lines are from the 40 m level and the third is from the 20 m level. The residence time of an air sample in the sampling line (between the top of the tower and the instrument inlets inside the observatory) is about 20 s.

1.2.2. CLIMATOLOGY

Fraserdale is in a region of convergent air masses and frontal activities. The mean latitudinal position of the summer Arctic frontal zone is north of the observatory. The summer Arctic frontal zone moves south of the observatory during the winter; this movement controls the seasonal pattern of the climate at Fraserdale. The mean annual temperature at Kapuskasing (a town located 100 km SEE of Fraserdale) is 0.6° C, which is close to the 0° C isotherm in annual mean temperature. Monthly mean temperatures are below 0° C for almost 6 months of the year. There are about 162 freeze-free days per year while the growing season (defined as starting after five consecutive days with temperatures

above 5° C) extends from May 5 to September 15 (133 days on average). This implies that biological influences on the measurements at Fraserdale start in early May. This is evident in the CO_2 mixing ratio time series, which reveals a small diurnal cycle at this time of year (see section 2.1.1.3 for details).

Cloud cover in the Fraserdale area is typical of the north-eastern middle latitudinal region with close to 50% overcast conditions (8-10 10th cloud cover) and an annual average of nearly 20% clear sky conditions (0-2 10ths cloud cover) [*Mortsch*, 1990]. Annual precipitation at Fraserdale reaches 800 mm water equivalent. Consequently, the forest influencing the observatory is a wet boreal forest in contrast to the dry boreal forest west of Ontario. The movement of the Arctic front controls the seasonal precipitation pattern over the region. Consequently, higher precipitation values are observed during the summertime (up to 100 mm per month) when the Arctic front is located just north of Fraserdale.

Changes in the position of the Arctic front affect the different air masses that are sampled at Fraserdale. In fact, Fraserdale is part of a region that is alternately influenced by Arctic, maritime tropical, and some modified Pacific air masses [*Bryson*, 1966]. Four main circulation patterns occur in the region: a winter pattern that brings air from the northwest between November and February; a spring pattern that transports air from due north between March and June; a summer pattern that brings air from due north as well as from the southwest between July and September; and a short transitional fall pattern that brings air from the west in October [*Bryson*, 1966]. During the wintertime and springtime, the circulation patterns bring clean air to Fraserdale while anthropogenic influence on the sampled air is more likely associated with the summer circulation, as indicated by *Jobson et al.* [1994].

Five-day Lagrangian back-trajectories [*Olsen et al.*, 1978] have been calculated for 0000, 0600, 1200 and 1800 UTC, for the period January 1990 to December 1996, for air parcels reaching Fraserdale at end point heights corresponding to the 1000, 925, 850, and 700 hPa pressure levels. The 925 hPa trajectories were chosen for the analysis because they were considered to be most representative of the air sampled at the observatory. In general, the back-trajectories that were calculated for pressure levels between 1000 hPa and 850 hPa were quite similar.

Six geographical sectors were used to associate the back-trajectories with air mass origins. The sectors were chosen so as to define the major source regions around Fraserdale. The sector classification scheme is shown in Figure 1.9. Also shown in Figure 1.9 is the frequency of occurrence of air parcel origin by sector for 1-day (grey bars) and 5-days (black bars) back in time. There is a tendency for air parcels approaching from the north to curve eastwards as they near Fraserdale because of the predominantly cyclonic curvature of airflow in this region of North America [*Barrie* 1986; *Barrie et al.*, 1992]. This is reflected in the high percentage of 1-day trajectory end points in sectors 1 and 2, and the small percentage of corresponding 5-day trajectory end points in the same sectors. Seventy-eight percent of the air parcels arriving at Fraserdale originate five days earlier in sectors 3 and 4, with 60% travelling over the HBL in sector 3. Less than 11% of the back-trajectories originate in sectors 1 and 6, which have a large anthropogenic influence. Due to the cyclonic curvature of the northerly trajectories, it is possible that some of the air parcels assigned as originating five days earlier in the wetlands sectors crossed sector boundaries and thus were influenced by urban and industrial areas en route to Fraserdale. However, the distances travelled during the first day back are relatively short. This is shown below by an assessment of the distances travelled by air parcels.

In order to define the *area of influence* for the Fraserdale observatory, the radial distances between Fraserdale and the location of an air parcel at the start of each trajectory five days earlier were calculated. The contours in Figure 1.9 show the distances travelled by 25%, 50% (median value), 75% and 100% of the air parcels associated with each sector over five days. The median distances travelled by back-trajectories originating in sectors 3 and 4 were 2319 km and 1773 km, respectively. The back-trajectories from these sectors were similar in magnitude to those from sector 2. The distances travelled by air parcels in these sectors were significantly greater than by air parcels in the southern sectors 1 and 6, and sector 5. The 100% contour encloses all cases analyzed over the 7-year period thus defining the outer limit of the 5-day area of influence. The extreme maximum distance travelled by an air parcel occurred in sector 3. The air parcel originated south of the Arctic Circle (about 57°N) on the Russian side of the Arctic in northern Siberia. The same analysis was repeated for the 1-day travel period. The analysis yielded similar results. For example, the median distances travelled in sectors 1 and 3 were 379 km and 678 km, respectively. It is evident that air parcels reaching Fraserdale frequently originate in the Arctic, and this raises the possibility that the air may retain a chemical signature characteristic of the high Arctic, especially in the wintertime.

The same analysis for the area of influence and air parcel history was done for the individual months throughout the year. For the area of influence, the distances travelled in each sector did not vary significantly from month to month for the 1-day and 5-day back-trajectories. During the summertime, however, there was a shift from sector 3 to sector 4 as the predominant source sector for the origin of the air parcel five days earlier. Nevertheless, sector 3 is the predominant sector on an annual basis, and 70% to 80% of the air parcels originate from the northern sectors 3 and 4, indicating that the air parcels reaching Fraserdale predominantly represent "background" air often with an Arctic origin. For the remaining sectors, the seasonal changes are rather small with an overall tendency for the influence of sectors 1 and 2 to be slightly higher in the summertime than in the wintertime. Overall, the results presented in this section for the period 1990-1996 are similar to the frequency patterns and area of influence for Fraserdale reported by *Mortsch* [1990] for the period 1979-1989.

The predominant local wind directions observed at Fraserdale are from the north and south, which reflect the influence of the local topography, i.e., the Abitibi Canyon. This wind direction pattern is very different to that observed at the nearby weather stations in Kapuskasing, Cochrane (100 km SE of Fraserdale), and Moosonee.

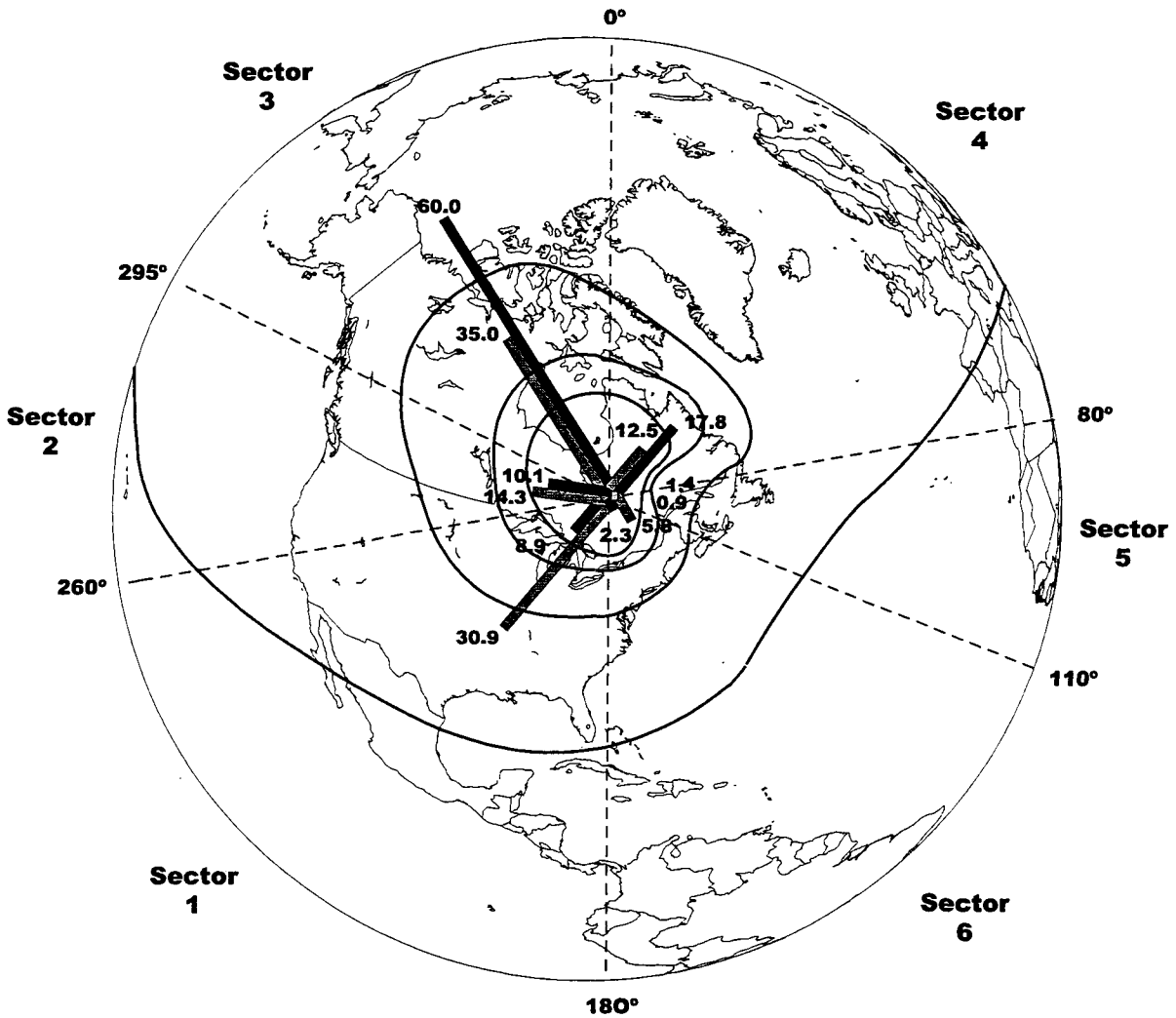

Figure 1.9 Fraserdale trajectory sectors associated with different source regions. The trajectory end point sector classification scheme uses a transformed coordinate system with Fraserdale (49°53'N, 81°34'W) defined as the center. The bars indicate the percent frequency of occurrence of air parcel origin by sector for 1-day (grey bars) and 5-days (black bars) back in time for the period 1990-1996. Also included are contours of the lower quartile (25%), median (50%), upper quartile (75%), and maximum distances travelled by 5-day back-trajectories.

1.3. SABLE ISLAND

Kaz Higuchi

1.3.1 SITE DESCRIPTION

Sable Island (43°N, 60°W) is about 275 km east-southeast of Halifax, Nova Scotia. The island is the dry summit of a sea ridge and has a maximum elevation of about 10 m. It is about 25 km long and 1 km wide. The terrain surrounding the measurement site is flat and bordered by a series of rolling sand dunes that are covered mostly by shrubs and grassy patches. Staff of the AES weather station occupies the island (along with the famed ponies and seals).

1.3.2. CLIMATOLOGY

Seasonally stratified windrose plots are shown in Figure 1.10. Throughout the year, most of the wind directions fall between northwesterly to southwesterly. Winds during the winter are mostly from westerly to northwesterly, shifting to a dominant southwesterly regime in the summer season. Winds during the fall and winter seasons can be very strong, with strength frequently greater than 20 m s^{-1}.

In an unpublished study, *Winter et al.* [1992] carried out a simple analysis of the CO_2 anomalies observed at Sable Island as a function of trajectory paths. Using the Interactive Model of Air Parcel Trajectories (briefly described in *Higuchi and Daggupaty*, 1985), *Winter et al.* calculated 850 mb 5-day back-trajectories of air parcels arriving at Sable Island on those days with CO_2 mixing ratio anomalies higher or lower than one standard deviation. The back-trajectory calculations were performed for the period 1987-1991. Consistent with the traditional concept of the basic westerly flow in the troposphere above the planetary boundary layer, the results of the trajectory study indicated that the Sable Island site is influenced mostly by winds from the North American continent west and northwest of the island. Even those surface winds classified as southwesterly to southerly in direction usually had 5-day back-trajectory "origins" from continental sites.

1.3.3. MEASUREMENT PROGRAMS

A grab flask sampling program for CO_2 has been carried out at Sable Island since 1975, using 2 L evacuated greased stopcock flasks. The sampling protocol at Sable Island dictates sampling from the northern shores of the island when the winds are from that direction, and on the southern shores when the winds are blowing from the southerly direction. Air samples are usually collected on a weekly basis and analyzed by NDIR analysis at AES in Downsview. A detailed description of the sampling program and procedures is given by *Trivett et al.* [1989]. Samples that do not meet the criteria of consistency are rejected, resulting in an irregularly spaced data set with an average spacing of about two weeks [*Winter et al.*, 1992].

1.4. CAPE ST. JAMES

Kaz Higuchi

1.4.1. SITE DESCRIPTION

Cape St. James, British Columbia, (52°N, 130°W), is located on the southeastern tip of St. James Island (one of the Queen Charlotte Islands) about 160 km west of the British Columbia mainland. In 1982, Cape St. James replaced Ocean Weather Station "P", which was located in the Gulf of Alaska. St. James Island has a maximum elevation of 115 km above sea level. The island is about 1 km long and 0.5 km wide. The actual sampling site is surrounded mostly with low growing vegetation such as grass, lichens and shrubs, with major forested areas to the north of the site. Sampling at Cape St. James was terminated in August 1992 when the weather station at the site was automated.

1.4.2. CLIMATOLOGY

Mean atmospheric circulation in the lower troposphere in the North Pacific is characterized by a very distinctive seasonal cycle [*Higuchi et al.*, 1995]. During the winter, a large cyclonic flow dominates the Pacific Ocean north of 20°N, bringing predominantly southerly winds to the Cape St. James site (see windrose plots in Figure 1.11). During the summer, this low system is replaced by a subtropical high, with its center near 40°N and 150°W, resulting in a dominant northwesterly flow over Cape St. James, consistent with the windrose plot. The transitional seasons of spring and summer are characterized by the northward and southward shifts, respectively, of the low and high systems. This is reflected in the windrose plots in Figure 1.11 as changes in the direction of the winds from southerly to northwesterly during the springtime, and vice versa in the fall.

Using US NMC meteorological data from September 1987 to April 1992, 30-day back-trajectories have been calculated every second day from the 800-900 mb layer

at 12z from Cape St. James [*Murayama et al.*, in preparation]. The trajectory model used in the calculations was developed and described in *Yamazaki et al.* [1989] and *Yamazaki* [1992]. A brief description of the model and various caveats related to trajectory analysis are also given in *Murayama et al.* [1995]. The results of the "climatology" of the trajectories show that during the summer (JJA), most of the air parcels spend much of their prior 30 days before arriving at the 800-900 mb layer over Cape St. James over the North Pacific Ocean, and do not "originate" in the Asian continent. It is therefore very likely that during the summer season, air parcels reaching Cape St. James are influenced by the air-sea fluxes over the ocean.

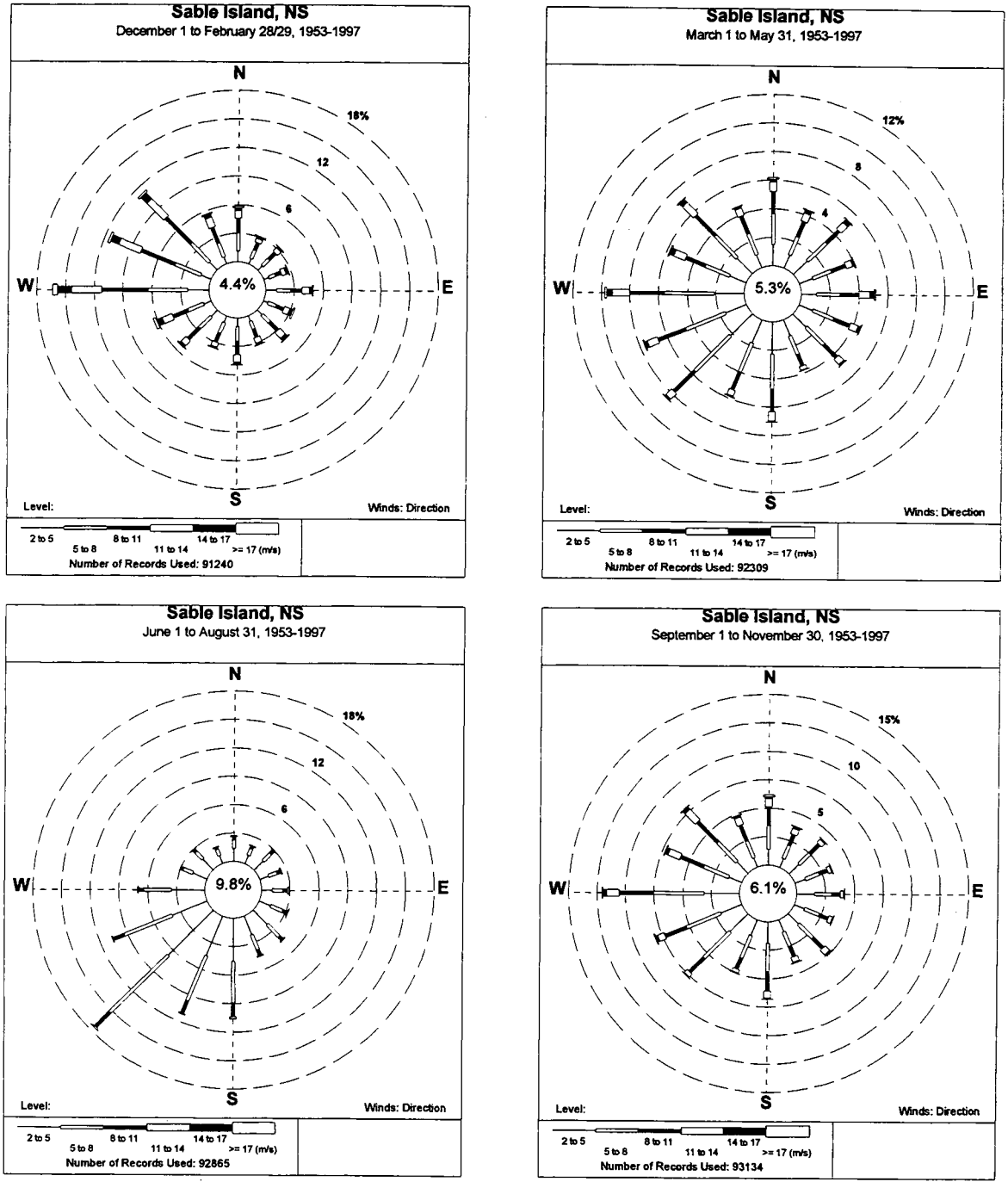

Figure 1.10 Seasonally stratified windrose plots for Sable Island.

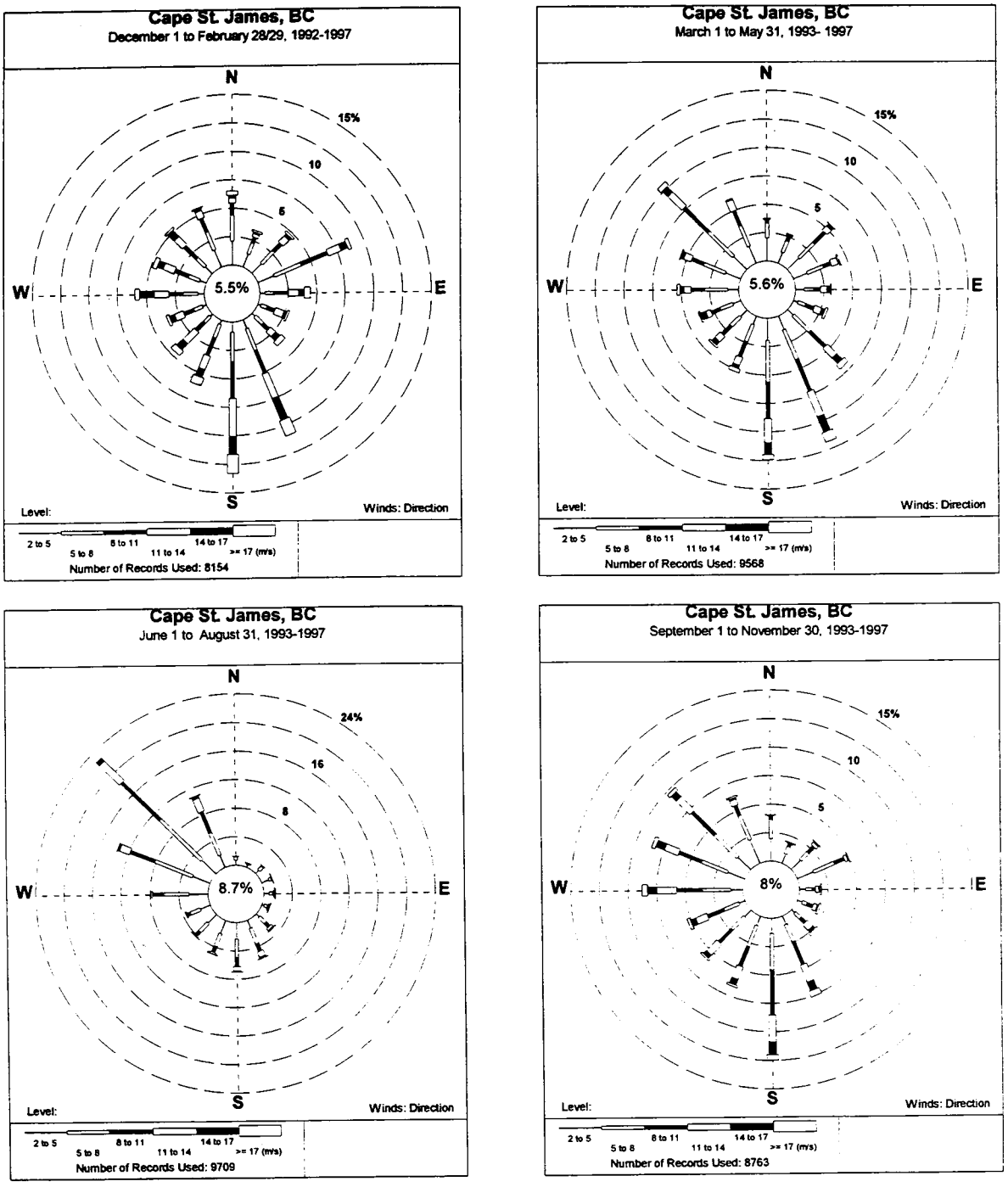

Figure 1.11 Seasonally stratified windrose plots for Cape St. James.

During the winter season (DJF), the westerly atmospheric flow is much stronger than in the summer, resulting in the 30-day back-trajectories coming from the Asiatic and European regions. The transit is very rapid, with air parcels usually spending less than 5 to 10 days over the North Pacific Ocean.

1.4.3. MEASUREMENT PROGRAMS

In May 1979, a CO_2 flask sampling program was initiated at Cape St. James. Grab samples were taken using 2 L evacuated greased stopcock flasks. A very stringent sampling protocol allowed sampling only when the winds were clearly blowing from areas away

from any major vegetated areas such as to the north and east, in an attempt to sample only the air coming off the Pacific Ocean.

The sampling protocol at Cape St. James called for a flask sampling frequency of one sample per week, but only when the station surface wind was off the water and its magnitude greater than 5 m s^{-1}. In addition to these constraints, logistic problems resulted in many missing observations at the site, the worst year being 1984 when only one measurement appears in the data set. In all, there are 230 accepted measurements in the Cape St. James CO_2 time series from May 1979 to August 1992. These values are listed in Table 1 in *Higuchi et al.* [1995].

1.5 ESTEVAN POINT

Kaz Higuchi

1.5.1 SITE DESCRIPTION

Estevan Point, British Columbia, (49°N, 126°W), is a lighthouse station located in the midsection of Vancouver Island's west coast. Due to a lack of road access, the site can be reached only by boat or helicopter. A northward aerial view of the site during a low tide is shown in Figure 1.12. The beach is about 100 m from the lighthouse. As can be seen in the figure, beyond the immediate area around the lighthouse complex, forests surround the sampling site to the north, east and south. To the west is the Pacific Ocean.

1.5.2. CLIMATOLOGY

The windrose plots for Estevan Point are shown in Figure 1.13 for the four seasons (winter, spring, summer, and fall). During the winter season, the flow is dominated by westerly to northwesterly winds, with the maximum strength a little less than 20 m s^{-1}. The winds gradually shift during the spring season to easterly and southeasterly, so that in the summer, there is almost equal probability of having westerly/northwesterly winds as easterly/southeasterly winds. However, the winds off the water tend to be a little stronger. The fall winds are characterized by flow from the southwesterly to northwesterly sector, as they gradually revert back to the winter pattern.

1.5.3. MEASUREMENT PROGRAMS

In June 1992, a weekly sampling program was started at Estevan Point, using 2 L evacuated o-ring flasks. Samples are taken on the beach when the wind speed is greater than 5 m s^{-1}. In January 1993, AES also began a pressurized flask sampling program using 2 L double-valve flasks. The samples are taken at the top of the 39 m lighthouse tower (see Figure 1.12). The samples are shipped back to AES in Downsview and are analyzed for CO_2, CH_4 and N_2O. Additional analyses of CO and SF_6 by gas chromatography are in the process of being evaluated.

Figure 1.12

Sampling site at Estevan Point.

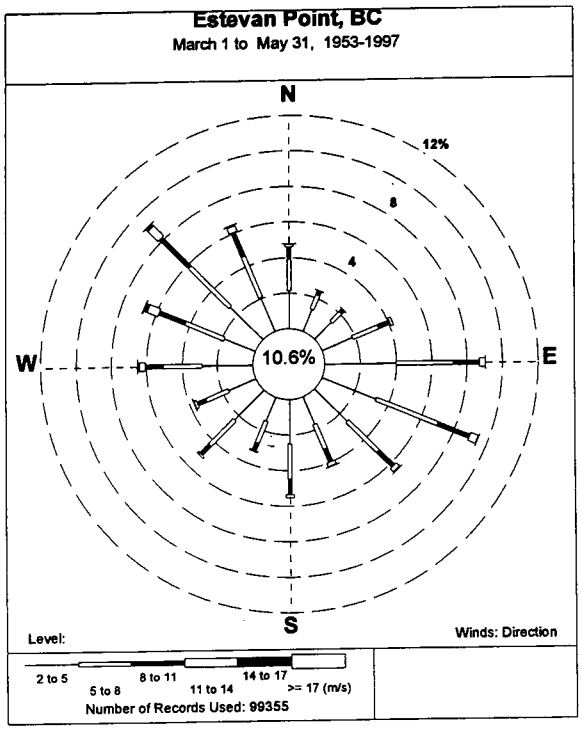

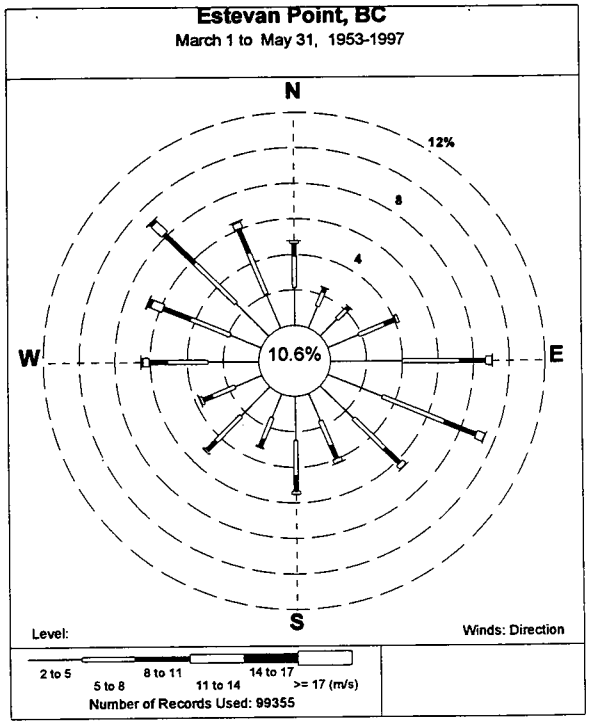

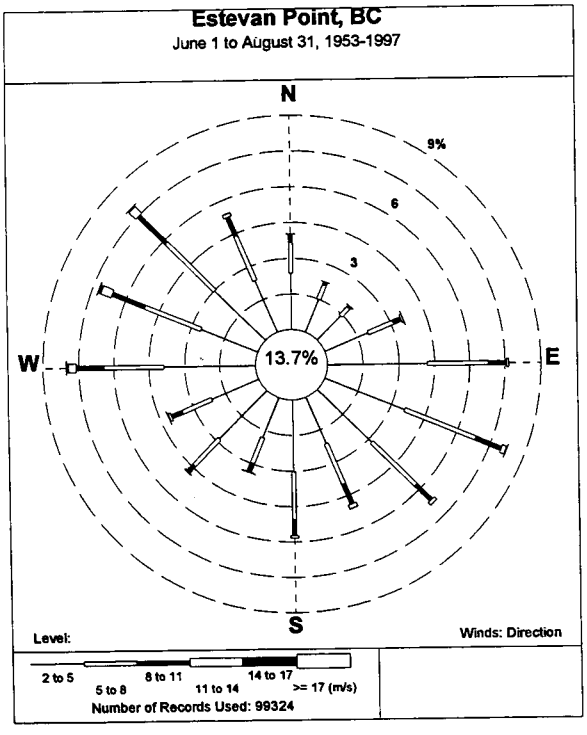

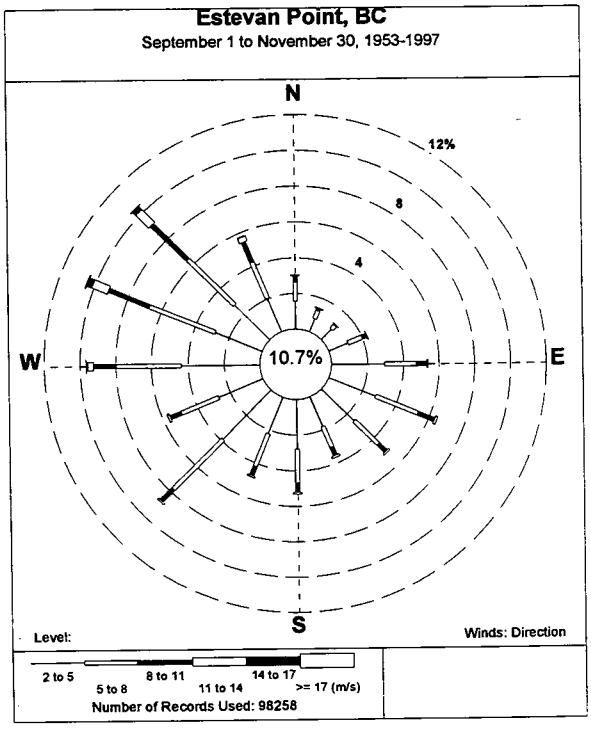

Figure 1.13 Seasonally stratified windrose plots for Estevan Point.

1.6. REFERENCES

Barrie L.A. Arctic air pollution: an overview of current knowledge, *Atmospheric Environment* 20, 643-663, 1986.

Barrie, L.A., D. Gregor, B. Hargrave, R. Lake, D. Muir, R. Shearer, B. Tracey and T. Bidleman, Arctic contaminants: Sources, occurrence and pathways, *The Science of the Total Environment*, 122 1-74, 1992.

Bryson, R.A., Air masses, streamlines, and the boreal forest, *Geographical Bulletin*, 4, No.3, pp. 228-269, 1966.

Conway, T., and L.P. Steele, Carbon dioxide and methane in the Arctic atmosphere, *J. Atmos. Chem.*, 9, 81-100, 1989.

Environment Canada, *Canadian Daily Climate Data on CD-ROM 1951-1995*, Environment Canada, 1997.

Higuchi, K. and S.M. Daggupaty, 1985: On variability of atmospheric carbon dioxide concentration at station Alert. Atmos. Environ., **19**, 2039-2044.

Higuchi, K., V. Hudec, N.B.A. Trivett, C.W. Yuen, D. Chan and C.S. Wong, 1995: A statistical comparison of the CO_2 measurements at Cape St. James and Station "P", Canada. Tellus, **47B**, 4-16.

Hopper, J.F. and W. Hart, Meteorological aspects of the 1992 Polar Sunrise Experiment, *J. Geophys. Res.* 99, No. D12, 1994.

Jackson, C. I., The Meteorology of Lake Hazen, N.W.T. Parts II, III, IV - Synoptic Influences, Local Forecasting, Bibliography, Arctic Meteor. Res. Group, Publ. Meteor. No. 16, McGill Univ., Montréal, pp. 295, 1960.

Jobson, B.T., Z. Wu, H. Niki, and L.A. Barrie, Seasonal trends of isoprene, C_2-C_5 alkanes, and acetylene at a remote boreal site in Canada, *J. Geophys. Res.* 99, 1589-1599, 1994.

Kuhlmann, A.J., D.E.J. Worthy, N.B.A. Trivett, and I. Levin, Methane emissions from Canadian wetlands: An atmospheric approach, Submitted to *J. Geophys. Res.*, 1997.

Maxwell, J.B., *The Climate of the Canadian Arctic Islands and Adjacent Waters*, Vol.1, Climatological Studies No. 30, Environment Canada, Downsview, pp. 531, 1980.

Mortsch, L. (Ed.) Climatological Studies, No. 42, Eastern Canadian boreal and sub-Arctic wetlands: A resource document, *Environment Canada*, 1990.

Murayama, S., T. Nakazawa, K. Yamazaki, S. Aoki, Y. Makino, M. Shiobara, M. Fukabori, T. Yamnouchi, A. Shimizu, M. Hayashi, S. Kawaguchi and M. Tanaka, 1995: Concentration variations of atmospheric CO_2 over Syowa Station, Antarctica and their interpretation. Tellus, 47B, 375-390.

Olsen, M.P., K.K. Oikawa, and A.W. Macafee, A trajectory model applied to the long-range transport of air pollutants: a technical description and some model intercomparisons, *Environment Canada/AES, Toronto, Canada, Internal report* LTRAP 78-4, 1978.

Raatz, W.E., The Climatology and Meteorology of Arctic Air Pollution, Chapter 2 in B. Stonehouse, *Arctic Air Pollution*, New York, Cambridge Univ. Press, 1986.

Roulet, N.T., R. Ash and T.R. Moore, Low boreal wetlands as a source of atmospheric methane, *J. Geophys. Res.*, 97, 3739-3749, 1992.

Trivett, N.B.A., D.E.J. Worthy, M. Glumpak, K. Higuchi and I. Levin, Defining "Clean" Air for the Canadian Arctic Baseline Observatory at Alert, N.W.T., Paper presented at the *Fourth Conference*, France, 1993.

Trivett, N.B.A., K. Higuchi and S. Symington, 1989: Trends and seasonal cycles of atmospheric CO_2 over Alert, Sable Island and Cape St. James, as analyzed by Forward Regression Stepwise Multiple Regression technique. In: *The Statistical Treatment of CO_2 Data Records* (ed. W.P. Elliott), NOAA Technical Memorandum ERL ARL-173, 27-42.

Winter, B., K. Higuchi, G.B. Lesins and N.B.A. Trivett, 1992: Variations with wind direction of CO_2 concentrations on Sable Island. (Unpublished).

Worthy, D.E.J., I. Levin, N.B.A. Trivett, A.J. Kuhlmann, J.F. Hopper and M.K. Ernst, *J. Geophys. Res. (accepted)* (1998).

Worthy, D.E.J., N.B.A. Trivett, J.F. Hopper, and J.W. Bottenheim, Analysis of long-range transport events at Alert, Northwest Territories, during the Polar Sunrise Experiment, J. Geophys. *Res.*, 99, No. D12, 25329-25344, 1994.

Yamazaki, K., 1992: The statistical analysis of long-term trajectory calculation based on the observed data. J. Meteorol. Soc. Japan, 70, 1167-1173.

Yamazaki, K., K. Okada and Y. Iwasaka, 1989: Where do aerosol particles in the antarctic upper troposphere come from? (a case study in Jaunary 1983). J. Meteorol. Soc. Japan, 67, 889-906.

Yuen, C.W., K. Higuchi, N.B.A. Trivett and H.-R. Cho, A simulation of a large positive anomaly over the Canadian Arctic Archipelago, J. Meteo. Soc. Japan, 74, No. 6, 781-795, 1996.

2. MEASUREMENT PROGRAMS

2.1 CARBON DIOXIDE

2.1.1. IN SITU CO_2 MEASUREMENTS

Kaz Higuchi, Neil B.A. Trivett, Alexander Shashkov, Lori Leeder and Darrell Ernst

2.1.1.1. BACKGROUND

As part of the Global Atmosphere Watch (GAW) Program under the World Meteorological Organization (WMO), Canada established a baseline observatory at Alert in 1986 on the northern tip of Ellesmere Island in the Canadian Arctic. The observatory is the most northerly monitoring station in the WMO network and, as such, it is far removed from the major industrial regions in the Northern Hemisphere. Alert has been regarded as an ideal location to monitor changes in the background atmospheric CO_2 concentration level due to anthropogenic activities. The temporal variability in the concentration of atmospheric CO_2 has been shown to reflect the CO_2 source/sink strength and distribution in the lower latitudes, particularly during the winter season [*Higuchi et al.*, 1987; *Worthy et al.*, 1994].

The high Arctic is a polar desert with minimal vegetation compared to the temperate regions. The region around Alert is covered with snow from September to June. During the snow-free season, rapid growth in vegetation, albeit sparse, is observed. The only "local" source of pollutants at Alert is the weather station and military camp, located about 7 km NNE of the observatory; however, only a very small fraction of the baseline data comes from this sector.

Three very distinctive features characterize the continuous measurements of CO_2 at Alert, each with its own time scale. These are: (1) variation in the short-term fluctuations, (2) interannual variability in the seasonal cycle, and (3) interannual variability in the secular trend. The last two features mainly reflect the year-to-year change in the source/sink strength and distribution on a hemispheric spatial scale. Alert CO_2 data constitute an important component in trying to resolve the issue of the role of the Northern Hemisphere mid-latitude terrestrial biosphere in the global carbon cycle.

The methodology description of the CO_2 measurements is found in Section 3.1.1.

2.1.1.2. IN SITU CO_2 MEASUREMENTS AT ALERT

Six-hourly averaged CO_2 concentration data measured at Alert since 1988 by NDIR are shown in Figure 2.1. Also shown in the figure are the seasonal cycle and long-term trend obtained by applying a digital filtering procedure [*Nakazawa et al.*, 1997] to the data. An outstanding feature of the CO_2 time series from Alert is the considerable variability (sometimes on the order of 5 to 6 ppm relative to the seasonal cycle) in the concentration values during the winter season. Given the absence of significant industrial and natural sources for CO_2 in the high Arctic wintertime, it has been demonstrated that long-range atmospheric transport plays an important role in causing the short-term variability, as well as in the long-term trend and seasonal cycle of CO_2 at Alert [*Higuchi et al.*, 1987; *Worthy et al.*, 1994; *Trivett et al.*, 1996; *Yuen et al.*, 1996].

In an earlier trajectory analysis study of CO_2 flask data from Alert, *Higuchi et al.* [1987] showed that the short-term positive CO_2 anomalies are usually associated with air masses arriving from northern Europe and Siberia, while the negative anomalies are typically related to air masses arriving from northern open oceanic areas. *Worthy et al.* [1994] showed that the variability on a synoptic time scale (5-7 days) during the months of January and February is caused by rapid long-range transport of air from anthropogenic sources in Eurasia and Siberia some 2500 to 3000 km from Alert. During the polar night, the Arctic atmosphere is usually very stable, forcing pollutants injected into the Arctic atmosphere to travel long distances as a cohesive plume without too much vertical and horizontal mixing. By the end of March, the short-term variability diminishes significantly, mainly due to increased mixing in the Arctic atmosphere.

Three distinctive tracer transport pathways from Eurasia to the Canadian Arctic were identified by *Yuen et al.* [1996]. These are: (1) direct cross-Arctic pathway, (2) transport via northern Siberia, across the pole, and (3) recirculation of Arctic air mass. Transport times for various pathways range from about 1-2 weeks (direct pathway) to over a month (transport via Siberia).

Besides the synoptic fluctuations, *Huang et al.* [1997] identified a low-frequency intraseasonal variability of 20-50 days in the CO_2 measurements. Even though both the synoptic fluctuations and the intraseasonal fluctuations are strongly modulated by the seasonal cycle, the origins of these fluctuations are quite different. The synoptic fluctuations reflect the quasi-

periodicity of the passage of synoptic systems with different air masses over Alert. The low-frequency intraseasonal variations are quite often associated with variability in the planetary wave structure, and appear to be correlated with convective activities in the tropics [*Knutson and Weickmann*, 1987].

The phase-locking relationship between the short-term fluctuations of CO_2 and the seasonal cycle also suggests that northern ecosystems could constitute a seasonally-dependent local CO_2 source [*Ciais et al.*, 1995; *Oechel et al.*, 1993; *Zimov et al.*, 1996].

Average Seasonal Cycle of CO_2 at Alert

The detrended mean seasonal cycle of CO_2 at Alert averaged over a 10-year period from 1988 to 1998 is shown in Figure 2.2, along with the detrended mean seasonal cycle of CO_2 at Fraserdale averaged over a 7-year period from 1990 to 1996. The relationship between these two average seasonal cycles is consistent with our expectations. Fraserdale is a continental site situated in a mixed boreal forest dominated mainly by black spruce in northern Ontario. Thus, the CO_2 data collected at Fraserdale are significantly influenced by the seasonal evolution of the carbon fluxes of the regional vegetation surrounding Fraserdale [*Shashkov et al.*, 1998; *Trivett et al.*, 1999]. During the non-growing season, the net flux of CO_2 from the ground to the atmosphere is mainly dominated by soil respiration. In the growing season, active photosynthetic process causes net drawdown of CO_2 from the atmosphere to the vegetation. The photosynthetic/decay cycle of the vegetation produces an average seasonal cycle at Fraserdale with the amplitude reaching around 20 ppm. Comparatively, the amplitude of the average (1988-1998) seasonal cycle at Alert is about 15 ppm with about a 1 month phase delay, which is consistent with the concept that the seasonal cycle of CO_2 in high latitudes is influenced greatly by the atmospheric transport of CO_2 from the mid latitudes.

Secular Trend of CO_2 at Alert between 1988-1998

The increase of CO_2 concentration in the Arctic atmosphere averaged about 1.5 ppm yr^{-1} from 1988 to 1998. Differentiation of the secular trend curve shown in Figure 2.1 gives the growth rate of CO_2 concentration. The growth rate curve of CO_2 from Alert is shown in Figure 2.3, along with the growth curve from Fraserdale for comparative purposes. Here, it is interesting to note that both Alert and Fraserdale show a positive growth rate in 1991, dropping almost concurrently to a negative growth rate in 1992. It has been speculated that the cool temperature during the summer of 1992 caused by the Mt. Pinatubo volcanic eruption reduced ecosystem respiration, thus enhancing the net uptake of the atmospheric CO_2 by the mid latitude biosphere.

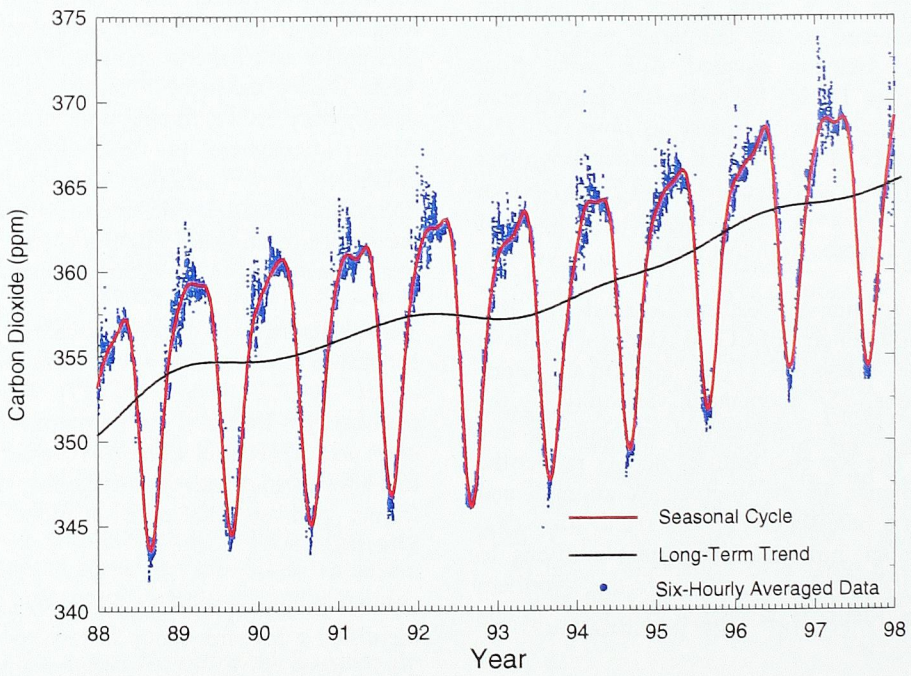

Figure 2.1 Secular trend (solid black line) and seasonal cycle (solid red line) fitted to six-hourly averaged CO_2 concentration data (solid blue dots) from 1988 to 1998. Note the interannual variability in the long-term trend, seasonal cycle and short-term fluctuations.

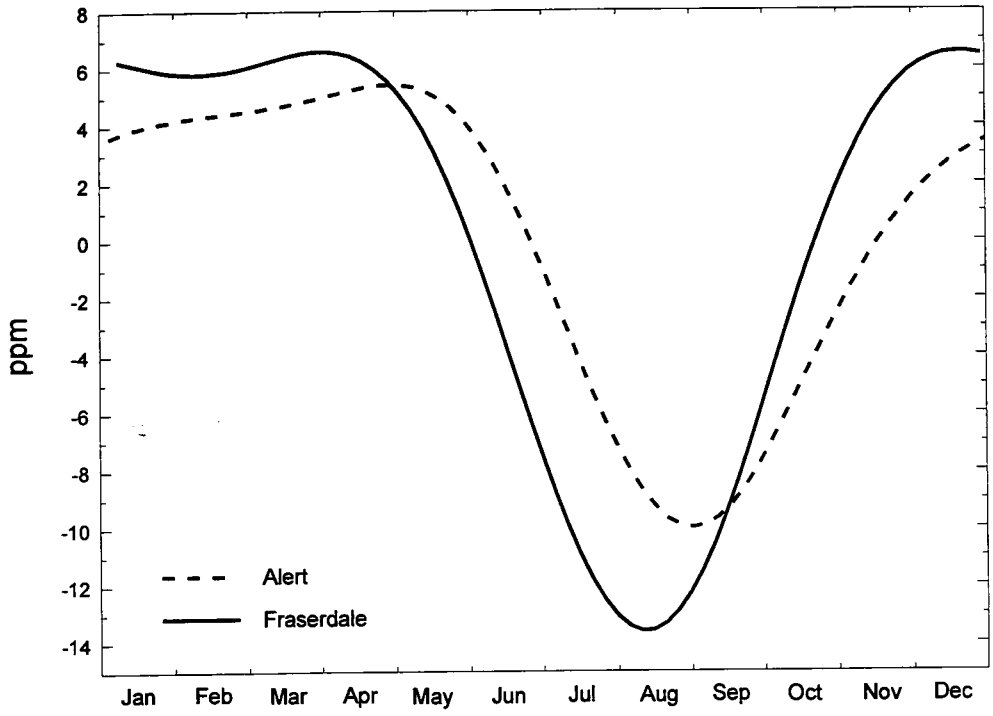

Figure 2.2 Mean seasonal cycle of CO_2 at Fraserdale (averaged over the period 1990-1996) and at Alert (averaged over the period 1988-1998). Note the difference in the amplitude and phase between Alert and Fraserdale.

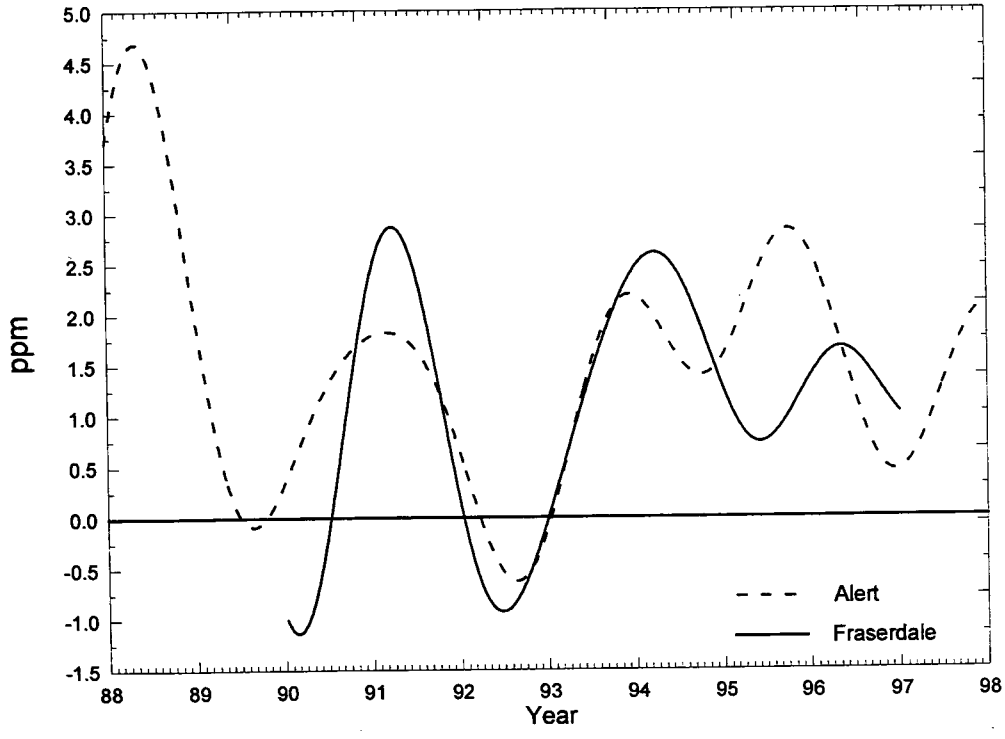

Figure 2.3 Growth rate curve at Alert and at Fraserdale. There is great deal of interannual variability in the growth of CO_2 concentration in the atmosphere. Note the correlation between Alert and Fraserdale in 1991 and 1992.

2.1.1.3 In Situ CO_2 Measurements at Fraserdale

The Fraserdale CO_2 concentration record (1990-1996) is unique in many respects and provides insight into the processes on various time scales responsible for CO_2 concentration changes in the atmospheric boundary layer at a continental site in boreal forest. As already mentioned in Section 1.2.1. Fraserdale is located in a mixed boreal forest dominated mainly by black spruce in northern Ontario.

The uniqueness of the Fraserdale station data record is derived primarily from the fact that Fraserdale is the first monitoring station to be established in an internal continental area with relatively flat topography. Other continental sites, such as Niwot Ridge in the United States and Shauinsland in Germany, are situated in elevated mountainous locations, causing complicated disturbed flow patterns and, thus, making the interpretation of the CO_2 concentration data from these stations very difficult [*Levin*, 1987].

An additional advantage of the Fraserdale site comes from its relative position to Alert. It has been found that about 60% of the air mass trajectories arriving at Fraserdale come from the Arctic [*Worthy et al.*, 1998]. This "coupling" between the two stations has been successfully exploited by *Worthy et al.* [1998] in calculating interannual variability in the methane flux from the Hudson Bay Lowland (see Section 2.2.3.1 for more detail). This relative geographical relationship between Fraserdale and Alert has also been exploited by *Shashkov et al.* [1998] in their calculation of the net biospheric flux of CO_2 around Fraserdale over the period 1991 to 1994 (see below for a brief summary of the results).

Atmospheric CO_2 Variability at Fraserdale

Hourly values of the CO_2 mixing ratio measured at Fraserdale, Ontario, from 1990 to 1996, are shown in Figure 2.4, along with "background" concentration values from Cape St. James, Cold Bay and Alert. The smooth seasonal cycles of Cape St. James and Cold Bay are obtained by applying the Forward Stepwise Multiple Regression (FSMR) [*Trivett et al.*, 1989] to the flask data from these stations. The continuous data from Alert, on the other hand, are smoothed with a 7-day running mean filter. Also plotted in the figure are the aircraft measurements obtained above the atmospheric boundary layer by Ray Desjardins (private comm., 1998) and *Anderson et al.* [1996]. Large diurnal variability during the growing season is quite noticeable. Also noticeable is the interannual variability in the amplitude of the diurnal cycle.

The diurnal cycle of the atmospheric CO_2 concentration is determined basically by the interactive effect of the daily cycle of the atmosphere/vegetation CO_2 exchange with the daily evolution of the boundary layer mixing regime. During the growing season, both the CO_2 exchange and the boundary layer mixing regime experience significant diurnal variations, driven primarily by daily changes in solar radiation. Figure 2.5 shows monthly averaged diurnal changes in the CO_2 mixing ratio during different months in 1991 and 1992.

During any particular day in the growing season, activation of photosynthesis after sunrise results in a rapid decrease in the CO_2 mixing ratio in the atmospheric boundary layer (see July and August in Figure 2.5). At the same time, convective turbulence causes growth of the well-mixed boundary layer, which usually becomes fully developed by the middle of the afternoon. After that time, the height of the convective boundary layer grows much slower and entrains less air from above the boundary layer. A combination of the change in the photosynthetic rate during the day and the "maturing" of the convective boundary layer by the early afternoon results in a period of quasi-constant CO_2 mixing ratio (afternoon "plateau") from some time in the mid afternoon to sunset.

At night, photosynthesis stops and there is a net transfer of CO_2 from land to the atmosphere, resulting from the heterotrophic and autotrophic respiration which continues to operate. At the same time, the surface radiative cooling causes a transformation of the near-surface air into a stable boundary layer through development of a temperature inversion. Carbon dioxide emitted into the stable layer accumulates there, causing rapid increase in the CO_2 mixing ratio during the nighttime. The accumulation continues until the stable layer collapses shortly after sunrise.

During the non-growing season, there is very little, if any, diurnal variation in the CO_2 mixing ratio (see January in Figure 2.5).

In Figure 2.4, we can also see variability of the diurnal cycle on a day-to-day basis. This is primarily due to synoptic weather events. For example, a high pressure system with relatively clear sky conditions during the daytime allows more intensive photosynthetic assimilation by the vegetation, giving lower CO_2 values than during those days with a low pressure system. During the nighttime, a clear sky condition typically causes calm winds and a strong near-surface inversion; these meteorological conditions usually result in high levels of CO_2 at night.

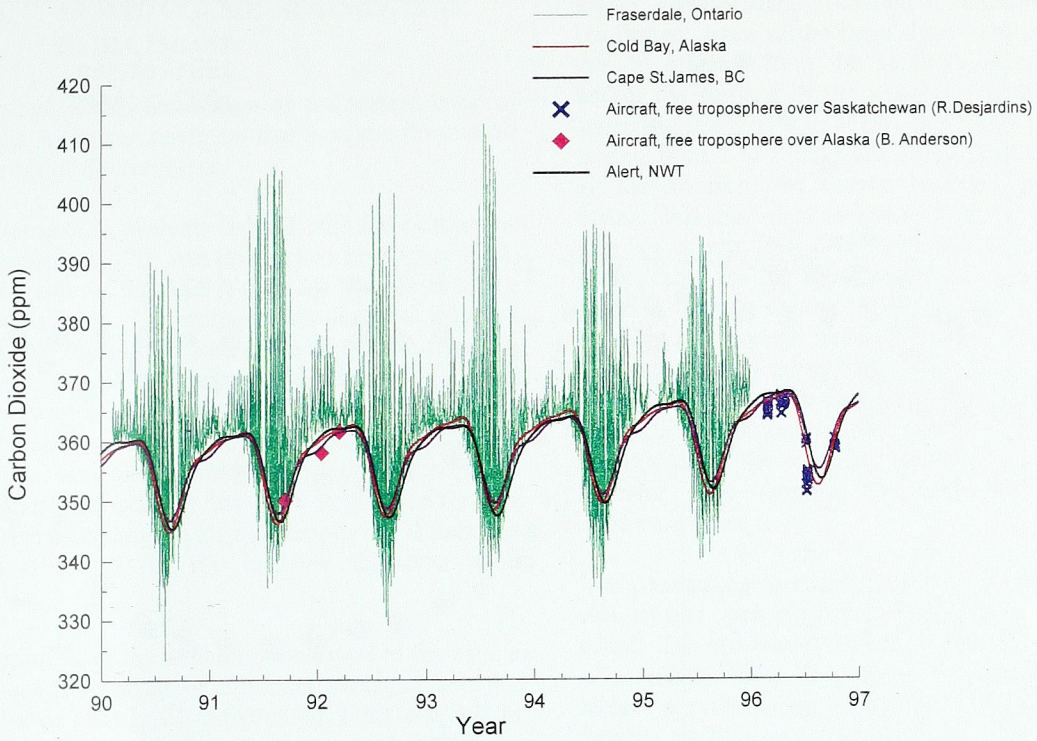

Figure 2.4 Hourly values of CO_2 mixing ratio (ppm) observed at Fraserdale between 1990 and 1996. Superimposed on the Fraserdale data are smooth curves fitted to the CO_2 data from Alert, Cape St. James and Cold Bay.

CO_2 Fluxes at Fraserdale

In a study just completed [*Shashkov et al.,* 1998], we used the CO_2 measurements from the Fraserdale site to calculate CO_2 fluxes over a 4-year period, from 1991 to 1994. For this purpose, we employed the "boundary layer budget" method, which was originally used to estimate regionally averaged water vapour exchange [*McNaughton and Spriggs,* 1986; *McNaughton*, 1989; *Munley and Hipps,* 1991]. *Raupach et al.* [1992] and *Deanmead et al.* [1996] published an excellent analysis of the technique and its application to CO_2.

Calculated annually averaged values from 1991 to 1994 of GEE (gross ecosystem exchange), NEE (net ecosystem exchange) and Resp. (Respiration) are shown in Table 2-1. Of the 4 years, 1992 and 1994 show noticeably larger NEE values of -2.0 metric tons of C per hectare and -1.7 metric tons of C per hectare, respectively. Although the photosynthetic absorption was relatively high during the growing season in 1994, respiration was also relatively high due to the above normal temperatures experienced at Fraserdale after the growing season. This resulted in a net annual transfer of CO_2 from the atmosphere to the vegetation in 1994 around Fraserdale slightly less than the NEE of -2.0 metric tons of C per hectare calculated for 1992. For comparative purposes, we also give in Table 2-1 the results obtained during BOREAS in 1994 [*Black et al.*, 1996]. The values of GEE, NEE and Resp. we obtained for the Fraserdale site are comparable with the values obtained at the southern BOREAS site. Our calculated value for 1994 is -1.7 metric tons of C per hectare, while the BOREAS value is -1.3 metric tons of C per hectare. Our calculations showed that the mixed boreal forest around Fraserdale in northern Ontario acted as a net sink for the atmospheric CO_2 from 1991 to 1994, with 1992 and 1994 showing the largest uptake values.

We also re-calculated the annual flux values for Fraserdale from day 300 to day 299 of the following year so that we could compare the resultant values with those obtained by *Goulden et al.* [1996] for Harvard Forest. These are also shown in Table 2-1. There are differences in the values. For example, the values we obtained for the 1992-1993 period for Fraserdale are noticeably lower in magnitude than those obtained for Harvard Forest. However, given that the Fraserdale site is a mixed forest dominated mainly by black spruce, while Harvard Forest is dominated mainly by aspen, the flux values for these two sites are not inconciliatorily different. But what is more interesting is the fact that the numbers are overall very similar.

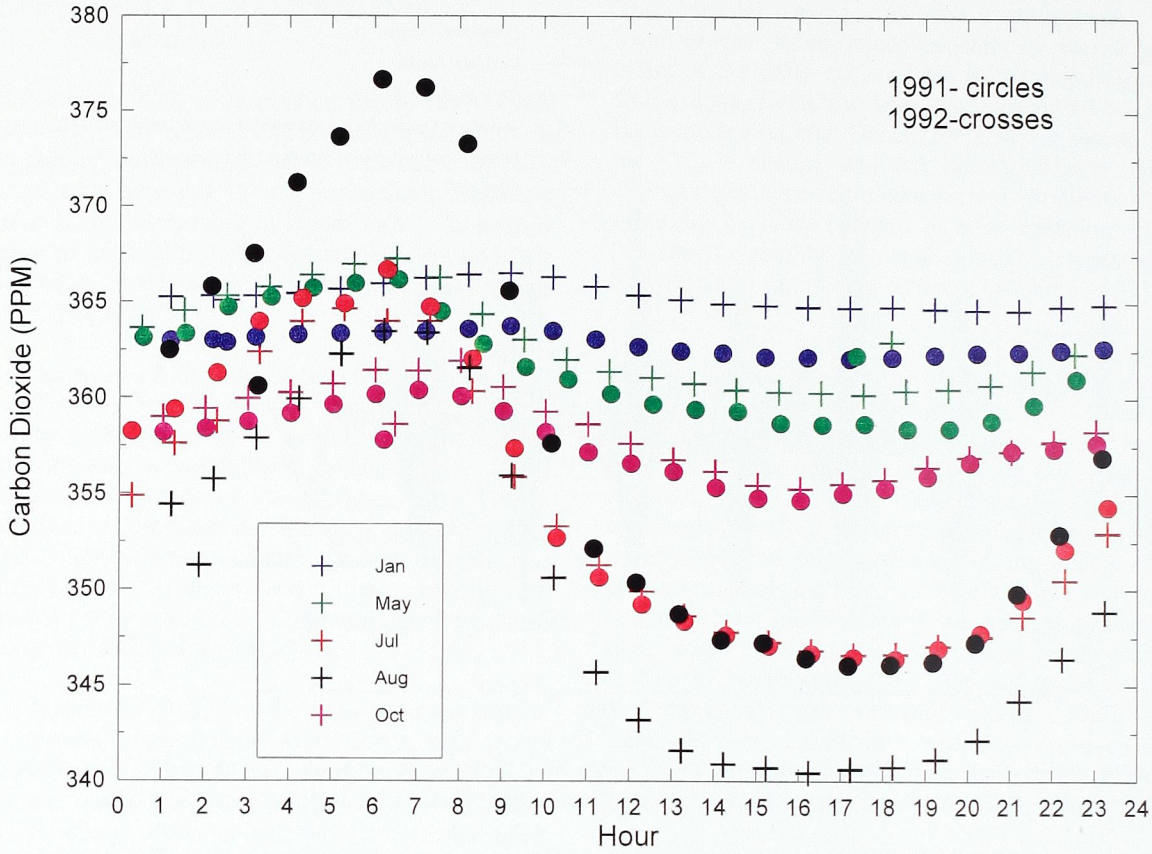

Figure 2.5 Average diurnal cycle of the CO_2 mixing ratio for different months in 1991 and 1992 at Fraserdale.

Table 2-1. Estimated annual CO_2 exchange fluxes.

Fraserdale: DOY 0 to DOY 365			
Year	NEE	GEE	Resp.
1991	-0.7	-9.8	9.1
1992	-2.0	-10.8	8.8
1993	-0.4	-9.4	9.0
1994	-1.7	-11.6	9.9

BOREAS (Black et al., 1996)			
Year	NEE	GEE	Resp.
1994	-1.3	-10.2	8.9

Units: metric tons of C per hectare

Fraserdale: DOY 300 to DOY 200 of the next year			
Period	NEE	GEE	Resp.
1991-1992	-2.4	-10.8	8.4
1992-1993	-0.5	-9.3	8.8
1993-1994	-1.3	-11.6	10.3

Harvard Forest (Goulden et al., 1996) DOY 300 to DOY 299 of the next year			
Period	NEE	GEE	Resp.
1990-1991	-2.8	-12.1	9.6
1991-1992	-2.2	-11.1	9.3
1992-1993	-1.4	-12.7	11.4
1993-1994	-2.1	-11.7	9.7
1994-1995	-2.7	-10.7	8.1

2.1.1.4. IN SITU CO_2 MEASUREMENTS AT SABLE ISLAND

Sable Island is the only station on the eastern coast of the North American continent that is in the flow of air coming out of the continent.

A pilot project to evaluate Sable Island for continuous measurements of CO_2 was established in August 1992, using the attic of the AES Upper Air Station to house the NDIR system. The sample intake line was installed on a nearby 20 m tower located about 0.5 km from the southern. One of the major objectives of the pilot program was to evaluate the effects of the island's vegetation on the CO_2 signal. Modelling studies of the wind flow over the island [*Wamsley*, AES personal communication] indicate that to be in the free flow of the marine boundary layer, the sample line should be located at the 80 to 100 m level for most wind directions.

As an example of the variability observed in the data, a continuous time series of 3-minute averaged data for the period of January 22 to March 30, 1993 is shown in Figure 2.6. The continuous data set reveals extremely highly variable data. Although it cannot be definitely confirmed, some of the large short-term peaks may be due to effluent from the station's diesel generators and/or the furnace in the weather office. Preliminary trajectory analysis also shows that some of the events lasting from 2 to 5 days are likely due to transport of air masses from the eastern seaboard of the United States. This short data set exemplifies the point that the analysis of any CO_2 data collected at Sable Island is complicated by the intrusion of air masses from the North American continent, which must be segregated from the maritime air masses coming in off the Atlantic Ocean. This is extremely difficult to do with a flask program. It should be noted that the Sable Island flask program is probably not affected by the local conditions, as the sampling protocol requires that the operator take samples from the north or south windward shore.

It is planned for the spring of 1999 to reinstall the in situ carbon dioxide measurement program at Sable Island. The instrument will be installed in the basement of a building next to a 40 m communication tower, located approximately 2 km away from the main camp. Sample air will be drawn from the top of the tower.

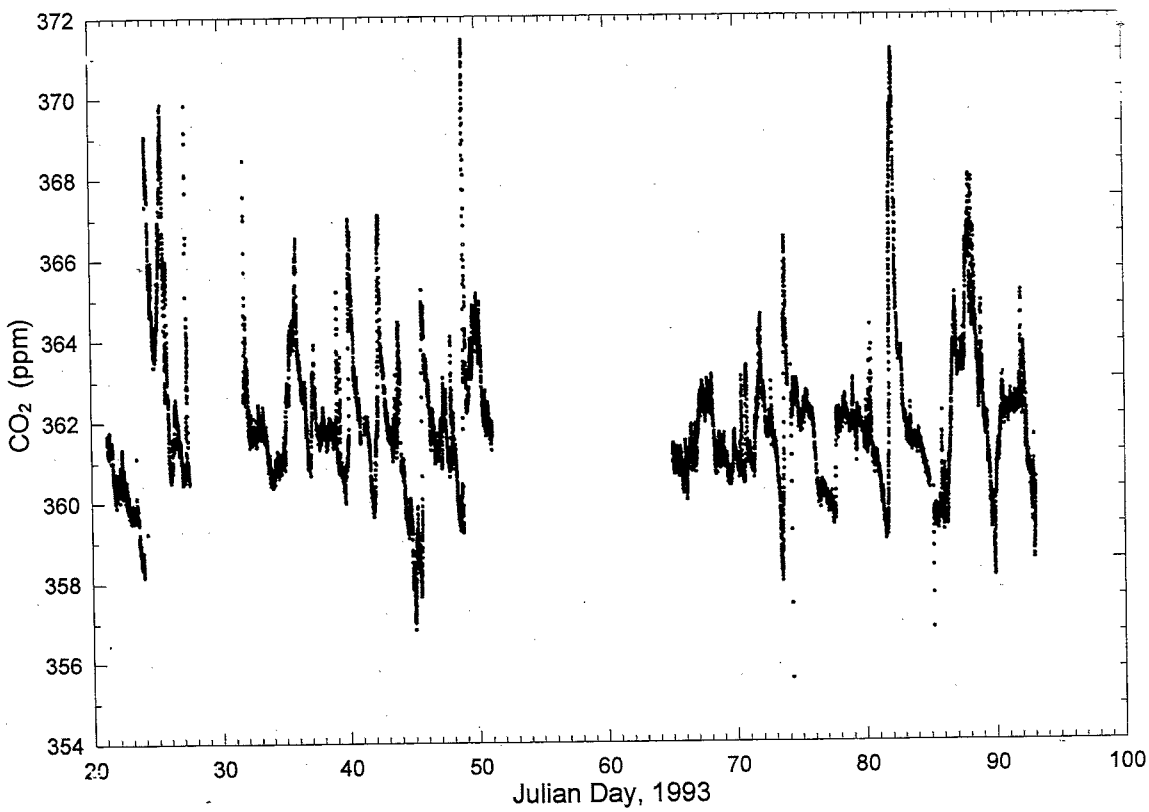

Figure 2.6 Time series of 3-minute averaged CO_2 data from Sable Island for the period Jan. 22 to Mar. 30, 1993.

2.1.1.5. REFERENCES

Anderson B.E., G.L. Gregory, J.E. Collins Jr., G.W. Sachse, T.J. Conway, and G.P. Whiting, 1996. Airborne observations of spatial and temporal variability of tropospheric carbon dioxide. J. Geophys. Res., 101, D1, 1985 – 1997.

Black T.A., G. den Hartog, H.H. Neumann, P.D. Blanken, P.C. Yang, C.Russel, Z. Nesic, X. Lee, S.G. Chen, R. Staebler and M.D. Novak, 1996. Annual cycles of water vapor and carbon dioxide fluxes in and above a boreal aspen forest. Global Change Biology, 2, 219-229.

Ciais, P., P.P. Tans, M. Trolier, J.W.C. White, and R.J. Francey, 1995: A large Northern Hemisphere terrestrial CO_2 sink indicated by the C^{13}/C^{12} ratio of atmospheric CO_2. Nature, 269, 1098-1102.

Deanmead O.T., M.R. Raupach, F.X. Dunin, H.A. Cleugh, and R. Leuning. Boundary layer budgets for regional estimates of scalar fluxes, 1996. Global Change Biology, 2, 255-264.

Goulden M.L., J.W. Munger, Song-Miao Fan, B.C. Daube, S.C. Wofsy, 1996. Exchange of Carbon Dioxide by a Deciduous Forest: Response to Interannual Variability, Science, 271, 1576-1578.

Higuchi, K., N.B.A. Trivett, and S.M. Daggupaty, 1987: A preliminary climatology of trajectories related to atmospheric CO_2 measurements at Alert and Mould Bay. Atmos. Environ., 21, 1915-1926.

Huang, J.-P., K. Higuchi, and N.B.A. Trivett, 1997: Multiresolution Fourier transform and its application to analysis of CO_2 fluctuations over Alert. J. Meteorol. Soc. Japan, 75, 701-715.

Knutson, T.R. and K.M. Weickmann, 1987: 30-60 day atmospheric oscillations: Composite life cycles of convection and circulation anomalies. Mon. Wea. Rev., 115, 1407-1436.

Levin, I. 1987. Atmospheric CO_2 in continental Europe - an alternative approach to clean air CO_2 data, Tellus, 39B, 21-28.

McNaughton, K.G., 1989. Regional interactions between canopies and the atmosphere. In: Plant Canopies: Their Growth, Form and Function. (G. Russel, B. Marshall and P.G. Jarvis, eds.). Cambridge University Press, Cambridge, U.K., 63-81.

McNaughton K.G. and T.W. Spriggs, 1986. A mixed-layer model for regional evaporation. Bound.-Layer Meteorology, 34, 243-262.

Munley W.G. and L.E. Hipps, 1991. Estimation of regional evaporation for a tallgrass prarie from measurements of properties of the atmospheric boundary layer. Water Res., 27, No.2, 225-230.

Nakazawa, T., M. Ishizawa, K. Higuchi, and N.B.A. Trivett, 1997: Two curve fitting methods applied to CO_2 flask data. EnvironMetrics, 8, 197-218.

Oechel, W.C., S.J. Hastings, G. Vourlitis, M. Jenkins, G. Riechers, and N. Grulke, 1993: Recent change of Arctic tundra ecosystems from a net carbon dioxide sink to a source. Nature, 361, 520-523.

Raupach M.R., O.T. Denmead, F.X. Dunin, 1992. Challenges in Linking Atmospheric CO_2 Concentration to Fluxes at Local and Regional Scales, Aust. J. Bot., 40, 697-716.

Shashkov A.A., K. Higuchi, N.B.A. Trivett, L. Leeder, S. Racki, and D.E.J. Worthy, 1998. Seasonal and Interannual Variability in CO_2 Fluxes Estimated from Atmospheric Concentration Measurements at Boreal Forest Site in Canada, (in preparation).

Trivett, N.B.A., K. Higuchi, and S. Symington, 1989. Trends and seasonal cycles of atmospheric CO_2 over Alert, Sable Island, and Cape St. James, as analyzed by forward stepwise multiple regression technique. In: The Statistical Treatment of CO_2 Data Records. (W.P. Elliot, ed.). NOAA Technical Memorandum ERL APL-173, Air Resource Laboratory, Silver Spring, Maryland, USA, 27-42.

Trivett, N.B.A., K. Higuchi, C.W. Yuen, and D.E.J. Worthy, 1996: The impact of Arctic circulation on trace gas measurements at Alert, Canada. Mem. Natl. Inst. Polar Res., Spec. Issue, 51, 165-176.

Trivett, N.B.A., K.Higuchi, and D.E.J. Worthy, 1999: Continuous measurements of ambient CO_2 concentration at Alert: 1988 to 1998. (In preparation.)

Worthy, D.E.J., N.B.A. Trivett, J.F. Hopper, J.W. Bottenheim, and I. Levin, 1994: Analysis of long-range transport events at Alert, N.W.T., during the Polar Sunrise Experiments. J. Geophys. Res., 99, 25329-25344.

Worthy, D.E.J., I. Levin, N.B.A. Trivett, A.J. Kuhlmann, J.F. Hopper, and M.K. Ernst, 1998. Seven years of continuous methane observations at a remote boreal site in Ontario, Canada. J. Geophys. Res., 103, D13, 15, 995-1007.

Worthy, D.E.J., I. Levin, J.F. Hopper, and N.B.A. Trivett, 1998: Evidence of a link between climate change and northern wetlands methane emissions. (In preparation.)

Yuen, C.W., K. Higuchi, N.B.A. Trivett, and H.-R. Cho, 1996: A simulation of a large positive CO_2 anomaly over the Canadian Arctic archipelago. J. Meteorol. Soc. Japan, 74, 781-795.

Zimov, S.A., S.P. Davidov, Y.V. Voropaev, S.F. Prosiannikov, I.P. Zimov, M.C. Chapin, and F.S. Chapin, 1996: Siberian CO_2 efflux in winter as a CO_2 source and cause of seasonality in atmospheric CO_2. Climatic Change, 33, 111-120.

2.1.2. FLASK CO_2 MEASUREMENTS

Victoria Hudec, Kaz Higuchi and Neil B.A. Trivett

2.1.2.1. BACKGROUND

The Canadian air sampling network was initiated in 1969 at Ocean Station Papa in the northeast Pacific Ocean to monitor the increase of carbon dioxide (CO_2) in the atmosphere. The program was a joint effort between the Scripps Institute of Oceanography (SIO) in San Diego, California, and the Institute for Ocean Sciences (IOS) in Patricia Bay, British Columbia. In 1975, AES established flask measurement programs at Alert and Sable Island. In 1978, IOS established a third flask measurement program at Cape St. James. Cape St. James became the replacement station for Ocean Station Papa in 1982, when the weather ship on site was taken out of service. In 1981, the partnership between SIO and IOS ended, and AES and IOS became jointly responsible for the Canadian CO_2 measurement program. IOS analyzed the flask samples collected at the three sites for CO_2 until 1988, when AES assumed responsibility for the analysis. In August 1992, the weather station at Cape St. James was automated with no requirement for a manned presence on site. This necessitated AES to terminate its flask measurement program at Cape St. James. AES chose Estevan Point, which is located on the west coast of Vancouver Island, as the replacement site for Cape St. James because it is well exposed to similar airflow off the Pacific Ocean. Flask sampling at Estevan Point began in June 1992.

AES has used evacuated 2 L glass flasks fitted with 6 mm bore high vacuum stopcocks (lubricated with Apiezon-N grease) at Alert, Sable Island and Cape St. James since 1975. This greased stopcock flask type is illustrated in Figure 2.7. AES introduced a new flask type into its sampling network at Alert and Estevan Point in 1992. This new flask type has a glass barreled valve with Viton® o-ring seals. It is more robust for field sampling and easier to open in extreme cold temperatures than the greased stopcock flasks. The design of this flask is illustrated in Figure 2.8. AES introduced a third flask type into its sampling network at Alert and Estevan Point in 1993. This flask has dual glass barreled valves with Viton® o-ring seals. The design of this flask is illustrated in Figure 2.9. Using a pumping unit, the volume of this flask can be completely flushed and pressurized with air from a sampling line. For a detailed description of flask sampling protocols and measurement techniques refer to Section 3.1.2.

2.1.2.2. FLASK DATA CLASSIFICATION

IOS maintained the flask analysis program from the inception of the program through to 1988. The data are published in a paper by *C.S. Wong et al.*, [1984]. For the period IOS was responsible for flask analysis, two aliquots from each flask were extracted and analyzed and a mean mixing ratio was calculated for each flask. The two flask mixing ratios were averaged to calculate a mean. Flask data was classified according to the "within flask difference" criterion for each aliquot and the "between flask difference" criterion for the flask pair.

If the analysis of the two aliquots, from a given flask, agreed within 0.3 ppm then the flask was classified as "**A**". If the analysis was not within 0.3 ppm then the flask was classified as "**L**" indicating a suspected laboratory problem. If both flasks, in a flask pair, were classified as **A** and agreed within 0.6 ppm then the flask pair average was classified as "**A**". If the two flasks agreed within 0.6 ppm, but the criterion for the within flask difference was not met, then the flask pair average was classified as "**B**". If the two flasks in the pair did not agree within 0.6 ppm then the flask pair average was classified as "**S**" indicating a suspected sampling problem. In the event that one of the flasks, in a flask pair, was broken or missing, the remaining flask was analyzed and classified as "**I**" for incomplete if the within flask difference for the flask was < 0.3 ppm. Only flask pair averages classified as "A" or "B" were used to determine CO_2 trends and seasonal cycles.

When AES assumed responsibility for the flask analysis in 1988, only a single aliquot from each flask was extracted and analyzed. Flask data were no longer classified according to the "within flask difference" criterion. Instead, data were classified according to the standard deviation of the analyzed flask and the "between flask difference" criterion for the flask pair.

A flask is classified as "+" when the standard deviation of the flask is less than three times the average standard deviation of the calibration gases. A flask is classified as "**L**" (suspected laboratory problem) if the standard deviation of the flask is greater than three times the average standard deviation of the calibration gases. The flask pair average is classified as "**A**" if both flasks are classified as "+" and agree within 0.6 ppm. The flask pair average is classified as "**B**" if the two flasks agreed within 0.6 ppm but one or both of the flasks are not classified as "+". The flask pair average is classified as "**S**" (suspected sampling problem) when both flasks in the pair do not agree within 0.6 ppm. In the event that one of the flasks, in a flask pair, is broken or missing, the remaining flask is analyzed. If

the standard deviation for the flask is less than three times the average standard deviation of the calibration gases, the flask is classified as "I" for incomplete pair. Only flask pair averages classified as "A" or "B" are used to determine CO_2 trends and seasonal cycles.

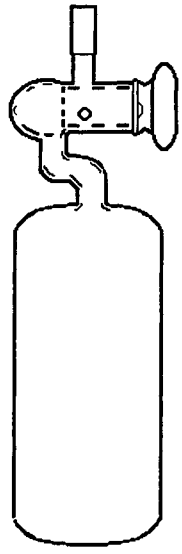

Figure 2.7 A 2 L flask with greased stopcock used for air sampling from 1975 to present.

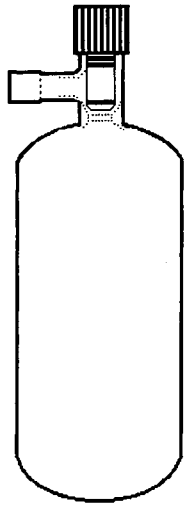

Figure 2.8 A 2 L flask with glass barreled valve (with Viton® o-ring seals) used for air sampling from 1992 to present.

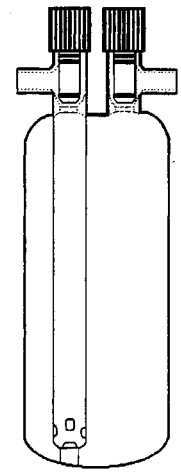

Figure 2.9 A 2 L flask with dual glass barreled valves (with Viton® o-ring seals) used for air sampling from 1993 to present.

2.1.2.3 CO_2 FLASK MEASUREMENTS AT ALERT

The CO_2 time series for flask samples collected at Alert using the three AES flask types is shown in Figure 2.10. Greased stopcock flasks were sampled at Alert from July 1975 to July 1997, evacuated o-ring flasks were sampled at Alert from August 1992, and dual valve pressurized flasks were sampled at Alert from June 1993. Flask samples are collected weekly at Alert, when the winds are greater than 1 m s^{-1} and from the clean air sector (the clean air sector excludes winds from the direction of the camp, i.e., 0-45 degrees).

Minimal scatter and no significant gaps are observed in the time series. The seasonal cycle and long-term trend for the greased stopcock data were determined using a forward stepwise harmonic regression (FSHR) technique [*Trivett et al.*, 1989]. The average growth rate is 1.52 ppm yr^{-1} for the period July 1975 to December 1994 [*Nakazawa et al.*, 1996]. The mean seasonal peak to peak amplitude is 15 ppm, with the seasonal decline in atmospheric CO_2 occurring in late May to early June, due to the transport of air from southern latitudes that is depleted in CO_2 from photosynthetic uptake.

Table 2-2 provides a summary of the Alert flask pair classifications for the three flask types. The highest percentage of field sampling problems occurred with the greased stopcock flasks.

The CO_2 time series for flask samples collected at Alert using the three AES flask types for the period 1992-1996 is shown in Figure 2.11. Differences can be seen in the CO_2 mixing ratios for the different flask types and sampling methodologies. In order to assess the quality of the data from the three different flask programs, the individual mixing ratios for each flask data set were compared to the corresponding Alert in situ CO_2 mixing ratios. (The Alert CO_2 in situ measurements are described in Section 2.1.1.2.)

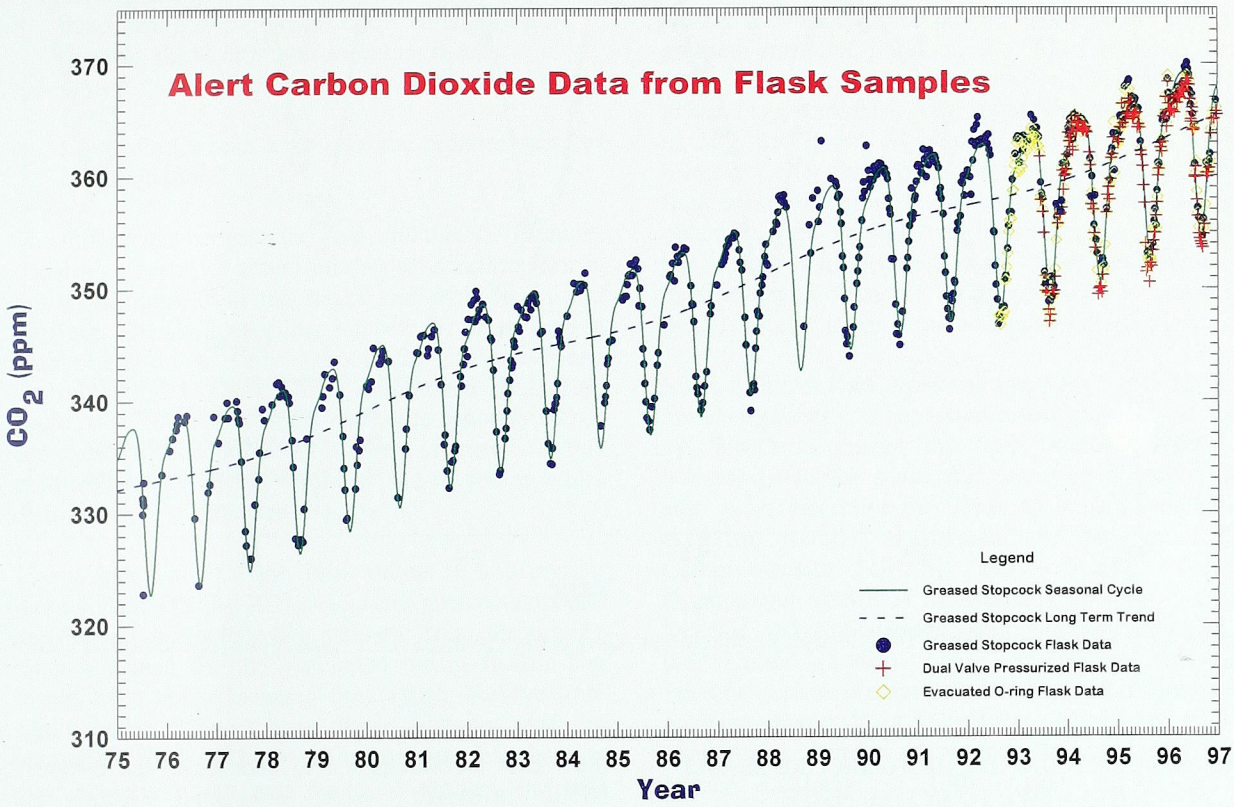

Figure 2.10 CO_2 time series of flask samples collected at Alert using the three AES flask types.

Table 2-2. Classification of AES weekly CO_2 flask pairs from Alert.

Flask Program	Sampling Period	%A Data	% I Data	% S Data	% L Data	Total # Pairs
2 L Evacuated Greased Stopcock	Mar. 1988 - 1996	73.5	2.9	20.7	2.9	377
2 L Evacuated O-Ring	Aug. 1992 - 1996	95.7	0.5	3.8	0	185
2 L Pressurized Dual Valve	Jun. 1993 - 1996	94.0	2.7	2.0	1.3	149

A - Data: Flask pair difference is <0.06 ppm.
I - Data: Incomplete pair (one flask is missing or broken).
S - Data: Flask pair difference is >0.06 ppm (suspected sampling problem).
L - Data: Flask pair difference is >0.06 ppm (laboratory analysis problem).

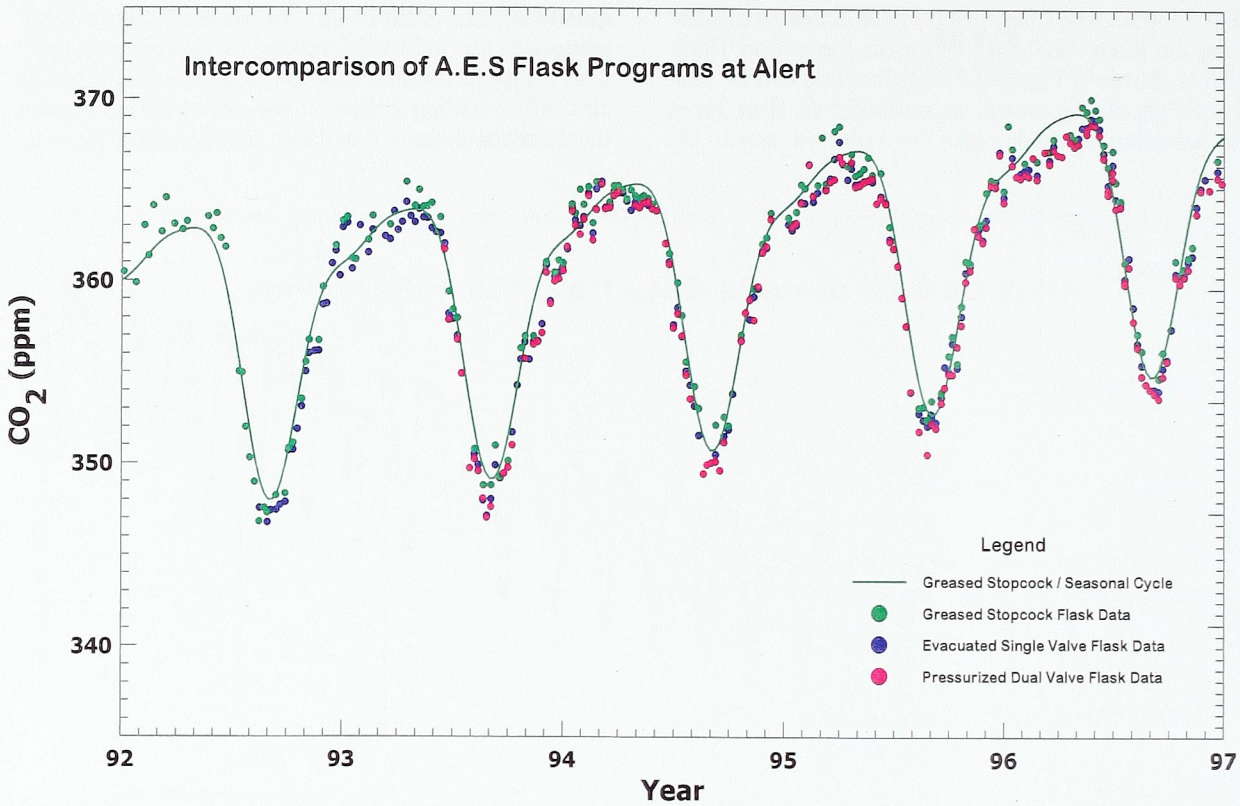

Figure 2.11 CO_2 time series of flask samples collected at Alert using the three AES flask types for the period 1992-1996.

2.1.2.4. Evaluation of Flask Programs Relative to In situ NDIR Program at Alert

Six-hour averages (ending at 6, 12, 18 and 24 GMT) and the corresponding standard deviations were calculated from the daily 5-minute NDIR CO_2 mixing ratio averages. Six-hour averages were selected for the evaluation to ensure that the flask sampling periods for all three flask programs were covered (flask sampling generally takes an afternoon to complete). The NDIR data were flagged for any irregularities (e.g., a vehicle at the site or adjustments to the analyser). A median analysis was performed on the standard deviation values of the 6-hourly NDIR averages to identify unstable mixing conditions; the resulting frequency distribution of standard deviations is given in Figure 2.12. An upper cut off value of 0.55 ppm was chosen. This is the upper quartile plus 1.5 times the inter-quartile range. Six-hourly averages with standard deviations greater than this were not used in the analysis. The resulting data set containing the individual 6-hourly NDIR values was then compared to the CO_2 mixing ratio values for the flask programs. The flask measurements are based on the same CO_2 scale as the NDIR measurements. In each case, the 6-hourly NDIR averages were subtracted from the corresponding flask pair averages. The frequency distributions for the differences between the three AES data sets and the NDIR are given in Figure 2.13 (a-e). A summary of these results is given in Table 2-3.

The results for the greased data set from 1988 to 1996 are given in Figure 2.13a. An analysis of the data revealed that the flask minus in situ values for the greased stopcock data were significantly greater for flask samples collected from 1993 to 1996. Thus, separate frequency distributions were plotted for the 1988-1992 greased stopcock data and for the 1993-1996 greased stopcock data. The average flask minus in situ value for the earlier data set (0.46 ± .75 ppm) is significantly lower than for the later data set (1.01 ± .72 ppm). This suggests that there is a significant contamination problem in the data after 1993. The data prior to 1993 have an average flask minus in situ value close to that of the other evacuated flask program, although the variability in the greased stopcock data is much higher than that for the o-ring data.

In general, the evacuated sampling methodologies (Figures 2.13 a, b, c and d) show the largest average flask minus in situ differences, the highest variability, and the largest number of positive outliers. The pressurized flasks produced results closest to the in situ measurements with the lowest variability. There are a number of possible explanations for these findings:

- evacuated flasks are more easily contaminated
- flushing flasks improves sampling results
- drying air reduces storage problems in o-ring flasks
- filling flasks from a sample line reduces operator contamination

The differences between the flask and the NDIR values could be a result of actual mixing ratio differences in the air sampled from the flasks and with the in situ analyser. The flask sampling interval for an evacuated grab sample is only about 20 seconds and approximately 5 minutes for a pressurized flask. This could be a problem when comparing to 6-hourly NDIR averages. If the differences were related to this problem, however, one would expect to see an equal distribution of differences about zero.

T-tests indicated that the flask minus in situ mixing ratios for the (1988-1992) evacuated, greased stopcock data were not significantly different from the mixing ratios obtained for the evacuated o-ring flasks. The results from both evacuated flask types, however, are significantly different than those obtained for the pressurized flasks. These results suggest that the two evacuated flask data sets could be merged, but that further studies are necessary before the pressurized flask data could be successfully merged with either data set.

This evaluation of AES flask sampling methodologies has clearly shown that the CO_2 mixing ratios from the pressurized flasks are closest to the in situ CO_2 mixing ratios, with the least amount of variability. It has also clearly shown that there is a serious problem with the greased stopcock flasks in the Alert program from 1993 onwards. For these reasons, the evacuated, greased stopcock flask program at Alert was terminated in July 1997. An adjustment will be made to the historical CO_2 data, obtained from greased stopcock flask samples, before it is merged with the CO_2 data, obtained from pressurized flask samples. This study has shown that different flask types and sampling methodologies do impact on the precision and accuracy of CO_2 mixing ratios obtained from flask samples.

Since different flask types and sampling methodologies are used globally, a concerted effort must be put forth by WMO to ensure the flask methodologies are intercompared for successful merging of global data sets. It is imperative that flask agencies cooperate to establish routine intercomparison programs. The Commonwealth Scientific and Industrial Research Organization (CSIRO) in Australia and the National Oceanic and Atmospheric Administration (NOAA) in the United States) have established such an intercomparison program, with both agencies analyzing air from shared flasks sampled at Cape Grim. AES is planning a similar intercomparison program with NOAA to begin in 1998, using NOAA 2.5 L pressurized flasks sampled at Alert.

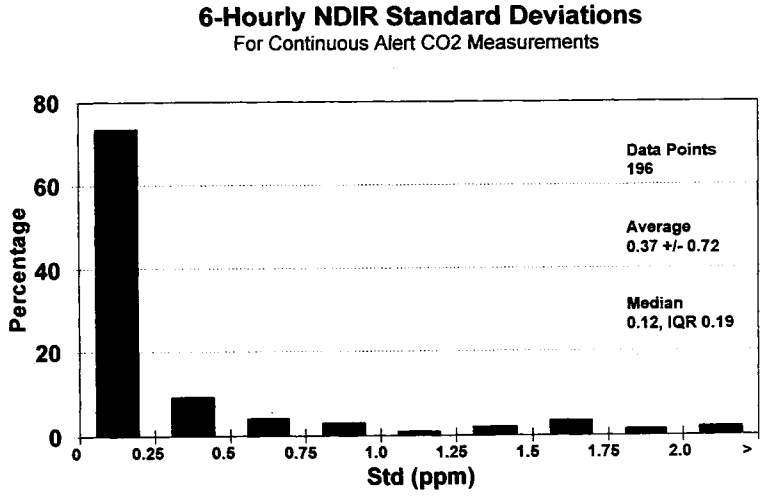

Figure 2.12 Six-hourly NDIR standard deviations for continuous CO_2 measurements at Alert.

Fig. 2.13a

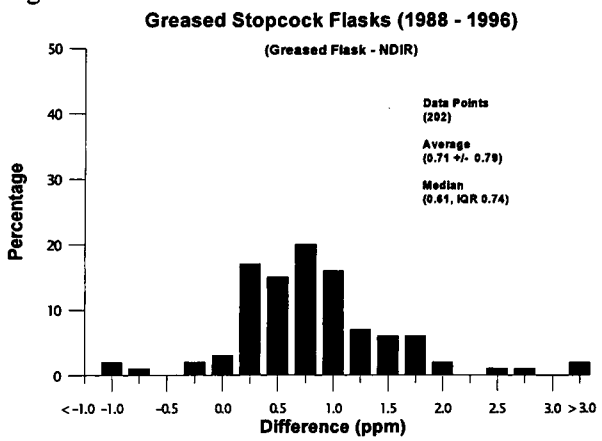

Fig. 2.13c

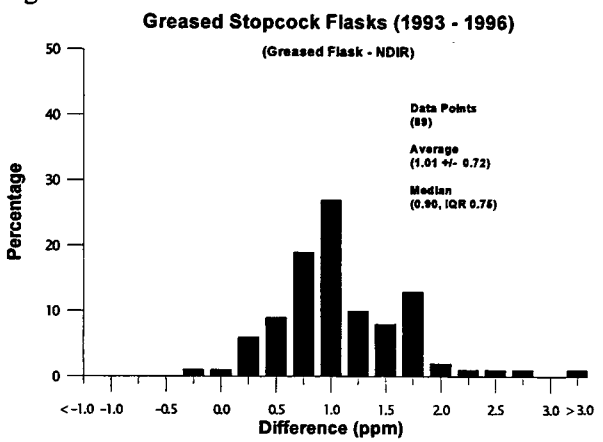

Fig. 2.13b

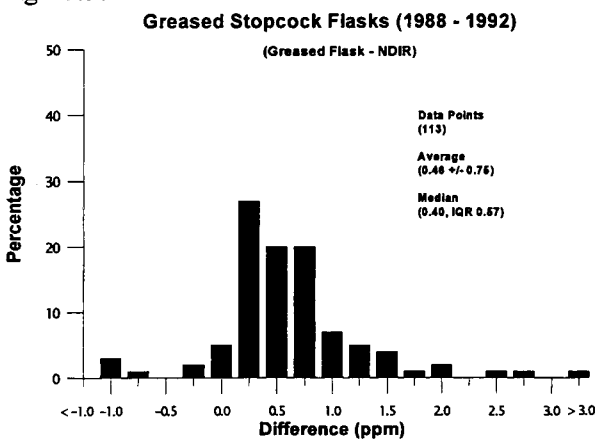

Fig. 2.13d

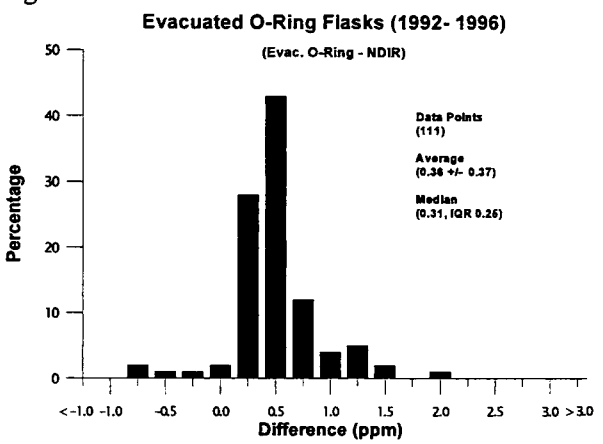

Fig. 2.13e

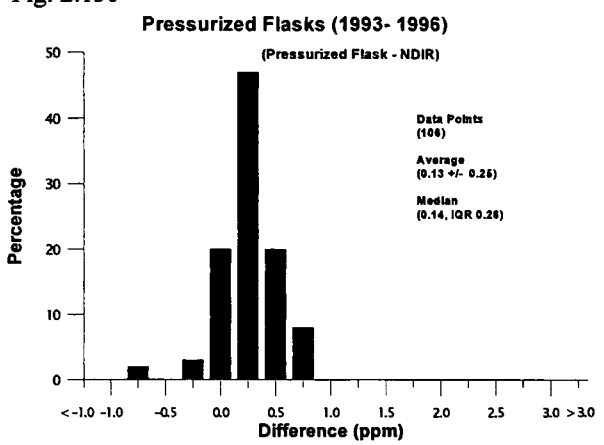

Figure 2.13 (a-e) Frequency distributions of the differences between the three AES flask data sets and the NDIR system.

Table 2-3. Comparison of in situ CO_2 measurements and flask sample CO_2 measurements from Alert.

Flask Program	Number of Data Points	[Flask – In Situ] Average (ppm)	[Flask – In Situ] Median (ppm)	[Flask – In Situ] IQR (ppm)
AES Greased Stopcock (1988-1996)	202	0.71 ± 0.79	0.61	0.74
AES Greased Stopcock (1988-1992)	113	0.46 ± 0.75	0.40	0.57
AES Greased Stopcock (1988-1996)	89	1.01 ± 0.72	0.90	0.75
AES Single Valve O-Ring (1992-1996)	111	0.36 ± 0.37	0.31	0.25
AES Dual Valve O-Ring (1993-1996)	106	0.13 ± 0.25	0.14	0.26

2.1.2.5 CO_2 FLASK MEASUREMENTS AT SABLE ISLAND

The CO_2 time series for flask samples collected at Sable Island using greased stopcock flasks is shown in Figure 2.14. Flask samples are collected weekly at Sable Island when the wind speeds are greater than 5 m s^{-1}. The flask samples are collected on the windward shore of the island to avoid sampling air that may be elevated in CO_2 mixing ratios from the sparse vegetation on the island. The practice of sampling on the windward shore was started in 1985. Prior to this, samples were taken at the same sampling location.

There are no significant gaps in the data set, however, in recent years the sampling frequency has decreased as a result of staff shortages on the island. Table 2-4 provides a summary of the flask pair classifications at Sable Island. Sampling problems affected a high percentage of the Sable data (36.2%). For the same flask type, this percentage is higher at Sable Island than at Alert, but similar at Cape St. James. It is possible that the samples at Sable Island are contaminated from elevated CO_2 mixing ratios from the island's vegetation or seal population, particularly for the period prior to 1985 when the samples were not strictly taken from the windward shore. It could also be a result of poor sampling practices by the staff on the island.

The seasonal cycle and long-term trend were determined using the FSHR technique as described earlier. There is a considerable scatter in the data set. The data collected at Sable Island shows larger scatter about its seasonal cycle than Alert and Cape St. James. The average standard deviation of the data from the seasonal is 3.11 ppm in the summer and 2.07 ppm in the winter [*Higuchi et al.*, 1995]. The average growth rate for Sable Island is 1.35 ppm yr^{-1} for the period from March 1975 to December 1994 [*Nakazawa et al.*, 1996]. A typical seasonal peak to peak amplitude at Sable Island is 15 ppm, with the seasonal decline in atmospheric CO_2 concentrations at Sable Island beginning in mid April, due to the transport of air from southern latitudes that is depleted in CO_2 from photosynthetic uptake [*Higuchi et al.*, 1995].

AES plans to implement the dual valve pressurized flasks at Sable Island in the summer of 1998. A one-year overlap with the greased stopcock flasks is planned. Steps are being taken by Sable Island administrative authorities to increase the number of staff on the island.

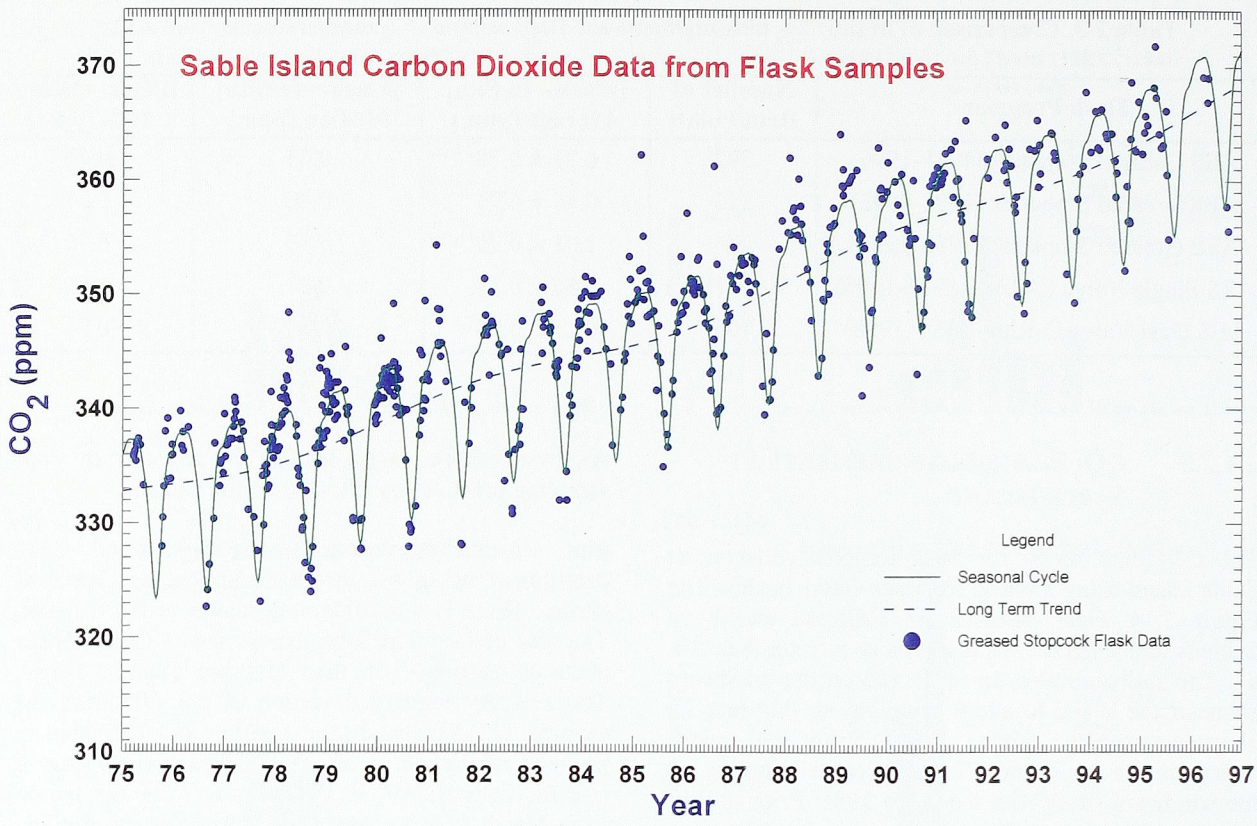

Figure 2.14 CO_2 time series of flask samples collected at Sable Island using greased stopcock flasks.

Table 2-4. Classification of AES weekly CO_2 flask pairs from Sable Island.

Flask Program	Sampling Period	%A Data	% I Data	% S Data	% L Data	Total # Pairs
2 L Evacuated Greased Stopcock	Mar. 1988 - 1996	55.3	7.1	36.2	1.3	309

A - Data: Flask pair difference is <0.06 ppm.
I - Data: Incomplete pair (one flask is missing or broken).
S - Data: Flask pair difference is >0.06 ppm (suspected sampling problem).
L - Data: Flask pair difference is >0.06 ppm (laboratory analysis problem).

2.1.2.6. CO_2 Flask Measurements at Cape St. James and Estevan Point

The CO_2 time series for flask samples collected at Cape St. James and Estevan Point is shown in Figure 2.15. Flask samples were collected weekly at Cape St. James from May 1979 to August 1992, using greased stopcock flasks. Samples were collected when winds were greater than 5 m s^{-1} and from a sampling sector between 180 to 300 degrees, in an attempt to sample air coming off the Pacific ocean. Logistical problems at Cape St. James resulted in significant gaps in the time series. A summary of the flask pair classifications for Cape St. James flask pairs is given in Table 2-5. Sampling problems affected a high percentage of the Cape St. James data (32.8%). This may have been the result of poor sampling techniques by Cape St. James staff.

Just prior to the termination of the flask program at Cape St. James, AES began sampling flasks at Estevan Point. AES intended to overlap the sampling at Cape St. James and Estevan Point for six months. This was not possible because the Cape St. James site was closed prematurely. Weekly sampling at Estevan Point began in June 1992 using evacuated o-ring flasks. Samples were collected on the rocky beach away from any vegetation when winds were greater than 5 m s^{-1} and from a sampling sector between 170 to 310 degrees for a minimum of 6 hours prior to sampling. During the spring months in particular, it was difficult for the operator to obtain samples because the wind direction was infrequently from the sector of interest. This resulted in gaps in the time series for those months. In May 1997, the sampling protocol was changed to include samples from other sectors if it was not possible to sample from the sector of interest. AES implemented dual valve pressurized flasks at Estevan Point in January 1993. A sampling line was extended from a mast on top of the lighthouse at a height of 39 metres. These flasks are sampled twice per week, using the same sampling criteria as outlined above.

The seasonal cycle and long-term trend were determined using the forward stepwise harmonic regression (FSHR) technique combining the Cape St. James (greased stopcock flasks) and Estevan Point (pressurized flasks) mixing ratios. AES plans to use the intercomparison results from the Alert flask study to adjust the Cape St. James greased stopcock mixing ratios before it can be correctly merged with the Estevan Point pressurized flasks. The average growth rate for the Cape St. James greased stopcock flask data set is 1.34 ppm yr^{-1} for the period May 1979-December 1994 [*Nakazawa et al.*, 1996]. The average seasonal peak to peak amplitude was 13 ppm with the minimum occurring during the latter half of August, due to the transport of air from southern latitudes that is depleted in CO_2 from photosynthetic uptake.

Table 2-5. Classification of AES weekly CO_2 flask pairs from Cape St. James and Estevan Point.

Flask Program	Sampling Period	%A Data	% I Data	% S Data	% L Data	Total # Pairs
2 L Evacuated Greased Stopcock (Cape St. James)	Mar. 1988 – 1992	56.1	9.6	32.8	1.5	198
2 L Evacuated O-Ring (Estevan Point)	Aug. 1992 – 1996	89.5	0	8.1	2.3	86
2 L Pressurized Dual Valve (Estevan Point)	Jun. 1993 – 1996	89.9	1.1	9.0	0	89

A - Data: Flask pair difference is <0.06 ppm.
I - Data: Incomplete pair (one flask is missing or broken).
S - Data: Flask pair difference is >0.06 ppm (suspected sampling problem).
L - Data: Flask pair difference is >0.06 ppm (laboratory analysis problem).

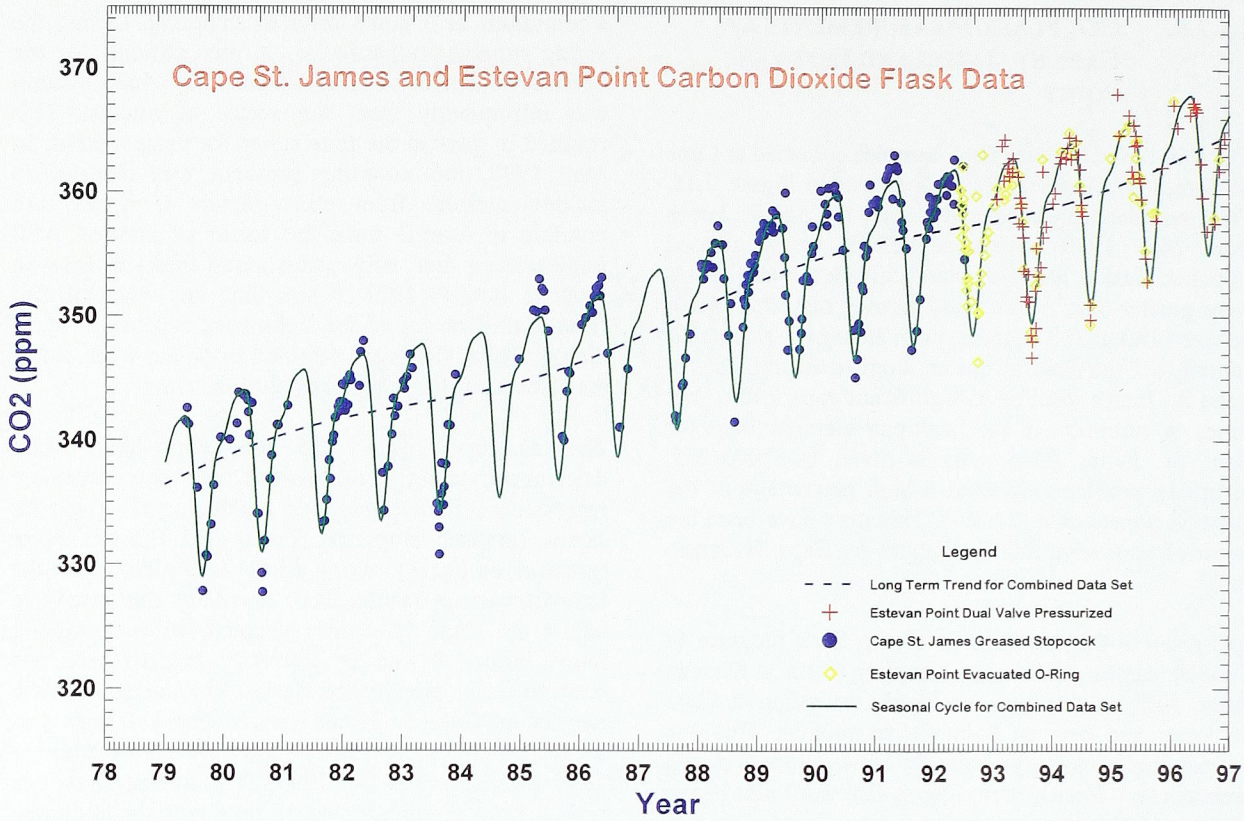

Figure 2.15 CO_2 time series of flask samples collected at Cape St. James and Estevan Point.

2.1.2.7. REFERENCES

Higuchi, K. V. Hudec, N.B.A. Trivett, C.W. Yuen, D. Chan and C.S. Wong, 1995: A statistical comparison of the CO_2 measurements at Cape St. James and Station "P", Canada. Tellus, **47B**, 4-16.

Komhyr, W.D. and L.S. Waterman, 1983: Semiautomatic nondispersive infrared analyzer apparatus for CO_2 air sample analyses. J. Geophys. Res., **88**, 1315 – 1322.

Nakazawa, T., M. Ishizawa, K. Higuchi and N.B.A. Trivett, 1997: Two curve fitting methods applied to CO_2 data. EnvironMetrics, Vol. 8, 197-218.

Trivett, N.B.A., K. Higuchi, and S. Symington, 1989: Trends and seasonal cycles of atmospheric CO_2 over Alert, Sable Island, and Cape St. James as analyzed by forward selection multiple regression technique. The statistical treatment of CO_2 data records. (ed. W.P. Elliot) NOAA Technical Memorandum ERL-173.

Wong, C.S., Y-H. Chan, J.S. Page, and R.D. Bellegay, 1984: Trends of atmospheric CO_2 over Canadian WMO background stations at Ocean Weather Station P, Sable Island, and Alert. J. Geophys. Res., **89**, 9527–9539.

2.1.3. MEASUREMENTS OF STABLE ISOTOPES OF CO_2

Fred Hopper, Ann-Lise Norman, Darrell Ernst, Alina Chivelescu, Douglas E.J. Worthy, Erika Wallgren and Michele K. Ernst

2.1.3.1. BACKGROUND

The stable isotope composition of gases such as CO_2 contain information indicative of sources of the gases and/or biogeochemical cycling processes. High precision measurements are necessary to distinguish CO_2 fluxes from the ocean ($\Delta\delta^{13}C$ = 0.005 ‰ / ppmv) and the terrestrial biosphere ($\Delta\delta^{13}C$ = 0.05 ‰ / ppmv). Accurate atmospheric isotope data will improve the ability to test and constrain general circulation models, particularly those linking the hydrological and atmospheric cycles. A number of low time resolution sampling programs (2-4 weeks) are currently in operation at Alert to support isotope analyses by various laboratories, but higher time resolution and more accurate data, particularly for $\delta^{18}O$, are desirable to better understand variability in CO_2 concentration due to changes in biomass respiration within the Northern Hemisphere.

2.1.3.2. INTERCOMPARISON RESULTS

The isotope composition of CO_2 in flask air collected at Alert and analysed by the AES stable isotope laboratory is shown in Figures 2.16 and 2.17. These data are compared with similar measurements performed by CSIRO for the same air samples. Flasks are shipped from Alert to Australia where a small portion of the air is removed for trace gas concentration measurements and isotope analysis. Flasks containing residual air sample are returned to AES where CO_2 is collected for a second isotopic analysis. Routine sample analysis began in late 1996 and data are only beginning to accumulate. Very good agreement is normally observed between initial results from paired flasks and between AES and CSIRO data (Figures 2.16 and 2.17). However, there are occasional significant deviations, the cause of which is currently under investigation.

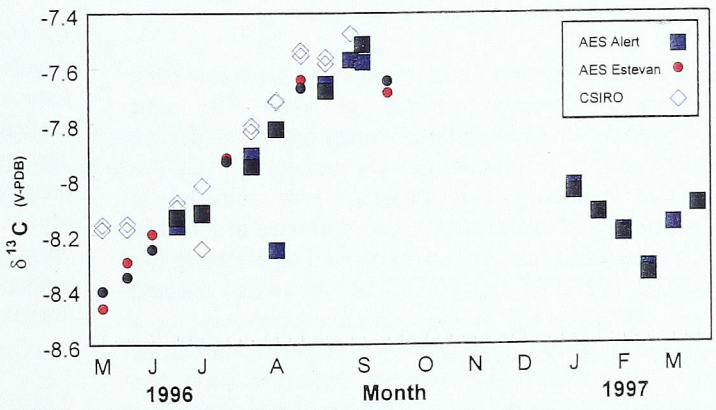

Figure 2.16 Intercomparison of $\delta^{13}C$ values measured by CSIRO and AES programs for CO_2 in air at Alert and Estevan Point. (The black dots are the pairs to the red dots. Pairs of samples were measured every two weeks.)

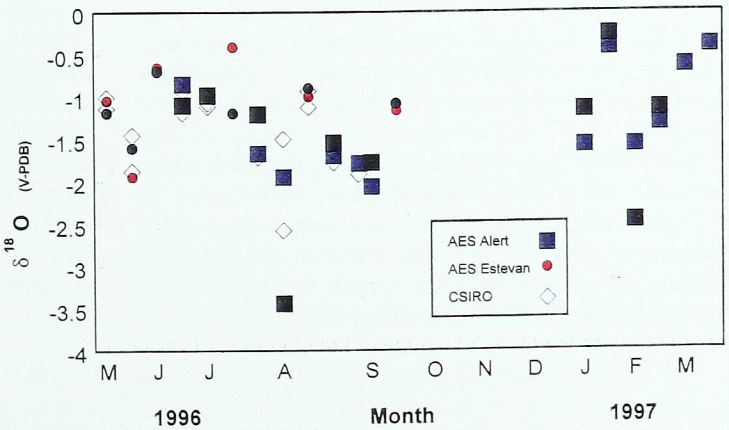

Figure 2.17 Intercomparison of $\delta^{18}O$ values measured by CSIRO and AES programs for CO_2 in air at Alert and Estevan Point. (The black dots are the pairs to the red dots. Pairs of samples were measured every two weeks.)

2.2. METHANE

Douglas E.J. Worthy and Michele K. Ernst

2.2.1. BACKGROUND

Over the past two decades, it has become evident that methane is increasing in the atmosphere [*Steele et al.*, 1992] although the rate of increase has diminished over the past few years [*Dlugokencky et al.*, 1994]. Methane is important in the atmosphere as a greenhouse gas, as a strong player in the balance of chemical reactions that influence OH, ozone and other greenhouse gases, and as a source of water vapour in the upper atmosphere [*Cicerone and Oremland*, 1988]. Since increased levels of methane can potentially have an impact on the global climate and affect the global chemistry of the atmosphere, there has been considerable interest in the causes of the increase as well as the source/sink relationship for the atmosphere, ocean and biosphere. Atmospheric methane observations from air sampling networks can be used to estimate the magnitudes of these sources and sinks.

Atmospheric observations of methane are routinely measured at the air chemistry observatories at Alert and Fraserdale. The measurement programs at these two sites are addressed separately below.

There are currently three separate programs that measure atmospheric methane at Alert. The most elaborate is the continuous measurement program, which uses an automated gas chromatograph (GC) to measure methane. This program was initiated in November 1987. Continuous measurements of methane were also made at Alert from a military transmitter building (82°27'N, 62°30'W; 142 m ASL) located about 500 m north of the current observatory for a three week period in April, 1986, as part of an Arctic Haze study. The measurements from the study are published in *Trivett et al.* [1989]. The two other programs are a weekly flask measurement program, which operates as part of the NOAA/CMDL Carbon Cycle Group cooperative flask air sampling network, and a methane stable carbon isotope program. The latter is a cooperative experiment between AES and the University of Heidelberg in Germany. The NOAA/CMDL flask sampling program was initiated in June 1985. Details about this program can be found in *Dlugokencky et al.* [1994a]. The methane stable carbon isotope program at Alert uses ambient air collected continuously over a two week period in high volume bags made of polyethylene coated weldable aluminium foil. The samples are approximately 1.5 m^3 at STP and are subsequently transferred to 10 L aluminium cylinders using a RIX oil-free compressor. The cylinders are first shipped to AES in Toronto, Ontario, for methane mixing ratio analysis and then to the University of Heidelberg for isotope analysis. The methane stable carbon isotope program was initiated in August 1990. More information about the program can be found in Section 5.1.

An in situ methane measurement program was initiated in December 1990 at Fraserdale, as part of the Canadian Northern Wetlands Study to evaluate wetland methane emissions from the Hudson Bay Lowland. Due to funding cuts, the observatory was closed in December 1996. The observatory, however, has since been deemed vital and was re-opened in the spring of 1998. The methane data from Fraserdale have proven to be extremely valuable scientifically. The uniqueness of the data has demonstrated the need for measurements at continental sites because atmospheric measurements from remote and coastal sites are not enough if our understanding of the methane cycle is to be improved. Details of the measurements made at Fraserdale are published in *Worthy et al.*, [1998a] and *Worthy et al.*, [1998b]. A brief summary of the results is given in Section 2.2.3.

In 1997, an automated flask analysis system was developed and the flask samples from Alert, NWT, and Estevan Point, BC, are now being analyzed for methane, nitrous oxide, sulphur hexafluoride and carbon monoxide. Because the GC flask measurement program is relatively new, it is not addressed in this report. The technical details of the in situ gas chromatographic system at Alert and Fraserdale, as well as the calibration scale and measurement protocol, are given in Section 3.2.

2.2.2. IN SITU CH_4 MEASUREMENTS AT ALERT

The time series of 6-hourly averaged methane concentrations obtained at Alert between January 1988 and December 1997 is shown in Figure 2.18 along with the annual cycle and long-term trend. The data show significant seasonal variations and an increasing trend along with high frequency variability most noticeably during winter. The annual cycle and long-term trend were determined using a digital filter technique described by *Nakazawa et al.* [1997].

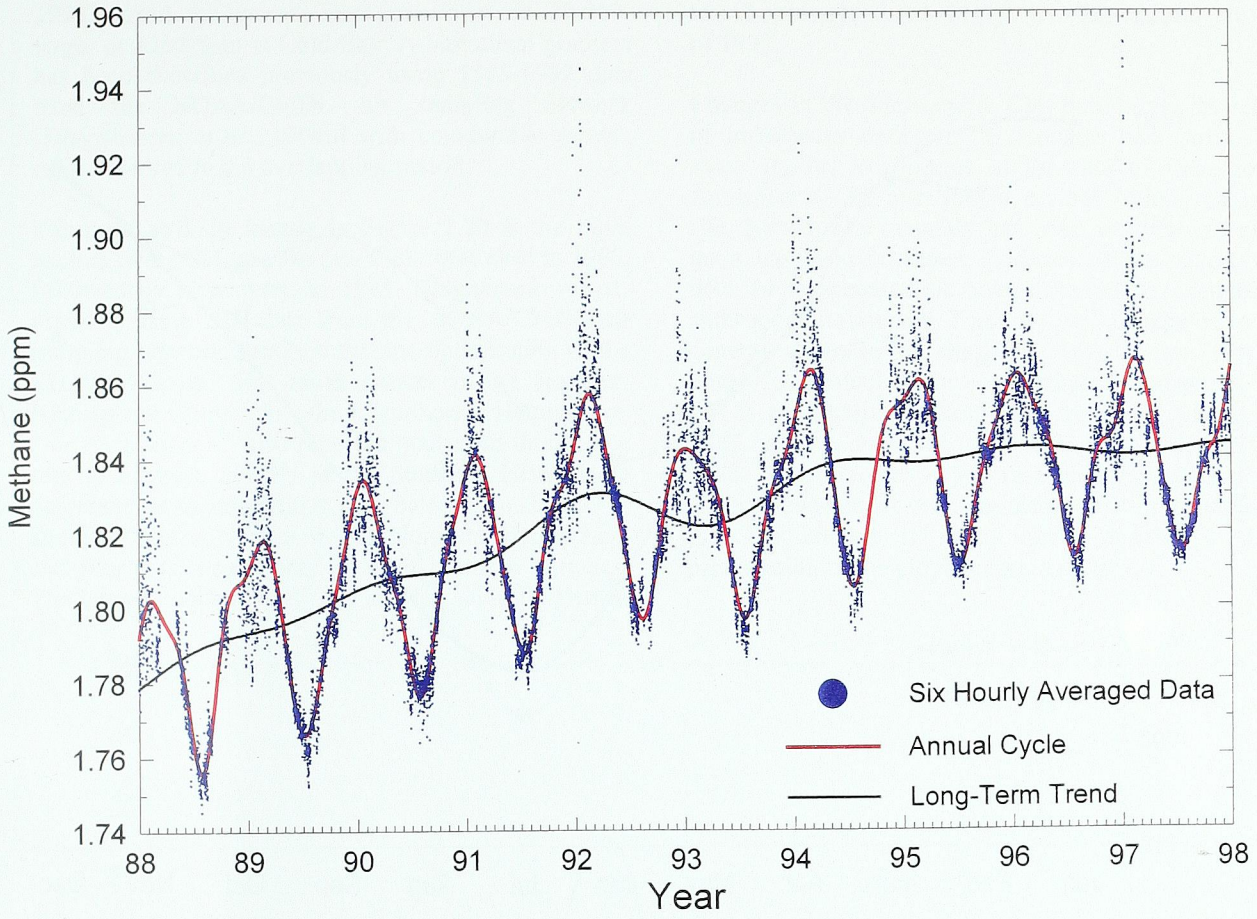

Figure 2.18 Time series of methane from Alert averaged over six hours along with the annual cycle and long-term trend. Large gaps in the record are due to system malfunctions.

Data obtained between February 24 and November 18, 1988, have been corrected for a calibration error, while the data obtained between May 4 and October 24, 1989, have been corrected for incomplete drying of the sample air. A glass tube (6 inches long and 0.5 inch diameter (o.d.)), filled with P_2O_5 had been placed in the sample line to remove water vapour between May 4 and October 24, 1989. However, when the carbon dioxide results from the NDIR were compared with the carbon dioxide measurements from the GC it became evident that the chemical trap was being saturated within 4 to 12 hours after the chemical absorbent was replaced. (The chemical absorbent was typically being replaced on a weekly basis.) The intercomparison between the CO_2 values from both the NDIR and the GC determined when the saturation point approximately occurred. All the CH_4 (and CO_2) data were then corrected using the hourly dew point data. The correction was validated by comparing the corrected CO_2 values from the GC with the CO_2 values from the NDIR. The methane data were then corrected using the same procedure.

The temporal changes in the concentration of atmospheric methane in the Arctic atmosphere reflect the source and sink strengths in the lower latitudes. With the exception of some areas in Siberia and northern Europe, there is very little industrial development north of 60° N to significantly modify the atmospheric concentration of methane in the high Arctic atmosphere. Given the lack of significant sources, especially in the winter, it is clear that long-range atmospheric transport plays an important role in the appearance and cycles of methane. The high frequency variability (episodes) seen in Figure 2.18 is primarily due to rapid long-range transport across the North Pole from Siberia and Eurasia to Alert [*Worthy et al.*, 1994]. Episodes also occur with rapid transport from the eastern Northern Hemisphere along the eastern side of the Greenland ice cap.

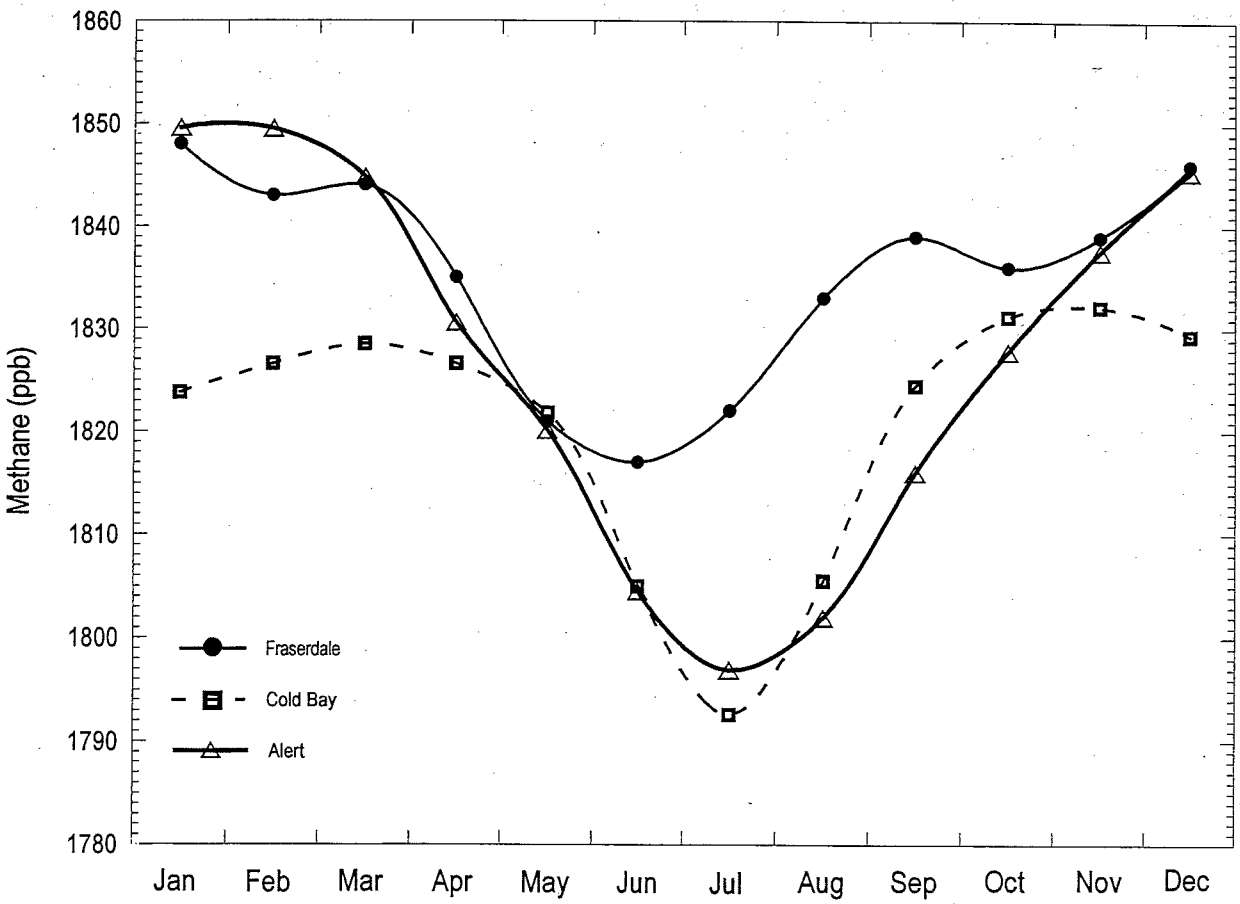

Figure 2.19 Mean annual cycle of methane observed at Alert, Fraserdale (only diurnal minimum data) and Cold Bay [*Dlugokencky et al.*, 1994b and unpublished data] determined using monthly averaged data for the period 1990-1995.

The mean annual CH_4 cycle at Alert has a peak-to-peak amplitude of about 55 ppb with the minimum occurring in August and the maximum occurring in February (see Figure 2.19). The characteristics of the mean CH_4 annual cycle at Alert are similar to those observed at other northern high latitude background monitoring sites such as Cold Bay, Alaska [*Dlugokencky et al.*, 1994b] (see Figure 2.19). The background annual cycle is driven by the seasonality of CH_4 sources and sinks in combination with a seasonally varying meridional circulation pattern. The high CH_4 observed at Alert during the winter months is caused by a negligible OH sink and transport of polluted air modified by CH_4 emissions (associated with fossil fuel use) in Siberia and Eurasia. During the winter, Alert, and the Arctic in general, is within a shallow stratified mixed layer. Anthropogenic pollution is transported and mixed into a relatively small volume of the atmosphere. During the spring, CH_4 begins to drop due to an increasing OH sink and dilution of northern air masses with air masses from southern latitudes and aloft that have lower CH_4 concentrations. During the summer, the tropospheric OH sink is strongest and produces a minimum in the annual CH_4 cycle in July. By late August and September, the CH_4 begins to increase as the effectiveness of the OH sink decreases, perhaps in combination with transport of air from lower latitudes [*Fung et al.*, 1991]. The timing of the seasonal minimum at Alert varies from year to year by as much as six weeks. This is believed to be due to interannual variability in CH_4 emissions from the northern wetlands.

The CH_4 growth rate observed at Alert, Fraserdale and Cold Bay is shown in Figure 2.20. The average trend between 1990-1995 (the period when data are available for all three sites) for Alert, Fraserdale and Cold Bay was 6.3 ppb yr^{-1}, 6.2 ppb yr^{-1} and 5.1 ppb yr^{-1}, respectively. Changes in the growth rate at Alert and Cold Bay are correlated temporally, but in the 1990-

1995 period the growth rate variations are 20-30% larger at Alert than at Cold Bay. A latitudinal gradient has been described previously using 1983-1992 data from the NOAA/CMDL air sampling network [*Dlugokencky et al.*, 1994b] with comparable growth rates observed in the overlapping period.

The most striking feature in Figure 2.20 is the rapid decline of the CH_4 growth rate at all three sites in 1992, followed by a recovery in 1993. *Dlugokencky et al.*, [1994a], using CH_4 data from the NOAA/CMDL air sampling network, reported that the deceleration of the CH_4 growth rate was much greater in the Northern Hemisphere than in the Southern Hemisphere. *Dlugokencky et al.* also reported that, even though the rate of increase in CH_4 in the Southern Hemisphere decreased, at no point did it drop below zero. The 1992 anomaly was only seen in the Northern Hemisphere and was most pronounced in high northern latitudes. The largest anomaly was seen at Alert with the growth rate dropping to about -14 ppb yr^{-1} CH_4 towards the end of 1992.

Changes in the atmospheric CH_4 burden are the result of imbalances between CH_4 sources and sinks. The same applies to changes in the rate of increase of atmospheric CH_4 over longer periods. While the 1992 CH_4 growth rate anomaly has been well documented, there has been no direct evidence of the cause(s) to date. Most speculations have centered on changes in anthropogenic sources. This may well be related to the general decrease of the CH_4 growth rate that is observed, particularly in the Northern Hemisphere, but this is not likely to account for the observed drop in 1992 and the quick recovery during the latter half of 1993. The fact that other trace gases, such as CO_2, experienced similar drops in their growth rate suggests that the change is more likely due to a short perturbation of the global climate system.

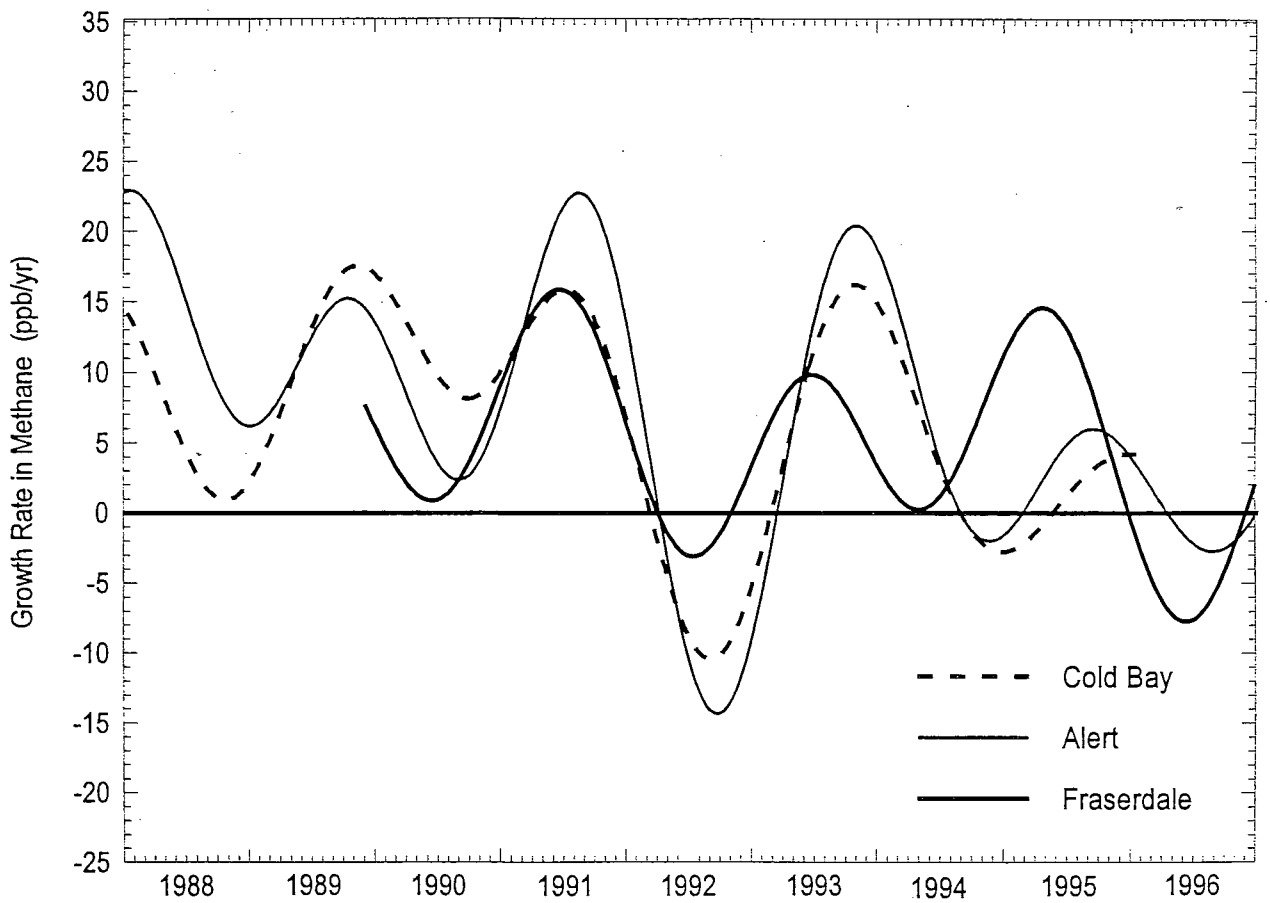

Figure 2.20 Growth rate of methane observed at Alert, Fraserdale and Cold Bay [*Dlugokencky et al.*, 1994b and unpublished data].

2.2.3. In Situ CH_4 Measurements at Fraserdale

The time series of hourly-averaged atmospheric CH_4 mixing ratios from Fraserdale, Ontario, for the period January 1, 1990, to December 7, 1996, is shown in Figure 2.21. The data show significant seasonal variations and an increasing trend along with high frequency variability (similar to what was observed at Alert, NWT).

During the winter, the CH_4 time series from Fraserdale often matches the short-term variability observed at Alert [*Worthy et al.*, 1998a]. As mentioned previously in Section 1.2.2, during the winter, Fraserdale is frequently under the influence of cold stratified air masses originating in the high Arctic. These air masses can encompass much of Eurasia and Canada and can accumulate significant loadings of pollutant gases and aerosols. During their transit in the cold stable Arctic atmosphere, they likely experience little vertical mixing. This has also been shown in many other studies [*Trivett et al.*, 1989; *Hopper et al.*, 1994; *Conway et al.*, 1989]. With the photochemical removal of CH_4 essentially being non-existent over high northern latitudes during the wintertime, the same air can be transported out of the high Arctic to Fraserdale without significant modification of its chemical composition. A detailed example of this transport phenomena is described in *Worthy et al.*, [1998a].

The variability in observed CH_4 during the summer is dominated by diurnal cycles (Figure 2.21). Under strong solar heating during the day the near surface mixed layer is unstable and generally well mixed throughout the boundary layer. At night, the radiation loss at the ground level leads to a cooling of the atmosphere at the surface, which gives rise to a shallow stable layer. The increase in CH_4 during the night is due to suppressed vertical mixing under the inversion. The magnitude of this nocturnal increase is variable and depends on the strength of the nocturnal inversion and the regional CH_4 source strength. Due to enhanced vertical mixing during the day, CH_4 is diluted through the rise of the boundary layer height up to a couple of thousand metres or more.

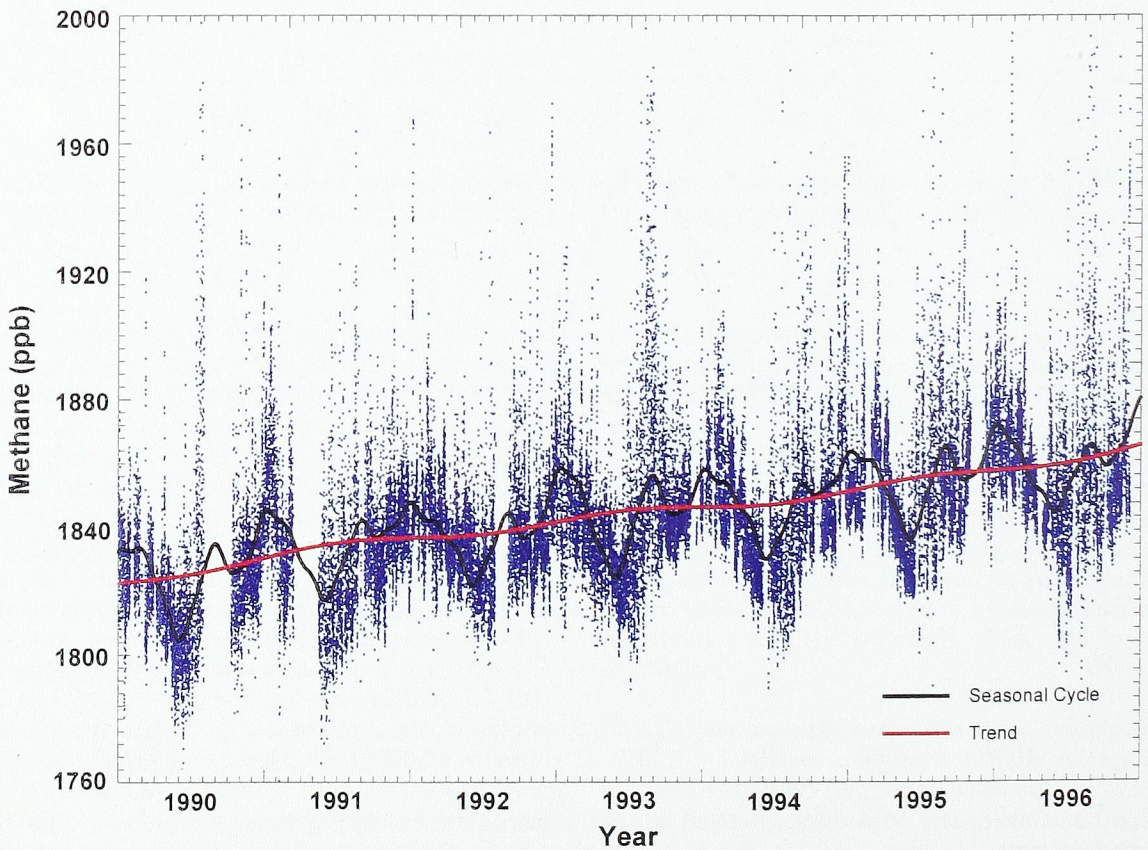

Figure 2.21 Time series of methane from Fraserdale averaged over one hour along with the seasonal cycle and long term trend. Large gaps in the record are due to system malfunctions.

Mean diurnal cycles of CH_4 are shown in Figure 2.22 for the months of January, May, July, August and October, determined from hourly averaged data for the period 1990-1996. Evident from Figure 2.22 is that the diurnal cycles are strongly dependent upon the season; during the wintertime the diurnal cycle is insignificant, however, by May the diurnal cycle begins to develop and reaches a maximum in August when emissions for CH_4 are highest. During the summertime, CH_4 mixing ratios have maximum values at around 0600 to 0800 local standard time in the morning and then decrease rapidly to reach a minimum in the afternoon at around 1600 to 1800.

There can be substantial variability in the diurnal cycle from day to day. During nights with low wind speed, increases in CH_4 under the nocturnal inversion are particularly large (up to 150 ppb) while high wind speeds suppress the build-up of strong inversions. In general, these nocturnal CH_4 accumulations are several times larger than the mean seasonal cycle amplitudes of about 35 ppb observed in background air at northern latitudes similar to Fraserdale. As well, the diurnal variability in CH_4 is often large enough to mask the CH_4 increase due to the arrival of air from the southern anthropogenic sectors. Further information on the seasonal cycle, trend and inter-annual variations observed at Fraserdale, as well factors that affect methane variability including diurnal cycles and long-range transport is provided in detail in *Worthy et al.*, [1998a].

From the preceding discussion, it is clear that measurements during the night are not representative of a large well-mixed volume of the lower troposphere and should not be included in the calculation of the large scale representative mean annual cycle and trend in CH_4 for Fraserdale. Excluding nighttime data is even more important when comparing the mean annual CH_4 cycle at Fraserdale with that at stations in other global baseline observing networks. The vertical homogeneity of the air has been evaluated at Fraserdale [*Worthy et al.*, 1998a] and the results show that air sampled during the afternoon from the 40 m level is representative of air that is well-mixed throughout the entire convective boundary layer.

Figure 2.19 shows the comparison between the mean CH_4 annual cycle at Fraserdale calculated using diurnal minima data (1700-1900 LST) and the mean annual cycle observed at Alert and Cold Bay. Cold Bay is the closest North American background CH_4 monitoring site (in latitude) to Fraserdale. The mean annual CH_4 cycle at Fraserdale and Alert was determined by averaging monthly data for the period 1990-1995. For each site, a spline curve was fit through the twelve monthly mean values to illustrate the annual cycle more clearly. The mean CH_4 annual cycle for Cold Bay was determined using the same procedure by averaging monthly values from the NOAA/CMDL air sampling network for data collected from 1990 to 1995 [*Dlugokencky et al.*, 1994b, and unpublished results].

Mean annual cycles observed at Fraserdale and Alert are similar during the wintertime and springtime (October to May). As discussed earlier, this would be expected since Fraserdale is essentially under the influence of the same northern air masses as Alert. In early summer, emissions of CH_4 from areas to the north of Fraserdale increase, leading to a secondary peak in late summer at Fraserdale. On average, the secondary maximum at Fraserdale occurs in September, and the minimum in the annual cycle occurs in June. These characteristics of the annual cycle at Alert are similar to those observed at many other northern high latitude background sites [*Dlugokencky et al.*, 1994b].

In the winter, CH_4 monthly means at Alert and Fraserdale are higher than at Cold Bay by about 25 ppb. By contrast, CH_4 monthly means at Alert and at Cold Bay are similar in the summer. This similarity, combined with the predominantly northern air flow at Fraserdale, shows that the higher CH_4 observed in the summer at Fraserdale relative to Alert (which appears as a secondary maximum in the Fraserdale annual cycle) must be the result of significant emission sources between Alert and Fraserdale. The sources that could potentially account for this substantial increase during transport from Alert to Fraserdale are oceans (including Hudson Bay), tundra, and the northern wetlands (principally HBL). However, global CH_4 emissions from oceans are small and the summer increase in CH_4 at Fraserdale begins when most tundra areas are still snow-covered, and extends beyond the time when Arctic and sub-Arctic tundra are likely to have been frozen and snow-covered for some time. In addition, it has been shown elsewhere [*Harris et al.*, 1994] with aircraft measurements that the mid-continental region is characterized by relatively uniform mixing ratios of CH_4 and CO and that the emissions of CH_4 from the HBL are the primary source for enhanced CH_4 under the boundary layer. Therefore, the HBL, which is well documented as a source of CH_4 [*Roulet et al.*, 1992], is the most likely cause of the secondary CH_4 maximum observed at Fraserdale in the summer.

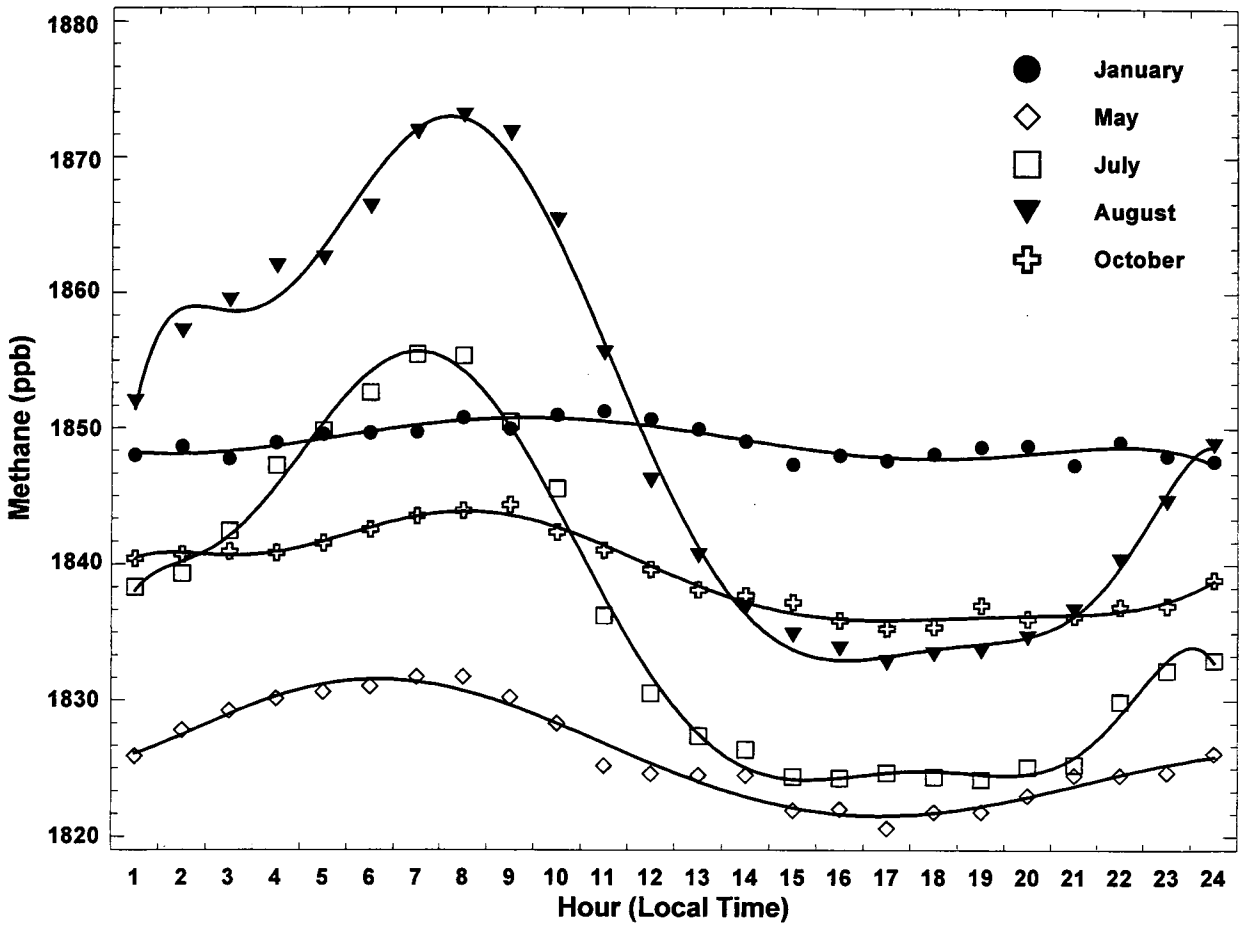

Figure 2.22 Average diurnal cycles of CH_4 for January, May, July, August and October determined from hourly averaged data for the period 1990-1996.

2.2.3.1 METHANE SOURCE ESTIMATE OF THE HUDSON BAY LOWLAND USING DATA FROM ALERT AND FRASERDALE

Typically, there are more than 10 days each month when air parcels reach Fraserdale from high latitudes after crossing some portion of the Hudson Bay Lowland (HBL). During the biologically active summer months, CH_4 mixing ratios at Fraserdale relative to CH_4 mixing ratios observed at Alert, frequently increase in proportion to the residence time of air parcels over the HBL. This observed correlation between residence time and CH_4 increase suggested the use of the atmospheric boundary layer as an integrating medium for emissions from regional ground-level sources. A conceptually simple approach was used to calculate the methane flux F for days with northerly flow across the HBL:

$$F = h * \Delta[CH_4] / \tau \qquad (1)$$

Daily differences in CH_4 concentration ($\Delta[CH_4]$) were calculated from continuous ambient measurements at Fraserdale using only afternoon observations when the boundary layer was normally well mixed and the air masses were at Alert five days earlier. (Five days is the typical transport time for air masses to arrive at Fraserdale from the high Arctic.) The residence time τ of an air parcel reaching Fraserdale at the 925 mb level (typically 1.5 days) was determined from its path over the HBL as calculated by a Lagrangian back-trajectory model. Monthly mean afternoon mixing heights were used as estimates of the atmospheric boundary layer thickness h. This approach has the advantage of integrating net emissions from a large area with substantial spatial inhomogeneities in emission strength. Net emissions are usually estimated using static chambers but extrapolation over large areas involves large uncertainties because point flux measurements can vary by several orders of magnitude

even within the same ecosystem. Our regional boundary layer integration approach for quantitative large-scale flux estimates also has uncertainties due to a number of assumptions. The most important of these assumptions are as follows:

1. No significant CH_4 emission source exists between Fraserdale and Alert other than the HBL.
2. The surface CH_4 mixing ratios at Fraserdale in the afternoon are representative of a homogeneous boundary layer.
3. Mean climatological mixing heights can be used in individual years.
4. Insignificant losses occur from the boundary layer to the free troposphere.

The validity of the first two assumptions has been addressed in *Worthy et al.*, [1998a]. The validity of the third assumption can be supported by the fact that the variability in monthly mean mixing heights from year to year is small. Even if this were not the case, higher mixing heights are generally associated with higher temperatures, which would lead to smaller flux estimates for warmer years. If the use of monthly mean mixing heights does introduce a small error, it would be towards an underestimate of the temperature sensitivity of northern wetland emissions. The uncertainty associated with neglecting diffusive or convective losses from the boundary layer to the free atmosphere is difficult to quantify, but other studies suggest that it is in the range of 10 to 20%. The total HBL emissions calculated here have not been corrected for this omission, and hence are likely lower by this amount. This error also affects the temperature sensitivity estimate because entrainment losses are proportional to the rate of development of the afternoon convective boundary layer *dh/dt*. This rate will be higher in warmer years, again potentially underestimating the temperature sensitivity of CH_4 fluxes from the HBL.

The monthly mean fluxes from this study are consistent with results from other wetland studies, although there is substantial variability in individual months (see Figure 2.23a). The negative fluxes determined for February and March are within the uncertainties for the monthly flux estimates. Results for the biologically active summer months compare favourably with independent empirical estimates of HBL fluxes [*Roulet et al.*, 1992]. This provides some measure of assurance that the assumptions for the regional boundary layer integration approach were reasonable and did not introduce large errors.

These emission rates for the HBL are much lower than many empirical flux measurements observed at other northern wetland sites and are 3 to 12 times lower than the estimates derived from recent global CH_4 models (listed in *Worthy et al.*, 1998) for all northern wetlands. Of greater importance, however, is that the flux can vary up to 50% from one year to the next (see Figure 2.23b). This is likely to be a characteristic of all northern wetlands shared through common climatic controls. The most important environmental parameters controlling production and release of CH_4 from wetlands to the atmosphere are the availability of organic carbon to bacteria, plant cover, water table depth, and soil temperature. Of these, soil temperature and water table depth, or parameters related to them, are likely to be the most sensitive to inter-annual changes caused by climate variability. Air temperatures from Fraserdale and soil temperatures from Kapuskasing (located 100 km southwest of Fraserdale) show similar correlations when compared to the monthly mean CH_4 fluxes calculated by the regional boundary layer integration approach. Less scatter is observed in the relationship between flux and air temperature because air temperature is more spatially representative of regional mean temperatures throughout the HBL than localized soil temperatures at individual sites.

Substantial year-to-year variations in air temperatures are observed at Fraserdale (see Figure 2.23b). These seasonal temperature anomalies are not a local effect but are observed over a large area of central Canada and are correlated with changes in seasonal CH_4 flux from the HBL (see Figure 2.23b). Mean CH_4 fluxes are positively correlated with mean air temperatures in July and August, when more than 50% of the annual CH_4 emissions occur. The slope of the exponential regression corresponds to a Q_{10} value of 6.8 ± 1.5 ($n = 7$, $R^2 = 0.74$). A similar strong relationship is not observed for annual integrated emissions (May through October) until a phase shift of two months is applied to the temperature data (March through August) ($Q_{10} = 6.7 \pm 1.8$; $n = 7$; $R^2 = 0.62$). This is interpreted as evidence of the effect of late winter temperatures on May and June fluxes through changes in the duration and depth of the snow cover and the rate at which the area density of frozen wetlands soils decreases. Moreover, the seasonal temperature anomalies persist in the same direction for several months (Figure 2.23b) such that there is an effective modulation of annual emissions. That is, years with lower temperatures in late winter are often associated with lower temperatures and lower fluxes throughout the spring and summer.

The large value of Q_{10} derived here indicates significant positive feedback between temperature and CH_4 emissions from wetlands. Similar Q_{10} values have been reported from some empirical studies (listed in *Worthy et al.*, 1998a) but these are based on temperature variations over a day to a few months. Our

Q_{10} estimates are derived from inter-annual variations in emission rates and temperature over a large area, on the same temporal and spatial scales as the direct effects of climate change on regional ecosystem emissions. Recent global CH_4 budget models typically use $1.5 \leq Q_{10} \leq 2$ to estimate climate feedback effects. In fact, with $Q_{10} > 2$ some models produce unrealistic CH_4 annual cycles at high northern latitudes [*Fung et al.*, 1991]. This is likely to be a consequence of over-estimating total CH_4 emissions from northern wetlands, such that even a small temperature increase leads to large increases in total emissions. A comparison of annual CH_4 emissions with precipitation records from sites in the HBL was inconclusive. This may be due to precipitation amounts being a poor surrogate for water table depth. There was, however, a tendency for July and August in anomalous years to be warm and dry, or cool and wet. This observation and the strong correlation between CH_4 fluxes and temperature suggest that, while temperature and precipitation are not independent climate parameters, seasonal variations in emission strength are most directly associated with temperature.

The results obtained here using the regional boundary layer integration approach indicate that CH_4 emissions from the HBL have a greater sensitivity to seasonal temperature than previously thought. If these findings are applicable to other northern wetlands, especially the Western Siberian Lowlands (540,000 km^2) which is the other principal semi-continuous wetland area north of 50°N, then the global CH_4 budget needs substantial revisions with respect to emissions from northern wetlands and their degree of climate feedback. As well, such a high sensitivity of northern wetland emissions to temperature can well produce inter-annual variations in total emissions of the required magnitude needed to account for the variability observed in the northern hemispheric CH_4 growth rate. With the possibility of higher temperatures in mid- and high-northern latitudes due to climate change, the strong feedback implied by $Q_{10} = 7$ suggests that CH_4 emissions from northern wetlands could rapidly increase in significance on a global scale.

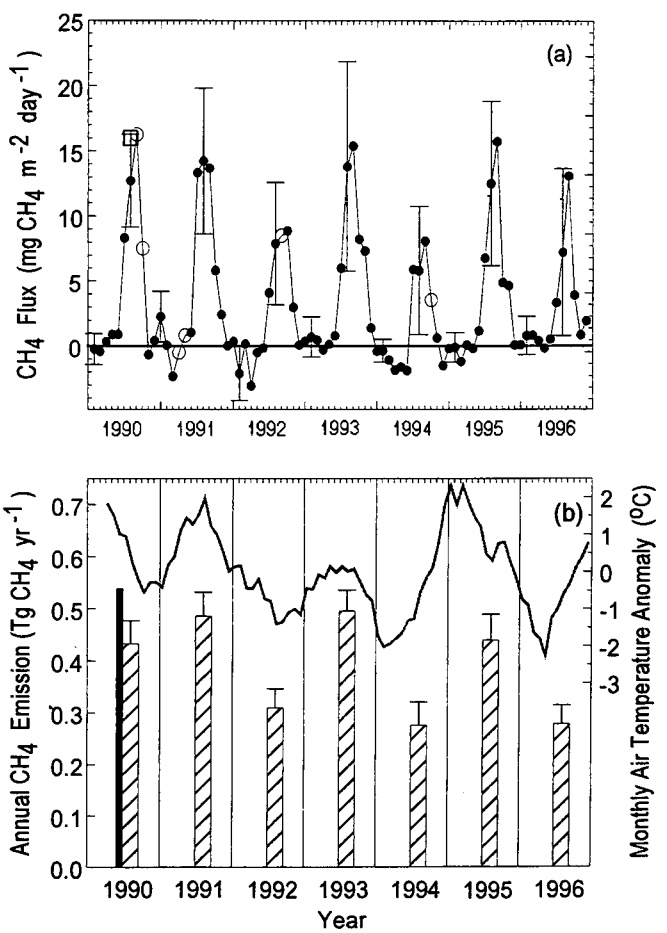

Figure 2.23 (a) Mean flux density for individual months from 1990 to 1996. Values for four months (o) were interpolated due to missing data from either Fraserdale or Alert. Also shown is the independent mean flux estimate of HBL CH_4 flux derived using continuous eddy correlation measurements for July, 1990, during the NOWES (Northern Wetlands) experiment. (b) Annual CH_4 emissions from the HBL (shaded bars) calculated by integrating the mean flux densities over the area of the HBL (320,000 km^2) for the biologically active months of May through October (180 days total). The error bars represent the standard error of the annual mean values. The solid bar is the total HBL flux in 1990 (0.54 ± 0.19 Tg CH_4 yr^{-1}) calculated from NOWES data. The red line is a smoothed time series (7-point moving average) of monthly anomalies in air temperature at Fraserdale plotted with a lag of two months.

2.2.4 REFERENCES

Cicerone R.J. and Oremland R.S. (1988) Biogeochemical aspects of atmospheric methane. *Global Biogeochem. Cycles,* 2, 299-328.

Conway, T.J., and L.P. Steele, Carbon dioxide and methane in the Arctic atmosphere, *J. Atmos. Chem.*, 9, 81-100, 1989.

Dlugokencky, E.J., and K.A. Masarie, P.M. Lang, P.P. Tans, L.P. Steele and E.G. Nisbet, A dramatic decrease in the growth rate of atmospheric methane in the Nothern Hemisphere during 1992, *Geophys. Res.*, Lett., 21, 45-48, 1994a.

Dlugokencky, E.J., L.P. Steele, P M. Lang and K.A. Masarie, The growth rate and distribution of atmospheric methane, *J. Geophys. Res.*, 99, 17, 021-17, 043, 1994b.

Fung, I., J. John, J. Lerner, E. Matthews, M. Prather. L. Steele, and P. Fraser, Global budget of atmospheric methane: Results from a three dimensional global model synthesis, *J. Geophys. Res.*, 96, 13, 033-13, 065, 1991.

Harris, R.C., G. W. Sachse, J.E. Collins, Jr., L. Wade, K.B. Bartlett, R.W. Talbot, E.V. Browell, L.A. Barrie, G.F. Hill, and L.G. Burney, Carbon monoxide and methane over Canada: July-August 1990, *J. Geophys. Res.*, 99, 1659-1669, 1994.

Hopper, J.F., D.E.J. Worthy, L.A. Barrie, and N.B.A. Trivett, Atmospheric observations of aerosol black carbon, carbon dioxide and methane in the high arctic, *Atmospheric Environment.* 28, 3047-3054, 1994.

Nakazawa, T., M. Ishizawa, K. Higuchi and N.B.A. Trivett, 1997: Two curve fitting methods applied to CO_2 flask data. EnvironMetrics, Vol 8, 197-218.

Roulet, N.T., R. Ash and T.R. Moore, Low boreal wetlands as a source of atmospheric methane, *J. Geophys. Res.*, 97, 3739-3749, 1992.

Steele L.P., Dlugokencky E.J., Lange P.M., Tans P.P., Martin R.C., and Masarie K.A. (1992) Slowing down of the global accumulation of atmospheric methane during the 1980's, *Nature 358*, 313-316.

Trivett, N.B.A., D.E.J. Worthy, and K.A. Brice, Surface measurements of carbon dioxide and methane at Alert during an Arctic Haze event in April, 1986, *J. Atmos. Chem.*, 9, 383-397, 1989.

Worthy, D.E.J, M.K. Ernst, and E.J. Dlugokencky, An intercomparison of methane standard gas scales between AES and NOAA/CMDL, *Environment Canada Internal report* ARD 93-001, 1993.

Worthy, D.E.J., N.B.A. Trivett, J.F. Hopper, J.W. Bottenheim, and I. Levin, Analysis of long range transport events at Alert, N.W.T., during the Polar Sunrise Experiment, *J. Geophys. Res.*, 99, 25329-25344, 1994.

Worthy, D.E.J., Levin, I., Trivett, N.B.A., Kuhlmann, A. J., Hopper, J.F., and Ernst, M. K., Seven years of Continuous Methane Observations at a Remote Boreal Site in Ontario, Canada, *J. Geophys. Res. (accepted)* (1998a).

Worthy, D.E.J, Levin, I., Hopper, J.F. and Trivett, N.B A., Evidence of a link between climate change and northern wetlands methane emissions, *Submitted* (1998b).

2.3. CARBON MONOXIDE

Douglas E.J. Worthy and Michele K. Ernst

2.3.1. BACKGROUND

Carbon monoxide (CO) has little direct radiative impact on the atmosphere however, due to its strong influence in ozone and hydroxyl chemistry, it has a large indirect impact [*IPCC*, 1994]. Major sources of CO are combustion, biomass burning and the oxidation of methane and non-methane hydrocarbons. The most important removal mechanism (~90%) is the reaction with OH radicals [*IPCC*, 1994]. Almost 50% of all OH present in the atmosphere is involved with the removal of CO [*Crutzen and Zimmermann,* 1991]. Atmospheric measurements show that the CO mixing ratios in the northern troposphere range from 40 to 250 ppb with lower values generally being observed in the summer and higher values being observed in the winter [*IPCC*, 1994].

CO is currently begin measured at Alert as part of the cooperative air sampling program with the National Oceanic and Atmospheric Administration's Climate Monitoring and Diagnostics Laboratory (NOAA/CMDL) in Boulder, Colorado, USA. The CO flask measurement program began prior to April 1992, however the grease used on the stopcocks at that time contaminated the samples for CO, and therefore the measurements are not reported. The greased glass stopcocks were replaced with Telfon® o-ring stopcocks in April 1992. The mean monthly values calculated using a curve fit through the weekly flask samples from April 1992 to October 1995 are shown in Figure 2.24 [*Novelli et al.,* 1992, and unpublished results]. The use of a curve fit to generate monthly values reduces the effects of short-term variability of the individual samples and of inhomogeneous sampling density through the year. The distinct annual cycle can be seen along with a non-discernible trend. In fact *Novelli et al.,* [1994] indicate that global CO levels have dropped by about 7% since 1990. There is no known explanation for the dramatic decrease at this time, although it is speculated that the decrease may be due to improved emission controls [*IPCC*, 1994].

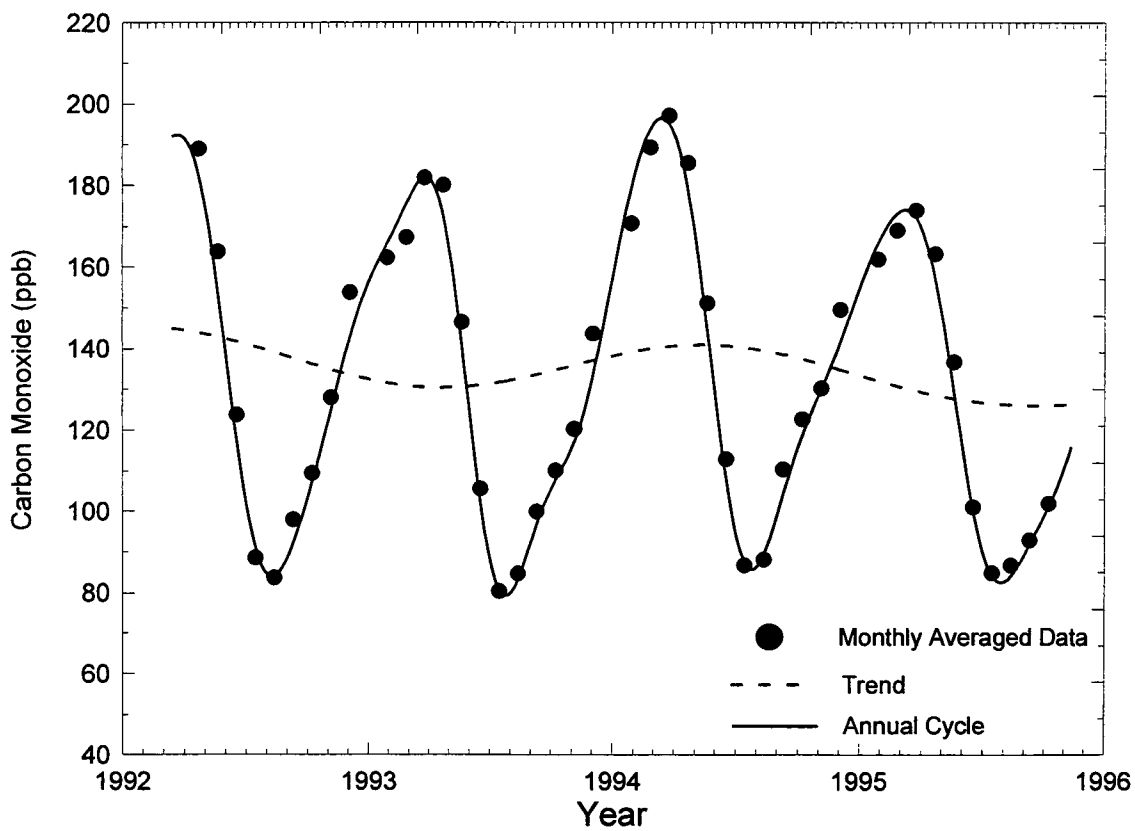

Figure 2.24 Time series of monthly averaged CO data from Alert collected by NOAA/CMDL.

In 1992, an in situ gas correlation system was installed at Alert. The main purpose of the measurements was to aid in the selection or screening of other trace species data. It was highly recommended at the Canadian Baseline Review meeting in May, 1997, that resources and effort should be made in establishing a precise and well-calibrated "baseline" CO measurement program at Alert, since CO occupies a central role in the chemistry of the atmosphere. Continuous measurements have a great advantage over flask measurements in that they have high time resolution, enabling the frequent episodes that occur in winter to be characterized. These measurements in conjunction with other in situ trace gas measurements, such as methane and carbon dioxide, as well as aerosols, have the potential to elucidate important information on regional source distributions.

The in situ CO program at Alert was initiated in January 1998. Because this program is new, there is no section in this report on the in situ CO data from Alert. Details on the measurement system, calibration and sampling protocols, and the gas standards utilized in the program are summarized in Section 3.3.

2.3.2 REFERENCES

IPCC 1994, Intergovernmental Panel on Climatic Change; Climate Change 1994. *Radiative Forcing of Climate Change and An Evaluation of the IPCC IS92 Emission Scenario*, Edited by J.T. Houghton, L.G. Meira Filho, J. Bruce, H. Lee, B.A. Callander, E. Haites, N. Harris and K. Maskell, Cambridge University Press, New York (1995).

Crutzen, P.J., and P.H. Zimmermann. The changing photochemistry in the troposphere, Tellus, 3(AB). 136-151, 1991.

Novelli, P.C., L.P. Steele and P.P. Tans, Mixing ratios of carbon monoxide in the troposphere. *J. Geophys. Res.* 97, 20731-20750, 1992.

Novelli, P.C., K. Masarie, P.P. Tans and P. Lang, Recent changes in atmospheric carbon monoxide. *Science*, 263, 1587-1590, 1994.

2.4. BLACK CARBON

Fred Hopper, Joe Kovalick and Armand Gaudenzi

2.4.1. BACKGROUND

Aerosol black carbon (BC) is produced by incomplete combustion, primarily from fossil fuels and biomass burning. BC is of interest because it is the dominant light absorbing component in atmospheric aerosols. BC is also a very good tracer of combustion emissions to the atmosphere. It can be transported long distances and because it has low background levels, is a more sensitive indicator of contaminated air (order of magnitude increases in concentration) than other combustion products such as CO_2 (increases of a few per cent). However, since it is in particulate form, BC is subject to more atmospheric removal processes (e.g., wet deposition) than gases.

BC measurements have been made at Alert (1989-1996) and Fraserdale (1990-1996) using commercially available aethalometers from Magee Scientific. The instruments made hourly measurements of the optical attenuation of aerosol deposits collected on quartz fibre filters. BC concentrations were calculated using the following equation:

$$BC = k * \Delta ATN / (\alpha * V)$$

where ΔATN is the change in optical attenuation over measurement period, V is the volume of air sampled, k is a constant, and α is the specific attenuation. Note that the optical attenuation is representative of the aerosol/filter matrix within the aethalometer and is not equivalent to optical attenuation caused by the aerosols in the free atmosphere.

Investigations by others have suggested that the specific attenuation α of aerosols in the atmosphere is not constant but is a function of location, time, aerosol origin, internal/external mixing, etc. Aethalometer sensitivity to these factors is not known. Consistent BC data sets for Alert and Fraserdale have been prepared using a specific attenuation of $\alpha = 19\ m^2\ g^{-1}$ to convert aethalometer optical attenuation to BC concentration, based on the original aethalometer calibrations by the instrument developers. Absolute calibrations of the aethalometers for typical Alert and Fraserdale aerosol samples have not been carried out. There is no consensus regarding an absolute method for determining the BC concentration in aerosols, necessitating a modest research and development program to develop a technique for calibration. Resources have not been provided for this activity.

2.4.2. IN SITU BC MEASUREMENTS AT ALERT

At Alert, two aethalometers were normally operated at each site for redundancy and QA/QC purposes. Instrument flow rates of 5 L min^{-1} were used in order to balance periods of lost data due to lower sensitivity and optical saturation (filter over-loading). Filters were normally changed weekly, but in recent years filters were changed twice per week in one aethalometer at each site, permitting use of a higher flow rate (10 L min^{-1}) for 2x increase in sensitivity. Aethalometer sensitivities are on the order of 5 ng m^{-3} to 15 ng m^{-3} (assuming the specific attenuation is 19 $m^2\ g^{-1}$).

BC concentrations at Alert (see Figure 2.25) and Fraserdale (see Figure 2.26) are best described as event-driven with frequent episodic increases in concentration lasting one to several days. The events are superimposed on longer-term seasonal cycles. The seasonal cycle at Alert is highly correlated with the cycle of Arctic Haze (see Section 2.9). BC concentrations at both sites are positively correlated with concentrations of other components that have pollution sources. While the winter maximum is also observed at Fraserdale, there is a secondary summer maximum in BC concentrations due in some part to boreal forest fires.

There has been a significant decline in aethalometer BC concentrations over the period 1990-1996 at Alert. A decline also occurred at Fraserdale but is less obvious due to closer proximity to anthropogenic and wildfire sources. These changes are in contrast to the positive growth rates in concentrations of other radiatively important components such as CO_2 and CH_4, which share some sources in common with BC.

The methodology description of the BC measurements is found in Section 3.4.

2.4.3. IN SITU BC MEASUREMENTS AT FRASERDALE

Sample air for the Fraserdale aethalometers was drawn from a 10 m tower through dedicated lines of aluminum tubing. Sample air for the initial Alert aethalometer was initially drawn from a 10 m tower through a manifold system supplying other instruments. This Alert system was abandoned in late 1992 because of gross contamination of the original sample lines. It was replaced by a dedicated stainless steel aerosol-sampling stack (10 m height) with (approximately) isokinetic sample probes. Size-selective devices have not been used in the Alert and Fraserdale sampling systems due to lack of funds.

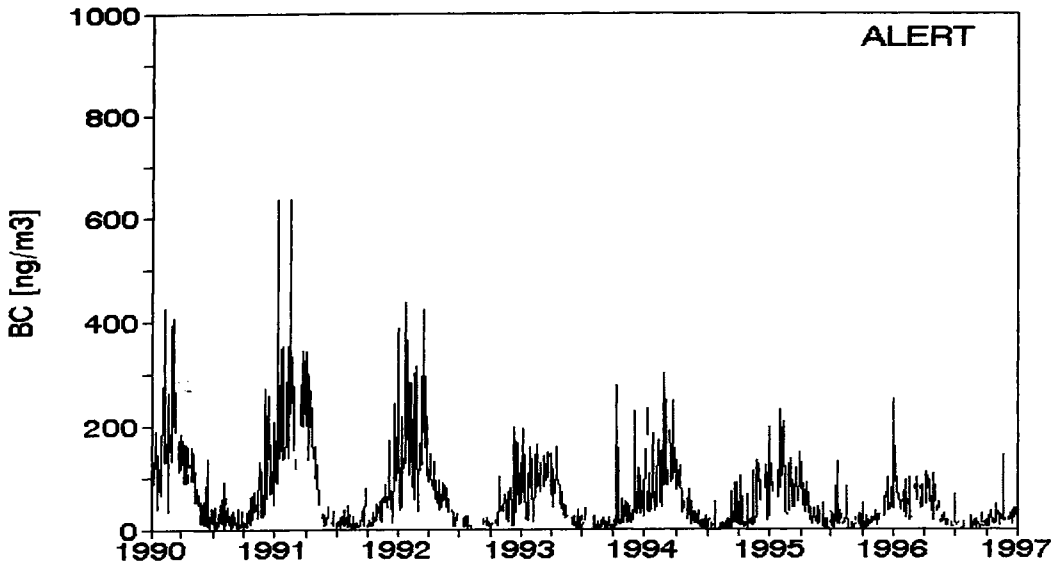

Figure 2.25 Time series of aerosol black carbon concentrations (ng m^{-3}) at Alert in the Arctic from 1990 to 1996 estimated using aethalometer observations of optical attenuation (specific attenuation is assumed to be 19 m^2 g^{-1}).

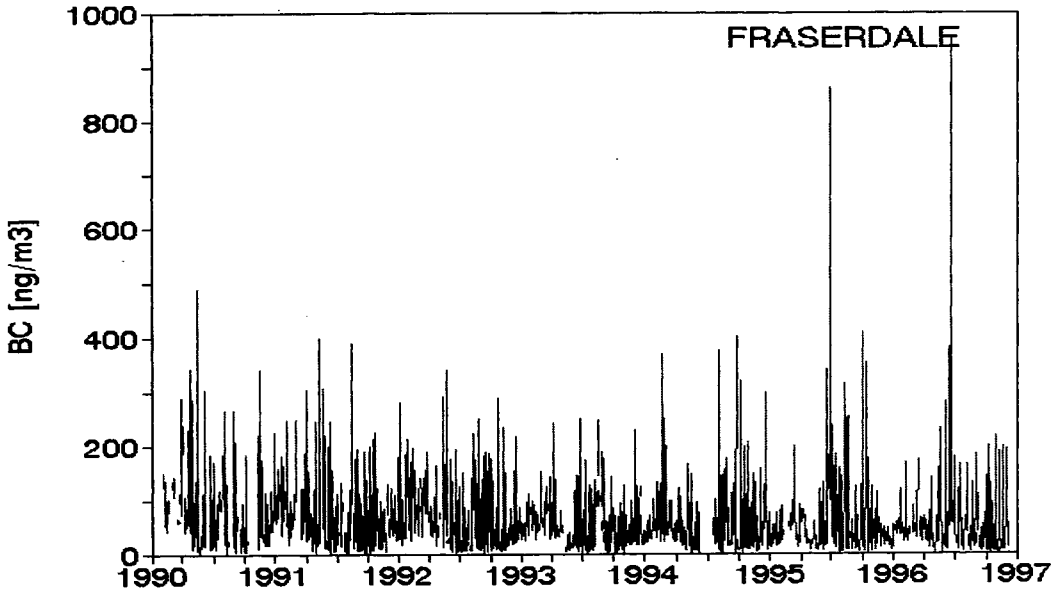

Figure 2.26 Time series of aerosol black carbon concentrations (ng m^{-3}) at Fraserdale in the central boreal region of Canada from 1990 to 1996 estimated using aethalometer observations of optical attenuation (specific attenuation is assumed to be 19 m^2 g^{-1}).

2.4.4. PUBLICATIONS

Hopper, J.F., D.E.J. Worthy, N.B.A. Trivett, L.A. Barrie. Atmospheric Observations of Aerosol Black Carbon, Carbon Dioxide, and Methane in the High Arctic. *Atmospheric Environment*, **28**, 3047-3054, 1994.

Hopper, J.F., W. Hart. Meteorological Aspects of the 1992 Polar Sunrise Experiment. *Journal of Geophysical Research*, **99(D12)**, 25,315-25,328, 1994.

Worthy, D.E.J., N.B.A. Trivett, J.F. Hopper, J.W. Bottenheim, I. Levin. Analysis of Long-Range Transport Events at Alert, Northwest Territories, During the Polar Sunrise Experiment. *Journal of Geophysical Research*, **99(D12)**, 25, 329-25, 344, 1994.

Hopper, J.F., A.-L. Norman. Analysis of Aerosol Black Carbon Events in the Arctic and at a Mid-Continental Site. Presented at *AGU Western Pacific Meeting*, Brisbane, 1996.

Hopper, J.F. Seven Years of Aerosol Black Carbon Measurements at Two Remote North American Sites. Presented at *Sixth International Conference on Carbonaceous Particles in the Atmosphere*, Vienna, 1997.

Blanchard, P., J.F. Hopper, L.A. Barrie. TD-GC/MSD Determination of PAHs and n-Alkanes in Atmospheric Aerosols at Four Sites in Ontario. *In preparation*, 1997.

2.5. IN SITU SURFACE OZONE MEASUREMENTS

Kurt Anlauf, Kathy Hayden and Maurice Watt

2.5.1. BACKGROUND

Ozone has been continuously measured at Alert, NWT, since January 1992. In the Hudson Bay Lowland at Fraserdale, Ontario, ozone was measured from March 1990 until June 1997 when the program was terminated due to funding cuts.

The ozone measurement program at both sites is in support of determining any trend in background ozone in Canada. In addition, the measurement at Alert is of particular interest, namely, in connection with the annual appearance of surface level ozone depletion starting in mid-March, just after the time of polar sunrise, and extending into June. Many field studies have been carried out at Alert to unravel the reason for this phenomenon. As a result, the accurate measurement of ozone is of crucial importance (see list of publications in Section 2.5.1.3). Just recently, this ozone depletion has also been correlated with a corresponding atmospheric mercury depletion (see list of publications in Section 2.5.1.3).

The methodology description of the ozone measurements is found in Section 3.5.

2.5.1.1. IN SITU SURFACE OZONE MEASUREMENTS AT FRASERDALE

Diurnal: Typical of low-elevation continental mid-latitude sites, Fraserdale shows large diurnal variations with a pronounced maximum in mid to late afternoon. However, the degree of diurnal variation is highly seasonally dependent. Figure 2.27 shows a plot of the diurnal ozone mixing ratios averaged for four months of the year. The largest day/night differences occur in the spring to fall months; in contrast, only a minimal variation is seen in the winter months. The basic reason for this is that low-elevation continental sites, like Fraserdale, frequently experience nighttime ground-based temperature inversions, thus maximizing the contact of ozone with the ground during the night. In the summer, the ground is covered with vegetation, which is an efficient scavenger for ozone. As a result, there is a rapid loss of ozone to the vegetation and frequently ozone mixing ratios rapidly decrease to near zero on many such nights. Then, during mornings, as the inversion is broken up by surface heating, the upper layer ozone (at higher mixing ratios) is brought down to the surface so that the surface ozone steadily increases until complete mixing has been established in the boundary layer at midday and continues until late afternoon. In contrast, during winter months, the loss of ozone to the snow or ice covered ground is minimal because ozone is relatively stable on these surfaces. Thus, there is only a slight diurnal variation in the winter months of November - January.

Seasonal: Figure 2.28 shows a box and whisker plot of hourly ozone values for each month of the year using data from March 1990 to February 1997; the solid line joins the monthly medians. There is a moderate increase in average ozone from about 30 ppb in January to about 37 ppb in March and April. This is followed by a slow decrease over several months leading to a steady minimum of about 22 ppb during July-October. Subsequently, the ozone increases again into the winter months. Major ozone episodes were observed from late spring until early fall - these are thought to be associated with the frequent southerly flows from polluted regions further south on the continent (only a few back-trajectories have been run to confirm this).

Annual: Figure 2.29 shows a plot of the average hourly ozone mixing ratio for each successive month of the April 1990 to March 1997 period. Applying a simple linear regression on the monthly means for this period shows no apparent significant trend in ozone, at 0.2 ppb per year (or about 0.7% per year).

2.5.1.2. AMBIENT MEASUREMENTS AT ALERT

Diurnal: There is virtually no diurnal variation at the Arctic Alert site where full daylight exists from April to September and total darkness extends from November to mid-February. This site, being snow-covered for the major part of the year, experiences minimal ozone deposition losses to the ground during this period. Only in mid-summer is the rocky ground exposed and dry deposition would take place throughout the 24-hour day.

Seasonal: Figure 2.30 shows a box and whisker plot of hourly ozone mixing ratios for each month of the year using data from January 1992 to December 1997; the solid line joins the monthly medians. There is a slight increase from January to February; this is followed by obvious depletion events from mid-March to mid-June. After this, the ozone exhibits a steady minimum at about 23 ppb during July-August, but increases again during September to October toward a steady mixing ratio of about 35 ppb during the polar dark months of November to January.

Annual: Figure 2.31 shows a plot of the average hourly ozone mixing ratio for each successive month of the January 1992 to December 1997 period. Applying a simple linear regression on the monthly means, there is an apparent positive trend in ozone over this period, namely 0.6 ppb per year (or about 2% per year). However, one must be cautioned that the measurement period is somewhat short for yielding conclusive information on surface ozone trend.

2.5.1.3. PUBLICATIONS

"Measurements of photolyzable chlorine and bromine during the Polar Sunrise Experiment 1995", G. Impey, P. Shepson, D. Hastie, L. Barrie and K.Anlauf, *J. Geophys. Res.* 102, 16, 005-16, 010 (1997).

"Measurement of ozone during Polar Sunrise Experiment 1992", K. Anlauf, R. Mickle and N. Trivett, *J. Geophys. Res.* 99, 25, 345-25, 353 (1994).

"Relationships between organic nitrates and surface ozone destruction during Polar Sunrise Experiment 1992", K. Muthuramu, P. Shepson, J. Bottemheim, T. Jobson, H. Niki and K.Anlauf, *J. Geophys. Res.* 99, 25, 369-25, 378 (1994).

"Serial gas chromatographic/mass spectrometric measurements of some volatile organic compounds in the Arctic atmosphere during the 1992 Polar Sunrise Experiment", Y. Yokouchi, H. Akimoto, L. Barrie, J. Bottenheim, K. Anlauf and T. Jobson, *J. Geophys. Res.* 99, 25, 379-25, 389 (1994).

"Mercury vapor mimics ground-level ozone depletion in Arctic air during springtime", W. Schroeder, K. Anlauf, L. Barrie, J. Lu, A. teffen, D. Schneeberger and T. Berg, *Nature* 394, 331-332 (1998).

"Measurements of C_2-C_7 hydrocarbons during the Polar Sunrise Experiment 1994: Further evidence for halogen chemistry in the troposphere", P. Ariya, B. Jobson, R. Sander, H. Niki, G. Harris, J. Hopper and K. Anlauf, *J. Geophys. Res.* 103, 13, 169-13, 180 (1998).

"Polar Sunrise Experiment 1995: Hydrocarbon measurements and tropospheric Cl and Br-atom chemistry", P. Ariya, H. Niki, G. Harris, K. Anlauf and D. Worthy, submitted for publication in *Atmos. Environ.* (1998).

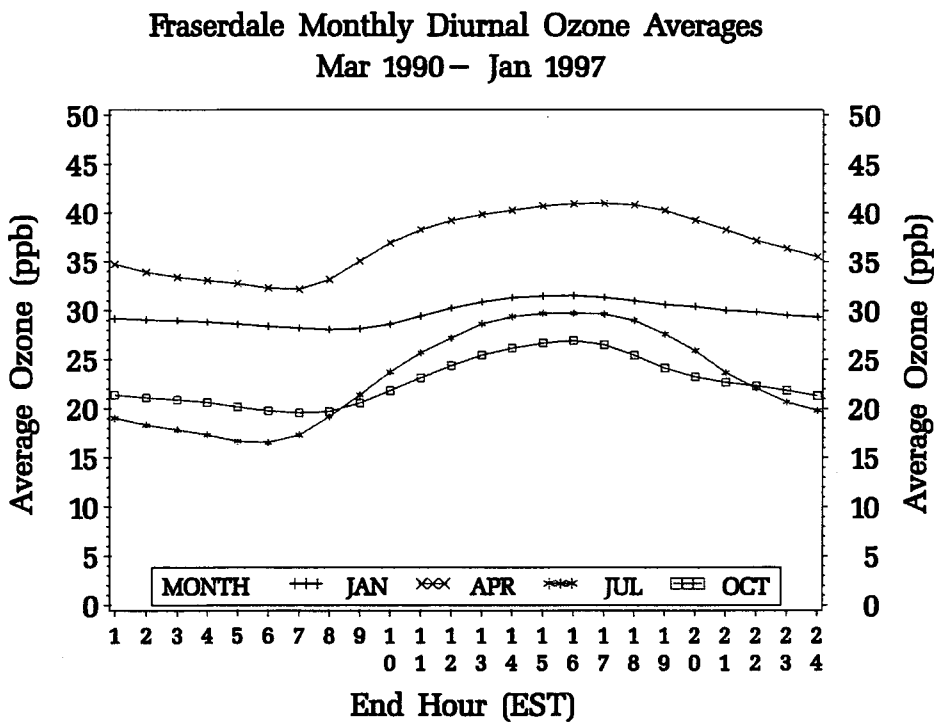

Figure 2.27 Averaged monthly diurnal ozone mixing ratios for four specific months as measured at Fraserdale over the period March 1990 to January 1997.

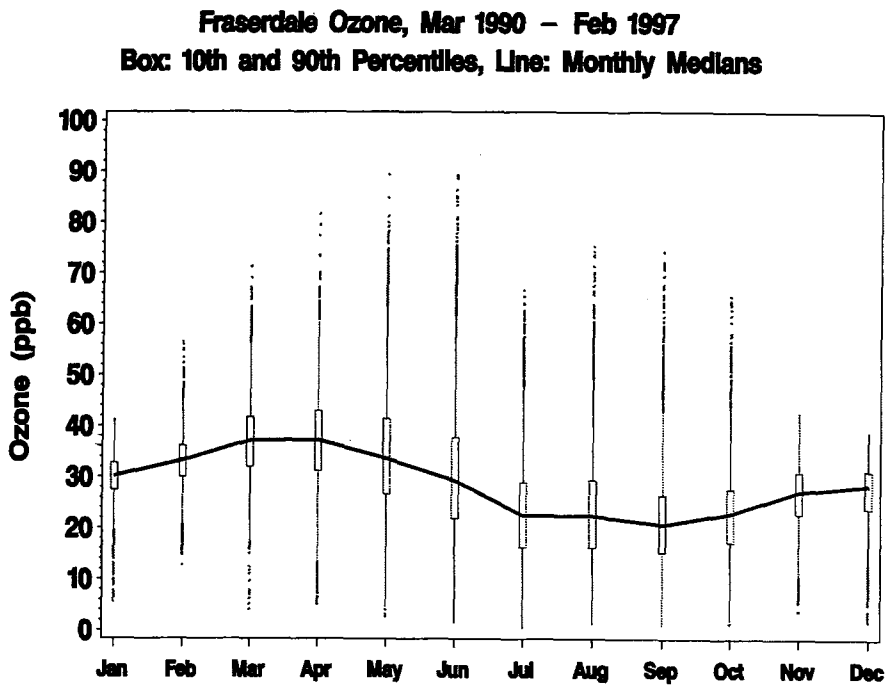

Figure 2.28 Box and whisker plots of hourly Fraserdale ozone mixing ratios for each month of the period: March 1990 to February 1997.

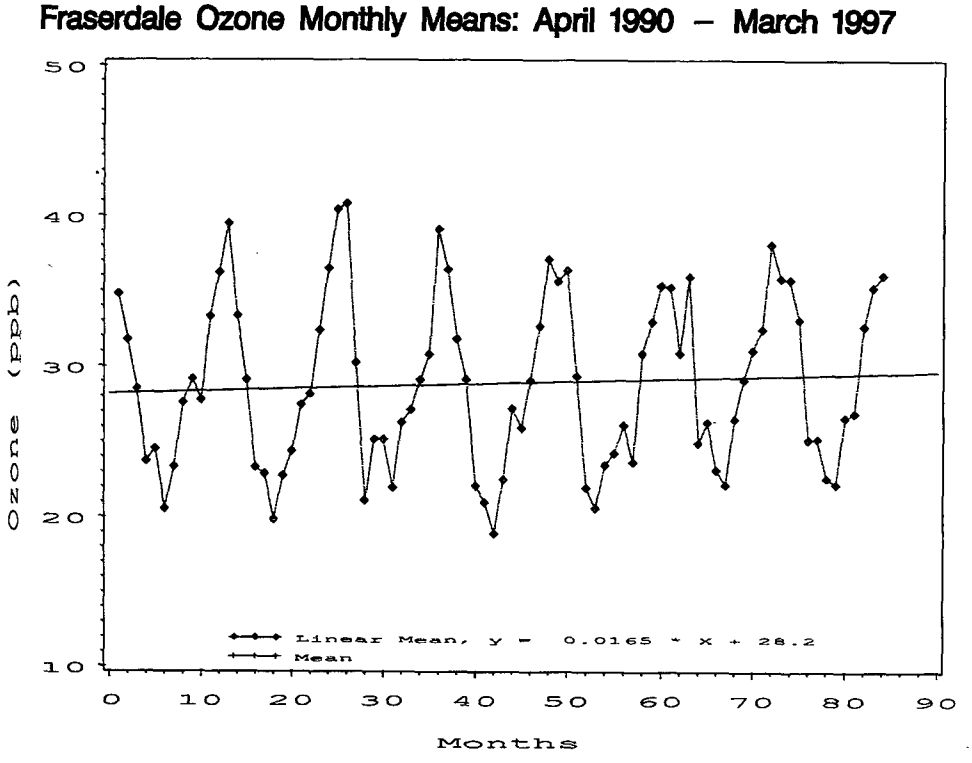

Figure 2.29 Hourly Fraserdale ozone mixing ratios averaged over each month of the year for the period: April 1990-March 1997.

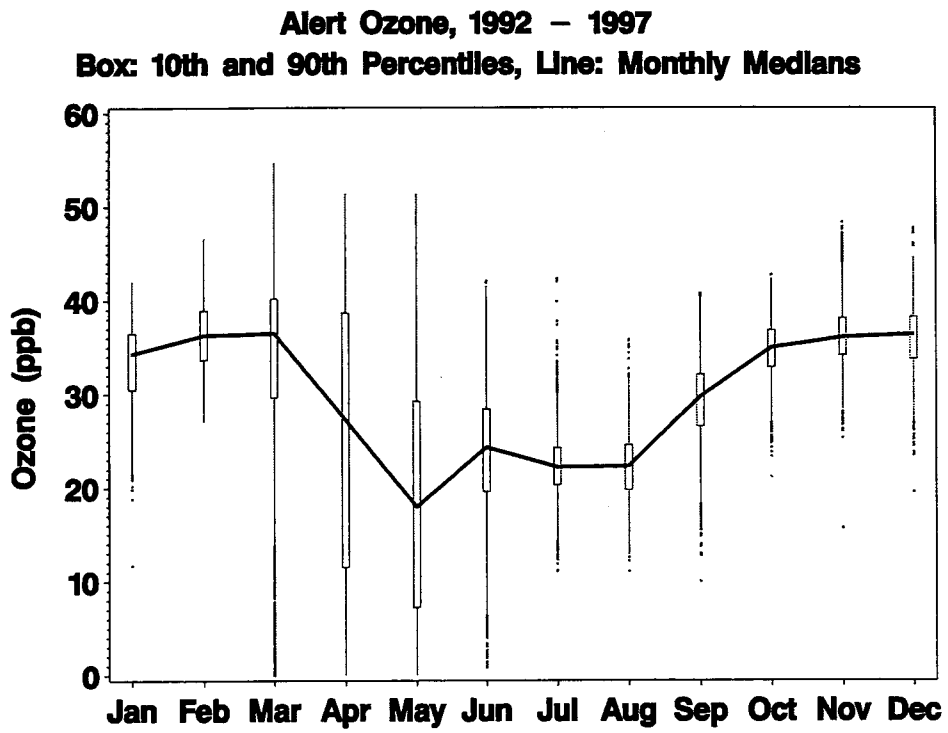

Figure 2.30 Box and whisker plots of hourly Alert ozone mixing ratios for each month of the period: January 1992 to December 1997.

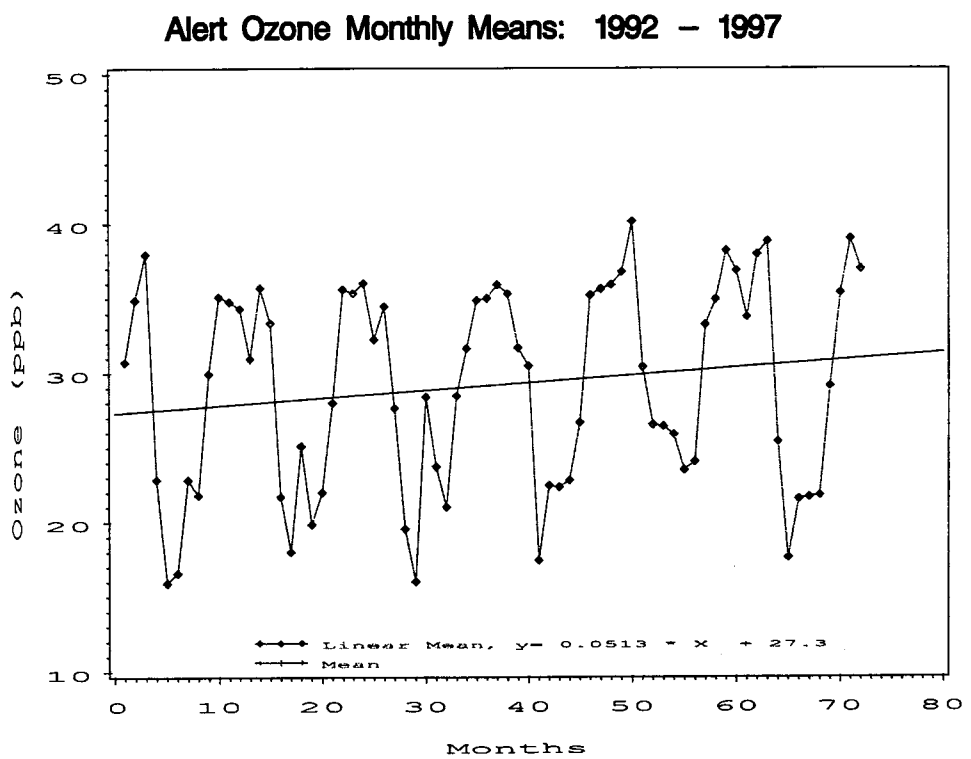

Figure 2.31 Hourly Alert ozone mixing ratios averaged over each month of the year for the period: January 1992 to December 1997.

2.5.2. STRATOSPHERIC OZONE AND UV-B MEASUREMENTS

Jim B. Kerr and David I. Wardle

2.5.2.1. BACKGROUND AND RESULTS

Significant decreases in the amount of springtime column ozone over Antarctica were reported by *Farman et al.* [1985]. This discovery, now known as the Antarctic ozone hole, prompted significant research aimed at quantifying and explaining the mechanisms of the massive ozone losses which recurred each October and became more prominent over the years. Research efforts of Environment Canada focussed on the Arctic, where it was thought that similar ozone losses might occur but would be more difficult to observe because of the greater natural variability of the Arctic stratosphere. Brewer spectrophotometer measurements of column ozone [*Kerr et al.*, 1980] and ultraviolet-B (UV-B) radiation [*Kerr and McElroy*, 1993] and ozonesonde measurements of the ozone profile [*Tarasick et al.*, 1995] were started at Alert (82.5°N, 62.3°W) as part of the Atmospheric Environment Service (AES) research program to study stratospheric ozone over the Arctic.

The ground-based total ozone and ozonesonde profile measurements began in 1987 [*Kerr et al.*, 1990]. Figure 2.32 shows the record of total ozone measured between 1987 and 1995. Maximum ozone depletion occurs during the late winter and early spring so the research has been more extensive at this time of year. Many of the total ozone measurements during the polar night have been made using the moon as a light source [*Kerr*, 1989].

Examples of the ozonesonde results are shown in Figure 2.33 for 1992 (top) and 1997 (bottom). Comparison between the two years indicates that there was significantly less ozone in the lower stratosphere (15 to 20 km altitude) in the winter/spring of 1997 than there was for the same period in 1992. The cause for the low levels in 1997 has been attributed to unusually cold temperatures that caused large amounts of polar stratospheric clouds (PSCs), which play a key role in the process of rapid ozone destruction (ozone hole) in the polar stratosphere. These findings are reported in *Fioletov et al.* [1997] and *Wardle et al.* [1997].

The UV-B measurements began in 1992 when the Canadian UV Index program was introduced [*Kerr*, 1994]. Figure 2.34 shows the measured erythemally (skin reddening) weighted daily irradiation at Alert for 1992. The values of 3000 Joules m^{-2} in the summer can be compared with values in Toronto, which can exceed 5000 Joules m^{-2} in the summer. Even though the sun reaches a significantly higher elevation at Toronto (~70°) than it does at Alert (~30°), the daily accumulated values are only about 70% more at Toronto since Alert has 24-hour daylight in the summer.

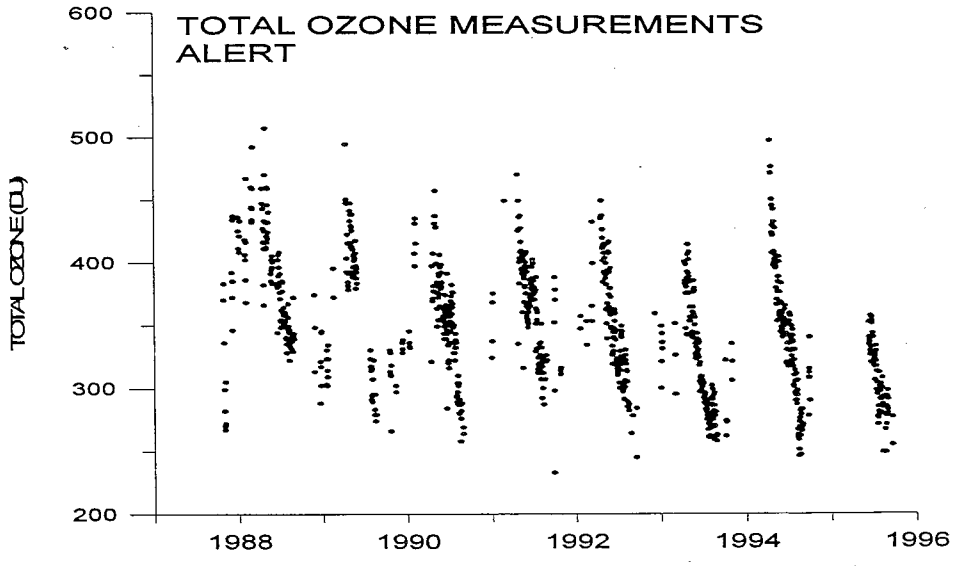

Figure 2.32 Ground-based measurements of total ozone made with the Brewer spectrophotometer at Alert. Measurements made during the summer are mostly direct sun. Those between October and February are made using the moon.

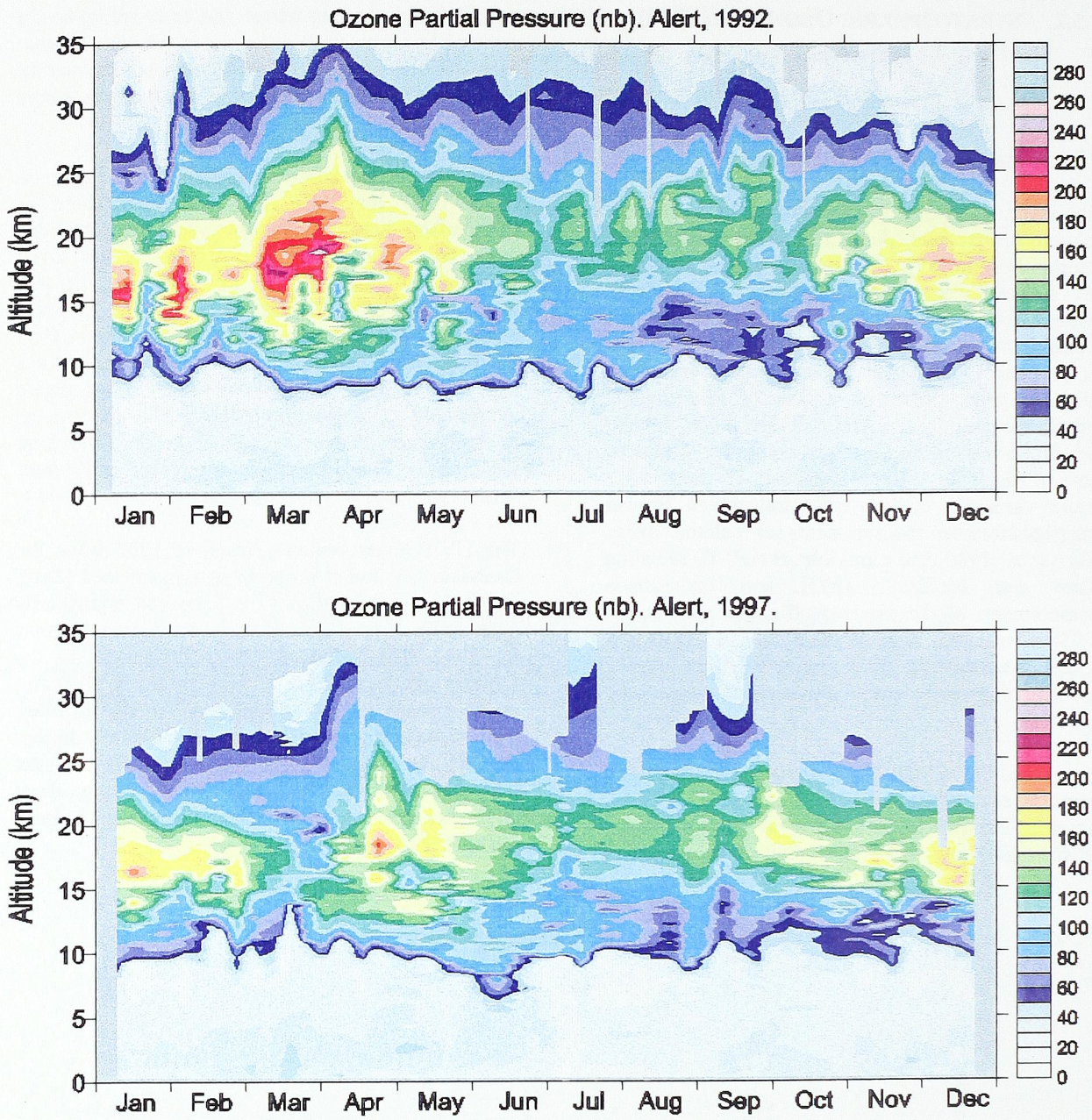

Figure 2.33 Results of ozonesonde profile measurements for 1992 (top) and 1997 (bottom). During March 1997, ozone values between 15 and 20 km were about 50% those of March 1992.

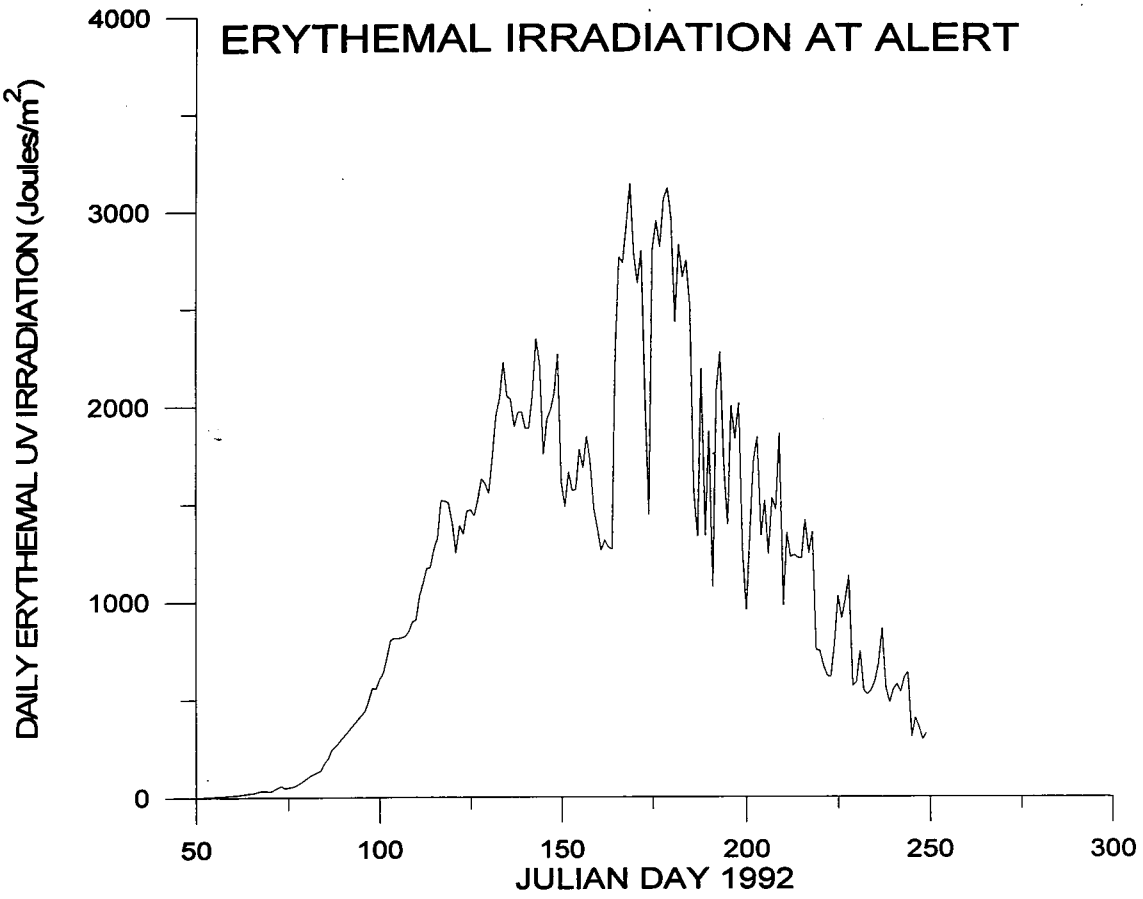

Figure 2.34 Daily erythemal irradiation values at Alert for 1992.

2.5.2.2. REFERENCES

Farman, J.C., B.G. Gardiner and J.D. Shanklin, Large loses of total ozone in Antarctica reveal seasonal ClO_x/NO_x interaction, *Nature,* **315**, 207-210, 1985.

Fioletov, V.E., J.B. Kerr, D.I. Wardle, J. Davies, E.W. Hare, C.T. McElroy and D.W. Tarasick, Long-term ozone decline over the Canadian Arctic to early 1997 from ground-based and balloon observations, *Geophys. Res. Lett.*, **24**, 2705-2708, 1997.

Kerr, J.B., Observations of Arctic total ozone with the Brewer spectrophotometer during the polar winter using the moon as a light source, In *Ozone in the Atmosphere,* R.D. Bojkov and P. Fabian (Eds), Proc. Quadrennial Int. Ozone Symp., DEEPAK Publ., Hampton, Va., 728-731, 1989.

Kerr, J.B., Decreasing ozone causes health concern, *Environ. Sci. Technol.*, **28**, 514A-518A, 1994.

Kerr, J.B., C.T. McElroy and R.A. Olafson, Measurements of ozone with the Brewer spectrophotometer, Proc., Quadrennial Int. Ozone Symp., Vol. I, J. London (Ed.), Int. Ozone Comm. (IAMAP), 74-79, 1980.

Kerr, J.B., C.T. McElroy, D.I. Wardle and V. Dorokhov, Measurements of Arctic total ozone during the polar winter, *Atmosphere-Ocean*, **28**, 383-392, 1990.

Kerr, J.B. and C.T. McElroy, Evidence for large upward trends of ultraviolet-B radiation linked to ozone depletion, *Science*, **262**, 1032-1034, 1993.

Tarasick, D.W., D.I. Wardle, J.B. Kerr, J.J. Bellefleur and J. Davies, Tropospheric ozone trends over Canada: 1980-1993, *Geophys. Res. Lett.*, **22**, 409-412, 1995.

Wardle, D.I., J.B. Kerr, C.T. McElroy and D.R. Francis eds., Ozone science: a Canadian perspective on the changing ozone layer, *Environment Canada Internal Report # CARD 97-3*, 119 pp, 1997.

2.6. CFC-11 AND CFC-12

Douglas E.J. Worthy and Michele K. Ernst

2.6.1 BACKGROUND

Chlorofluorocarbons (CFCs) are powerful greenhouse gases because they strongly absorb terrestrial infrared radiation and have long atmospheric lifetimes [*IPCC*, 1994]. The major sources of CFCs are from refrigeration, air conditioning and from the production of aerosols and foams. The tropospheric growth rates of CFC-11 and CFC-12, based on measurements spanning the last 15 years including data from Alert [*Elkins et al.*, 1993], have slowed significantly in response to substantially reduced emissions, as required by the Montreal Protocol and its subsequent amendments and adjustments. Current atmospheric measurements indicate that the mixing ratios of CFC-11 and CFC-12 in the northern troposphere are about 275 ppt and 545 ppt, respectively. Atmospheric CFC-11 mixing ratios at Alert are decreasing and CFC-12 mixing ratios are presently increasing, but will eventually decrease due to the reduced emissions.

CFC-11 and -12 are currently being measured at Alert as part of the cooperative air sampling program with the National Oceanic and Atmospheric Administration's Climate Monitoring and Diagnostics Laboratory (NOAA/CMDL) in Boulder, Colorado, USA [*Elkins et al.*, 1993]. The CFC flask measurement program began in February 1988 and continues today (see Section 5.4 for details). In May 1993, an in situ gas chromatographic (GC) system was installed at Alert. The main purpose of the program is to monitor changes in these two species and better understand the interannual and annual changes observed in their respective mixing ratios. Even though the interest in these two species has diminished due to their decreasing trend in the atmosphere, it was still highly recommended at the recent Canadian Baseline Review meeting (in May 1997) that resources and effort be maintained to maintain the precise and well-calibrated "baseline" CFC measurement program at Alert. The in situ measurements have a great advantage over flask measurements in that they have high time resolution, enabling the frequent episodes that occur in the winter to be characterized. Furthermore, continuous measurements of CFCs in conjunction with other in situ trace gas measurements along with accurate tracking of emissions, will help to define the chemical lifetimes of these species and may provide a more complete understanding of the transport properties of the atmosphere. This is of particular interest at Alert where air masses are often observed from Siberian or Eastern European origins and, therefore, there is a potential to elucidate important information on regional source distributions.

In March 1995, a comparison of the in situ data with flask data from the NOAA sampling program revealed inconsistencies within the two data sets. It was determined that there were errors in the AES in situ data. The errors could not be associated with a possible error in a calibration standard because the ratio of the in situ data with the NOAA flask data changed with time. The problems with the GC were never definitively determined but it is speculated that they were due to the sample flows being controlled by a rotometer that was located at the end of sampling module. This may have caused the pressures for the ambient and calibration samples to be sensitive to their delivery pressures. Therefore, the pressure of the sample loop was not consistent between standards and ambient air injections. Since flows were checked weekly, it was too difficult to track and correct the data. It was also determined that the Nafion® dryer used to dry the samples caused CFC-11 contamination. In August 1995, the changes to the sample flow adjustment protocol were made and the Nafion® dryer was removed. The in situ and the NOAA flask data from August 1995 to present compare well to each other. Only data obtained during this period are reported here. Details about the measurement system, calibration and sampling protocols, and the gas standards used in the program are summarized in Section 3.6.

2.6.2. IN SITU CFC-11 AND CFC-12 MEASUREMENTS AT ALERT

The time series of daily averaged CFC-11 and CFC-12 at Alert from September 2, 1995 to September 19, 1997 are shown in Figures 2.35 and 2.36, respectively. Gaps in the records are due to system malfunctions including the period between September 19 and December 31, 1997, which was due to an accidental bleed of the gas standard. (Periods when the gas standards were replaced are indicated on the figures as crosses.) The data are preliminary and subject to correction due to a drift in one or both of the standard gas scales maintained at NOAA/CMDL. Both data sets show significant seasonal variations and high frequency variability that occur throughout the year, unlike the methane and carbon dioxide data time series which have more pronounced variability during the winter.

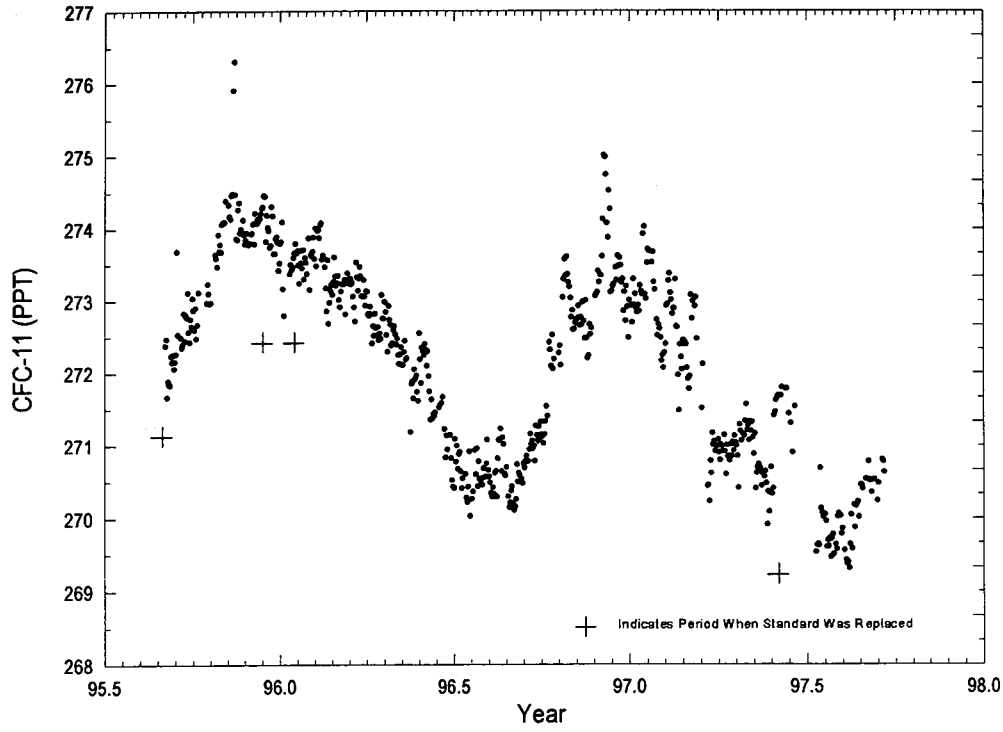

Figure 2.35 Time series of daily averaged CFC-11 from Alert.

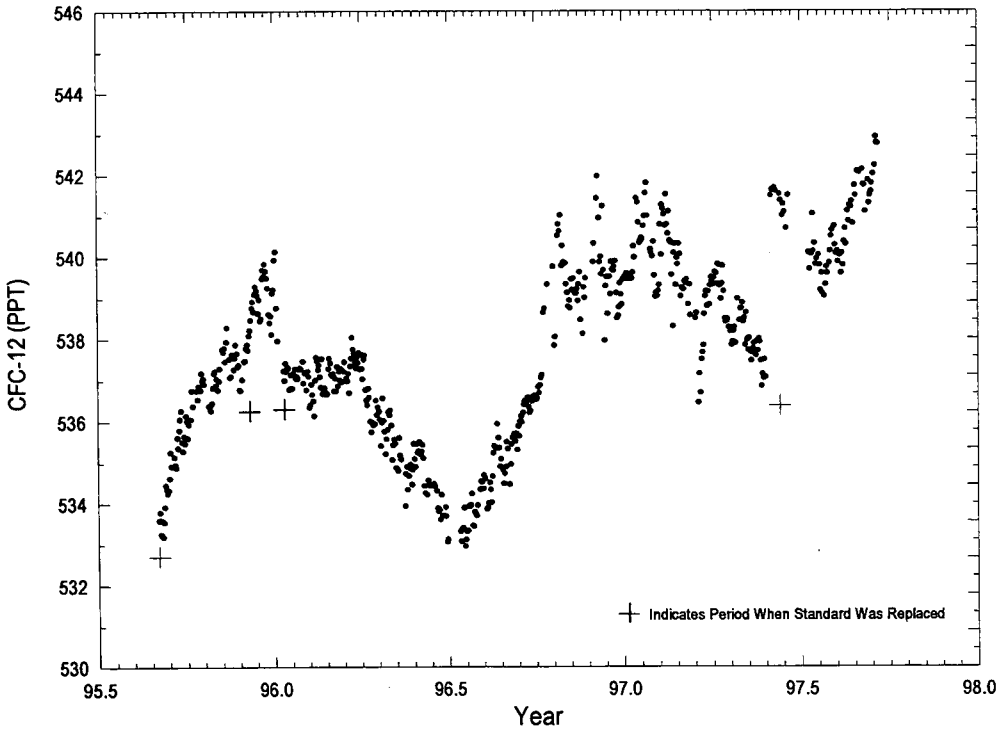

Figure 2.36 Time series of daily averaged CFC-12 from Alert.

Preliminary analysis reveals that most of the episodes are primarily due to rapid long-range transport from either across the pole in Siberia and Eurasia to Alert or from the eastern Northern Hemisphere along the eastern side of the Greenland ice cap. Air mass trajectories are used to characterize such periods of transport. This may reveal information on whether countries of the Former Soviet Union are adhering to the mandatory reduction protocols.

The mean CFC-11 annual cycle has a peak-to-peak amplitude of 4.5 ppt with a minimum in occurring in the months of July and August and a maximum occurring in the winter during the months of November to February. The mean CFC-12 annual cycle has a peak-to-peak amplitude of around 8 to 10 ppt with the minimum and maximum values occurring at the same time period as that observed in the CFC-11 annual cycle. The characteristics of the annual cycles for CFC-11 and CFC-12 can be used to verify transport models that in turn are used to understand many aspects of atmospheric chemistry and their processes.

2.6.3 REFERENCES

IPCC 1994, Intergovernmental Panel on Climatic Change; Climate Change 1994. *Radiative Forcing of Climate Change and An Evaluation of the IPCC IS92 Emission Scenario*, Edited by J.T. Houghton, L. G. Meira Filho, J. Bruce, H, Lee, B. A. Callander, E. Haites, N. Harris and K. Maskell, Cambridge University Press, New York (1995).

Elkins, J., T. Thompson, T. Swanson, J. Butler, B. Hall, S. Cummings, D. Fishere and A. Raffo, Decrease in the growth rates of atmospheric chlorofluorocarbons 11 and 12, Nature, 364, 780-783 (1993).

2.7. PAN

Jan W. Bottenheim

2.7.1. BACKGROUND

The tropospheric chemistry of nitrogen oxides plays a central role in determining the oxidizing capacity of the atmosphere. Nitrogen oxides are emitted in the atmosphere largely as nitric oxide (NO), which very rapidly establishes an equilibrium with nitrogen dioxide (NO_2) through reaction with O_3. Subsequent oxidation products are expected to dominate the total nitrogen oxide balance with transport away from major source areas. The main oxidation products are the inorganic compounds nitric acid (HNO_3) and particulate nitrate (pNO_3^-), and organic nitrates such as peroxyacetyl nitrate (PAN) and the alkyl nitrates (with the generic denomination $RONO_2$). Until the mid 1980s methods to perform routine measurements of organic nitrates were not available and in Arctic research all attention was focused on the inorganic nitrates; its concentrations were found to be low which led to the hypothesis that nitrogen oxides played a minor role in Arctic atmospheric chemistry. However, *Crutzen* [1979] had already suggested that in more remote regions of the globe PAN should be expected to be an important species, and our pioneering measurements of PAN at Alert in 1985 confirmed this hypothesis [*Bottenheim et al.*, 1986]. As a result, beginning in the fall of 1986, a routine measurement program of PAN was initiated at Alert. This ongoing program is truly unique in the world in that it is the only long-term PAN measurement program at a remote location of the globe.

There are some very good reasons for this program. Since PAN is the dominant nitrogen oxide species [*Bottenheim et al.*, 1993], it may be expected to be an excellent indicator of the long-term trend in the global atmospheric nitrogen oxide content. In particular, as with the sulphur oxides, efforts to reduce the emission of nitrogen oxides from anthropogenic activities should eventually be reflected in the long-term PAN trend. To date, little progress has been made in this respect, and hence no long-term trend in PAN has been observed. Its levels peak in the spring due to a combination of at least two factors. At that time, most air parcels observed at Alert originate from major Eurasian pollution source regions. Spring is also the period of increasing solar radiation and hence photochemical activity in the Northern Hemisphere. As with the sulphur oxides, the increase of PAN levels in the spring can be related to increasing levels of OH radicals during that time of the year [*Bottenheim and Barrie*, 1996]. Since PAN is not entirely stable and will decompose (albeit very slowly under prevailing Arctic conditions) it may play a role in local oxidant chemistry which is largely unexplored.

The methodology description of the PAN measurements is found in Section 3.7.

2.7.2. IN SITU PAN MEASUREMENTS AT ALERT

PAN monitoring has continued since the fall of 1986 essentially without any instrumental changes. A record of over 10 years of data now exists and a manuscript devoted to an analysis of the data is being prepared for submission in a peer-reviewed journal. On several occasions, the data have been reported at scientific meetings [*Bottenheim*, 1987; *Bottenheim*, 1992; *Bottenheim et al.*, 1994] and they have been included in other published material [*Barrie and Bottenheim*, 1991; *Bottenheim and Barrie*, 1996; *Bottenheim et al.*, 1993; *Worthy et al.*, 1994]. Typical examples of the data are shown in Figures 2.37 to 2.39.

Figure 2.37 shows the annual cycle of PAN; clearly showing the spring maximum as discussed earlier. The period of November to June is plotted. During the summer and early fall, PAN mixing ratios drop to levels well below 100 pptv. While the method can detect mixing ratios as low as 10 pptv, these numbers are much less accurate and not used for trend calculations.

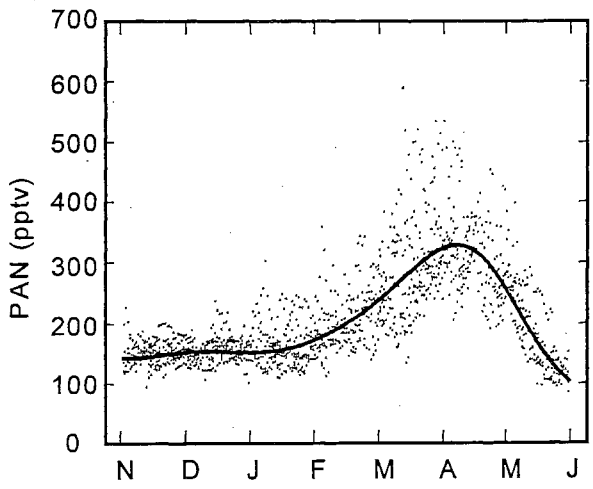

Figure 2.37 Daily PAN data for the period 1987-1997.

Figure 2.38 compares PAN data with concurrent O_3 mixing ratios in the spring during typical O_3 depletion events in 1992. These measurements were made during

the Polar Sunrise Experiment 1992 [*Barrie et al.*, 1994] and show that whatever causes the depletion of O_3 appears not to have an impact on PAN. If, as is generally accepted, the depletion of O_3 is due to Br atom chemistry, then it would seem that the reaction of PAN + Br is slow. No kinetic data exist for this reaction at the present time. Figure 2.39 compares data for inorganic and organic nitrates during two winter seasons at Alert. There are two comments to be made. Firstly, levels of PAN are almost an order of magnitude higher than those of the inorganic nitrate. In *Bottenheim et al.* [1993] it is argued that this is due to more efficient deposition loss of the inorganic nitrates during the transport from source regions to Alert. Secondly, it would appear that while the inorganic nitrates maximize in late fall or early winter, PAN maximizes in the spring. This may well be due to differences in chemical formation mechanisms where the inorganic nitrates are formed in the winter from the initial reaction of NO_2 with O_3 [*Bottenheim and Sirois*, 1996] while the PAN formation is due to OH chemistry as remarked earlier [*Bottenheim et al.*, 1994].

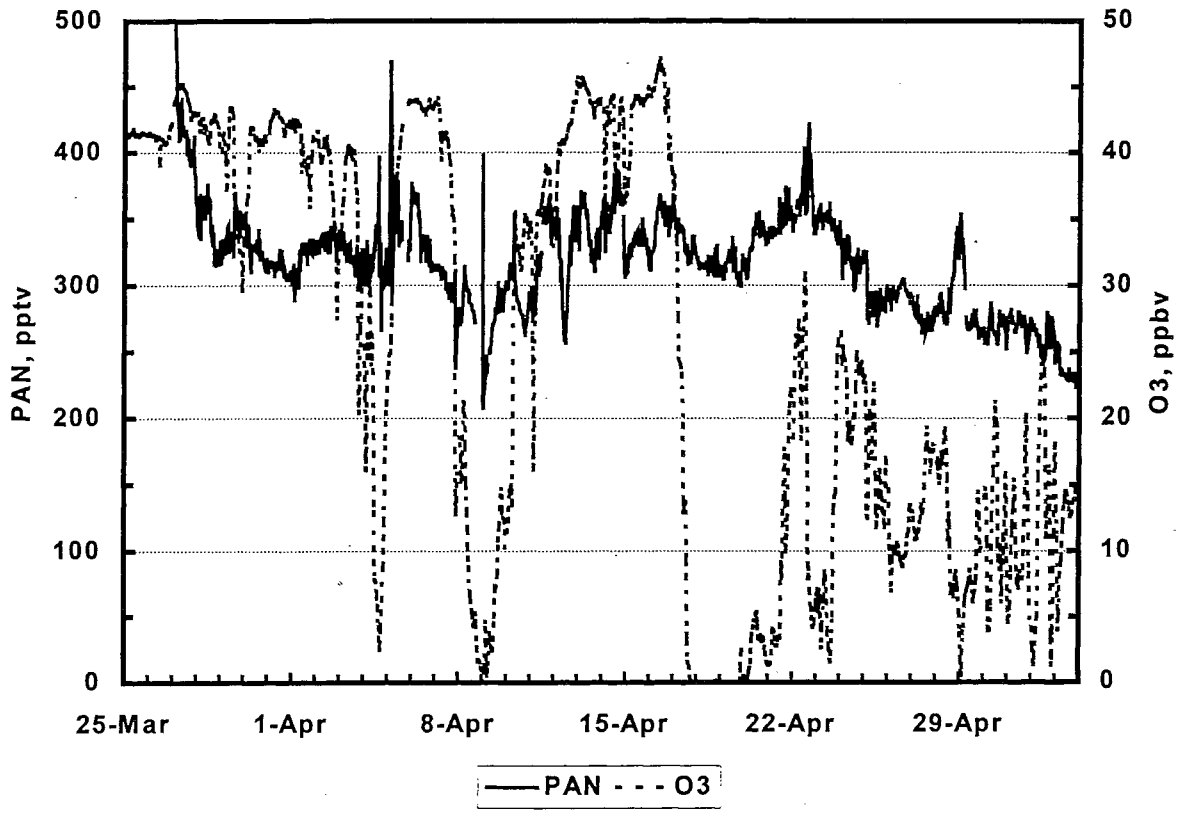

Figure 2.38 Hourly PAN and O_3, spring 1992. (O_3 data courtesy K.G. Anlauf, AES.)

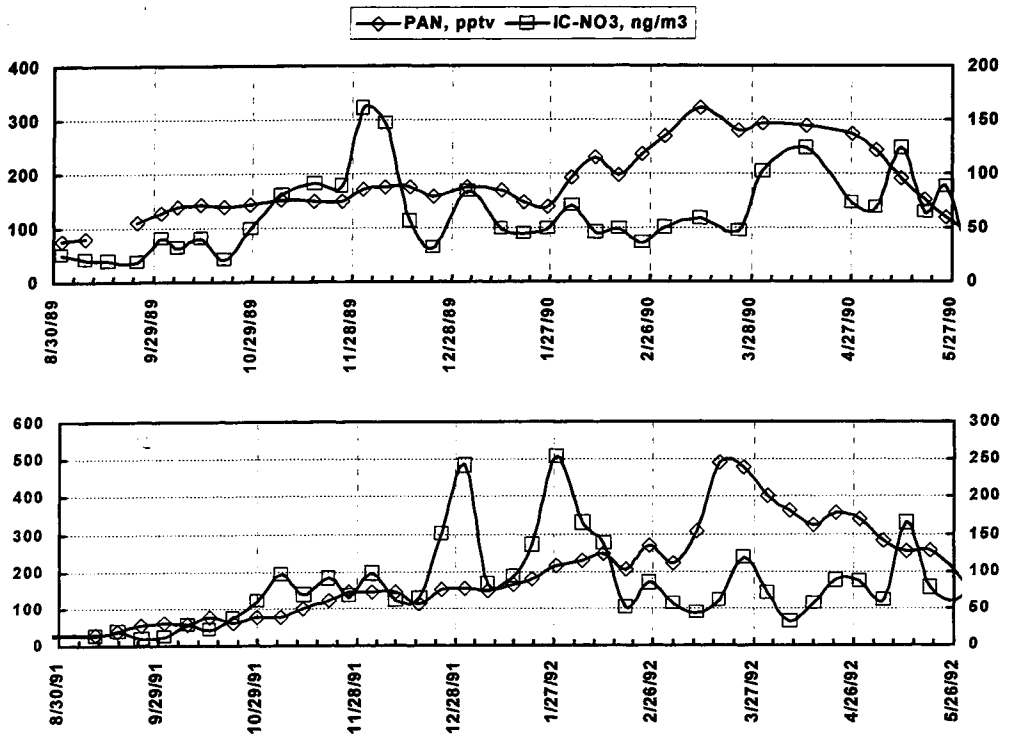

Figure 2.39 Weekly averaged PAN and total nitrate (from HiVol) for 1989/90 and 1991/92. (NO_3 data courtesy L.A. Barrie, AES.)

2.7.3 REFERENCES

Barrie, L.A., and J.W. Bottenheim, Sulphur and Nitrogen Pollution in the Arctic Atmosphere, in *Pollution of the Arctic Atmosphere*, edited by W.T. Sturges, pp. 155-183, Elseview Science Publishers, London and New York, 1991.

Barrie, L.A., J.W. Bottenheim, and W.R. Hart, Polar Sunrise Experiment 1992 (PSE 1992): Preface, *J. Geophys. Res.*, *99* (D12), 25313-25314, 1994.

Bottenheim, J.W., PAN and ozone during late winter and early spring in the Canadian high arctic, in *4th International Symposium on arctic air chemistry*, Hurdal, Norway, 1987.

Bottenheim, J.W., Six years of observations of PAN at Alert, N.W.T., Canada, in *5th International Symposium on arctic air chemistry*, Roskilde, Denmark, 1992.

Bottenheim, J.W., and A. Sirois, Long-term daily mean mixing ratios of O_3, PAN, HNO_3, and particle nitrate at a rural location in eastern Canada: Relationships and implied ozone production efficiency, *J. Geophys. Res.*, *101* (D2), 4189-4204, 1996.

Bottenheim, J.W., and L.A. Barrie, Chemical reactions in the polar troposphere relevant to C, S, and N compounds, in *Chemical exchange between the atmosphere and polar snow*, edited by E.W. Wolff, and R.C. Bales, pp. 201-224, Springer Verlag, Berlin, 1996.

Bottenheim, J.W., L.A. Barrie, and E. Atlas, The partitioning of nitrogen oxides in the lower arctic troposphere during spring 1988, *J. Atmos. Chem.*, *17*, 15-27, 1993.

Bottenheim, J.W., L.A. Barrie, and A. Sirois, Analysis of seven years of continuous observations of peroxyacetyl nitrate (PAN) at the high arctic station Alert, in *Joint meeting on global atmospheric chemistry, CACGP/IGAC*, Fuji-Yoshida, Japan, 1994.

Bottenheim, J.W., A.J. Gallant, and K.A. Brice, Measurements of NOy species and O3 at 82 N latitude, *Geophysical Research Letters*, *13*, 113-116, 1986.

Crutzen, P.J., The role of NO and NO_2 in the chemistry of the troposphere and stratosphere, Ann. Rev. Earth Planet. Sci., 7, 443-472, 1979.

Worthy, D.E.J., N.B.A. Trivett, J.F. Hopper, J.W. Bottenheim, and I. Levin, Analysis of long-range transport events at Alert, Northwest Territories, during the Polar Sunrise Experiment, *J. Geophys. Res.*, *99* (D12), 25329-25344, 1994.

2.8. MERCURY

William H. Schroeder, Alexandra Steffen and Julia Lu

2.8.1. BACKGROUND

During the 1990s, the perception of environmental mercury contamination has evolved from one of primarily local or regional-scale issues (e.g., point source releases; fish consumption advisories) to the recognition of mercury as a global pollutant. This shift in perception of the spatial scale and importance of this issue is clearly reflected in the titles and contents of the papers presented at the series of International Mercury Conferences held since 1990 [*Lindqvist*, 1991; *Watras and Huckabee*, 1994; *Porcella et al.*, 1995; *Atmospheric Environment*, 1998]. Because of its toxicity (especially in the form of methyl mercury), persistence (global atmospheric residence time: ~ 1 year) and ability to bio-accumulate in the human food chain (up to a million-fold or more), mercury has been designated as a priority chemical in the Canadian Northern Contaminants Program [*Jensen et al.*, 1997], the Arctic Monitoring and Assessment Program [*AMAP*, 1997] and the North American Free Trade Agreement/Commission of Environmental Cooperation (NAFTA/CEC) Sound Management of Chemicals Program [*CEC*, 1997]. Mercury is also one of the three heavy metals (besides cadmium and lead) for which a Protocol has recently been signed under the UN - ECE Long-Range Transport of Air Pollutants (LRTAP) Convention.

The methodology description of the Hg measurements is found in Section 3.10.

2.8.2. IN SITU HG MEASUREMENTS AT ALERT

The Arctic ecosystem is exhibiting disturbing evidence of contamination by a host of persistent, bio-accumulating toxic chemicals, including heavy metals such as mercury [*Barrie et al.*, 1997]. Prior to 1990, few data were available for atmospheric concentrations of mercury in Canada [*Schroeder*, 1981; *Schroeder and Jackson*, 1987; *Schroeder and Fanaki*, 1988; *Schroeder and Markes*, 1994] and no data at all existed for atmospheric mercury concentrations in the Canadian Arctic. From August 1992 to August 1993, using manual sampling and analysis methodology, weekly-integrated measurements of total gaseous mercury (TGM) were carried out at Alert. Results from that historic, exploratory survey yielded the first time series of atmospheric mercury concentrations anywhere in the Arctic [*Schroeder et al.*, 1995a; *Schroeder*, 1996a]. Encouraged by the success of the exploratory study, continuous automated measurements of TGM concentrations in surface-level air were initiated at Alert in January 1995.

2.8.3. DATA FROM MERCURY MEASUREMENTS AT ALERT

Prior to 1992, no data existed on atmospheric concentrations of mercury in northern Canada. The series of exploratory, ground-level mercury measurements conducted at Alert from August 1992 to August 1993 provided the first results for atmospheric mercury concentrations in the Canadian Arctic [Schroeder et al., 1995a]. Some results from this one year pilot study are shown in Figure 2.40. Interesting features of the resulting time-series of TGM measurements at Alert include: a log-normal frequency distribution of ambient air TGM concentrations, and a "weak" ($r^2 = 0.14$) annual correlation between (weekly-average) ambient air concentrations of TGM and air temperatures (measured routinely at the Alert GAW observatory) averaged over the same time periods [*Schroeder et al.*, 1995a]. Through the application of a numerical modelling technique called the "Potential Source Contribution Function" (PSCF) source-receptor model [*Cheng et al.*, 1993; *Cheng and Schroeder*, 1996], our results from this pilot study have been used to identify possible source regions of atmospheric mercury emissions in Europe, Asia and North America which may contribute to ground-level concentrations of atmospheric mercury observed at Alert. Furthermore, our Canadian baseline mercury measurement program at Alert is making a substantial contribution as well to the current scientific knowledge of the atmospheric transport, transformation and removal/deposition mechanisms and processes operating on mercury which is present in the Arctic troposphere due to releases from either natural or anthropogenic emission sources in the circumpolar regions [*Mackay et al.*, 1995].

While our manual method atmospheric TGM measurements were in progress at Alert, we were also providing scientific guidance, advice and direction to a newly incorporated Canadian company located in Toronto (Tekran, Inc.) which was developing an automated atmospheric mercury vapour analyzer. During fiscal year 1994-95, we assessed the suitability, ruggedness and reliability of this new, sophisticated Canadian instrument–the Tekran (Model 2537A) Mercury Vapour Analyzer–for possible application in making continuous real-time atmospheric TGM measurements in the Arctic. This instrument assessment process was performed in three phases: (1) extensive laboratory-based testing and evaluation

during the spring and summer of 1994 (under a variety of operating conditions, including experiments with dry and moist mixtures of other common air pollutants–sulphur dioxide, nitrogen dioxide, hydrogen sulphide–individually or in combination); (2) during September 1994, the analyzer was evaluated in a field interlaboratory intercomparison study (at a remote continental site in North-Central Wisconsin, U.S.A.) and compared well against results obtained using the traditional manual method for the measurement of total gaseous mercury in ambient air [*Schroeder et al.*, 1995c]; (3) In January 1995, with funding from the (Canadian) Department of Indian Affairs and Northern Development (DIAND) under the aegis of the federal Northern Contaminants Program, we installed and evaluated (in parallel) two of these instruments at Alert.

On the basis of the success of the three-pronged evaluation performed on the Tekran automated mercury vapour analyzer, we began an atmospheric mercury monitoring program at Alert in January 1995 with this instrument. The high frequency (either 5- or 30-minute cycles) of the real-time atmospheric TGM measurements being made at Alert since the beginning of 1995 is one of the major features distinguishing these ongoing measurements from those made during 1992 and 1993 using the traditional manual methodology, which (for logistical reasons) relied on a weekly-integrated sampling schedule. With the assistance of D. Schneeberger (Tekran Inc.) and a Co-Op student from the University of Waterloo (T. Lees), the data acquired during 1995 were processed, quality-assured and subjected to detailed analysis, both statistically and graphically [*Schroeder and Schneeberger*, 1996]. Additionally, as part of a collaborative effort with the University of Connecticut, intermittent sampling for the determination of airborne particulate-phase mercury, and mercury in snow, has also been undertaken (with the chemical analyses of these samples being performed in the ultra-trace, metal-free laboratory of W. Fitzgerald at the University of Connecticut). Results for the chemical analyses of a set of snow samples, which were collected at Alert by Alert GAW Observatory staff/students during May 1995, are shown in Figure 2.41. These results demonstrate the pronounced variability in the concentrations of mercury in snow, which are encountered at Alert during that time of the year.

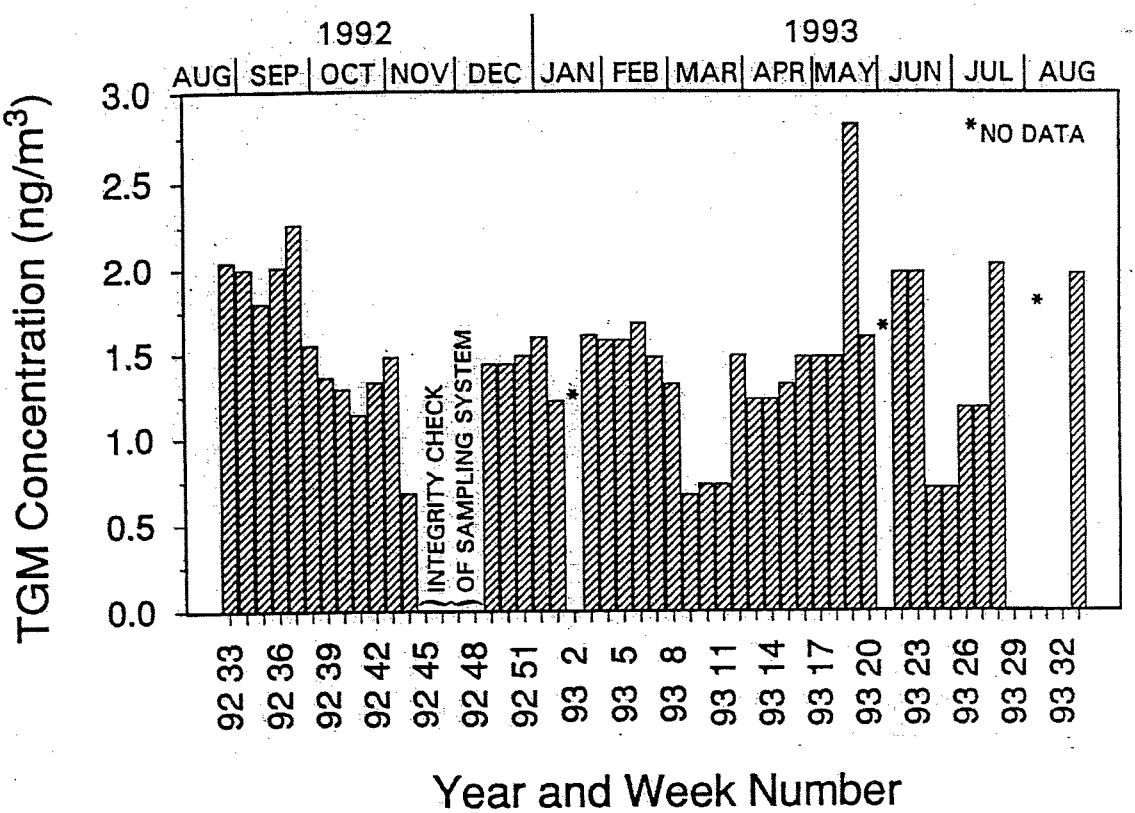

Figure 2.40 Weekly average TGM concentrations at Alert (August 1992-August 1993).

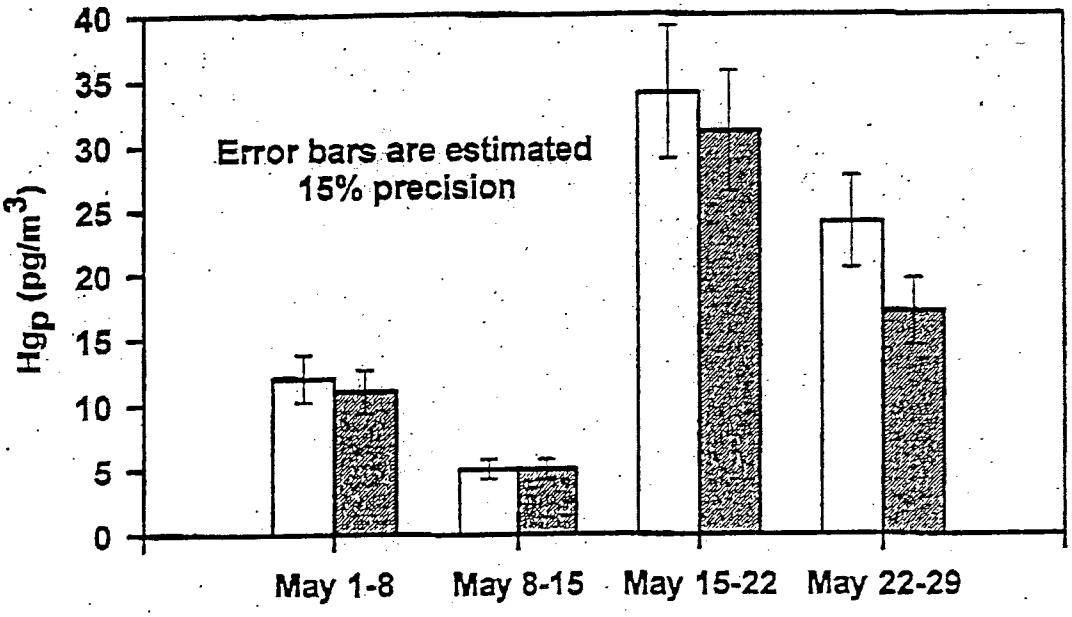

Figure 2.41 Concentrations of total and reactive mercury fractions in samples of snow collected at Alert during May 1995.

Continuous measurements of ground-level TGM concentrations have now been on-going at Alert with the Tekran mercury vapour analyzer since January 1995. At a background site such as Alert, atmospheric TGM is expected to consist predominantly of (atmospherically long-lived) elemental mercury vapour. Figures 2.42a and 2.42b show, on a seasonal basis, the total gaseous mercury concentrations that were observed at Alert during 1995. In these two (and subsequent) figures, data gaps–indicated by an asterisk–arise either from the absence of data (e.g., due to a power failure, or human error) or data which was acquired but was not included in the final (QA/QCed) data set because it did not meet our existing data quality criteria. For the purposes of this report, the four seasons of the year are defined as follows: winter = January, February, March; spring = April, May, June; summer = July, August, September; and autumn = October, November, December.

It is readily apparent that each season of the year has a distinctive pattern of TGM concentrations. During the winter months, TGM values are between 1-2 ng m^{-3}, generally oscillating around a value of about 1.6 ng m^{-3} to 1.7 ng m^{-3}. TGM values between 1 ng m^{-3} and 2 ng m^{-3} are typical of rural and remote continental locations [*Fitzgerald et al.*, 1991; *Iverfeldt*, 1991]. In spring (after polar sunrise), the variability of the observed TGM concentrations at Alert is much greater than at any other time of the year: with 6-hour average concentrations at times exceeding 2 ng m^{-3} and at other times dropping below 0.5 ng m^{-3}. Only in Antarctica have ambient air TGM values less than 0.5 ng m^{-3} been reported previously [*deMora et al.*, 1993; *Dick et al.*, 1988]. During the summer, values of TGM are generally between 1.5 ng m^{-3} and 3 ng m^{-3}, becoming increasingly less "noisy" throughout September. From October to December, the ambient air TGM concentrations at Alert are very consistent, with values between 1.4 ng m^{-3} to 1.7 ng m^{-3} being the norm. This is the type of signal one might intuitively expect to see for a substance, such as mercury vapour, which has an average global atmospheric residence time (τ) of the order of a year [*Schroeder and Munthe*, 1998], with estimates for τ ranging from ~ 0.4 to ~ 3 years [*Slemr et al.*, 1981; *Fitzgerald et al.*, 1983]. In light of the consistency demonstrated by the ground-level atmospheric mercury concentrations measured at Alert during the autumn of 1995 (Figure 2.42b) and a globally-averaged tropospheric residence time for Hg^0 of about one year, the large variability (from < 0.5 ng m^{-3} to > 2.5 ng m^{-3}) in TGM concentrations that occurred at Alert during April, May and June 1995 (Figure 2.42a) is quite anomalous and totally unexpected. This extremely interesting feature will be discussed in more detail later in this report.

Meteorological data, such as air temperature, wind speed and wind direction, are monitored routinely at the Alert observatory. The data for the year 1995 were

obtained from Mr. D. Worthy [*Personal Communications*, 1996] for the purpose of facilitating the interpretation of the atmospheric mercury measurements. Utilizing (10-metre height anemometer) wind direction data for 1995, pollution roses, based on median TGM concentrations and 30° wind direction sectors, were calculated. The resulting "spider web plots" for the first six months of 1995 (January through June) are reproduced in Figure 2.43a. During the winter months, wind directions between 120° and 300° are associated with median TGM concentrations near 1.6 ng m^{-3} to 1.7 ng m^{-3}, but TGM concentrations are somewhat lower (near 1.5 ng m^{-3}) for wind directions between 330° and 90°. In the springtime (April to June), TGM values indicative of atmospheric background concentrations (in the northern hemisphere) are only found with south-westerly winds, i.e., winds which have recently passed over the mountainous terrain typical of Ellesmere Island. For a more detailed description of the geographical features surrounding Alert, the reader is referred to *Hopper and Hart* [1994]. With the exception of the TGM values measured when the prevailing wind direction was around 30 ± 15 degrees, all other remaining wind directions produced median TGM concentrations which were below the expected background levels for a remote site such as Alert. It is conceivable that the elevated TGM value obtained at the Alert observatory for wind directions between 15 to 45° may be due to human activity (e.g., fossil fuel combustion for heating, waste incineration, periodic burning of old construction/building materials, vehicular and aircraft traffic) at the Canadian Forces Station (CFS) Alert, which is about 6 km to the north-northeast on the edge of the Lincoln Sea, or human activity at the observatory itself. The most pronounced depression in TGM concentrations occurred with winds from the north to northwest (i.e., in air having recently come from over the Arctic Ocean).

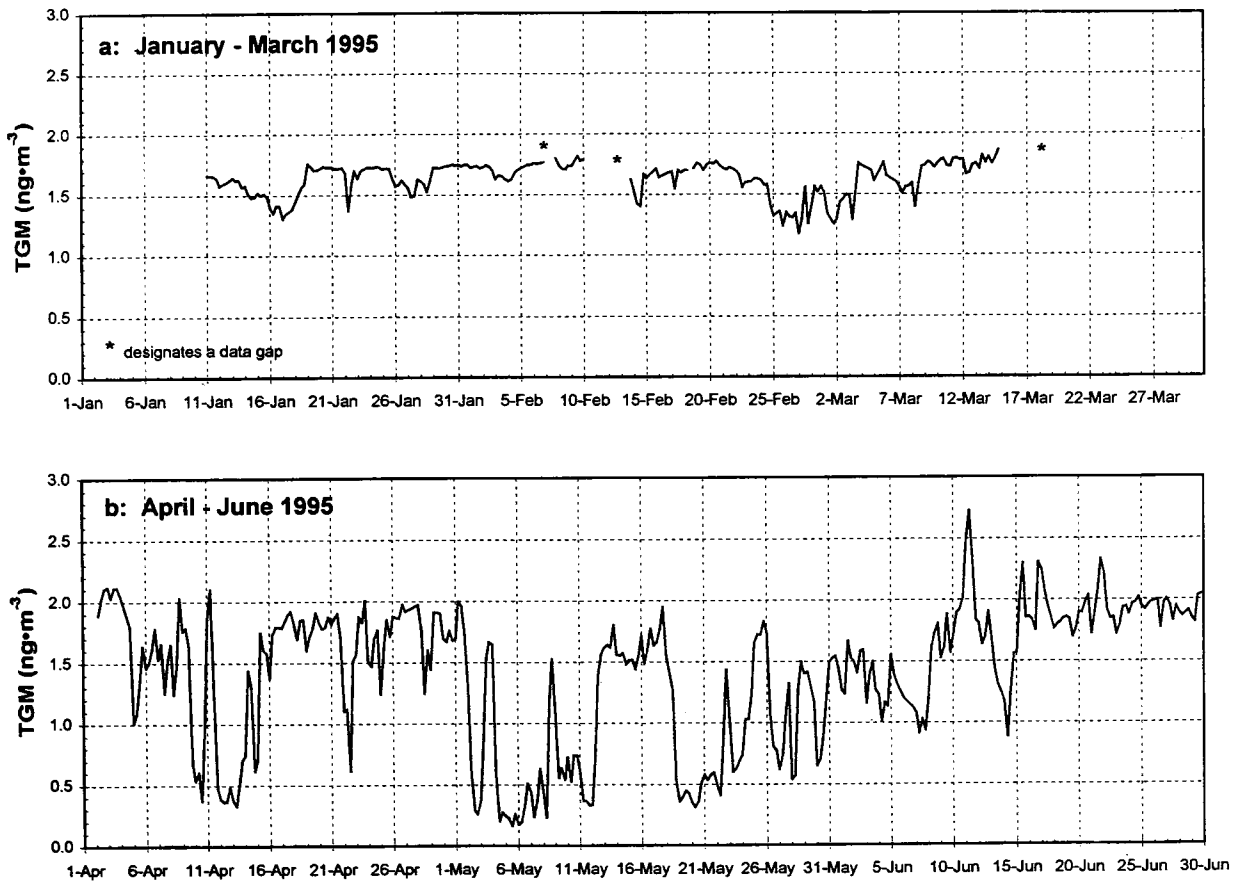

Figure 2.42a Atmospheric concentrations (6-hour averages) of total gaseous mercury (TGM) measured at Alert during 1995 (January to June).

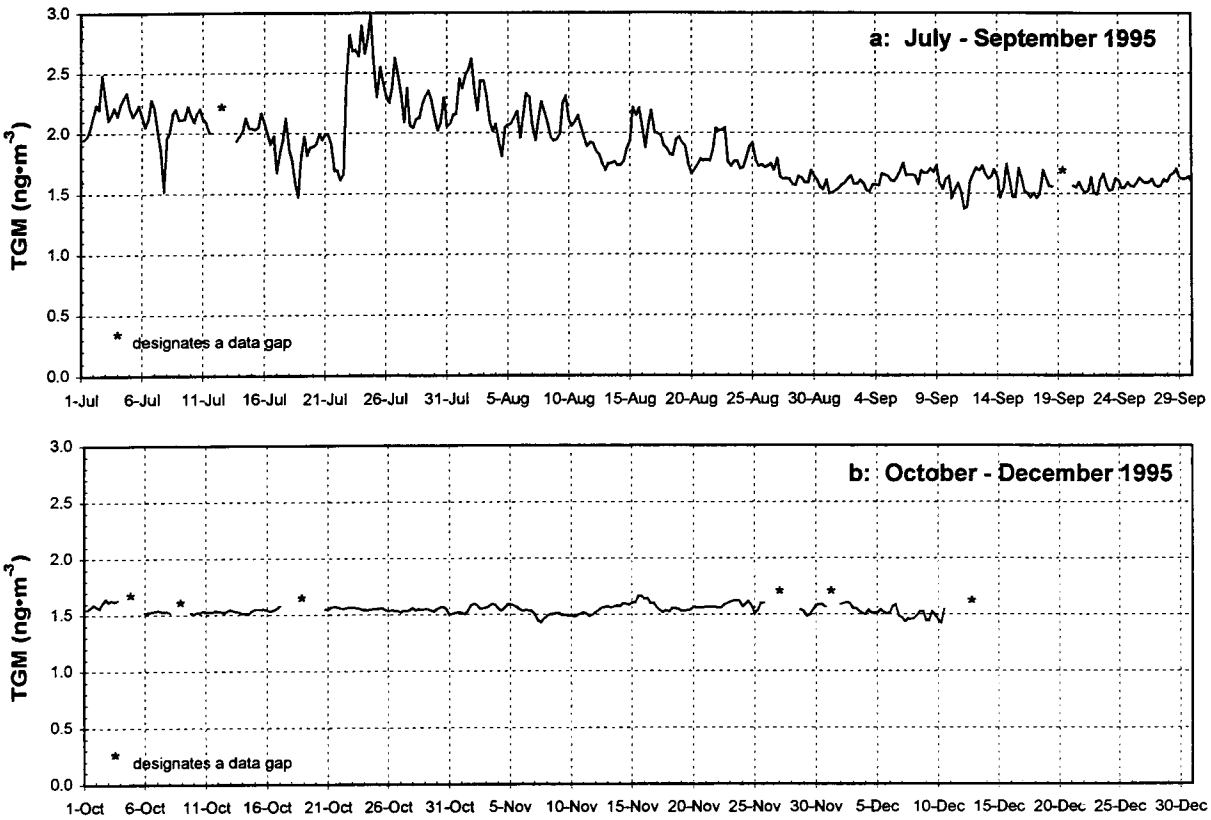

Figure 2.42b Atmospheric concentrations (6-hour averages) of total gaseous mercury (TGM) measured at Alert during 1995 (July to December).

However, as is evident from Figure 2.43b, during the summer (July to September) of 1995 TGM levels higher than the typical background values were observed with all wind directions other than the southwesterly sector. Median values higher than 2 ng m^{-3} occurred when winds were coming from the sector bounded by ~ 350 to ~ 65° (i.e., north-to-northeast winds). Yet another significantly different temporal pattern existed during the period from October to December 1995, when the median values of the TGM concentrations which existed in ground-level ambient air at Alert (practically invariant at around 1.5 ng m^{-3} to 1.6 ng m^{-3}, viz., the present-day northern hemispherical background values) were virtually independent of surface level (10 m) wind direction. This is the type of pattern one might expect to see, at least at remote (baseline) sites, for an atmospheric pollutant that is long-lived and well-mixed throughout the troposphere. This hypothesis is supported rather well by the pollution roses for January to March and for October to December, which are nearly symmetrical in their shape. Experimental evidence that mercury vapour is, indeed, well-mixed in the atmosphere (at least up to an altitude of 5 km) has recently been obtained from aircraft measurements in Atlantic Canada [*Banic et al.*, 1997].

Ground-level ozone is one of a number of air quality parameters which have been measured at Alert for more than a decade [*Anlauf et al.*, 1994; *Bottenheim et al.*, 1986]. Thus it was of interest to us to obtain these data for the year 1995 for the purpose of comparison with our TGM data. In Figures 2.44a and 2.44b we have plotted, on the same graph, the time series for our 6-hour average concentrations of surface-level TGM and for the similarly-averaged surface-level ozone concentrations measured simultaneously at the Alert GAW Observatory by K. Anlauf and his colleagues at AES. A striking similarity is immediately recognizable in the concentration profiles of these two air contaminants, at least during the period from January to the end of May 1995 and again from September onwards until December of the same year.

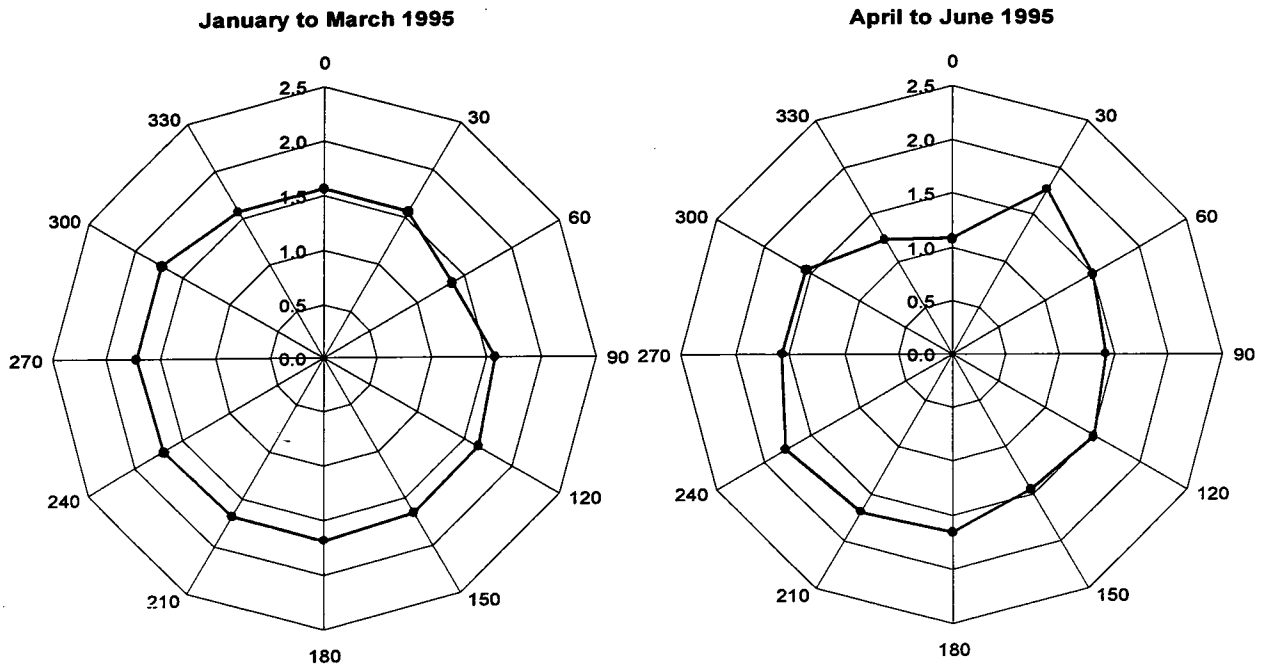

Figure 2.43a Pollution roses of median TGM concentrations in ambient air from twelve different 30° wind direction sectors at Alert during 1995 (January to June). TGM values shown as solid circles are given in ng m^{-3}. (Each wind direction sector encompasses 15° on either side of the given directional value).

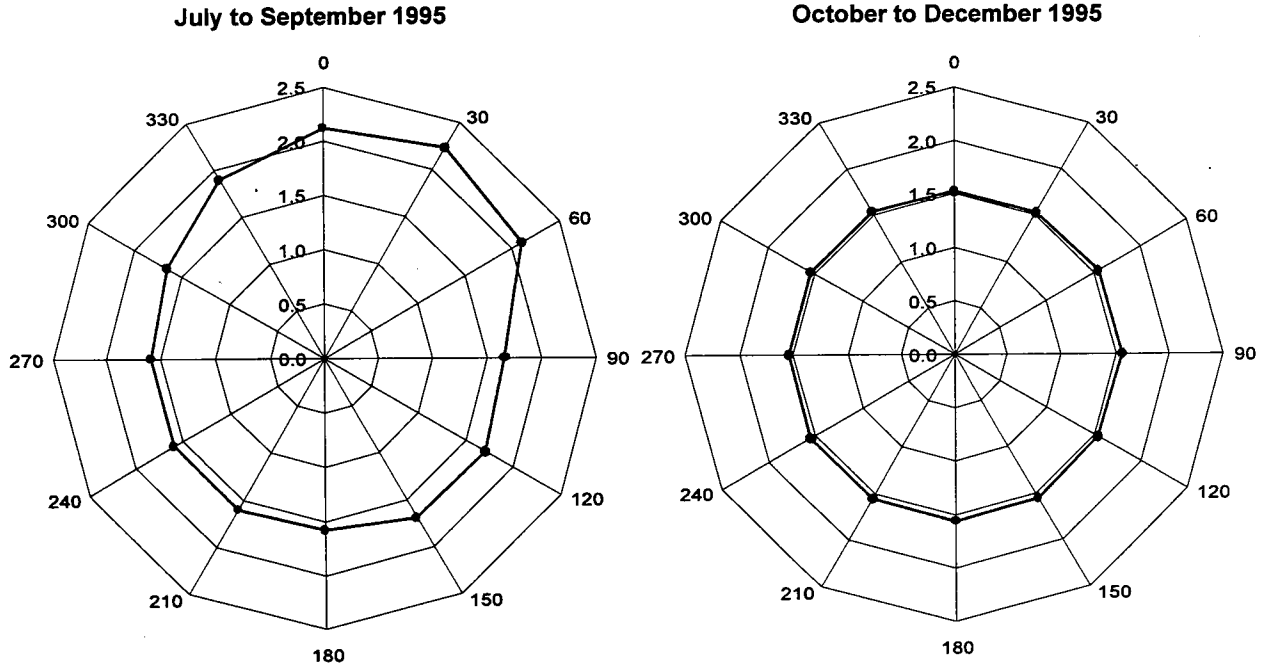

Figure 2.43b Pollution roses of median TGM concentrations in ambient air from twelve different 30° wind direction sectors at Alert during 1995 (July to December). TGM values shown as solid circles are given in ng m^{-3}. (Each wind direction sector encompasses 15° on either side of the given directional value).

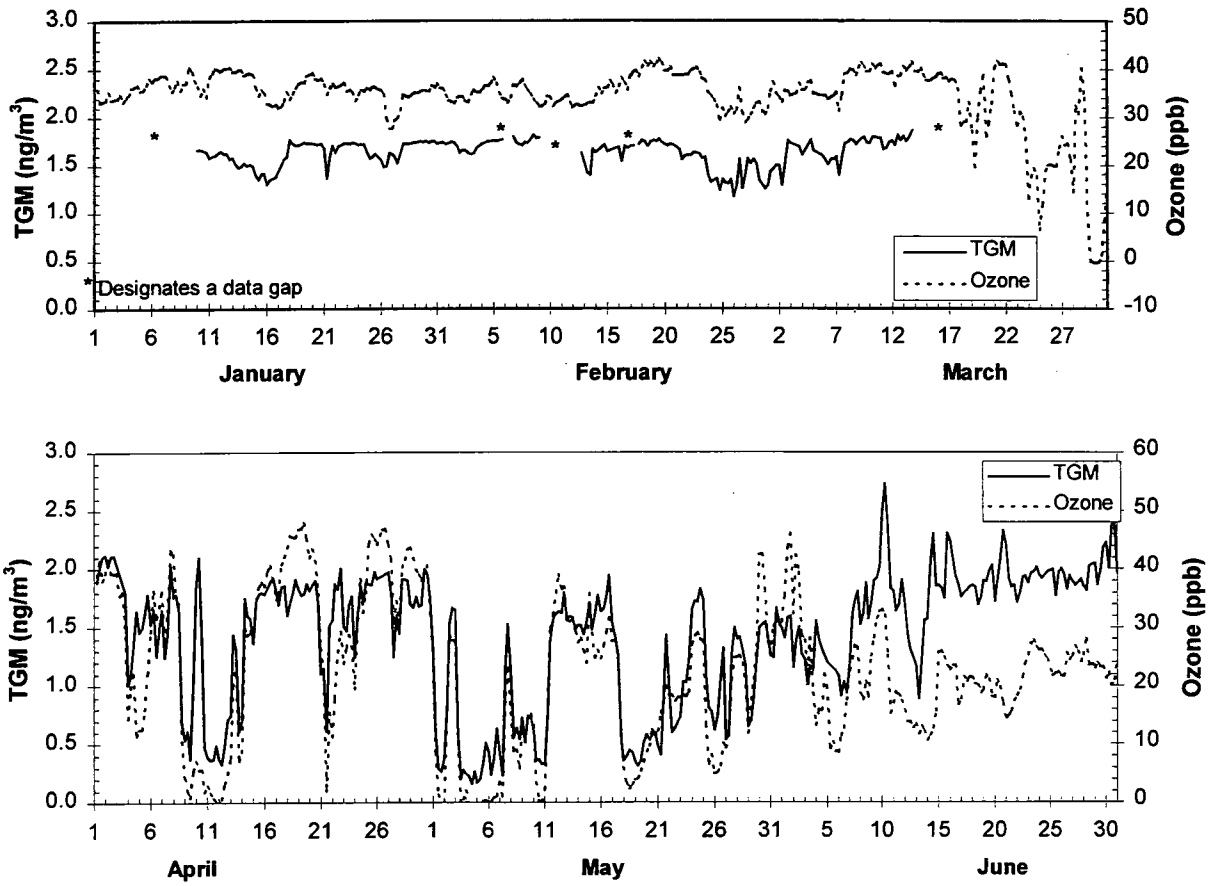

Figure 2.44a Atmospheric concentrations (6-hour averages) of total gaseous mercury (TGM) and ground-level ozone measured at Alert, NWT, during 1995 (January to June).

This co-variance between ground-level (boundary-layer) ozone and mercury vapour is directly supported by the method-of-least-squares linear correlation plots, which are shown in Figures 2.45a and 2.45b, on a seasonal basis. For the winter period, the coefficient (r^2) for the positive correlation between Hg^0 and O_3 was determined to be 0.26, but it increased to 0.51 for the springtime. If we select the time period from the beginning of April to the end of May (that period during which there was the most pronounced variability in both the TGM and the O_3 concentrations) the correlation coefficient (r^2) reaches a value of 0.8 [*Schroeder et al.*, 1997a]. In other words, TGM and ozone are co-varying with an 80% probability.

Interestingly, the data suggest that a weak anti-correlation (with an r^2 value of only 0.07, however) existed between ozone and TGM concentrations during the summer of 1995, which then reverted to a positive correlation in the autumn months. The strong correlation between the fluctuations of the atmospheric concentrations of ozone and mercury is completely unexpected, since the only physical-chemical property that these two substances have in common is that they are both present in the atmosphere in the gas phase. In all other respects these two chemicals are vastly different. For example, mercury is released into the atmosphere from both natural as well as anthropogenic sources (emissions from the latter making it an important primary air pollutant) whereas ozone is a secondary pollutant (associated with "smog") which is produced in ambient air by the interaction of sunlight with mixtures of volatile organic compunds, VOCs (primarily unsaturated hydrocarbons from vehicular emissions) and nitrogen oxides, NO_x, from a variety of combustion sources. Also, O_3 exists in ambient air as a molecule with a molecular weight of 48 Daltons, whereas mercury is present in the troposphere predominantly in the mono-atomic (elemental) gaseous form (with an atomic weight of 200 Daltons).

Several laboratory investigations have been conducted into the gas phase reaction between elemental mercury (Hg^0) vapour and ozone [*Hall*, 1995; *Schroeder et al.*, 1991; *Lindqvist and Rodhe*, 1985; *P'yankov*, 1949]. From these studies, it has been concluded [*Hall*, 1995] that the chemical reaction between these 2 substances is slow (in the case of a first-order dependence on the ozone concentration), especially when extrapolated to environmental conditions and typical non-urban or non-industrial atmospheric concentrations, and that the "partly heterogeneous" reaction has a rate constant of $3\pm2 \times 10^{-20}$ cm^3 $molec^{-1}$ s^{-1} at 20° C. This would correspond, in temperate climatic zones, to an atmospheric half-life of Hg^0 of about 1 year at a mean global O_3 concentration of 30 parts per billion, in good agreement with estimates made by other means [*Lindqvist and Rodhe*, 1985]. Kinetic (laboratory) experiments of the aqueous phase reaction between O_3 and Hg^0 [e.g., *Iverfeldt and Lindqvist*, 1986; *Munthe*, 1992] and results obtained in a recent field study [*Poissant*, 1997] suggest, however, that the (heterogeneous) reaction between these two air pollutants might be of atmospheric significance, at least in warmer climates. Thus, under conditions representative of the Arctic (low concentrations of both Hg^0 and O_3, and temperatures well below 0° C except for the months of July and/or August), one could certainly expect that this reaction would be too slow to be of importance in converting Hg^0 to Hg^{2+} in polar regions.

Previously we saw that, in 1995, the near-surface tropospheric TGM concentrations at Alert exhibited a very pronounced increase in their variability after polar sunrise. Furthermore, there was a striking, yet completely unexpected, similarity in the TGM and near-surface ozone concentration patterns observed at Alert [*Schroeder et al.*, 1997; *Schroeder et al.*, 1998]. The TGM concentrations measured at Alert during 1996 are given in Figures 2.46a and 2.46b.

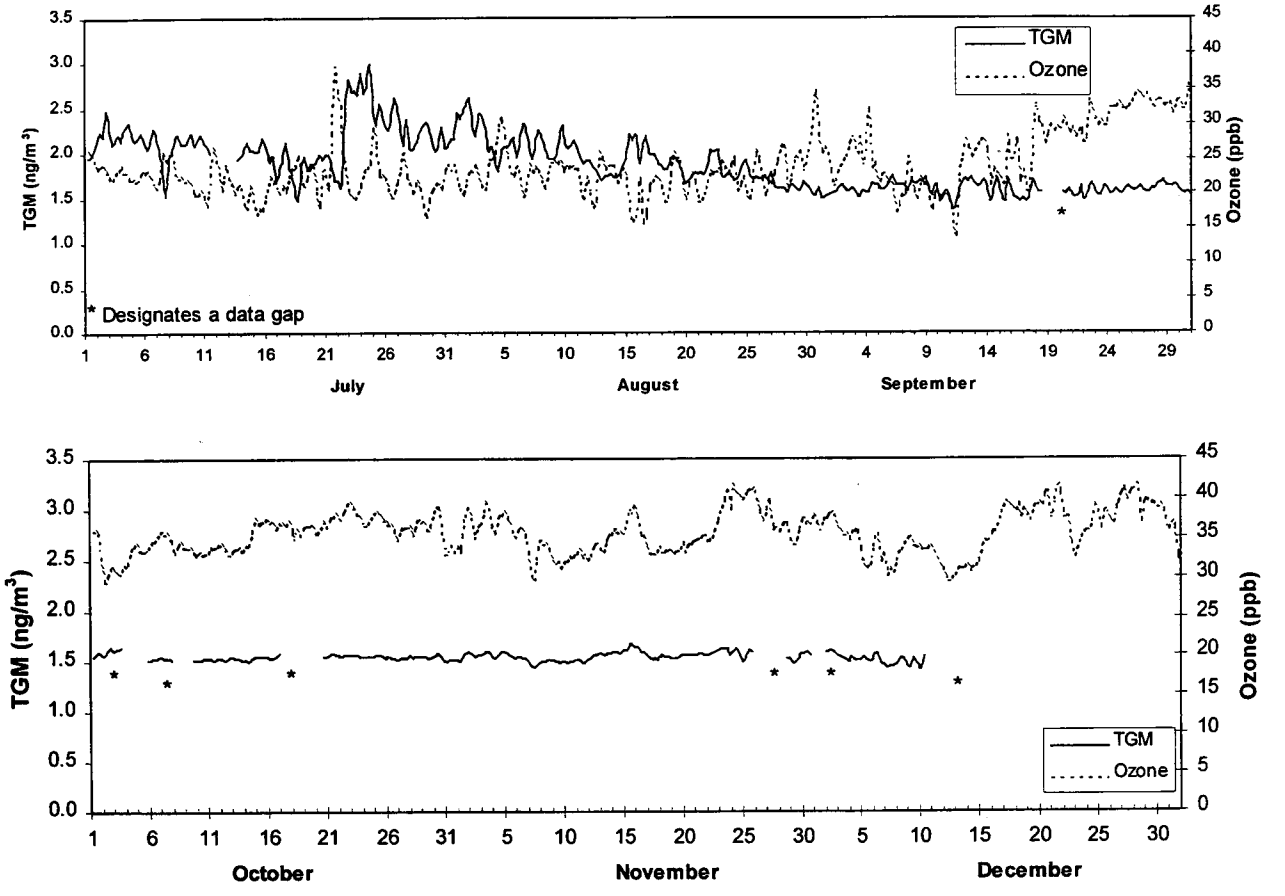

Figure 2.44b Atmospheric concentrations (6-hour averages) of total gaseous mercury (TGM) and ground-level ozone measured at Alert, NWT, during 1995 (July to December).

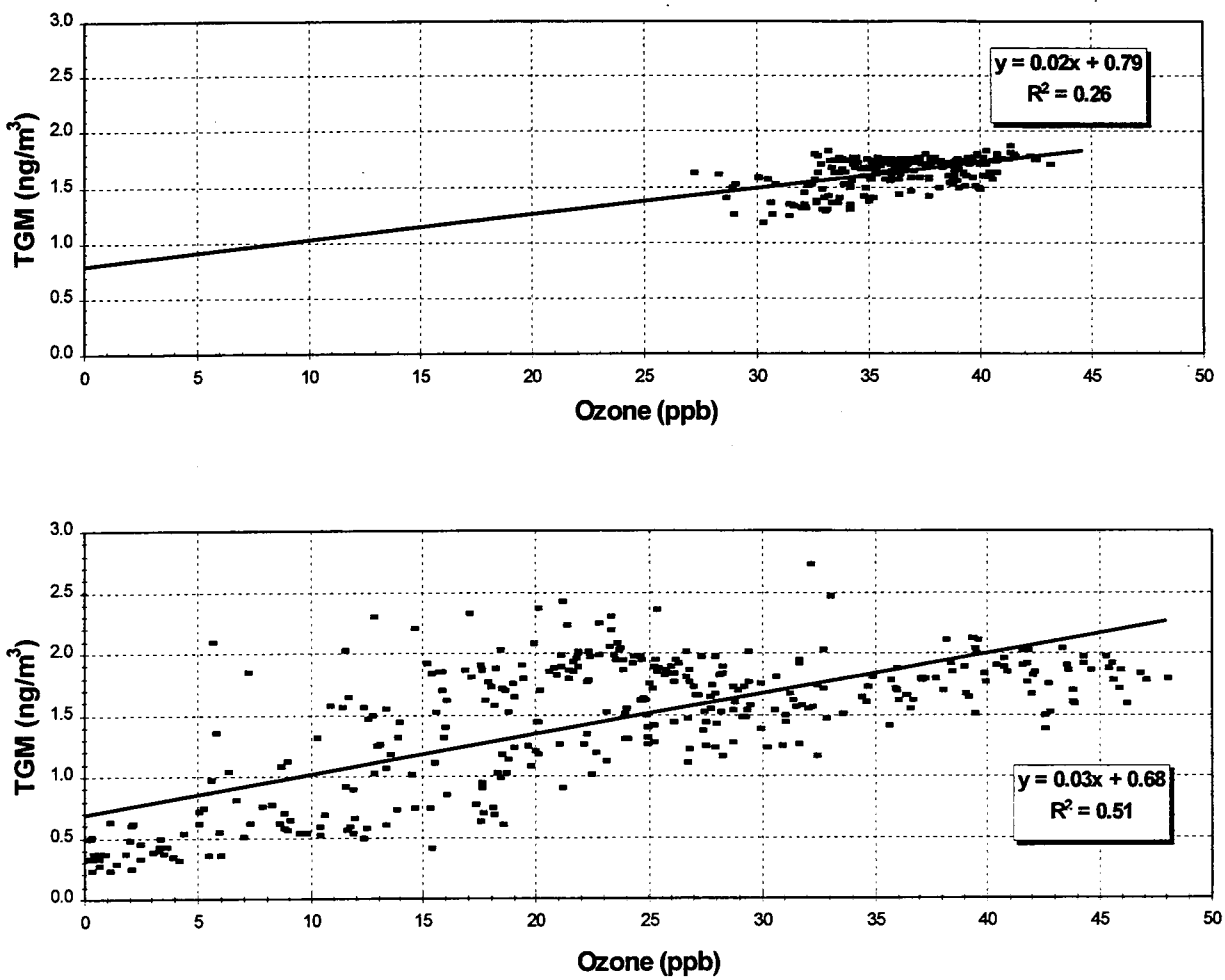

Figure 2.45a Correlation of ground-level ozone and TGM concentrations (6-hour averages) measured at Alert, NWT, during 1995 (January to June).

Inspection of Figures 2.46 a and b shows that, starting in March (i.e., after polar sunrise) and continuing throughout the April to mid-June period, the surface-level atmospheric concentrations of TGM are again much more variable than at other times of the year and anomalously low concentrations (values significantly less than 0.5 ng m^{-3}) occur periodically. This is also the time of the year during which severe ozone depletion episodes are observed at Alert [*Bottenheim et al.*, 1986; *Barrie et al.*, 1988; *Anlauf et al.*, 1994; *Barrie*, 1996; *Barrie and Platt*, 1997]. In the case of ozone, the depletion has been attributed to advection from over the Arctic Ocean of a shallow layer of air in which O_3 has been consumed through its interaction with highly reactive chemicals/free radicals (notably inorganic bromine- and possibly other halogen-species). These highly reactive halogen species are photochemically generated in the lower troposphere when sunlight returns to the Arctic after several months of continuous darkness. The reason(s) for the highly variable and, at times unusually low, TGM concentrations observed at Alert during the two to three months following polar sunrise are not yet known, but work is in progress to elucidate this special springtime polar atmospheric chemistry phenomenon.

One possibility for the unusually low values of TGM that occur at Alert in the springtime is a sampling/measurement artifact: a so-called gold cartridge "passivation" or "blocking effect" which has been previously described by *Brosset and Iverfeldt* [1989] and by *Schroeder et al.* [1995b]. Such an artifact could result from incomplete collection of mercury vapour by the pre-concentrating gold

cartridges in the automated analyzer, caused by the presence of highly reactive chemical species which are produced through chemical/photochemical processes taking place in the polar atmosphere during that time of the year. Another (less likely) possibility could be quenching of the fluorescence signal measured by the instrument, owing to incomplete flushing of the air (or a chemical 'contaminant') introduced into the instrument with the sample being analyzed.

Hence, during March/April 1997 (in conjunction with *Polar Sunrise Experiment 1997*), a variety of tests and diagnostic experiments/procedures were performed at Alert to either confirm, or rule out, the existence of such a sampling/measurement artifact. Two Tekran mercury vapour analyzers were operated in parallel (with sample integration periods reduced from 30 minutes to 5 minutes). By activating the internal permeation source of the Tekran analyzer, "standard additions" of precisely known amounts of Hg^0 vapour (to yield resultant TGM concentrations of close to 18 ng m^{-3}) were regularly 'spiked' into the ambient air sample of one of the instruments (Serial No. 007) near the end of the sampling period. Meanwhile the other instrument (Serial No. 012) was monitoring the TGM concentrations in the ambient air. As can be seen in Figure 2.47, the response expected for instrument No. 007 (i.e., TGM concentrations close to 18 ng m^{-3}), obtained by subtracting the ambient air TGM concentration from the total concentration (standard addition plus ambient air concentration), was registered consistently, even at times when depletion events were being recorded by the other instrument (Serial No. 012). Furthermore, at times in between the standard addition runs, the concentration readings of both instruments tracked each other very well. These diagnostic *in situ* field experiments, in addition to sampling line integrity checks and Hg^0 vapour spike recovery tests, provided conclusive evidence that the very low concentrations of TGM associated with the spring-time (post polar sunrise) mercury vapour depletion events – which are coincident with surface-level ozone depletion – are indeed real and are not caused by a sampling/measurement artifact affecting the automated instrumental measurement procedure (Tekran analyzer) used at Alert.

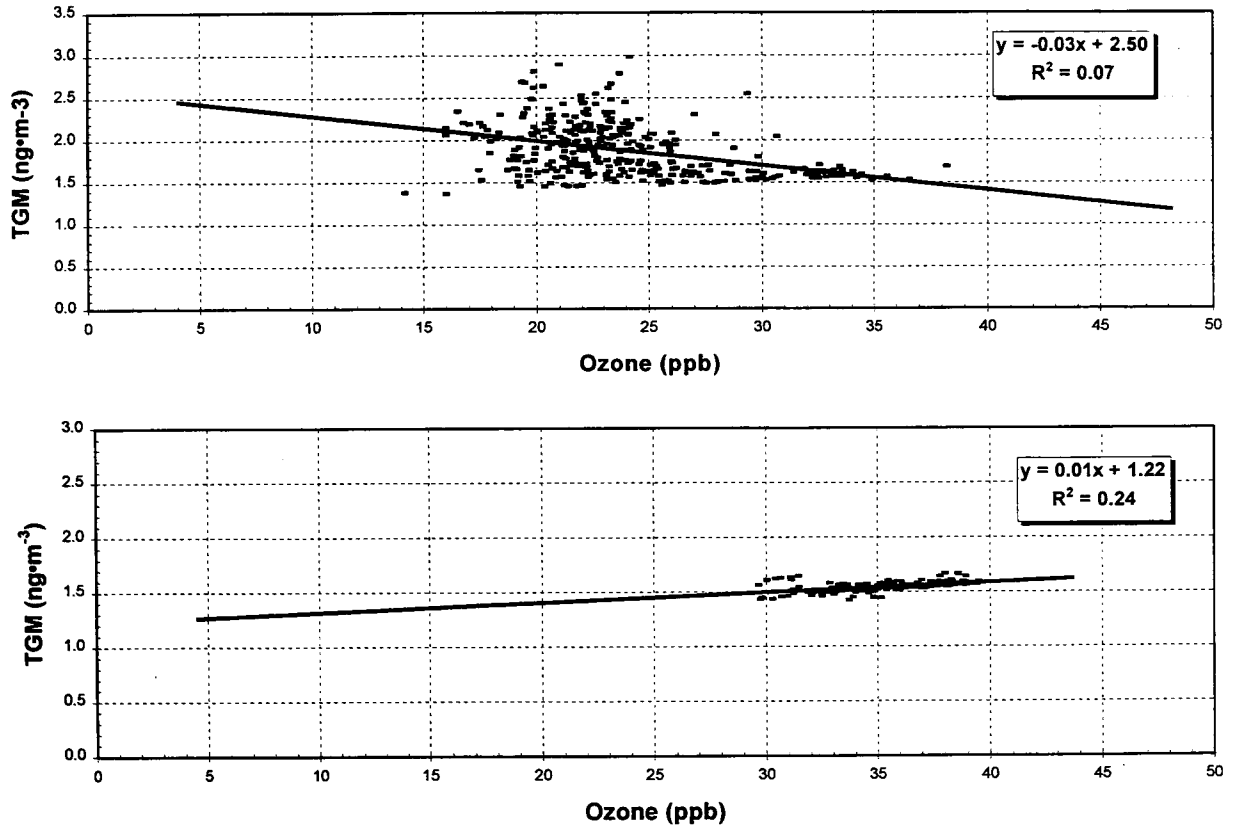

Figure 2.45b Correlation of ground-level ozone and TGM concentrations (6-hour averages) measured at Alert, NWT, during 1995 (July to December).

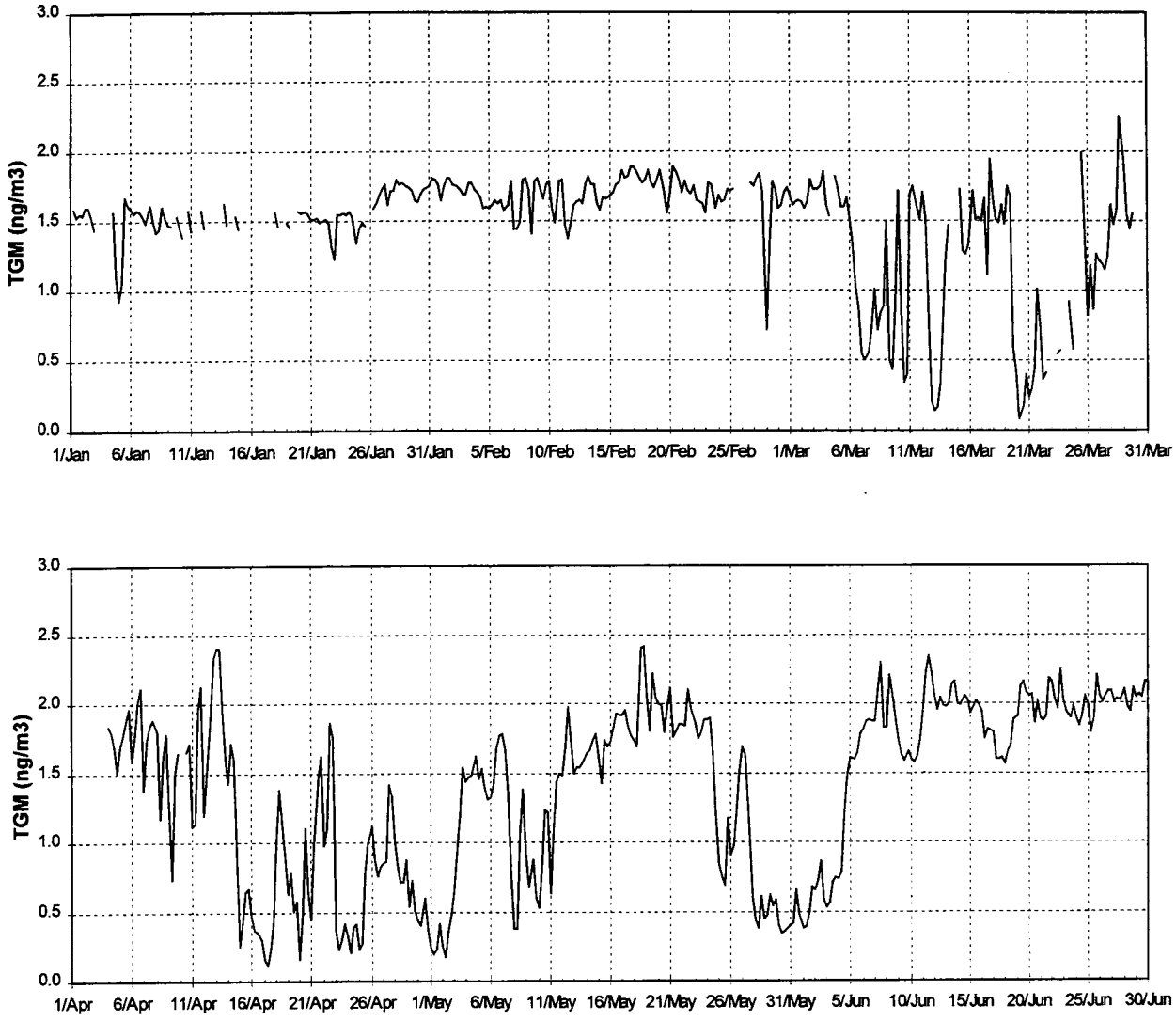

Figure 2.46a Atmospheric concentrations (6-hour averages) of total gaseous mercury (TGM) measured at Alert, NWT, during 1996 (January to June).

Using a novel method recently developed at AES [*Schroeder*, 1996b; *Lu* 1997; *Lu et al.*, 1997; *Lu et al.*, 1998] alongside the traditional weekly-integrated sampling procedure, particulate-phase mercury samples were also collected at Alert during April 1997. Preliminary results (Figure 2.48) indicate that the concentrations of total particulate-phase mercury (TPM) increased substantially during those times following polar sunrise when the TGM concentrations were well below 1 ng m^{-3} (i.e., during TGM depletion periods). This is what would be expected if a chemical reaction mechanism is responsible for the observed depletion of the gaseous-phase mercury in ambient air. In this scenario, one or more of the highly reactive chemical species which are known to be produced in the Arctic boundary layer after polar sunrise [*Barrie et al.*, 1988; *Bottenheim et al.*, 1990; *Li et al.*, 1994; *Mozurkewich*, 1995; *Pearce*, 1997; *Schroeder et al.*, 1997b] react(s) with and oxidizes the normally inert, gaseous mercury fraction (consisting mainly of elemental mercury vapour) to one or more compound(s) of mercury with vapour pressure(s) substantially below that of Hg°. The much less volatile compound(s), such as a mercury halide or an oxide, for example, would preferentially exist in the particle-phase rather than in the gas-phase under the environmental conditions prevailing in the Arctic.

The significance of our discovery of springtime depletion of TGM concentrations at Alert (and most

likely in other polar regions as well) lies in the fact that the associated reaction(s) provide(s) an environmental pathway for converting the normally inert (and hence long-lived) and relatively insoluble gaseous form of mercury (viz., Hg°), which constitutes the predominant species of mercury in the atmosphere, to the particulate phase (containing oxidizing Hg species) having a much shorter atmospheric residence time, since particles/aerosols are more readily deposited from the atmosphere to (Arctic) terrestrial and aquatic ecosystems.

Probably of even more importance for the Arctic environment and its biosphere/food chain is that this chemical transformation of Hg° presumably yields Hg^{2+}, which is the substrate (i.e., starting material) for the biological (and/or abiotic) methylation of inorganic mercury to organo-metallic methyl mercury, the most toxic form of this heavy metal [*Fitzgerald et al.*, 1994]. It is the methyl mercury species which has the unique ability to bio-accumulate in the human food chain and cross the blood-brain barrier as well as the walls of the placenta. This invasive potential of the methylated form of mercury can lead to serious neurological damage, particularly in fetuses and young children, once it is taken up into the human body through consumption of fish from mercury-tainted waters. Thus, our finding has considerable ecological and toxicological implications for people living in the north.

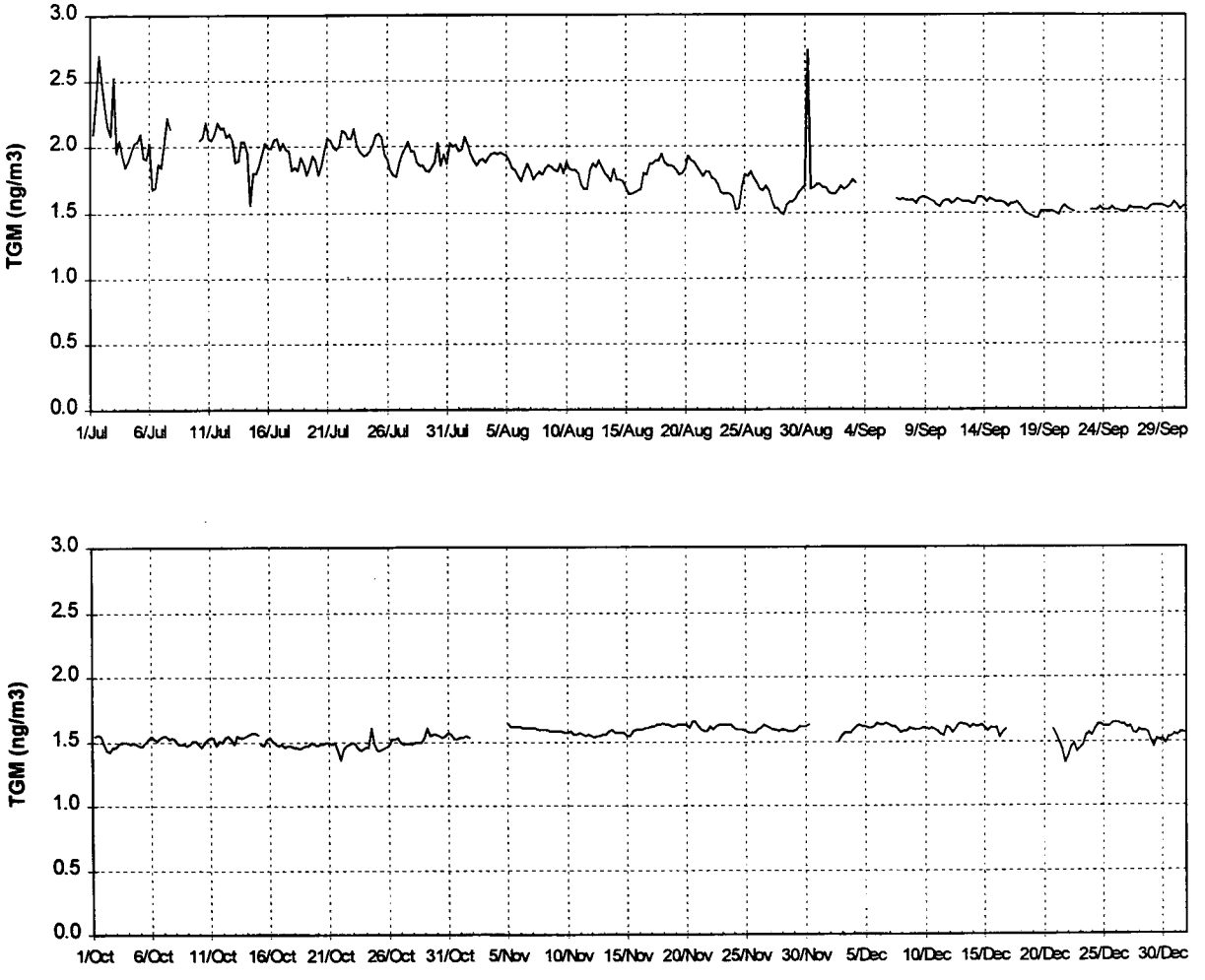

Figure 2.46b Atmospheric concentrations (6-hour averages) of total gaseous mercury (TGM) measured at Alert, NWT, during 1996 (July to December).

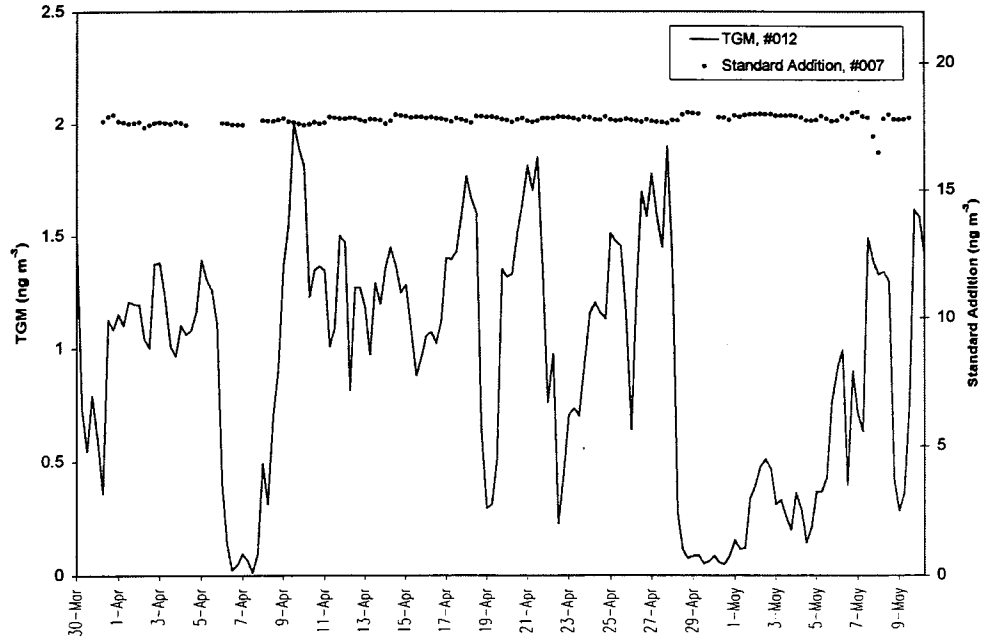

Figure 2.47 Results of standard addition diagnostic tests performed with the Tekran mercury vapour analyzers at Alert during spring 1997.

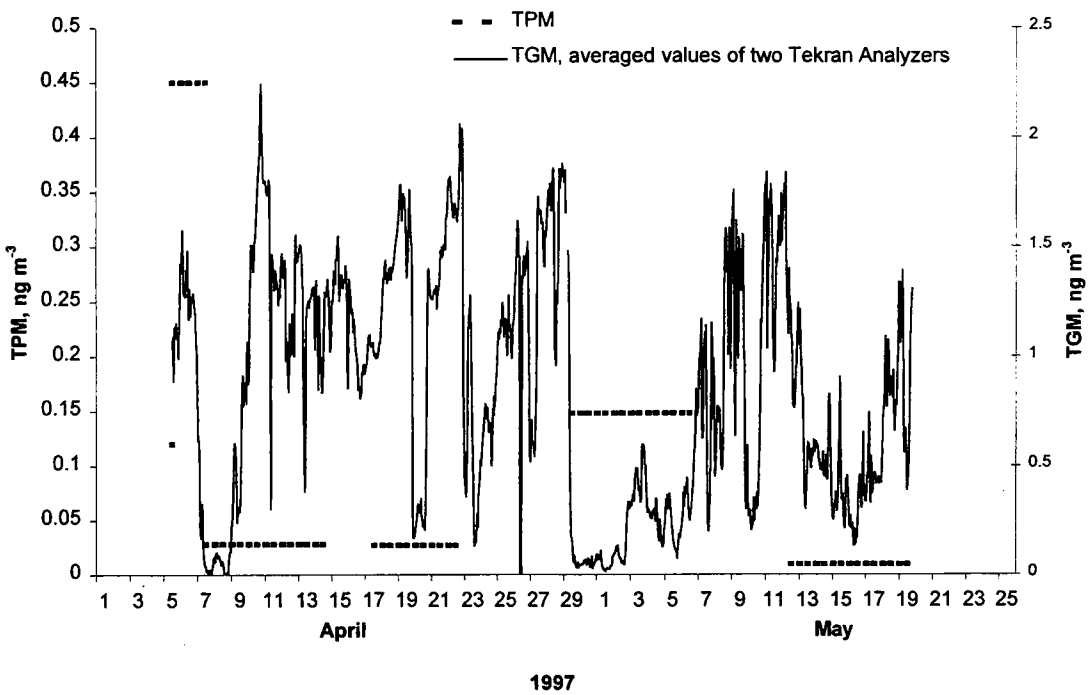

Figure 2.48 Results of concurrent measurements of total gaseous mercury (TGM) and total particulate-phase mercury (TPM) in ground-level ambient air at Alert during April and May 1997.

2.8.4. REFERENCES

AMAP, 1997. *Arctic Pollution Issues: A State of the Arctic Environment Report.* Arctic Monitoring and Assessment Programme, Oslo, Norway. 188 pp.

Anlauf K.G., Mickle R.E. and Trivett N.B.A., 1994. Measurement of ozone during polar sunrise experiment 1992. J. Geophys. Res. **99**(D12): 25, 345-25, 353.

Banic C.M., Schroeder W.H., Beauchamp S.T. and Tordon R.J., 1997. Concentrations of mercury in the troposphere at altitudes up to 5 km in the vicinity of southern Nova Scotia, Canada. Fall Meeting, American Geophysical Union, San Francisco, California. December 8-12.

Barrie L.A., Bottenheim J.W., Schnell R.C., Crutzen P.J. and Rasmussen R.A., 1988. Ozone destruction and photochemical reactions at polar sunrise in the lower Arctic atmosphere. Nature **334**: 138-141.

Barrie L.A., 1996. Occurrence and trends of pollution in the Arctic troposphere. In: *Chemical Exchange Between the Atmosphere and Polar Snow.* Wolff E.W. and Bales R.C. (Eds.), NATO ASI Series, Vol. I 43. Springer-Verlag, Berlin.

Barrie L.A. and Platt U., 1997. Arctic tropospheric chemistry: an overview. Tellus **49B**: 450-454.

Barrie L., Macdonald R., Bidleman T., Diamond M., Gregor D., Semkin R., Strachan W., Alaee M., Backus S., Bowers M., Gobeil C., Halsall C., Hoff J., Li A., Lockhart L., Mackay D., Muir D., Pudykiewicz J., Reimer K., Smith J., Stern G., Schroeder W., Wagemann R., Wania F. and Yunker M., 1997. Chapter 2. Sources, Occurrence and Pathways. In: Jensen J., Adare K. and Shearer R. (Eds.), *Canadian Arctic Contaminants Assessment Report*, Indian and Northern Affairs Canada, Ottawa.

Bottenheim J.W., Gallant A.C. and Brice K.A., 1986. Measurements of NO_y species and O_3 at 82° N latitude. Geophys. Res. Lett. 13: 113-116.

Bottenheim J.W., Barrie L.A., Atlas E., Heidt L.E., Niki H., Rasmussen R.A. and Shepson P.B., 1990. Depletion of lower tropospheric ozone during Arctic spring: the polar sunrise experiment 1988. J. Geophys. Res. **95**(D11): 18,555-18,568.

CEC, 1997. *Continental Pollutant Pathways.* Commission for Environmental Cooperation, Montreal, Que. 44 pp.

Cheng M.-D., Hopke P.K., Barrie L., Rippe A., Olson M. and Landsberger S., 1993. Qualitative determination of source-regions of aerosol in the Canadian High Arctic. Environ. Sci. Technol. **27**: 2063-2071.

Cheng M.-D. and Schroeder W.H., 1996. Identification of sources of atmospheric mercury in the Canadian Arctic using Potential Source Contribution Function (PSCF) modelling. Fourth International Conference on Mercury as a Global Pollutant. Hamburg, Germany, August 4-8.

deMora S.J., Patterson J.E. and Bibby D.M., 1993. Baseline atmospheric mercury studies at Ross Island, Antarctica. Antarctic Science **5**: 323-326.

Dick A.L., Orange C.J., Sheppard D.S. and Patterson J.E., 1988. Ultratrace determination of mercury in air, water and snow using photoacoustic mercury analysis. In: *Trace Elements in New Zealand: Environmental, Human and Animal. Proc. New Zealand Trace Elements Group Conference.* Lincoln College, Canterbury, New Zealand. 30 Nov.- Dec. 2.

Fitzgerald W.F., Gill G.A. and Hewitt A.D., 1983. Air-sea exchange of mercury. In: *Trace Metals in Sea Water*, Wong C.C.S., Boyle E., Bruland K.W., Burton J.D. and Goldberg E.D. (Eds.), Plenum Press, New York.

Fitzgerald W.F., Mason R.P. and Vandal G.M., 1991. Atmospheric cycling and air-water exchange of mercury over mid-continental lacustrine regions. Water, Air, Soil Pollut. **56**: 745-767.

Fitzgerald W.F., Mason R.P., Vandal G.M. and Dulac F., 1994. Air-water cycling of mercury in lakes. In: *Mercury Pollution–Integration and Synthesis.* Watras C.J. and Huckabee J.W. (Eds.), Lewis Publishers, Ann Arbor, MI. pp. 203-220.

Hall B., 1995. The gas phase oxidation of elemental mercury by ozone. Water, Air, Soil Pollut. **80**: 301-315.

Hopper J.F. and Hart W., 1994. Meteorological aspects of the 1992 polar sunrise experiment. J. Geophys. Res. **99**(D12): 25, 315-25, 328.

Iverfeldt Å. and Lindqvist O., 1986. Atmospheric oxidation of elemental mercury by ozone in the aqueous phase. Atmos. Environ. **20**: 1567-1573.

Iverfeldt Å., 1991. Occurrence and turnover of atmospheric mercury over the Nordic countries. Water, Air, Soil Pollut. **56**: 251-265.

Jensen J., Adare K. and Shearer R., 1997. *Canadian Arctic Contaminants Assessment Report.* Indian and Northern Affairs Canada, Ottawa, Ontario. 460 pp.

Lindqvist O. (Ed.), 1991. *Mercury as an Environmental Pollutant.* Water, Air, Soil Pollut. **56**: 1-847 (Special Volume).

Li S.-M., Yokoouchi Y., Barrie L.A., Muthuramu K., Shepson P.B., Bottenheim J.W., Sturges W.T. and Landsberger S., 1994. Organic and inorganic bromine compounds and their compositions in the Arctic troposphere during polar sunrise. J. Geophys. Res. **99**(D12): 25,415-25,428.

Lindberg S.E., Petersen G. and Keeler G. (Eds.), 1998. Atmospheric Transport, Chemistry and Deposition of Mercury. Atmos. Environ. **32**: 807-944.

Lindqvist O. and Rodhe H., 1985. Atmospheric mercury -- a review. Tellus **37B**: 136-159.

Lu J., 1997. Method development for sampling and analysis of particulate-phase mercury in ambient air. *Spring 1997 Seminar Series*. Air Quality Research Branch, Atmospheric Environment Service, Downsview, Ontario. May 8.

Lu J., Schroeder W.H. and Steffen A., 1997. Sampling and determination of particulate-phase mercury in ambient air. In: *Proceedings of the AMAP International Symposium on Environmental Pollution of the Arctic*. Arctic Monitoring and Assessment Programme, Oslo, Norway. pp. 352-353.

Lu J., Schroeder W.H., Berg T., Munthe J., Schneeberger D. and Schaedlich F., 1988. A Device for Sampling and Determination of Total Particulate Mercury in Ambient Air. Analytical Chemistry, **70** (11): 2403-2408

Mackay D., Wania F. and Schroeder W.H., 1995. Prospects for modeling the behavior and fate of mercury, globally and in aquatic systems. Water, Air, Soil Pollut. **80**: 941-950.

Mozurkewich M., 1995. Mechanisms for the release of halogens from sea-salt particles by free radical reactions. J. Geophys. Res. 100(D7): 14,199-14,207.

Munthe J., 1992. The aqueous oxidation of elemental mercury by ozone. Atmos. Environ. **26A**: 1461-1468.

Pearce F., 1997. Mercurial storms rage in the Arctic. New Scientist **154**: 17.

Poissant L., 1997. Field observations of total gaseous mercury behaviour: interactions with ozone concentration and water vapour mixing ratio in air at a rural site. Water, Air, Soil Pollut. **97**: 341-353.

Porcella D.B., Huckabee J.W. and Wheatley B. (Eds.), 1995. *Mercury as a Global Pollutant*. Kluwer Academic Publishers, Dordrecht, The Netherlands. 1336 pp.

P'yankov V.A., 1949. Kinetics of the reaction between mercury vapor and ozone. Zhur. Obshchev Khim. (J. Gen. Chem.) **19**: 224-229.

Schroeder W.H., 1981. Recent developments in the measurement of atmospheric mercury. Can. Res. **14**: 33-41.

Schroeder W.H. and Jackson R.A., 1987. Environmental measurements with an atmospheric mercury monitor having speciation capabilities. Chemosphere **16**: 183-199.

Schroeder W.H. and Fanaki F.H., 1988. Field measurements of water-air exchange of mercury in freshwater systems. Environmental Technology Letters **9**: 369-374.

Schroeder W.H., Yarwood G. and Niki H., 1991. Transformation processes involving mercury species in the atmosphere -- results from a literature survey. Water, Air, Soil Pollut. **56**: 653-666.

Schroeder W.H. and Markes J., 1994. Measurements of atmospheric mercury concentrations in the Canadian environment near Lake Ontario. J. Great Lakes Res. **20**: 240-259.

Schroeder W.H., Ebinghaus R., Shoeib M., Timoschenko K. and Barrie L.A., 1995a. Atmospheric mercury measurements in the northern hemisphere from 56° N to 82.5° N Latitude. Water, Air, Soil Pollut. **80**: 1227-1236.

Schroeder W.H., 1996a. Atmospheric mercury measurements in the Canadian Arctic. In: *Synopsis of Research Conducted under the 1994/95 Northern Contaminants Program*. Murray J.L., Shearer R.G. and Han S.L. (Eds.), Environmental Studies Series Report No. 73, Department of Indian Affairs and Northern Development (DIAND), Ottawa, Ontario. pp. 21-29.

Schroeder W.H., 1996b. Mercury at Alert: particulate-phase mercury sampling and analysis methodology development. *Hazardous Air Pollutants (HAPs) Mid-Term Review Meeting*. Atmospheric Environment Service, Downsview, Ontario. October 22-23.

Schroeder W.H. and Schneeberger D.R., 1996. High-temporal-resolution measurements of total gaseous mercury in air at Alert, Northwest Territories, Canada. Fourth International Conference on Mercury as a Global Pollutant. Hamburg, Germany. August 4-8.

Schroeder W.H., Anlauf K., Barrie L.A., Berg T. and Schneeberger D.R., 1997a. Atmospheric mercury and polar sunrise tropospheric ozone depletion at Alert in the Canadian High Arctic. In: *Proceedings of the AMAP International Symposium on Environmental Pollution in the Arctic,* Arctic Monitoring and Assessment Programme, Oslo, Norway. pp. 354-356.

Schroeder W.H., Anlauf K., Barrie, L.A., Berg T., Lu J. and Schneeberger D., 1997b. Polar tropospheric ozone depletion chemistry transforms mercury and increases its input to the biosphere. In: *Proceedings of the International Symposium on Atmospheric Chemistry and Future Global Environment*, Nagoya, Japan. International Global Atmospheric Chemistry Program and Science Council of Japan.

Schroeder W.H., Anlauf K.G., Barrie L.A., Lu J.Y., Steffen A., Schneeberger D.R. and Berg T., 1988. Arctic springtime depletion of mercury. Nature **394**: 331-332.

Schroeder W.H. and Munthe J., 1998. Atmospheric mercury: an overview. Atmos. Environ. **32**: 809-822.

Slemr F., Seiler W. and Schuster G., 1981. Latitudinal distribution of mercury over the Atlantic ocean. J. Geophys. Res. **86**: 1159-1166.

Watras C.J. and Huckabee J.W. (Eds.), 1994. *Mercury Pollution -- Integration and Synthesis*. Lewis Publishers, Ann Arbor, MI. 727 pp.

Worthy D., 1996. Personal Communications. Atmospheric Environment Service, Environment Canada, Downsview, Ontario.

Acknowledgements

The authors wish to express their gratitude to all of the Alert GAW observatory staff, contractors and students who have been extremely helpful during the conduct of this work at Alert. We are especially indebted to Lori Leeder, Erika Wallgren, Tina Scherz, Vicky Hudec and Korb Whale for their cheerful assistance and advice.

2.9. AEROSOL CHEMISTRY

Leonard A. Barrie

2.9.1. AEROSOL CHEMISTRY OBSERVATIONS AND RESULTS: 1980-1995

2.9.1.1. INTRODUCTION

Under-lain by an ice-covered biologically-active Arctic Ocean and surrounded by open northern Pacific and Atlantic oceans and industrialized continents, the Arctic troposphere (0 to ~8 km) is affected by anthropogenic and natural sources of aerosols. Since the late 1970's when observations of aerosols were first made for a whole year in the Alaskan Arctic [*Rahn and McCaffrey*, 1980], widespread anthropogenic aerosol pollution in the polar troposphere known commonly as Arctic haze has been studied and characterized [*Heidam*, 1984; *Barrie*, 1986; *Ottar*, 1989; *Shaw*, 1995, *Barrie*, 1996]. For meteorological reasons, there is a strong seasonality in the lifetime of aerosols in the Arctic air mass. Because of very stable thermal stratification in the atmospheric surface boundary layer and less than 10 mm-H_2O/month of precipitation in the cold-half of the year from October to May, aerosol residence times are much longer in winter (~3 to 7 weeks) than in summer (~3 to 7 days). Furthermore, there is a strong seasonality in the north-to-south transport of aerosols [*Barrie et al.*, 1989a, *Iversen*, 1996; *Christensen*, 1997]. Thus, via long-range atmospheric transport the Arctic region is subjected to a variety of aerosol sources that are seasonally modulated by atmospheric circulation and precipitation.

In Canada at three widely separated high Arctic stations (Alert, Mould Bay and Igloolik), routine observations of aerosol composition were made from 1980 to 1984 [*Barrie et al.*, 1981; *Barrie and Hoff*, 1985]. They showed that measurements made at Alert on the northern tip of Ellesmere Island (82.5°N, 62.3°W) were representative of the composition of the high arctic troposphere. Thus, for the purpose of measuring long term trends in aerosol composition, routine measurements were continued at Alert. Results of 6 years of aerosol chemistry observations at Alert were analyzed using principal component analysis [*Barrie and Barrie*, 1990] to reveal four major components: soil, sea salt, anthropogenic and photochemical. The last was associated with gas-particle conversion at polar sunrise of anthropogenic sulphur dioxide to form sulphuric acid aerosols and of marine halogens to form particulate Br and I. In addition, it showed that there was a distinct peak in aerosol I in the period August to October presumably of marine biogenic origin. This confirmed the previous analysis of seasonal variation in halogens based on four years of observations at all three high Arctic sites [*Sturges and Barrie*, 1988]. The photochemical aerosol component was first linked to lower tropospheric ozone depletion at polar sunrise at Alert [*Barrie et al.*, 1988]. It was later observed in the Norwegian Arctic at Spitsbergen [*Maenhaut et al.*, 1993].

Archived samples of Alert aerosols were analyzed for trends in the marine biogenic sulphur compound methane sulphonic acid (MSA) for the period 1980 to 1991 by *Li et al.* [1993]. It was found that MSA concentration had a bimodal seasonal distribution with one peak in April to May and one in July to August. In addition, it decreased by 33% over the 11-year period. Analysis of the isotopic composition of $SO_4^=$ -S in aerosols at Alert showed that in the period September to May, they were predominantly of anthropogenic origin but in summer were also influenced by marine sea salt and biogenic sulphur [*Nriagu et al.*, 1990; *Norman et al.*, 1999]. Principal component analysis as well as a quantitative source apportionment based on sulphur isotopes and sea salt sodium [*Li and Barrie*, 1993] showed that aerosol $SO_4^=$ in summer is 25 to 30% biogenic, 1 to 8% sea salt and the rest of anthropogenic origin. At other times of year, it is <14% biogenic, 1% to 8% sea salt and the rest anthropogenic.

Lead isotopes have been used to differentiate Pb aerosols from different source regions in Europe [*Hopper et al.*, 1991]. When applied to Arctic aerosols at Alert and Barrow Alaska [*Sturges and Barrie*, 1989; *Sturges et al.*, 1994], they are consistent with apportionment's to sources within Eurasia deduced from chemical transport modelling [*Akeredolu et al.*, 1994], namely, equal contributions from the former USSR, western Europe and E. Europe.

Since the inception of sampling at Alert in 1980, fifteen years of data for eighteen aerosol constituents are available to examine, with greater statistical confidence than previously, the seasonality, long-term variation and source apportionment of arctic aerosols constituents.

The methodology description of the aerosol measurements is found in Section 3.8.

2.9.1.2. RESULTS

In Figure 2.49, the time series and mean seasonal variation of $SO_4^=$, H^+, NH_4^+ and NO_3^- are shown. Also included is the long term trend in the observations deduced from time series analysis of the data.

Generally, the major ion composition of polluted winter Arctic haze is an acidic ammonium sulphate salt with a stochiometric composition between NH_4HSO_4 and H_2SO_4. It becomes more acidic in March and April after polar sunrise when *in situ* oxidation of SO_2 in the Arctic troposphere adds H_2SO_4 to the mix [*Barrie and Hoff*, 1984; *Barrie et al.*, 1994]. Nitrates in particles are a minor constituent. Most end-product oxides of nitrogen are in the form of peroxyacetylnitrate (PAN, see Section 2.7) and other organic nitrates[*Bottenheim et al.*, 1993]. There was no significant change in $SO_4^=$ between 1980 and 1991 but thereafter it has shown a significant decline. This is likely due to the disintegration of the former Soviet Union and the attendant decline in industrial production and hence pollution thereafter.

The seasonal variation of anthropogenic sulphates are very different than those of the halogens shown in Figure 2.50. Sea salt ions Na^+ and Cl^- undergo a sesonal variation somewhat similar to that of anthropogenic sulphates peaking in winter and lowest in summer. This is due to maximum sea salt production in the noerhtern oceans during the windy winter motnhs as well as longer aerosol residence times in the winter rather than the summer half of the year. Br and iodine show a spring time peak just after polar sunrise that is related to photochemistry in the Arctic atmosphere [*Barrie and Platt*, 1997]. Iodine also has a second maximum in autumn which may be related to biological production at this time of the year.

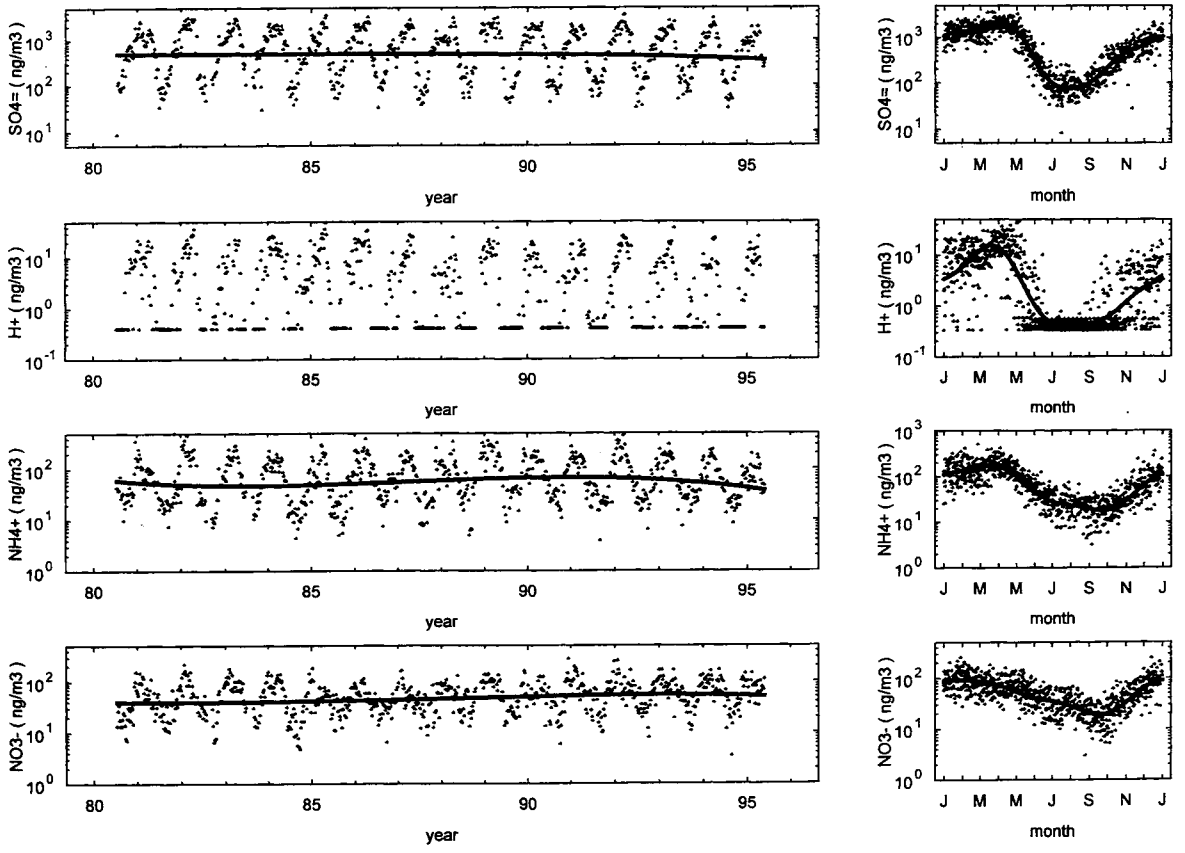

Figure 2.49 The time series and mean seasonal variation of $SO_4^=$, H^+, NH_4^+ and NO_3^- (from *Sirois and Barrie*, 1999). If the de-seasonalized long-term trend was statistically significant, it is also shown on the left-hand plot.

The mean seasonal variation of soil dust (represented by aerosol Al) at Alert is shown in Figure 2.51. The seasonal variation for all weeks of observation as well as for low wind weeks when the 90th percentile of local hourly wind in a week is less than 20 km/hr are shown. This is to separate local wind blown dust from dust that has been transported long distances. Clearly, local wind blown dust peaks in autumn while llong range transported dust paeks in May. The latter is consistent with generation of dust from Asian deserts in spring.

The long-term trend in atmospheric concentrations of several heavy metal aerosol elements of anthropogenic origin are shown in Figure 2.52. Pb decreased from 1980 to 1995 by approximately 60% which is consistent with decreased usage of this metal as a fuel additive in European gasoline. Similar trends as for Pb were observed for non-soil V (xV) and non-soil Mn (xMn). xV is largely a product of oil combustion. Cu and Zn are heavily influenced by smelting and both declined markedly after the disintegration of the former Soviet Union. Soluble K^+ is in part from sea salt and in part from wood combustion. It has a very different seasonal variation than the others.

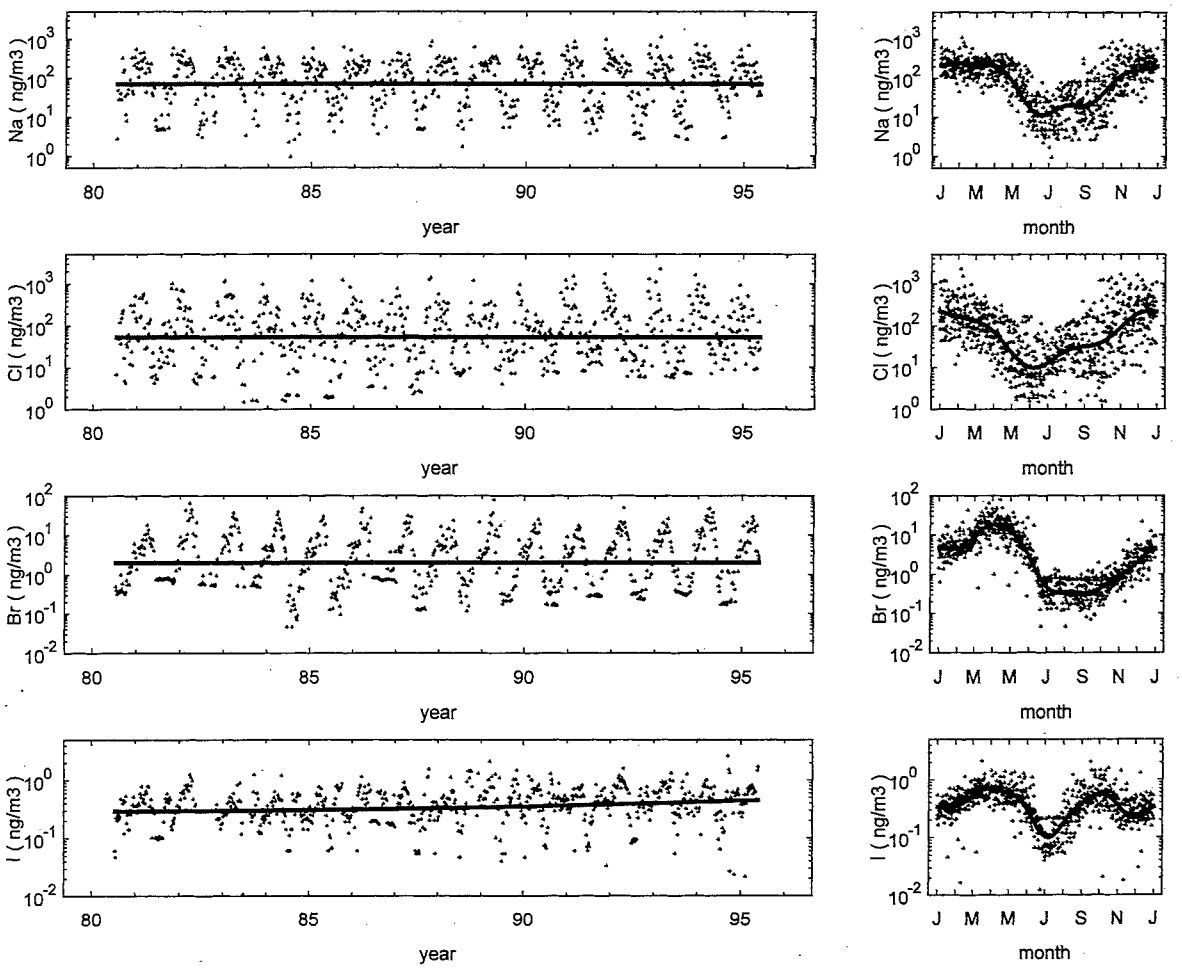

Figure 2.50 The time series and mean seasonal variation of Na^+, Cl^-, Br^- and I at Alert (from *Sirois and Barrie*, 1999). The de-seasonalized long-term trend is also shown on the left-hand plot.

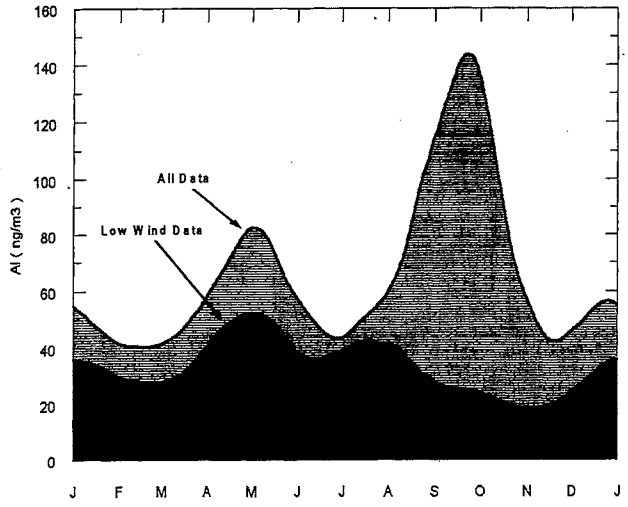

Figure 2.51 The mean seasonal variation of wind blown dust at Alert (represented by aerosol Al) for all samples from 1980 to 1989 and for low wind weeks when the 90th percentile of local hourly wind in a week is less than 20 km/hr. (from *Sirois and Barrie*, 1999).

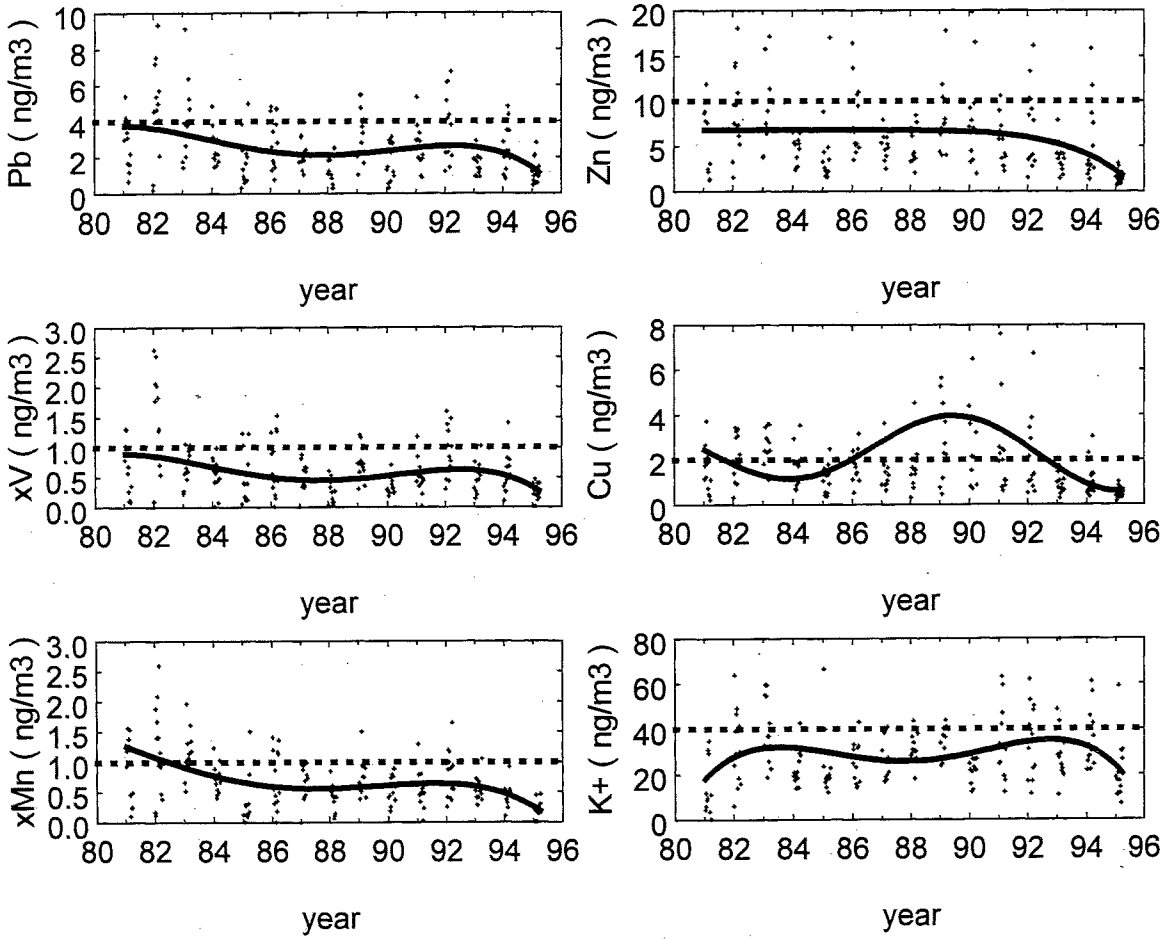

Figure 2.52 For the winter months, the estimated long-term and seasonal trends of weekly concentration of Zn, Cu, Pb, K+, xV(non-soil V) and xMn (non-soil Mn) at Alert (from *Sirois and Barrie*, 1999).

2.9.1.3. REFERENCES

Akeredolu, F.A., L.A. Barrie, M.P. Olson, K.K. Oikawa, J. Keelerand J. Pacyna,1994, The flux of anthropogenic metals into the Arctic from the mid-latitudes in 1979/80, *Atmos. Envir., 28,* in press.

Barrie, L.A., 1986, Arctic air pollution: an overview of current knowledge, *Atmos. Environ., 20,* 643-663.

Barrie, L.A. 1996, Occurrence and trends of pollution in the Arctic troposphere, in *"Chemical Exchange Between the Atmosphere and Polar Snow"*, eds. Wolf and Bales, NATO ASI Series I: Global Environmental Change, 43, 93-130.

Barrie, L.A., R.M. Hoff and S.M. Daggupaty, 1981,The influence of mid-latitudinal pollution sources on haze in the Canadian Arctic, Atmos. Environ., 15, 1407-1419.

Barrie, L.A. and R.M. Hoff, 1984, The oxidation rate and residence time of sulphur dioxide in the Arctic atmosphere, *Atmos. Environ., 18,* 2711-2722.

Barrie, L.A. and R.M. Hoff, 1985, Five years of air chemistry observations in the Canadian Arctic, Atmos. Environ., 19, 1995-2010.

Barrie, L.A., J.W. Bottenheim, R.C. Schnell, P.J. Crutzen and R.A. Rasmussen, 1988, Ozone destruction and photo-chemical reactions at polar in the lower Arctic atmosphere, Nature, 334, 138-141.

Barrie, L.A., M.P. Olson and K.K. Oikawa, 1989a,The flux of anthropogenic sulphur into the Arctic from mid-latitudes, Atmos. Envir., 23, 2502-2512.

Barrie, L.A. and M.L. Barrie, 1990, Chemical components of lower tropospheric aerosols in the high Arctic: Six years of observations, *J. Atmos. Chem., 11,* 211-266.

Barrie, L.A., S.M. Li, D.L. Toom, S. Landsberger and W. Sturges, 1994, Lower tropospheric measurements of halogens, nitrates and sulphur oxides by denuder and filter systems during Polar Sunrise Experiment 1992, *J. Geophys. Res., 99D,* 25453-25469.

Barrie, L.A. and U. Platt, 1997, Arctic tropospheric chemistry: overview to Tellus special issue, 49B, 450-454.

Bottenheim, J.W. L.A. Barrie and E. Atlas, 1993, The partitioning of nitrogen oxides in the lower Arctic troposphere during spring 1988, *J. Atmos. Chem., 17,* 15-27.

Christensen, J. 1997, The Danish eulerian hemispheric model–a three-dimensional air pollution model used for the Arctic, Atmos. Envir., 31, 4169-4191.

Heidam, N.Z., 1984, The components of the arctic aerosol, *Atmos. Envir., 18,* 329-343.

Hopper, J.F., H.B. Ross, W.T. Sturges and L.A. Barrie, 1991, Regional source discrimination of atmospheric aerosols in Europe using the isotopic composition of lead, *Tellus, 43B,* 45-60.

Iversen, T. ,1996, Atmospheric pathways for the Arctic, in *"Chemical Exchange Between the Atmosphere and Polar Snow"*, eds. Wolf and Bales, NATO ASI Series I: Global Environmental Change, 43, 71-92.

Li, S.M., L.A. Barrie and A. Sirois, 1993, Biogenic Sulfur Aerosol in the Arctic Troposphere: 2. Trends and Seasonal Variations. *J. Geophys. Res., 92,* 20, 623-631.

Li, S.M. and L.A. Barrie, 1993, Biogenic sulphur aerosols in the Arctic troposphere: I Contributions to sulphate, J. Geophys. Res., 98D, 20613-20622.

Maenhaut, W., G. Ducastel and J.M. Pacyna,1993, Atmospheric aerosol at Ny Ålesund during winter 1989: Multielement composition, receptor modelling, and comparison with data from previous winters, *Proc. Fifth Intern. Symp.on Arctic Air Chemistry*, Copenhagen, Denmark, September 8-10, 1992, Edited by N.Z. Heidam, NERI Technical Report No. 70 (1993) 11 p. (ISBN: 87-7772-094-6).

Norman, A.L., L.A. Barrie, D. Toom-Sauntry, A. Sirois, H.R. Krouse, S.M. Li, and S. Sharma, 1999, Sources of aerosol sulphate at Alert: apportionment using stable isotopes, *J. Geophysic. Res.*, 104D, in press.

Nriagu, J.O., R.D. Coker and L.A. Barrie, 1990, Origin of sulphur in Canadian Arctic haze from isotope measurements, *Nature, 349,* 142-145.

Ottar, B., 1989, Arctic air pollution: a Norwegian perspective, *Atmos. Envir., 23,* 2349-2356.

Rahn, K.A. and R.J. McCaffrey, 1980, On the origin and transport of winter Arctic aerosol, *Ann. N.Y. Acad. Science, 338,* 486-503.

Sirois, A. and L.A. Barrie, 1999, Arctic lower tropospheric aerosol trends and composition at Alert, Canada: 1980-1995, *J. Geophysic. Res.*, 104D, in press.

Shaw, G. 1995, The arctic haze phenomenon, *Bull. Amer. Met. Soc.*, 76, 2403-2413.

Sturges, W.T. and L.A. Barrie, 1988, Chlorine, bromine and iodine in Arctic aerosols, *Atmos. Environ., 22,* 1179-1194.

Sturges, W.T. and L.A. Barrie, 1989, Stable lead isotope ratios in Arctic aerosols: evidence for the origin of Arctic air pollution, *Atmos. Envir., 23,* 2513-2520.

Sturges, W.T., J.F. Hopper, L.A. Barrie and R.C. Schnell, 1994, Stable lead isotopes in Alaskan Arctic aerosols, *Atmos. Envir., 28,* in press.

2.10. LONG-TERM OBSERVATIONS OF TOXIC ORGANIC SUBSTANCES: 1992-1998

Leonard A. Barrie and Crispin Halsall

2.10.1. INTRODUCTION

Over the last two decades, concern has grown about anthropogenic pollutants contaminating the arctic environment [*Barrie et al.*, 1992; AMAP, 1997; CACAR, 1997]. Consequently, three classes of compounds have been measured at Alert on a routine weekly basis since January 1992: persistent organic pollutants (POPs), polycyclic aeromatic hydrocarbons (PAHs) and polychlorinated byphenyls (PCBs). Alert has been the long-term baseline station in a larger measurement program that undertook two year surveys of atmospheric composition of these substances at Tagish, Yukon, Cape Dorset, Baffin Island, and Dunai Island, Russia (at the mouth of the Lena River). The same methodologies were used everywhere. Given the scarcity of data from the polar region, this study has provided a unique long-term database. For further details, the reader should consult *Fellin et al.*, [1997], *Halsall et al.*, [1997], *Stern et al.*, [1997] and *Halsall et al.*, [1998].

The methodology description of the toxic organic substances measurements is found in Section 3.9.

POPs

Persistent organic pollutants (POPs) such as the organochlorine pesticides (OCs) have now been widely detected in both abiotic and biotic matrices within the Arctic region, with concern focused on the indigenous Arctic. Indeed, recent modelling efforts have predicted an accumulation of many semi-volatile organic compounds in the polar regions [*Wania and Mackay*, 1996], the atmosphere being key to the movement of POPs from southerly source regions. Organohalogen pesticides as a chemical group cover a wide range of physical-chemical properties. Furthermore, their usage on a global scale has varied tremendously; while some of them have been banned/restricted (i.e., DDT, toxaphene) in western/industrialized countries, their use prevails in other parts of the globe (e.g., DDT production and use in India). However, many of these compounds are still in current use in industrialized countries. Lindane (alpha-HCH), endosulfan and trifluralin are examples of current-use pesticides applied both in Europe and N. America. This diversity in properties as well as usage makes fate prediction for the whole halogenated class extremely difficult, however, by examining trends in a remote atmosphere it is possible to identify processes that may affect their global distribution.

PAHs

PAHs in the arctic environment are present through both anthropogenic and natural sources (petrogenic/biogenic). The influence of these source types has been undertaken through the analysis of sediments taken from the Beaufort and Barents Seas (Arctic Ocean). Aside from riverine inputs of petrogenically derived PAHs, the atmosphere is seen as one of the key sources. Evidence of long-range atmospheric transport from southerly source regions in Eurasia and North America has been demonstrated in both the Norwegian and Canadian Arctic

PCBs

PCBs are an example of an industrial OC. They were previously used as hydraulic and transformer fluids, but production and use has been largely discontinued in developed countries. However, dumping in the environment and their persistence makes them an ever-present chemical group of concern.

2.10.2. RESULTS

OCs

Annual contaminant levels for 1993 are displayed in Figure 2.53 including the 1993 Norwegian data. Spatially, the annual concentrations at the various sites do not show remarkable differences, indicating a degree of uniformity in contamination of the arctic atmosphere. Note, however, that the y-axis is a log scale, significant variations can be seen in the levels of the chloro-veratroles, these being metabolites of chlorinated catechols released in bleached kraft mill effluent. Higher levels of the chloro-veratroles in the Tagish atmosphere may be indicative of the wood pulp industry located in north western Canada. Seasonal variations were evident in the observations. An increase in air concentrations during the summer months was apparent for a range of compounds. The strongest correlation with temperature tended to be with the transformation/metabolite daughters of the original pesticides, i.e., oxychlordane, heptachlor epoxide and dieldrin. This reflects: 1) the widespread distribution of these compounds and their persistence in the global environment and 2) the likelihood that a large percentage of the parent

compounds, many of which are no longer in use, have now been degraded into these secondary compounds. To support this second point, levels of heptachlor and p, p-DDT were often below the minimum detection limits. In contrast, the respective metabolites heptachlor epoxide and p, p-DDE were found above the detection limit in the majority of the samples. Other compounds which also displayed a significant correlation included endosulfan, cis-chlordane and cis-nonachlor. Endosulfan is still currently used in many northern countries as a contact insecticide, with application rates being highest during the warmer months.

PAHs

Figure 2.54 displays a box-and-whisker plot of monthly total PAH (t-PAH) concentrations (sum of 16 compounds) for Alert. A seasonal fluctuation in air concentrations was clearly evident, with the colder months of the year (October-April) displaying higher concentrations than the warmer months (May-September). The mean t-PAH concentration during the cold period was an order of magnitude higher than the rest of the year, with elevated concentrations coinciding with the haze period. Sporadic increases in PAH levels were also evident during months outside of the haze season. Local contamination from the combustion of waste materials and fuels at the nearby military base resulted in elevated concentrations observed between July 20 and August 15, 1993.

PCBs

Mean total PCB (sum of 99 congeners) concentrations for 1993, the year when all three sites were running simultaneously, were 27.4 pg m^{-3}, 17.0 pg m^{-3} and 34.0 pg m^{-3} at Alert, Tagish and Dunai, respectively (Figure 2.55). Tagish had the lowest mean ΣPCB concentrations during both the warm and cold monitoring periods. *Oehme et al.*, [1996], observed a mean annual total PCB concentration of 13.1 pg m^{-3} at Ny-Ålesund, Spitzbergen, in 1993. As this study was part of the Arctic Monitoring Assessment Program (AMAP), the number of PCB congeners was restricted to the 10 that were routinely monitored in biota, sediments and other sample matrices. The equivalent annual mean concentrations for the same 10 congenors at Alert, Tagish, and Dunai were 5.8 pg m^{-3}, 3.7 pg m^{-3} and 8.1 pg m^{-3}, respectively.

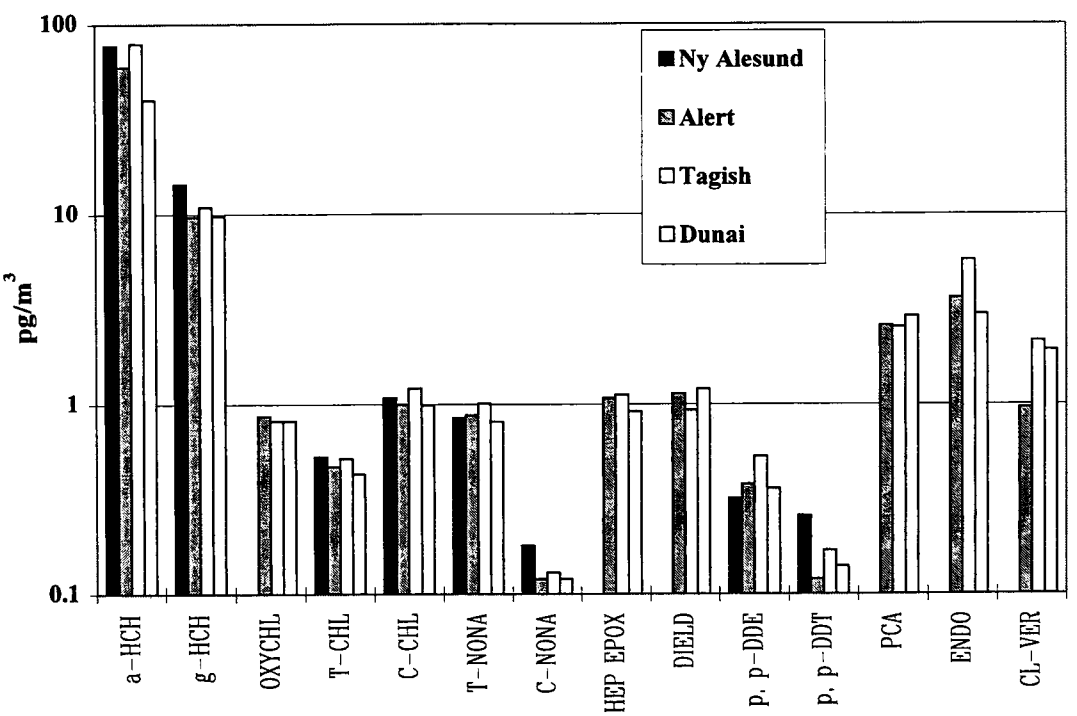

Figure 2.53 A comparison of mean annual (1993) total (filter + PUF) organochlorine concentrations.

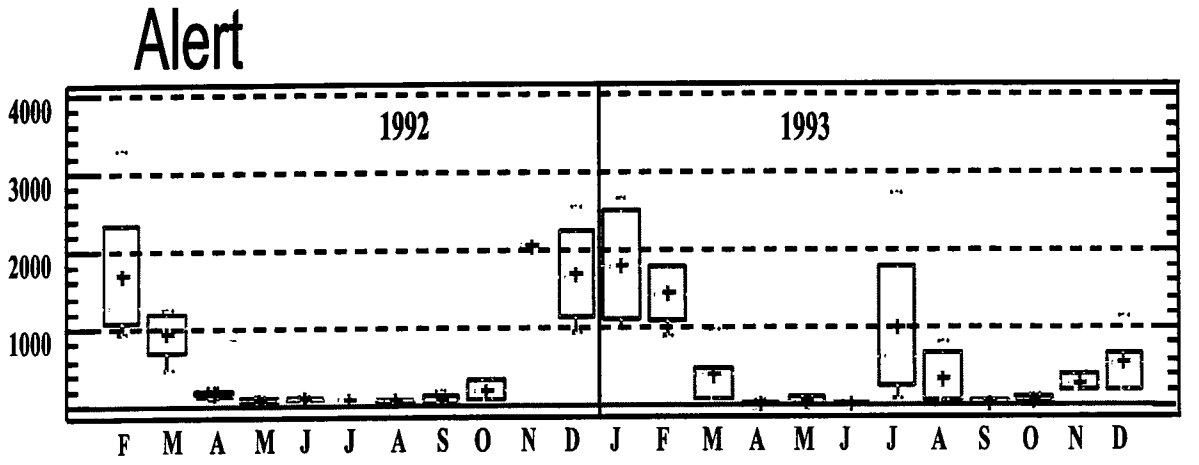

Figure 2.54 Box-and-whisker plots of weekly mean t-PAH concentrations (pico g m^{-3}) at Alert. Each month comprises four weekly samples.

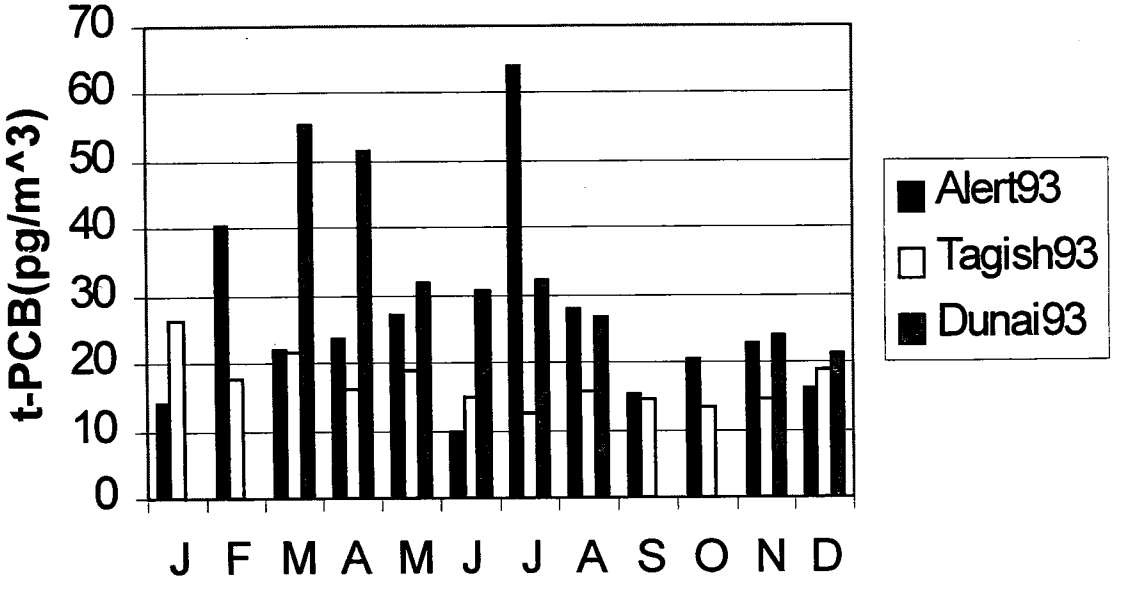

Figure 2.55 A comparison of the seasonal variation of t-PCB (sum of 99 congeners) observed at three widely separated locations in the Arctic in 1993.

2.10.3. REFERENCES

AMAP (Arctic Monitoring Assessment Programme) (1997) Arctic pollution issues: a state of the Arctic environment report. AMAP, Oslo, Norway.

Barrie, L.A., D. Gregor, B. Hargrave, R. Lake, D. Muir, R. Shearer, B. Tracey and T. Bidleman, 1992, Arctic contaminants: sources, occurrence and pathways, Sci. of the Total Envir., 122, 1-74.

CACAR (Canadian Arctic Contaminants Assessment Report) (1997) Northern Contaminants Program. Dept. of Indian Affairs and Northern Development (DIAND), Ottawa, Ontario, Canada.

Fellin, P., L.A. Barrie, D. Dougherty, D. Toom, D. Muir, N. Grift, L. Lockhart and B. Billeck, (1996). Air monitoring in the arctic: results for selected persistent organic pollutants for 1992. Environmental Toxicology and Chemistry 15, 253-261.

Halsall C.J., R. Bailey, G.A. Stern, L.A. Barrie, P. Fellin, D.C.G. Muir, F. Ya. Rovinsky, E. Ya. Kononov, B.V. Pastukhov, 1998, Organohalogen pesticides in the arctic atmosphere, Environmental Pollution, 102, 51-62.

Halsall, C.J.; L.A. Barrie, P. Fellin, D.C.G. Muir, F. Ya. Rovinski, E. Ya. Kononov, and B.V. Pastukhov, (1997). Spatial and temporal variation of polycyclic aromatic hydrocarbons in the arctic atmosphere. Environmental Science Technology 31, 3593-3599.

Oehme, M. and J.-E. Schlabach. Seasonal changes and relations between levels of organochlorines in Arctic ambient air: first results of an all-year round monitoring program at Ny Alesund, Svalbard, Norway. Environmental Science and Technology, 1996, 30: 2294-2304.

Stern, G.A., C.J. Halsall, L.A. Barrie, D.C.G. Muir, P. Fellin, B. Rosenberg, F. Ya. Rovinski, E. Ya. Kononov, and B.V. Pastukhov, (1997). PCBs in the arctic atmosphere: 1. Spatial and temporal trends: 1992-1994. Environmental Science Technology 31, 3619-3628.

Wania, F. and D. Mackay. Tracking the distribution of persistent organic pollutants. Environmental Science and Technology, 1996, 30(9): A390-A396.

3. MEASUREMENT AND CALIBRATION PROTOCOLS

3.1. CARBON DIOXIDE

3.1.1. IN SITU CO_2 MEASUREMENTS

Neil B.A. Trivett, Lori Leeder, Darrell Ernst and Douglas E.J. Worthy

Carbon dioxide measurements in the Canadian Baseline program follow a set of principles and protocols established by a number of international agencies through the CO_2 Experts Meetings sponsored by the WMO. A typical measurement program is based on the non dispersive infrared (NDIR) measurement principle using commercial instruments developed for industry and fine-tuned for high precision measurements at remote field stations. Since the NDIR instruments are not absolute systems and their response functions are non-linear, a set of calibration gases are required to obtain the requisite precision. Although stations in the high northern latitudes have large seasonal cycles (14-16 ppm at Alert), southern latitude seasonal cycles are very much smaller (1-2 ppm at the South Pole). In addition, the small North-South gradient (approximately 3-4 ppm) and the consequences of small changes in the atmospheric growth rate to the global carbon balance require that the inter-station network precision be 0.1 ppm or better. While programs operated by individual agencies may have internal precision better than this, we have yet to achieve this across the global network.

3.1.1.1. CO_2 STANDARD GASES

All AES CO_2 measurements are directly traceable to the international scale of the WMO Central Calibration Laboratory (CCL) at the Scripps Institute of Oceanography (SIO) until 1996, when the CCL was moved to the NOAA/CMDL facilities in Boulder. A set of compressed reference gases (CO_2-in-N_2) form the basis of the WMO scale. These tanks were made gravimetrically but their concentration is monitored periodically using a manometer. The accuracy of the SIO manometer is 0.2 ppm to 0.3 ppm which is an order of magnitude larger that the precision of the typical NDIR measurement systems. The accuracy of the new manometer built by NOAA/CMDL is somewhat better at ± 0.1 ppm [*Zhao et al.*, 1997]. From these periodic manometric measurements of the CO_2 standards and calibration of the manometer itself, adjustments are made to the NDIR transfer scale, which is then dated accordingly. The last major cleaning and calibration of the manometric systems was in 1985 and gave rise to the WMO 1985 scale which many countries report their data on. The AES carbon dioxide data are reported on the WMO 1985 scale.

Until recently, most NDIR systems had large internal volumes requiring significant amounts of standard gases during calibrations and field operation resulting in rapid depletion of gas standards. As the pressure in the cylinder decreases, the CO_2 mixing ratio tends to drift, particularly when the pressure drops below 500 psi. The exact principle behind this drift is not yet fully understood. Therefore, to prolong the life of the primary standards and to maintain the consistency of the CO_2 measurements over a long period of time, SIO transfers CO_2 concentration values from their primary set of reference gases to a secondary set via NDIR calibrations. This secondary set is used to calibrate working tanks. These are then used to calibrate the CO_2 gas standards from outside agencies.

The AES maintains a set of National Standards that are regularly calibrated by SIO and NOAA/CMDL approximately every two years. In relation to the WMO standards, the Canadian National Standards (1986) are at the quaternary level. For simplicity in the naming convention, the National Standards are referred to as the AES primary standards. To prolong the lifetime of the AES primary standards, AES has established a hierarchy of CO_2 standard gases for which the CO_2 content is determined by transferring concentrations via NDIR calibrations. The AES hierarchy of standards is depicted in Figure 3.1 and the gas concentration ranges of the standards are summarized in Table 3-1.

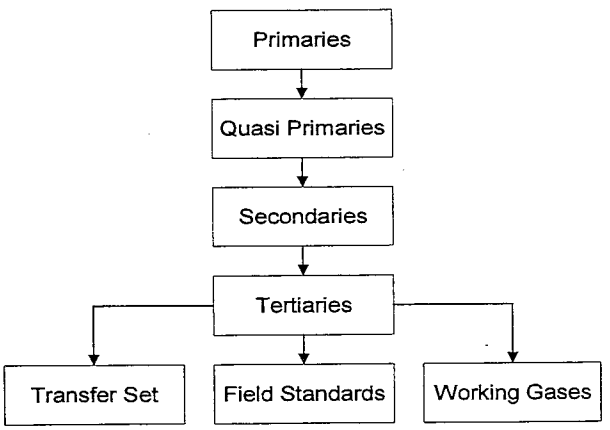

Figure 3.1 AES CO_2 laboratory standards hierarchy.

While the hierarchy shown in Figure 3.1 certainly complicates the database system, it was considered necessary to maintain the primary tanks as long as possible. Nevertheless, the main AES primary tanks, produced in 1986 by SIO, have come to the end of their useful life. A new set will be used starting in 1998 and to simplify things there will only be 3 levels – primary, secondary and station standards. This is possible because the current high volume (200 ml) NDIR analyzers will be replaced with new low volume (8 ml) ones.

Table 3-1. Concentration ranges of the CO_2 standards.

Class	Number of Tanks	Concentration Range (ppm)
Primary (1986)	9	310 to 390
Quasi Primary	11	310 to 410
Secondary	5	320 to 380
Tertiary	5	320 to 380
Transfer Set	5	310 to 390

The AES CO_2 standard gas hierarchy is maintained by periodically transferring concentration values from the primary standards via NDIR calibration to the quasi-primary standards. As a general rule, the quasi-primary standards are referenced to the primary standards once for every five sets of calibrations referenced to the quasi-primary standards. Similarly, the CO_2 concentrations from the quasi-primary standards are transferred to the secondary standards. As above, the secondary standards are referenced to the quasi-primary standards once for every five sets of calibrations referenced to the secondary standards. The secondary standards are used to establish the tertiary standards. The tertiary standards are also calibrated once for every five sets of calibrations referenced to them. The tertiary standards are used for routine calibrations of working gases, field standards, GC and flask system standards, and all international calibrations. The tertiary standards are also used to regulate a set of transfer standards that are taken into the field to calibrate field standards. The transfer standard set is calibrated before and after each trip to the field.

3.1.1.2. CALIBRATION HISTORY

The AES primary standards were calibrated twice by SIO in 1986 and 1991 and four times by NOAA/CMDL in 1989, 1993, 1995, and 1997. The mean values and standard deviations for these calibrations are given in Table 3-2. In addition, the new primary standards made and calibrated by SIO in 1994 were used to provide interim transfer calibrations of the 1986 primary tanks using the CCRL calibration system. While these are not a direct calibration by the CCRL they provide a good check on the standards. Because of the major discrepancy between the 2 SIO calibrations in 1986 and 1991 compared to the NOAA/CMDL, all of the current CCRL data from 1987 to July 1991 are directly traceable to an interpolation between the two SIO calibrations. Carbon dioxide measurements from August 1991 are fixed at the 1991 calibration values for the primary tanks.

The discrepancy between the SIO and NOAA/CMDL numbers on our standards has not been fully resolved. The CCRL and NOAA/CMDL standards are both traceable to the SIO standards. SIO calibrates the NOAA/CMDL primary tanks as well as those from CCRL. When NOAA/CMDL calibrates our tanks, they should agree well with the SIO numbers. Unfortunately, the SIO CCL was not able to calibrate our tanks after the 1991 calibration so we had to rely on NOAA/CMDL. After the last calibration in 1997, we decided to use the NOAA/CMDL numbers and the SIO 1991 numbers to determine the long-term drift in our 1986 primary standards (Figure 3.2). The worst case drift of > 0.2 ppm in our standards are for the HA2190 (310 ppm) and HA2202 (330 ppm) tanks. However, this has negligible effect on our scale in the range of ambient concentration of 340-370 ppm. When the standards are corrected for drift in the primaries using the equations in Figure 3.2, the ambient air concentrations will be corrected and submitted to the data centres.

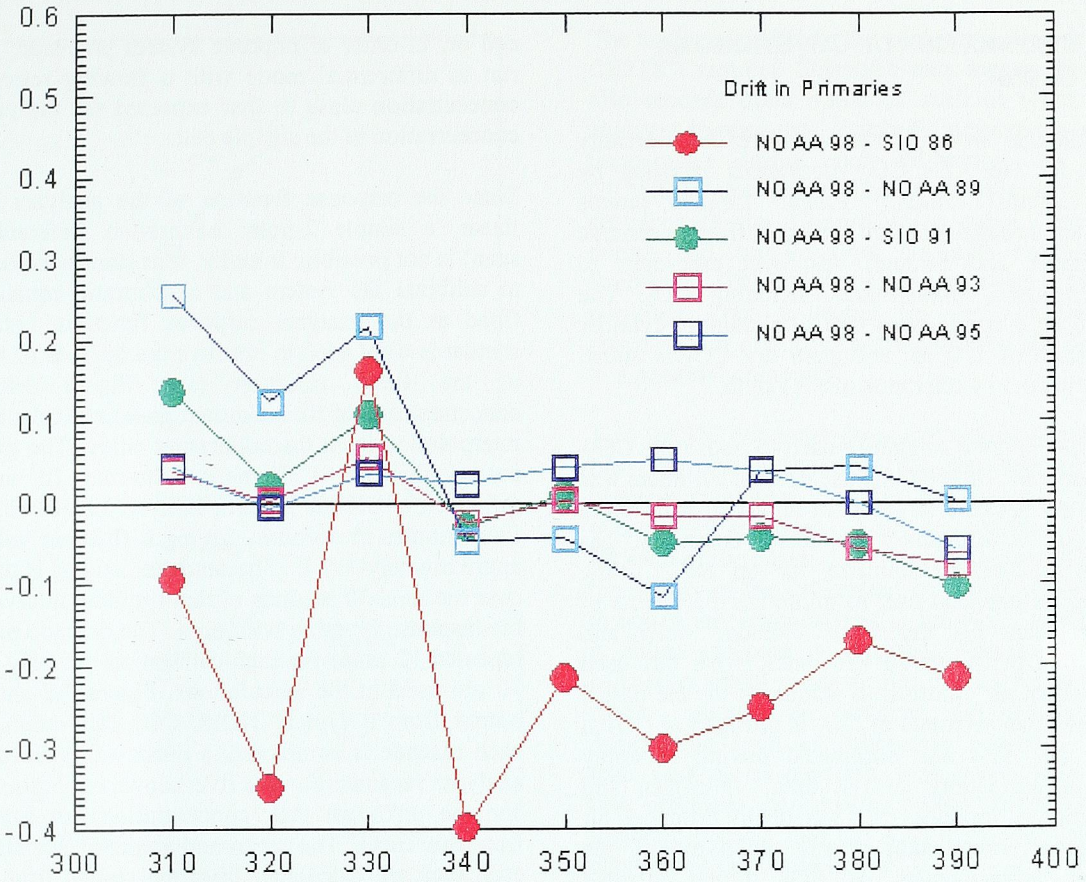

Figure 3.2 Drift in the primary standards calculated as the difference between the last calibration in 1998 by NOAA/CMDL and previous calibration by NOAA/CMDL and SIO.

Table 3-2. Calibration history of CCRL Primary CO_2-in-air tanks by SIO and NOAA/CMDL.

Cal. Date	HA2190 (ppm)	HA2194 (ppm)	HA2202 (ppm)	HA2217 (ppm)	HA2222 (ppm)	HA2223 (ppm)	HA2225 (ppm)	HA2286 (ppm)	HA2312 (ppm)
86/04/04	310.75±.04	319.63±.04	330.06±.06	339.31±.06	350.84±.05	360.45±.05	370.49±.08	381.38±.11	391.05±.10
89/05/09	310.4±.01	319.16±.01	330.00±.01	338.96±.07	350.67±.00	360.27±.05	370.20±.00	381.17±.03	390.83±.06
91/04/18	310.51±.04	319.26±.04	330.11±.05	338.94±.03	350.62±.03	360.20±.07	370.28±.06	381.27±.07	390.94±.07
93/06/24	310.60±.01	319.28±.01	330.16±.01	338.94±.02	350.62±.01	360.17±.01	370.26±.02	381.27±.00	390.91±.02
94/04/05*	310.71±.01	n/a	330.22±.01	n/a	350.7±.01	n/a	370.41±.01	n/a	391.13±.01
95/02/25*	310.67±.01	n/a	330.23±.00	n/a	350.71±.01	n/a	370.44±.01	n/a	390.15±.01
95/05/10	310.61±.02	319.29±.01	330.18±.00	338.89±.02	350.58±.01	360.10±.02	370.20±.01	381.21±.02	390.89±.00
95/06/19**	310.69±.01	319.32±.01	330.22±.00	338.96±.01	350.72±.00	360.27±.01	370.43±.00	381.47±.00	390.15±.00
97/12/19	310.65±.01	319.28±.01	330.22±.01	338.91±.01	350.63±.02	360.15±.02	370.24±.01	381.21±.01	390.83±.01

* Transfer calibration from new AES suite of primaries using original numbers.
** Transfer calibration from new AES suite of primaries after calibration by NOAA.

3.1.1.3. PREPARATION OF CO_2 STANDARD GASES

Carbon dioxide working standards are commercially prepared for the AES CO_2 monitoring program by Praxair Canada Limited. Praxair Limited pumps ambient air through a set of cooled baffles to remove water vapour and through adsorbent cartridges to remove residual contaminants including CO_2. The processed air is compressed into an aluminum cylinder to a pressure of 220 psi and pure dry CO_2 is added gravimetrically to a tolerance of ±0.1 ppm.

Steel cylinders were originally used to house the CO_2-in-air standards. In 1987, the use of steel cylinders was discontinued because larger concentration drifts were evident than in aluminum cylinders. Generally, gas standards are left to stabilize for up to 2 years, depending on intended use, to minimize the effects of CO_2 adsorption on the inner cylinder walls and concentration drifts within the tanks. AES has used CO_2 in natural air mixtures as standards for the past 8 years rather than mixtures of CO_2 in nitrogen or CO_2 in synthetic air. This has eliminated having to apply carrier gas corrections to the data. Nitrogen and disproportionate mixtures of synthetically produced air cause pressure broadening effects which modify the absorption characteristics of CO_2 during infrared analysis.

3.1.1.4. CO_2 CALIBRATION PROTOCOL

A schematic of the typical NDIR is given below in Figure 3.3. The system consists of an infrared source, a beam splitter, a sample and a reference cell and two IR detectors. The output of the analyzer is proportional to the difference in concentration of CO_2 between the sample cell and the reference cell. The analyzer may be run in absolute mode with zero CO_2 in the reference cell or, in order to improve system precision, may be run in differential mode with a flowing reference of concentration close to that expected for the unknown concentration in the sample cell.

Since the response function of the analyzer is non-linear, a simple 2-point calibration (reference plus span) is not possible. Initially, four standards were used to calibrate the system and a quadratic equation was fitted as the analyzer response function. Later, five standards were used to improve the degrees of freedom of the fitted equation (see Figure 3.4). The concentrations of the unknown gases are calculated by interpolation from the calibration curve. The gases are passed through a Siemens Ultramat III analyzer, following a *cascade* pattern. Each step in the cascade is four minutes in duration, giving a flushing volume of approximately 1.5 L. The analyzer output is averaged over the final 30 seconds of the 4-minute interval when the response is stable with time. The cascade pattern is repeated 12 times for each calibration but only the last 10 are used in the calculations. Figure 3.5 shows the output from a typical NDIR CO_2 calibration. When each cascade is completed, a quadratic is fitted to the analyzer response for the five known calibration gases and the unknown tank concentrations are calculated from this curve. The mean and standard deviations for each tank are calculated from the results from the 10 cascades.

A 12-port electronic stream selection valve is used to switch between gases every four minutes. This allows a maximum of five unknown gases to be calibrated against five known standards during each calibration. A target gas is also included in one of the suites of gases to monitor the system stability between calibrations. The 12th port is used to pass the reference gas through the analyzer to determine stability of the zero point, which is used in subsequent calculations to normalize the calibration curve.

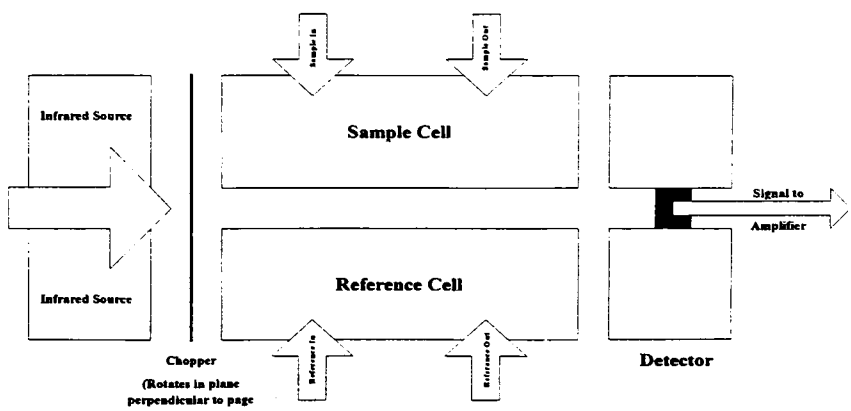

Figure 3.3 Schematic of an NDIR taken from the Siemens Ultramat III.

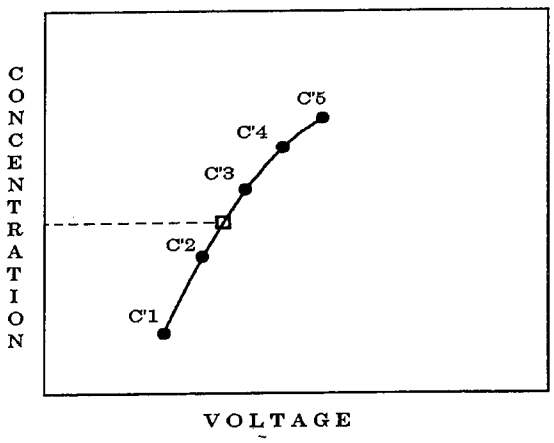

Figure 3.4 A typical response curve for an NDIR.

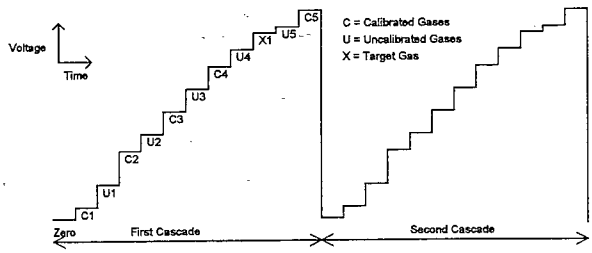

Figure 3.5 Typical chart recording of an NDIR CO_2 calibration.

Scott-1002 nickel-plated high purity regulators are used to regulate the outlet pressures of the gases during analysis. A Spangler 8262C90VH electric solenoid valve is incorporated into the zero gas stream to terminate the gas flow once the calibration is finished. After exiting the stream selection valve, the sample gas flow passes through a stainless steel sintered mesh filter and into an electronic mass flow controller (Tylan FC260 with RO28 readout). The sample flow is controlled at a rate of 300 cm^3 min^{-1}. Similarly, the reference gas flow is filtered and regulated at a rate of 30 cm^3 min^{-1}. Both sample and reference gases are dried as they pass through vapour traps immersed in a methanol cryobath maintained at -65° C. Reference and sample gases are equilibrated to room temperature by passing through 1/8-inch equilibration coils upstream of the analyzer. All the tubing used in the system, including the vapour traps, is 1/8-inch o.d. stainless steel tubing connected with stainless steel Swagelok® fittings. The NDIR analyzer has diffusion coils attached to the exits of both the sample and reference cells to minimize the back diffusion of water vapour from the room into the analyzer.

The analog signal from the analyzer is recorded using a CR21X Campbell Scientific data logger. The CR21X also records other variables such as room pressure, analyzer temperature, cryobath temperature and room temperature during each calibration. As well, the CR21X is used to control the automatic switching sequence of the 12-port Valco valve. The analyzer output and sample flow are also recorded on a Panasonic PM8252A chart recorder for visual purposes. Data collected for each calibration run sequence are directly transferred from the data logger to a personal computer.

Two BASIC computer programs are used to reduce the raw data output file from the data logger. The first program calculates averages and standard deviations, over the 10 cascades, of all the measured parameters for each of the gases. This allows the operator to assess the quality of the calibration over the 10 cascades and to notice any irregularities in the run. Calibration data is either accepted or rejected. The second program calculates actual concentration values for all unknown gases, creates an archive containing ancillary information such as calibration number, calibration date, tank serial numbers, tank types, port numbers, tank pressures, and creates output files which can be imported directly into the AES custom drift-correction database as described below.

3.1.1.5. Evaluation of Transfer Effects

To achieve the best possible measurement precision, the errors accrued in transferring concentrations from one level of standards to the next need to be quantified and minimized. To evaluate this, a "closing the loop" experiment is conducted at regular intervals in which the CO_2 mixing ratios are transferred from one level of standards to the next, following the sequence: AES primary $\rightarrow$ AES secondary $\rightarrow$ AES tertiary $\rightarrow$ AES working gases $\rightarrow$ AES primaries (same set used at the starting point). A variation of this protocol is to calibrate a set of tanks directly against the Primary set and then against the Tertiary set.

The intention of the experiment was to determine the magnitude of the error introduced by transferring concentration values via infrared analyses. The results are summarized in Table 3-3 and indicate that there is a systematic shift downwards by about 0.01 to 0.02 ppm after three transfers. It should also be noted that the P-Q values are generally higher than the T-Q values. The results given here are typical of these "closing-the-loop" experiments and indicate that there are no serious errors attributable to having 2-3 levels in the standards

hierarchy, however, the more levels you have the more complicated is the problem of tracking the calibration systems for drifts and transfer errors.

3.1.1.6. AES CUSTOM DATABASE FOR DRIFT CORRECTING CO_2 STANDARDS

A custom database was developed to correct the concentration drifts that usually occur in CO_2 standards. The database was written in Paradox PAL Version 4.0 and currently contains the CO_2 calibration data from 1986 to the present. The database is both relational and hierarchical with respect to the calibration data. Each cylinder is related through the database to the calibration gases used and those being calibrated. This allows a time history of calibrated concentrations to be extracted for each cylinder and provides a means for monitoring drifts in concentration. The calibration data is entered into the database based on the hierarchy given in Figure 3.6. Since the database is relational, changes in the concentration values of the AES primary standards are directly transferred to the AES secondary standards and from the AES secondary to the AES tertiary standards. All previous calibrations dependent on these cylinders are automatically recalculated. This lets the AES CO_2 program have current concentration values for each cylinder based on the latest calibration of the AES primary standards.

The drift-correction database is used to track drifts in the standards and currently holds all the CO_2 calibration data for the Canadian Baseline Program from 1986 to the present. There are several problems associated with the calibration data between 1987 and 1989. During this period, suites of calibration gases were inappropriately split up and the quality control of the calibration data was poor. Measures to improve the quality of the calibration data were implemented in 1990. These included:

- more periodic calibrations to characterize drifts in standards
- increased flushing times for gases during calibrations
- stricter criteria for the acceptance of calibration data
- system modifications

3.1.1.7. WMO INTERCALIBRATIONS

The WMO CO_2 Expert's Committee decided to implement a series of round robin calibrations as one means of comparing the scales in use by various laboratories. Two sets of tanks are prepared by the NOAA/CMDL laboratories in Boulder and sent to all the international laboratories making CO_2 measurements as part of the WMO GAW program. These tanks are first calibrated by NOAA and then sent in two loops (North America/Europe) and Austral-Asia. Upon their return to NOAA they are recalibrated to see if they have drifted. As can be seen from Table 3-4, the results from our laboratory are within 0.05 ppm or better which is well within the WMO objective to have all laboratories within 0.1 ppm. This is not the case for many of the participating laboratories. More details on these round-robin calibrations can be found in the WMO CO_2 Experts Meeting Reports.

3.1.1.8. NDIR MEASUREMENT SYSTEMS

Ambient CO_2 concentrations at Alert, NWT, Sable Island, NS, and Fraserdale, ON, are determined using NDIR technology. Similar experimental and calibration protocols are followed at each station with some minor variations depending on the requirements of the station. The setup for each station is a variation of that shown in Figure 3.7.

A typical NDIR measurement system consists of a filtered intake line pressurized to 15 psi, a large volume cryotrap maintained at -70° C to remove most of the water vapour, a 10 or 12 port rotary stream selection valve with mass flow controllers downstream for the sample and reference lines before the secondary cryotraps to remove any ice crystals escaping from the main trap prior to the NDIR analyzer.

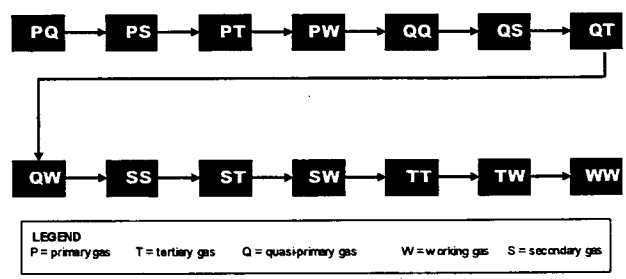

Figure 3.6 Hierarchy of drift-correcting database.

Table 3-3. Closing the loop experimental results using a set of tanks (referred to as "Q" tanks) which are calibrated directly against the Primary (P-Q) and then against the Tertiary (T-Q), after a top down calibration of Primaries to Secondary to Tertiary. The initial value for the tanks is the value from the last calibration. The tank AES111 is a surveillance tank included in all calibration to tract systematic errors

Serial Number	March 1993			April 1993		
	Initial Value	Transfer P-Q	Transfer T-Q	Transfer P-Q	Transfer T-Q	Initial-Final
76859	321.74	321.80	321.74	321.77	321.75	-0.01
76861	338.01	338.05	338.01	338.03	338.03	-0.02
76864	350.31	350.34	350.30	350.32	350.33	-0.02
76905	361.11	361.15	361.11	361.14	361.14	-0.02
AES123	377.43	377.47	377.44	377.48	377.45	-0.02
AES111	368.89	368.92	368.88	368.92	368.91	-0.01

Table 3-4. Canadian results for WMO round-robin interlaboratory calibrations.

Agency	Analysis Date			
USA NOAA Canada AES	June/July 1986 August 1986	**Cylinder 18049 (ppm)**	**Cylinder 8395 (ppm)**	**Cylinder 18502 (ppm)**
		335.48 335.53	341.49 341.47	350.54 350.51
USA NOAA Canada AES	September 1991 October 1991	**Cylinder 11413 (ppm)**	**Cylinder 13763 (ppm)**	**Cylinder 11051 (ppm)**
		341.47 341.45	347.41 347.36	375.16 374.76
USA NOAA Canada AES	August 1995 October 1995	**Cylinder 1357 (ppm)**	**Cylinder 1155 (ppm)**	**Cylinder 1230 (ppm)**
		342.16 342.14	358.92 358.91	376.77 376.76

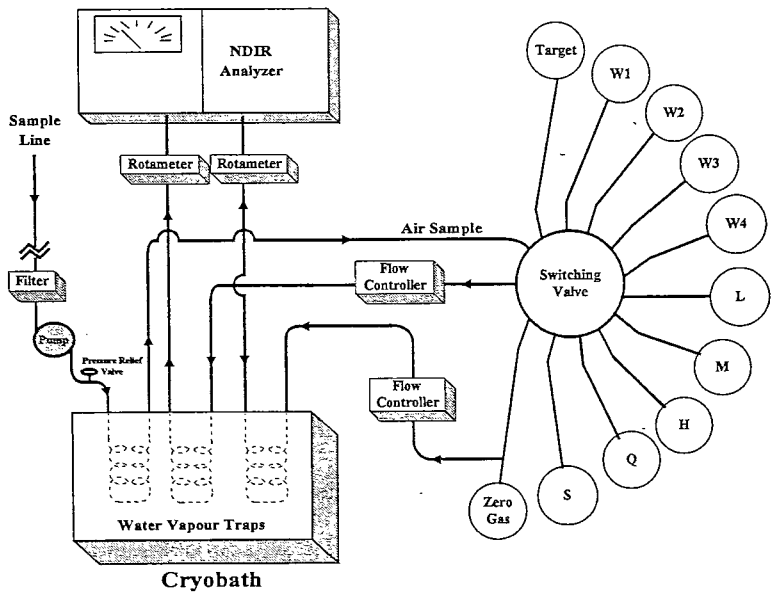

Figure 3.7 Schematic of a typical NDIR system used at one of the stations.

3.1.1.9. IN SITU CO_2 MEASUREMENTS AT ALERT

Continuous CO_2 measurements have been made at Alert since January 1987. However, reliable measurement are only available from June, 1987 when the systems was reconfigured from the then conventional solenoid gas switching to the rotary valve system described below. The NDIR analyzer used at the site is a Siemens Ultramat III throughout the period of record. The sample gas intake is a 20 cm heated glass line extending to 10 m above ground level. It is protected by a particle filter with a 15 micron cutoff. In the laboratory, the glass manifold reduces to 10 cm from which a ¼-inch stainless steel line is directed to the NDIR system.

A Neuberger (Model UN022SV1) vacuum pump is used with a pressure release valve to regulate the line pressure to 15 psig. The sample gas passes through a large bead-filled glass trap immersed in a cryogenic bath, set at -70° C, to permit analysis on a dry air basis. The sample gas flow is typically maintained at 300-400 cm^3 min^{-1} depending on the station. The reference or zero gas passes through a separate glass trap and flow controller and is maintained at 10-30 cm^3 min^{-1}. The CO_2 concentration is determined at about room pressure, since there are no restrictions downstream of the analyzer.

The drift of the analyzer is checked every hour by passing two calibrated working gases through the analyzer for five minutes each. The concentrations of the two working gases bracket the current concentrations being measured at Alert. Generally, there is a 10 to 15 ppm concentration difference between the two working standards. Ambient air is passed through the system for the remaining 50 minutes of each hour. In 1994, a target or surveillance gas was injected every five hours immediately after the span gases to check overall system performance.

The working gases, which are used to check the drift of the analyzer every hour, are calibrated against the station standards designated C1 to C5. The next set of working standards to be used on the system (W3 and W4) are also attached and are calibrated along with the current working gases. In 1994 a surveillance tank was added and was switched in every five hours immediately after the W2 gas as a check on overall system performance. The station standards are calibrated, approximately every 6 months, against a set of transfer standards maintained at the CCRL calibration facility in Toronto. The standards maintained in Toronto are referenced to the WMO 1993 scale. The analytical precision of the measurements is estimated to be better than 0.05 ppm.

The voltages from the analyzer are averaged over a 5-minute period and are stored in a data logger (CR21X) along with the maximum, minimum and standard deviation for that period. The loggers are connected via a local area network to a modem for external access and to a computer in the Alert GAW Observatory for local access and storage. The loggers are polled every 3 hours by a data collection computer in the Alert office located 7 km away at the main camp. The system parameters are plotted daily by the operator and checked to see that they are within acceptable limits. The QC/QA program (described below) is applied weekly to the accumulated data and the data are then flagged by the station operator to identify observed local problems.

The data collected from the NDIR are considered to be "raw" data, which are later subjected to correction for drifts in the standards and the hour to hour drifts in the system response. The data are flagged for known problems by the station operator, as described in Section 4.0. In addition, the data are run through a preliminary quality assurance program to check system performance. First a median analysis is done on the calculated concentrations and standard deviations for the hourly working standards and any outliers are identified. The first character of the QC/QA flag (see Table 3-5) is set to O if the value is identified as an outlier when compared to the other 23 hourly values for the standard, or + if there are no problems. The second character is set to V if the standard deviation for the standard gas is identified as an outlier when compared to the other 23 standard deviation or else it is set to +. A similar analysis is done for the mean values for the ambient air concentrations for the 24-hour period. Next, the system performance is evaluated using the following measurements (see Table 3-5):

- analyzer temperature
- room temperature
- cryocooler bath temperature
- flow rates,
- room pressure
- CN or PAH concentrations

Table 3-5. QC/QA flags set by preliminary QC/QA program.

Set by the principal investigator, the CO_2 NDIR QC/QA flag is a set of characters that is no greater than 30 characters in length. The space and comma characters may not present in the string. The following are the meanings of some of the character combinations.

@ Set by some extraction programs if not used immediately and to be set later by the principal investigator

Set by the extraction program, ALTCO2SP, which splits out the NDIR data

++ No system problems
O+ Outlier from daily median analysis of 5 minute means
+V Outlier from daily median analysis of 5 minute standard deviations
OV Combined from both above

These flags identify the calibration gases and are added to the above flags

W1 1st working gas
W2 2nd working gas
W3 3rd working gas
W4 4th working gas
TT Target gas
ZZ Zero gas
LL Low calibration gas
MM Mid calibration gas
HH High calibration gas
QQ Span calibration Gas

These flags are systems checks and are added to the above flags

PR Pressure variable (probably OK but needs checking)
TR Room temperature fluctuations (could be a problem for the NDIR)
ZC Analyzer zero chamber temperature fluctuations greater than 1° C
SC Analyzer sample chamber temperature fluctuations greater than 1° C
ZT Zero trap temperature fluctuations greater than 1° C
ST Sample trap temperature fluctuations greater than 1° C
ZF Zero flow fluctuations greater than 1 cm^3min^{-1}
UZ Unstable Zero regulation - maximum - minimum greater than 1%
SF Sample flow fluctuations greater than 1 cm^3min^{-1}
US Unstable Sample regulation - maximum - minimum greater than 1%
CN CNC fluctuations greater than 100 counts

Example: OVW1TRZFCN
++W1OK

3.1.1.10. In Situ CO_2 Measurements at Fraserdale

Except for the year-and-a-half period beginning 1997, continuous CO_2 measurements have been made at Fraserdale, Ontario, since February 1990. The NDIR analyzer used at the site is a Siemens Ultramat III until 1994 when a Siemens Ultramat V was installed. Because of the large diurnal range of concentration, the sampling protocol at Fraserdale is somewhat different from that of Alert. A fixed normalized quadratic calibration equation is entered into the logger to calculate preliminary concentrations. Every hour the drift of the analyzer is checked by passing a calibrated target gas (approximately 360 ppm) and a zero gas (approximately 310 ppm) through the analyzer for three minutes each. Ambient air is passed through the system for the remaining 54 minutes of each hour. Every five hours the target gas, zero gas, and three working gases are passed through the analyzer for three minutes each. Every 15 days the working and target gases are calibrated against the four station standards. These station standards are calibrated approximately every six months against a set of transfer standards maintained at the CCRL calibration facility in Toronto.

The voltages from the analyzer are averaged over a 3-minute period and the ambient concentrations are calculated from the fixed quadratic equation described above. In subsequent processing programs a quadratic system response function is calculated every five hours using the measured concentrations of the target and three working gases. This response function is used to recalculate the ambient CO_2 concentrations. The data are corrected for drift by linearly interpolating between the hourly target values and the calibrated target values. The hourly zero gas concentrations are used to normalize the data. Hourly averages (ppm) are then calculated from the 3-minute drift corrected data.

When the Ultramat V analyzer was installed in 1995, the Alert sampling protocol was adopted because the output of the Ultramat V is considered to be sufficiently linear to do a 2-point calibration. As with the Alert program, a target gas is injected every 5 hours to evaluate systematic errors.

3.1.1.11. In Situ CO_2 Measurements at Sable Island

A short continuous CO_2 measurement program at Sable Island was established in August 1992 for about seven months using the attic of the AES Upper Air Station. The sample intake line was installed on a nearby 50 ft tower located about 0.5 km from the southern shoreline. The NDIR analyzer used at the site was a Hartman & Braun URAS-3E. The sampling protocol was similar to that used at Fraserdale.

3.1.1.12. In Situ CO_2 Calibration Protocol

The calibration protocol for the stations is essentially the same as that used in the calibration laboratory described in Section 3.1.1.5. At each station there is a set of station standards (five levels), which are used to calibrate the working gases. Alert started initially with four standards but switched to five in 1990. Every seven to eight days at Alert and Sable Island and every 15 days at Fraserdale, a calibration is initiated automatically by the data logger to check the drift of the working gases in use at the time, as well as, the next set of working standards to be used at the station. The calibration data are extracted from the data files by the station operator to verify that the process was within specifications laid down in the standard operating procedures manual. If not, another calibration may be initiated manually. The calibration data are sent to the Downsview Laboratory where the supervising technician checks the calibration and may re-run it if errors are found. The calibrations are then entered into the main database from which drift equations are calculated.

3.1.1.13. References

Zhao, C.L., P. Tans and K. Toning, 1997, A high precision manometric system for absolute calibrations of CO2 in dry air, *J. Geophys. Res.*, 102 (5), 5885-5894.

3.1.2. FLASK CO_2 MEASUREMENTS

Victoria Hudec, Kaz Higuchi and Neil B.A. Trivett

AES has used evacuated 2 L glass flasks fitted with 6 mm bore high vacuum stopcocks (lubricated with Apiezon-N grease) at Alert, Sable Island and Cape St. James since 1975. Sampling problems associated with the greased stopcock and the delicate neck on the flask led AES to introduce a new flask type into its sampling network at Alert and Estevan Point in 1992. This new flask type has a glass barreled valve with Viton® o-ring seals. It is more robust for field sampling and easier to open in extreme cold temperatures than the greased stopcock flasks.

Grab sampling, i.e., opening an evacuated flask to the air, is a very convenient and economical technique, but can have contamination problems associated with it. Flask contamination can occur if there is not a complete vacuum in the flask prior to taking the sample. Most frequently, however, contamination is the result of poor sampling practices in which the flask becomes contaminated from the operator's breath. To eliminate the problems associated with evacuated flask methodologies, AES introduced a third flask type into its sampling network at Alert and Estevan Point in 1993. This flask has dual glass barreled valves with Viton® o-ring seals. The volume of this flask can be completely flushed and pressurized with air from a sampling line that is attached to a pumping unit. The three AES flask types are illustrated in Figures 2.7 to 2.9 in Section 2.1.2.2. The evacuated and pressurized flask sampling protocols used by AES are outlined below.

3.1.2.1. FLASK SAMPLING PROTOCOLS

2 litre, greased stopcock flask / 2 litre, single valve, o-ring - evacuated

These flasks are evacuated to pressures of 10^{-4} mb at AES using a vacuum system that operates with a mechanical and a turbo molecular pump. Up to eight flasks are housed in an oven that is set to 60 degrees. A Cajon fitting connects each flask to a 6-inch length of stainless steel flexible tubing ¼ inch in diameter. Each length of the flexible tubing is connected to a short ¼-inch stainless steel tube that is welded to a stainless steel manifold, which is 1 inch in diameter. The turbo and mechanical pumps are connected to this manifold via a stainless steel flexible hose that is 1 inch in diameter. The flasks are left to evacuate on the system for a minimum of 4 hours to reach a pressure of 10^{-4} mb. The flasks are heated to remove any residual water vapour from the walls of the flasks.

At the flask sampling sites, the flasks are sampled outside away from any sources of CO_2, approximately 100 metres upwind of the station. Flask samples are generally collected on days when the wind direction is from a "clean sector" and the wind speed is greater than 5 m s^{-1}. (For Alert the wind speed criterion is greater than 1 m s^{-1}.) The operator walks into the wind holding the flask overhead, pointing the nozzle of the flask into the wind. With quick rapid movements, the operator moves a dowel into and out of the nozzle of the flask to purge it of room air. Holding his/her breath, the operator walks three paces into the wind and opens the stopcock/valve of the flask. The operator continues to hold his/her breath and walks into the wind until the hissing sound of air rushing into the flask stops. The operator waits an additional 10 seconds to allow the pressure in the flask to equilibrate to ambient pressure and then closes the flask. The operator does not exhale until the flask is closed to avoiding contaminating the flask with CO_2 from his/her breath. The procedure is repeated with a second flask. A pair of flasks is sampled for quality control purposes. The time of the sample and relevant meteorological parameters are recorded on a flask log sheet.

For greased stopcock flasks, the stopcock grease hardens in cold temperatures making it difficult to open the flasks. At Alert and Sable Island, when sampling is required in cold temperatures, Thermo Pad® handwarmers are taped around the stopcocks to keep the grease warm and the stopcocks easy to turn.

2-litre, dual valve, o-ring flask - pressurized

This flask type has an inlet and outlet valve that can withstand pressures up to 60 psi. There is a glass delivery tube attached to the inlet valve of the flask that extends to the bottom of the inside of the flask. The delivery tube has four outlet ports for even distribution of airflow through the flask. A vacuum pump (KNF Neuberger pump, Model UN022-SV1) draws sample air from a sampling line that extends from a tower (10 m at Alert; 39 m at Estevan Point). The sample air is dried chemically using magnesium perchlorate (Estevan Point) or is passed through a glass trap submerged in a methanol bath set to -60° C (Alert).

A pair of flasks is flushed with sample air simultaneously at a flow rate of 2 L min^{-1} for 20 minutes at Alert or 500 ml min^{-1} for 40 to 60 minutes at Estevan Point. The flasks are then individually pressurized with sample air to 15 psi. The flushing time, the filling time and relevant meteorological parameters are recorded on a flask log sheet. Prior to being shipped to the sampling sites, the flasks are filled with dry air, which has a CO_2 mixing ratio of about 300 ppm.

3.1.2.2. FLASK MEASUREMENT TECHNIQUES

IOS maintained the flask analysis program from the inception of the program through to 1988. The data are published in a paper by *C.S. Wong et al.*, [1984]. A Hartman and Braun URAS-2T analyzer was used for the analyses. IOS used analysis and extraction techniques similar to those of *Komhyr and Waterman*, [1983].

In 1988, AES assumed responsibility for the flask programs at Alert, Cape St. James, and Sable Island. The analyses were initially made using a Hartman and Braun URAS-3E analyzer. In October 1989, the analyzer was changed to a Maihak UNOR-6N. All analyses were made using CO_2-in-air reference gases. Three CO_2 standard gases (340 ppm, 355 ppm and 365 ppm) and a reference gas (330 ppm) were used on the analysis system. The mixing ratios of the standard gases were calibrated at AES and are traceable to the SIO 1985 scale.

The AES CO_2 flask analysis system was designed to analyze a maximum of eight flasks per run. An 8-port stream selection valve was used to switch between flasks while a vacuum pump (KNF Neuberger pump, Model UN022-SV1) was used to extract the air from the flasks. The three calibration gases and eight flasks were switched manually. A Campbell Scientific CR21x data logger was used to collect the raw data. All measurements were made on a *dry air* basis, with both sample and reference gas air streams passing through stainless steel traps (¼ inch diameter) submerged in a methanol bath at –55° C. Only one aliquot was extracted and analyzed from each flask. A typical flask run sequence consisted of the calibration gases (C1 to C3), followed by eight flasks, and again followed by the calibration gases (C1 to C3).

For each run, the voltages of the calibration gases, before and after the flasks, were averaged. The averaged voltages and mixing ratios assigned to the calibration gases were used to generate a quadratic system response function for the run. The mixing ratios for the flasks were calculated by substituting the flask voltages into the system response function for each flask run. Minimal or no drifts were observed in the bracketing voltages of the calibration gases.

Changes were made to the flask analysis system in April 1991. The UNOR-6N analyzer was replaced with a Siemens Ultramat III analyzer. The change in analyzer was necessary because the UNOR-6N was sensitive to subtle changes in sample flow, which occurred even though mass flow controllers were used. Because the Siemens analyzer had a larger sample cell volume (100 cm^3) compared to the UNOR-6N analyzer (8 cm^3), it was necessary to increase the flushing volume from each flask. The system was modified for "static" measurements to compensate for the extra volume required for flushing. To achieve static measurements, the system is flushed with gas and then a solenoid valve shuts off the gas flow to the sample cell. The gas in the sample cells equilibrates to ambient pressure before a measurement is taken. Static measurements require less gas from a given flask.

Changes to the system included the addition of a 10-port stream selection valve, a target gas (350-360 ppm), two additional calibration gases (340-380 ppm), and a solenoid valve upstream of the sample cell. The reference gas, five calibration gases, target gas, and the outlet of the flask stream selection valve were connected to the 10-port valve (see Figure 3.8).

At present, a typical flask run has the following sequence: reference, calibration gases (C1-C5), reference, target, flasks (F1-F8), reference, calibration gases (C1-C5), reference and target. Prior to running the flask analysis system on any given day, the regulators on the reference tanks, calibration tanks and target tanks are flushed with about 3 L of gas. The gas is also passed through the system to stabilize the analyzer. To extract air from the ambient pressure flasks, an automated sequence is programmed into the data logger to control 1) the switching of the stream selection valves, 2) the opening and closing of the solenoid and 3) turning the pump on and off. The data logger also collects the raw data and calculates the average and standard deviation voltages for each sample. The following is the analysis protocol for a typical flask run.

- The stream selection valve is set to port one for the reference gas.
- The reference gas is flushed through the system for 140 seconds at 300 cm^3 min^{-1}.
- The solenoid valve upstream of the sample cell (see Figure 3.8) closes, allowing the gas to equilibrate to ambient pressure in the sample cell for 25 seconds.
- The signal and standard deviation of the signal (in volts) are averaged for 15 seconds and stored in the data logger.
- The stream selection valve is stepped to the next port.
- The same flushing, equilibration and averaging procedure is used for the calibration gases, reference gas, target gas and eight flasks.
- For ambient pressure flasks, the air is extracted from the flasks with the vacuum pump (the

CR21X controls the switching on and off of the pump).

- For pressurized flasks, a switch is manually set to disable the pump, although the air from the flasks passes through the pump.

Subsequent calculation of the mixing ratios for the individual flasks is done using a BASIC program run on a PC. Flask mixing ratios are determined as follows:

1. A quadratic function of voltage versus time is calculated using the four reference gas responses.
2. The flask, calibration and target voltages are normalized using the above quadratic function.
3. A linear response function of voltage versus time is calculated for each of the five calibration gases, using the before and after flask voltages.
4. For each flask and target, the sample time is substituted into each of the five linear response functions for the calibration gases to determine the interpolated voltages for C1-C5.
5. A quadratic response function of voltage versus mixing ratio is calculated for each flask using the five interpolated calibration voltages and their assigned mixing ratios.
6. A mixing ratio for each flask and target sample is determined by substituting their respective voltages into this quadratic function.

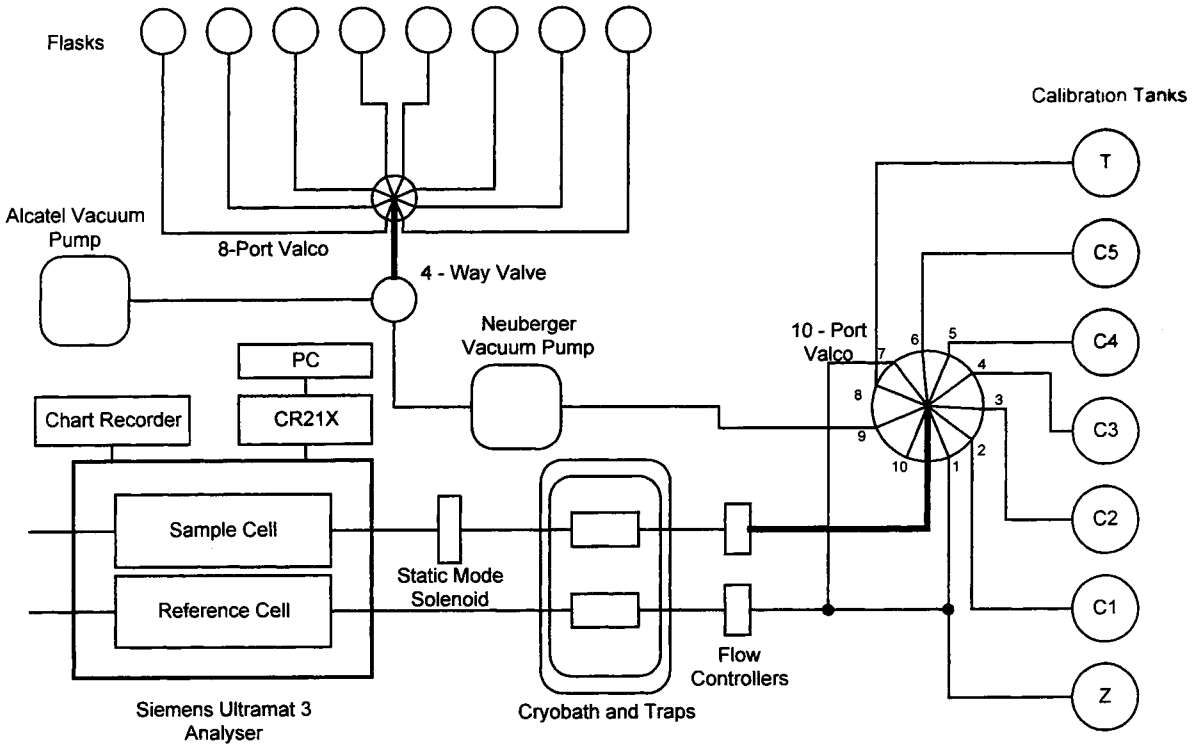

Figure 3.8 Configuration of the AES flask analysis system.

3.1.3. STABLE ISOTOPES OF CO_2

Ann-Lise Norman and Darrell Ernst

3.1.3.1. MEASUREMENT SYSTEM

As part of CCRL, the Stable Isotope Laboratory operates a Finnigan MAT 252 isotope ratio mass spectrometer (IRMS) capable of high precision measurements of light stable isotopes. Analytical methods have been developed to determine $\delta^{13}C$ and $\delta^{18}O$ in 0.5 to 1 ml of atmospheric CO_2 to within ±0.02‰ and ±0.05‰ respectively. Samples containing less than 1000th this amount can be analysed by GC separation but lower precision is realized.

Existing flask samples collected by other groups are utilized. Stable isotope determinations are made without any additional sampling or logistical requirements. CO_2 is cryogenically extracted and purified off-line from air remaining in weekly AES and CSIRO flask samples collected at Alert and Estevan Point, following concentration determinations for CO_2 and trace gases by CCRL at AES.

3.1.3.2. MEASUREMENT / CALIBRATION PROTOCOL

When analyzing AES flask samples, an aliquot of gas is removed by the CCRL concentration analyses. After this, the 2L flask is attached to a vacuum extraction line. A leak test is performed prior to each extraction by monitoring a static vacuum in the extraction line to ensure that all connections and valves in the system are sound. The sample is then slowly passed through three separate liquid nitrogen cooled traps to quantitatively remove all condensibles. Air in the flask is extracted until the line pressure reaches 2 mTorr. The sample flask valve is then closed and trace amounts of non-condensibles are evacuated from the extraction line. Condensibles are transferred from the first to second cold trap by replacing the liquid nitrogen with a dry ice/ethanol slush. After transfer, trace amounts of non-condensibles remaining are again evacuated to less than 1 mTorr. Sample gas transfer from the second to third loop is achieved in a similar manner. CO_2 is released into a calibrated volume using a dry ice/ethanol slush and the sample pressure is recorded. The sample is cryogenically transferred to a preheated 6 mm o.d. glass tube and flame sealed with a propane/oxygen torch. Samples sealed in these tubes have a relatively long shelf life (months) with no evidence of leakage or fractionation. Once the sample has been sealed in the tube, the approximate water content remaining in the vacuum line can be determined from the vapour pressure in the calibrated volume.

Quality control for the extraction procedures includes periodic extraction and analysis of a 2 L flask filled with "standard air" containing 360 ppmv CO_2 of known isotopic composition.

$\delta^{13}C$ and $\delta^{18}O$ are determined relative to two working standards of pure CO_2 (APB-2 and PR-1) and carbonates (Cal-1 and Cal-2) which have been calibrated against international standard reference materials (NBS-18, NBS-19) relative to Vienna PeeDee Belemite (Figure 3.9). These carbonates are used to generate carbon dioxide by acid digestion. Highly purified and concentrated (> 101%) phosphoric acid is prepared for the digestion procedure. Strict attention to protocol is observed in order to achieve quality standardization. The digestion is carried out in clean, preheated glass Y-tubes. Vessels and pipettes are warmed to minimize contamination from condensed water. The reaction is carried out in a constant temperature bath at 25 ± 2° C. Secondary and tertiary standards used on a daily basis are calibrated periodically (every six months). Secondary standards are comprised of other carbonates (CAL-1 and CAL-2) as well as other compressed CO_2 gases (e.g., Oztech standard). Tertiary standards (e.g., PR-1, APB-2 and MG-1 as supplied by commercial manufacturers) are used for daily standardization. Precision of the results is typically ≤ 0.02‰ for $\delta^{13}C$ and ≤ 0.05‰ for $\delta^{18}O$.

A number of laboratory investigations of possible sources of errors in isotope ratio determinations from flask samples of air have been carried out. As one example, an experiment showed an increase in water as a function of storage time (Figure 3.10). Because oxygen isotope exchange can occur between gaseous CO_2 and H_2O in flasks, the $\delta^{18}O$ ratio in CO_2 determinations may be altered between sample collection and analysis. This increase has been identified as resulting from water vapour diffusion across o-ring seals of flask valves. Preventive measures are under consideration.

Corrections must also be made for the presence of nitrous oxide, which is an isobar and is co-extracted with CO_2. N_2O is present in ambient air at a concentration of approximately 0.3 ppmv, or 0.1% of typical CO_2 concentrations in remote locations. The magnitude of this interference can be calculated and a correction applied if the ionization efficiency of N_2O relative to CO_2 is known (and the concentrations of CO_2 and N_2O are also known). Another factor involved in the N_2O correction is the assumed isotope ratio for

N_2O, which can affect the final values by 0.0006 ‰ permill change in $\delta^{15}N$ or $\delta^{18}O$. Taken together, these factors could contribute to differences as large as 0.045‰ in $\delta^{13}C$ and 0.05‰ in $\delta^{18}O$ in atmospheric CO_2.

An additional level of quality assurance is present through a comparative program with CSIRO, where $\delta^{13}C$ and $\delta^{18}O$ ratios in air remaining in a set of monthly flasks collected at Alert and Estevan Point are determined following CSIRO analysis, which provides a link to results from other isotope laboratories through the extensive CSIRO program.

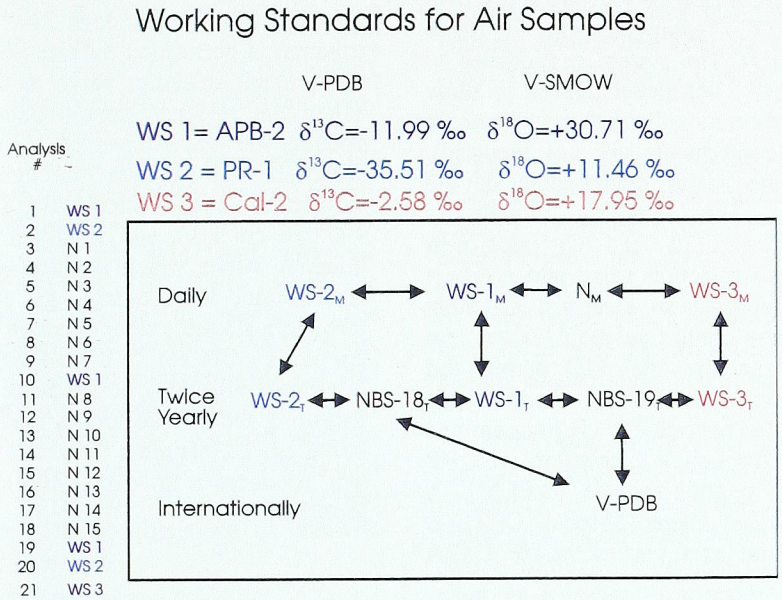

Figure 3.9 Schematic demonstrating sample and laboratory standard measurement protocols and how the data are calibrated to the international V-PDB scale.

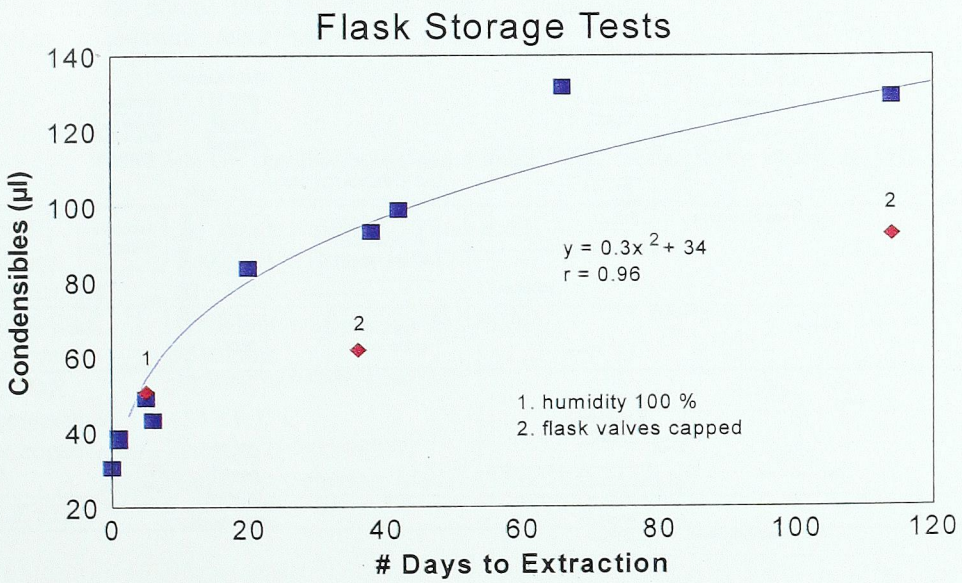

Figure 3.10 Air of known isotope composition was stored for up to 90 days. The amount of water increased over time and is attributed to diffusion of water vapour across the flask o-ring seals.

3.2. IN SITU CH_4 MEASUREMENTS

Douglas E.J. Worthy and Michele K. Ernst

3.2.1. MEASUREMENT SYSTEM AND SAMPLING PROTOCOL

The automated measurement of methane at Alert and Fraserdale is made using a Hewlett Packard (HP) 5890 gas chromatograph (GC), equipped with a flame ionization detector (FID). The system is modified to house and control an HP 5790 nickel catalyst to allow the measurement of carbon dioxide on the same sample run (the GC CO_2 measurements are not reported). Figure 3.11 shows the major components of the measurement system. The sampling module is comprised of a thermostated (30 ± 0.5 °C) Valco oven housing a 4-port stream selection valve and a 6-port sampling valve with appropriate electrical actuators (Valco), and on/off flow control solenoid valves. An HP 3392A integrator acquires the FID output and controls the automatic operation of the analysis procedure. The automated operation is via programmed external timed events through a connection to a HP 19405A sampler/event control module (S/ECM). A Campbell Scientific data logger (Model CR21X), which is connected to the serial port of the HP 3392A integrator, is used to acquire the integrator report generated by the integrator.

The automated sampling module is designed to sample from four separate gas streams supplied to the instrument at about 10 psig. Standard gases are provided from pressurized cylinders equipped with high-purity two-stage regulators. Selection of the gas stream for presentation to the sampling injection system (with simultaneous flow interruption of "off" streams) is performed by electrical actuation of the 4-port stream selection valve to the required position. When the relevant stream-control solenoid valve is opened, the gas fist passes through the 4-port stream selection valve, then through a stainless steel temperature equilibration coil (183 cm x 0.159 cm o.d. x 0.076 cm i.d.), and finally into the 6-port sample injection valve, which is fitted with a 3 cm^3 stainless steel sample loop. Sample gas flow exits the system through a stainless steel isolation coil (183 cm x 0.159 cm o.d. x 0.076 cm i.d.). To maintain dead-volume at a minimum, all tubing downstream of the inlet solenoid, including the sample loop s made of 0.159 cm o.d. x 0.076 cm i.d. stainless steel. An input pressure of ~ 5 psig produces a flow of ~ 100 cm^3 min^{-1} through the loop system.

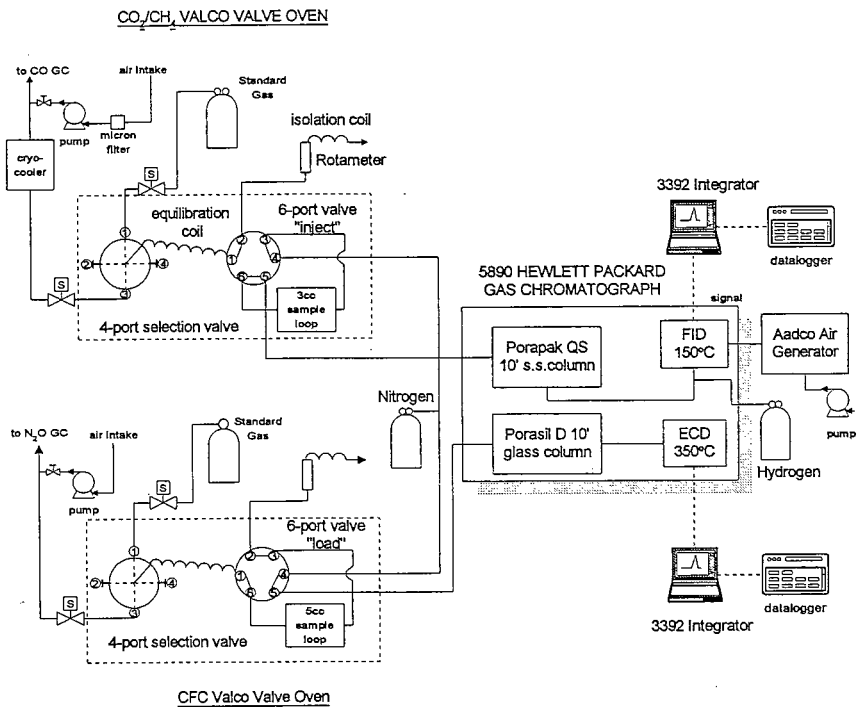

Figure 3.11 Schematic of the AES automated gas chromatographic CO_2/CH_4 and F-11/F-12 measurement system.

After a 46 seconds purging flow, the flow control solenoid valve is shut to allow the gas in the sample loop to equilibrate to atmospheric pressure and the valve oven temperature. Following an equilibration time of 72 seconds, the 6-port sample injection valve is switched to transfer the contents of the sample loop into the carrier gas stream and onto the GC column. The carrier gas supply of the gas chromatograph to the packed column injection port (unheated) was plumbed to pass first to the 6-port valve, and then on to a stainless steel column (366 cm x 0.32 cm o.d. x 0.22 cm i.d.) packed with Porapak QS (100-120 mesh), maintained at 40° C. A carrier gas flow of 25 cm^3 min^{-1} ultra high pure nitrogen (>99.9998%) provides retention times of around 2.2 minutes for methane and 4.8 minutes for carbon dioxide. On leaving the column, the carrier gas mixes with ultra high pure hydrogen (>99.99999%) flow of 30 cm^3 min^{-1} and enters the catalyst unit maintained at 350° C to affect the conversion of carbon dioxide to methane. The nitrogen/hydrogen stream then passes to the flame jet of the FID (150° C) and is combusted with 425 cm^3 min^{-1} of purified dry air (Aadco Model 737-1A air generator). This combination of flow and detector conditions provides good resolution of methane and carbon dioxide from oxygen and carbon monoxide, and gives high response. The specifications of the GC systems are given in Table 3-6.

At Fraserdale, ambient air is delivered to the GC at approximately 5 L min^{-1} by a KNF Neuberger N2202 vacuum pump via a 0.95 cm o.d. sample line (Dekoron) from a 40 m intake on a tower. The ambient air passes through a 7 μm stainless steel membrane filter upstream of the pump. The ambient air then passes through a pressure relief valve set at 1 atmosphere to release excess pressure. The ambient air is then dried to a dew point of around -60° C by passing it through a glass trap submerged in an -80° C methanol bath. The flow of dried air is then split between the inlet to the GC and the inlet to nondispersive infrared (NDIR) analyzer. Standard gas is supplied to the GC from a pressurized gas cylinder equipped with a high-purity, two-stage gas regulator. Stainless steel tubing (0.32 cm o.d. x 0.22 cm i.d.) is used for the standard gas sample line and for the ambient sample line after the cold trap. An additional stainless steel filter is used in the sample line to the GC.

At Fraserdale, each GC measurement cycle consists of a standard gas injection followed by two ambient air injections repeated every 30 minutes (96 ambient air measurements per day). The peak height for the standard injection is used to calculate a system response factor, which is then used to calculate the CH_4 mole fraction of the two subsequent ambient injections and the standard injection of the next cycle.

At Alert, the ambient air is drawn from a glass manifold, which extends to 10 m outside the laboratory, at approximately 5 L min^{-1} by a KNF Neuberger N2202 vacuum pump. The ambient air is passed through a cryogenic trap and filter similar to what is done at Fraserdale. Measurements initially began in November 1987 with a five-injection cycle of standard, ambient, standard, ambient, and standard, repeated every hour. In January 1990, the five-injection-per-hour protocol at Alert was changed to a half-hourly three-injection protocol as done in Fraserdale.

Table 3-6. GC specifications for automated CH_4 measurement system at AES

COLUMN	10' stainless steel (3/16 inch o.d.)
Packing	Porapak QS (Mesh 100-120)
Temperature	40 ± 0.1° C
CARRIER GAS	Ultra high purity N_2 (> 99.9995%)
Flow rate	25 ml min^{-1}
DETECTOR	FID
Temperature	150 ± 0.1° C
Hydrogen	Zero Gas (> 99.9999%)
Air	Aadco Air Generator Model 737 or UHP cylinder
SAMPLE SIZE	3 ml

Peak areas were initially used at Alert, however, in May 1991, the integration procedure was changed from peak areas to peak height. The peak height integration procedure increased the CH_4 precision by approximately 30 percent to give a relative repeat precision (1s) of the analysis of approximately 0.3%. All CH_4 measurements at Alert and Fraserdale are reported in nmole $mole^{-1}$ (parts per billion (ppb) mole fraction) dry air. Ambient CH_4 measurements are included in the final data set only if the re-evaluation of the standard gas is within 10 ppb of its assigned value. Approximately 90% of the data are accepted at both sites using this criterion. The data are also manually inspected and examined using quality control routines before being accepted as valid ambient measurements (refer to Section 4 for data management procedures).

3.2.2. METHANE STANDARD GASES

As with the CO_2 trace gas program, methane gas standards are classified as primary, secondary or working gas. The standard CH_4 scale, to which the AES CH_4 measurements are referenced, is based on a set of primary CH_4 Standard Reference Materials (SRMs) purchased from the National Institute for Standard Technology (NIST). The NIST certified methane mixing ratios in the cylinders are referenced to a secondary standard set that is intercompared with a set of gravimetric primary standards. Table 3-7 lists the NIST cylinders purchased by AES. The given limits of inaccuracy (column two in Table 3-7) represent the uncertainty in the methane mixing ratios in the primary gravimetric standards and the imprecision of the intercomparison.

The mixing ratios in the primary standards CAL-8246 and CAL-8313 have been intercompared in the AES laboratory several times. The intercomparisons disclosed a small discrepancy between the two cylinders. CAL-8246 appeared to be between 1.8 ppbv and 2.1 ppbv higher in concentration than CAL-8313. However, this difference is within the estimated NIST uncertainty for the cylinders. Linearity tests were also done by evaluating the mixing ratio of CAL-8297 against both CAL-8313 and CAL-8246. Tests were completed on three distinct GC systems. All system responses were linear within the estimated uncertainties of the standards, verifying the validity of 1-point calibrations.

In 1986, three large steel cylinders (serial numbers 76878, 76876 and 76895) that were previously used in the CO_2 program were adopted as secondary standards for the methane program. These cylinders were calibrated yearly against a primary NIST standard until 1991 when the pressure in the NIST cylinders dropped below acceptable levels. The mixing ratio of cylinder 76878 was determined against both the 1 ppb NIST primary standards. The results of the calibrations are outlined in Table 3-8. The results showed that the mixing ratio of secondary standard 76878 was stable over the initial 4-year period of the program. The 2 ppb discrepancy is also evident in the calibration due to which NIST primary standard was used (see Table 3-8). Because of this discrepancy, the methane measurement scale utilized at AES is propagated only from cylinder CAL-8313.

In order to prolong the lifetime of primary calibration cylinder CAL-8313, the secondary cylinder (76878) is used to calibrate the other assigned secondary cylinders 76876 and 76895. The calibration results, which are given in Table 3-9, clearly indicate that there has not been an appreciable drift in the mixing ratios of these additional secondary standards since the inception of the program in 1987. To date, these secondary standards are used to calibrate all subsequent working standards that are used to determine ambient CH_4 mixing ratio observations at Alert and Fraserdale.

In 1994, in order to preserve the main suite of secondary standards (serial numbers 76878, 76878 and 76895), three additional standards were purchased with the intent that they will eventually replace the existing secondary set. These new standard gases are 37.5 L aluminum tanks (purchased from Scott Marin), which have been internally treated by a proprietary process referred to as Aculife Treatment. The new standards have been periodically checked for stability against cylinder 76878. The results are given in Table 3.10.

Table 3-7. NIST standards purchased by AES.

Serial Number	Certified Mixing Ratio	Batch Number	Year Purchased
CAL 8246	913 ± 10 ppbv CH_4	NIST SRM 1658	1986
CAL 8313	913 ± 10 ppbv CH_4	NIST SRM 1658a	1988
CAL 8297	9790 ± 20 ppbv CH_4	NIST SRM 1659	1988

Table 3-8. Calibration history of cylinder 76878.

Calibration Against Cylinder CAL-8246			Calibration Against Cylinder CAL-8313		
Date	Mixing Ratio (ppb)	Variability (ppb)	Date	Mixing Ratio (ppb)	Variability (ppb)
August 14, 1987	1726.8 ppb	2.0	June 27, 1988	1725.0	4.4
August 18, 1987	1727.2 ppb	3.1	December 7, 1989	1725.0	4.0
March 21, 1990	1727.8 ppb	3.1	March 30, 1991	1724.9	3.8

Table 3-9. Secondary calibration relative to gas standard 76878 (1725.0 ppb).

	Cylinder 76876		Cylinder 76895	
Date	Conc. (ppb)	Std. Dev.	Conc. (ppb)	Std. Dev.
September 1987	1734.2	6.2	-------	-------
August 1987	1733.5	2.5	-------	-------
October 1987	1735.0	2.2	-------	-------
May 1988	1734.0	4.1	1726.5	2.3
June 1988	1734.0	4.4	1726.8	4.4
March 1989	1734.8	3.0	1732.0	4.1
March 1989	1734.0	3.3	1728.0	3.2
March 1991	1734.1	2.7	1726.6	2.1
November 1992	1733.8	1.7	1726.3	1.8
March 1994	1733.8	0.8	1726.7	1.8
September 1994	1733.6	2.8	-------	-------
November 1995	1734.2	1.5	1726.8	1.8
March 1998	1734.3	2.1	1727.0	2.5

Unlike in the previous suite of secondary tanks, these standards were purposely made to cover the measurement range of ambient observations observed at background stations. Similar to the results seen previously, essentially no drift has been observed in these tanks as well.

It should be note that working standards used in Alert and Fraserdale are aged for at least 3 months and then calibrated at least three times before being used in the field. In addition, any replacement working standards are calibrated against current working standards at the site to ensure the consistency of the scale during working tank changes.

All standard cylinders are only used to pressures of about 500 psi since drifts in the mixing ratio are more prone to happen at low pressures. The working standards are also calibrated several times before and during the time period of use, and at least once afterwards. During the past 10 years of the methane measurement program at AES, there have been no appreciable drifts in the working standards, demonstrating the stability of the methane gas standard hierarchy utilized in the Canadian Baseline Program.

3.2.3. CALIBRATION INTERCOMPARISON WITH NOAA/CMDL

Most network monitoring stations are generally established under the guidelines of the World Meteorological Organization's (WMO) Global Atmospheric Watch (GAW) program, but are owned and operated by individual national agencies. The ability to intercompare data sets from these stations is necessary if one is to quantify the effects of human activities on the climate and the source/sink distribution of the biogeochemical cycles.

The data sets that are useful in understanding high latitude Northern Hemispheric sources and sinks are those from AES and NOAA/CMDL's Carbon Cycle Group. As mentioned previously, the AES methane calibration scale is propagated from a methane standard purchased from NIST. The NOAA/CMDL methane

calibration scale is propagated from two standards purchased from the Oregon Graduate Institute for Science and Technology (OGIST) in Portland, Oregon. In order to intercompare the data sets, a methane intercalibration experiment was performed between AES and NOAA in April 1990. Additionally, in 1992, NOAA circulated a pressurized 6.7 L stainless steel gas cylinder filled with natural air as part of a round-robin methane intercalibration experiment. The cylinder was calibrated by two independent Japanese agencies, the Scripps Institute of Oceanography (SIO), the University of Irvine California, NOAA and AES. The objective of the round-robin experiment was to quantify any differences in the methane scales used by the individual agencies and to provide evidence of any offsets existing in the various data sets. Specific details of the study between AES and NOAA can be found in *Worthy et al.*, [1993] (see Section 2.2.4 for the reference). In January 1994, six additional AES owned cylinders, which were assigned to the carbon monoxide program, were sent to NOAA/CMDL for CO calibration analysis. (The CO measurements program is described in Section 2.3.) Since the cylinders were already at NOAA, they were also calibrated for methane. The results of the three independent calibration studies are summarized in Table 3-11.

The methane scale employed at AES is a factor of 1.0151 higher (approximately 25 ppb at ambient level) than the methane scale employed by the NOAA/CMDL group. The results from the intercomparisons revealed three important points:

1. There is a consistent scale factor for the methane scales employed at NOAA and AES.
2. There is a need for international round-robin intercalibration experiments to permit methane carbon modellers to use methane data sets from various international agencies
3. It is important for an agency, such as WMO or NOAA, to intercede and ensure that a standard methane scale is available and adopted for all WMO measurement network programs.

Table 3-10. Secondary calibration of the new aluminum cylinders relative to gas standard 76878.

	Cylinder CA1083		Cylinder CA01467		Cylinder CA01464	
Date	**Conc. (ppb)**	**Std. Dev.**	**Conc. (ppb)**	**Std. Dev.**	**Conc. (ppb)**	**Std. Dev.**
Sept. 1994	1970.9	1.9	1847.7	1.8	1694.6	2.6
Sept. 1994	1970.8	2.8	1847.4	2.7	1694.8	2.4
Apr. 1995	1971.0	0.9	1847.9	0.8	1694.4	0.9
*Nov 1996	1971.1	1.5	1847.6	1.7	1693.3	1.5
*Jan. 1998	1.9719	1.6	1.8483	1.8	1694.9	1.5

**Tanks were checked by independent standards, which were calibrated directly against cylinder 76878.*

Table 3-11. Intercomparison of methane standard gas scales between the Atmospheric Environment Service of Canada and the National Oceanic and Atmospheric Administration's Climate Monitoring and Diagnostics Laboratory. Results are reported in ppb.

Date	Cylinder Number	NOAA Result	AES Result	Ratio (NOAA/AES)
April 1990	CC64026	1670.8 ± 2.8	1696.0 ± 3.0	0.98514
April 1990	CC64027	1716.5 ± 2.5	1740.0 ± 4.1	0.98649
April 1990	AES-092	1793.7 ± 2.8	1819.2 ± 1.7	0.98598
November 1992	FF30507	1731.6 ± 1.0	1756.4 ± 1.6	0.98588
January 1994	AES-1863	1640.3 ± 0.3	1665.9 ± 0.8	0.98463
January 1994	AES-1852	1642.0 ± 0.4	1668.6 ± 0.9	0.98406
January 1994	AES-1864	1645.2 ± 0.5	1671.3 ±1.6	0.98438
January 1994	AES-1860	1648.8 ± 0.2	1674.0 ± 0.8	0.98495
January 1994	AES-1869	1639.8 ± 0.4	1665.2 ± 0.8	0.98475
January 1994	AES-1875	1647.6 ± 0.2	1674.2 ± 1.2	0.98411

**The NOAA/CMDL results for each cylinder are averages of 3 calibrations of 20 aliquots each. The reported 1σ values are determined from the 3 calibrations. The reported 1σ values for the AES results are determined from combining all individual injections for each calibration.*

3.3. IN SITU CO MEASUREMENTS

Douglas E.J. Worthy and Michele K. Ernst

3.3.1. MEASUREMENT SYSTEM AND SAMPLING PROTOCOL

The automated measurement of CO at Alert is made using a commercial RGA3 Reduction Gas Analyzer purchased from Trace Analytical in California. The principle of analysis is as follows: after eluting from the analytical column, the CO is passed immediately through a heated bed of mercuric oxide in which the reaction CO + HgO (Solid) → CO_2 + Hg (vapour) occurs. The resultant mercury vapour is quantitatively determined by a precise ultraviolet photometer located immediately downstream of the reaction bed. Figure 3.12 shows the major components of the system. The sampling module is comprised of a 16-port stream selection valve and a 10-port sampling valve with appropriate electrical actuators (Valco), and an on/off flow control solenoid valve. A HP 3392A integrator acquires the detector output. The automated operation is via a Campbell Scientific data logger (Model CR21X) which also acquires the integrator report.

The automated sampling module is designed to sample from 16 separate gas streams supplied to the instrument. Standard gases are provided from pressurized cylinders equipped with high-purity, two-stage regulators. Selection of the gas stream for presentation to the sampling injection system is performed by electrical actuation of the 16-port selection valve to the required position (see Figure 3.12a). At this point, the stream control solenoid valve is opened, allowing the gas to pass through the 16-port stream valve, and into the 10-port sample injection valve fitted with a 3 cm^3 stainless steel sample loop. Sample gas flow exits the system through a rotometer attached to the end of the sampling system.

Following a purging flow for 30 seconds, the flow control solenoid valve is shut, allowing the gas in the sample loop to equilibrate to atmospheric pressure. Following an equilibration time of 12 seconds, the 10-port sample injection valve is switched to inject and the contents of the sample loop are transferred into the carrier gas stream and on to the GC column. The contents are first passed on to a pre-column. CO elutes from the pre-column after about 1 minute and then is passed on to a second analytical column. At this point, the pre-column is back-flushed allowing late eluting components to be passed back to the room. Back-flushing allows the analysis time to be minimized by removing late eluting compounds. The nitrogen carrier gas supply is first pre-purified with a heated metallic oxide combustion filter and then split and connected to two inputs of the 10-port selection valve (ports 1 and 8). In the load position, the carrier gas connected to port 1 back-flushes the pre-column whereas the carrier gas connected to port 2 is used as a carrier gas to pass the contents of the analytical column to the detector. In the inject position, the carrier gas connected to port 1 is used to pick up the contents in the sample loop and transfer them on to the pre-column. The carrier gas connected to port 2 is vented to the room. Needle valves (F1 and F2 in Figures 3.12a and 3.12b) are used to adjust the restriction in the lines to permit similar flows through the detector for both positions.

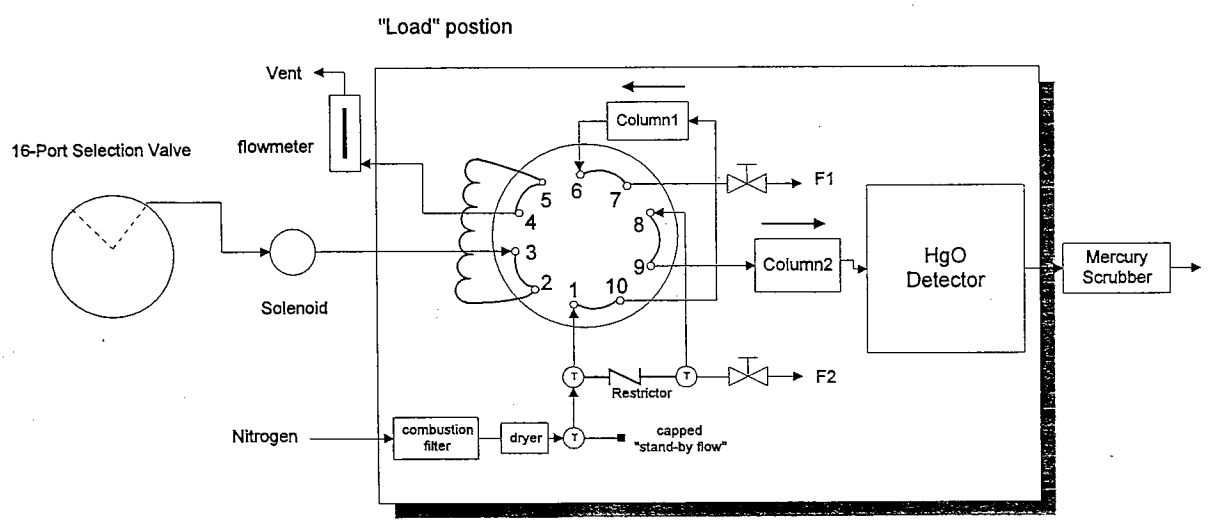

Figure 3.12a Schematic of CO automated gas chromatographic RGA analyzer with the sampling valve in the load position.

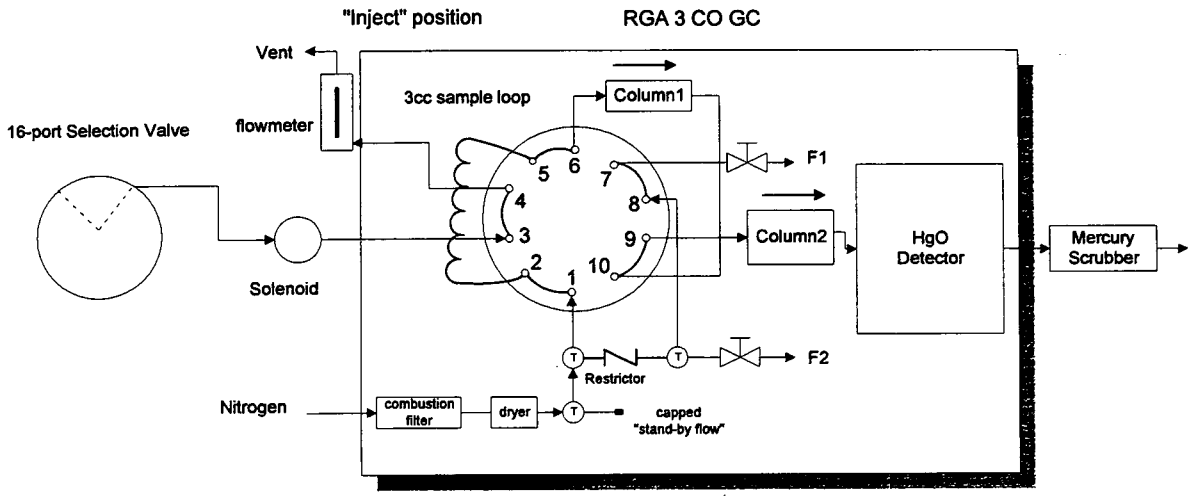

Figure 3.12b Schematic of CO automated gas chromatographic RGA analyzer with the sampling valve in the inject position.

Table 3-12. GC conditions for automated CO measurement at Alert.

COLUMN 1	30 ¼ inch stainless steel (0.32 cm o.d. x .076 cm i.d.)
Packing	Unibeads 1S (Mesh 60 – 80)
Temperature	105 ± 0.1° C
COLUMN 2	30 ¼ inch stainless steel (0.32 cm o.d. x .076 cm i.d.)
Packing	Mole Sieve 5A (Mesh 60 – 80)
Temperature	105 ± 0.1° C
CARRIER GAS	Ultra high purity N_2 (> 99.9998%)
Flow rate	25 ml min^{-1}
DETECTOR	Mercury Vapour
Temperature	265 ± 0.1° C
SAMPLE SIZE	3 ml

At Alert, ambient air is supplied to the GC at approximately 5 L min^{-1} by a KNF Neuberger N2202 vacuum pump sampling through a 0.95 cm o.d. sample line (Dekoron®) from a 10 m intake stack attached to the outside of the laboratory. Prior to the pump, ambient air passes through a 7 micron stainless steel membrane filter. The air then passes through a pressure relief valve set at 1 atmosphere to release excess pressure. The sample air is then dried to a dew point of around -60° C by passing the sample air through a glass trap submerged in a methanol bath set at -80° C. The dried airflow is split between inlets for the CH_4 GC and the CO GC. Stainless steel tubing (0.32 cm o.d. x 0.22 cm i.d.) is used for the standard gas sample line and the ambient sample line after the cold trap.

Each GC measurement cycle consists of the following injections repeated every hour. A single injection last four minutes (15 injections per hour):

1 Working High
Ambient Air
Working Low
Ambient Air (or Target every 5th hour)
10-15 Ambient Air

The RGA CO GC is non-linear and therefore a single calibration point is insufficient to determine the ambient mixing ratios. The ambient data is determined as follows: A quadratic calibration curve is determined every month by passing 6 calibration gases through the system. The calibration gases range from 50 ppb to 300 ppb in 50 ppb concentration steps (ports 6 to 11 on the 16-port stream selection valve). Every hour the response (in peak height counts) of the working high (WH port 2) and the working low (WL port 4) are passed through the calibration curve to determine "predicted" mixing ratios. Correction ratios for both the WH and WL are determined by dividing the assigned mixing ratio for each tank by the predicted

mixing ratio. Analysis tests in the lab have shown that the correction ratio is concentration dependent. That is, the correction ratio can be different at 250 ppb then at 100 ppb. A linear correction ratio equation is determined from the correction ratios for the WH and WL and their assigned concentrations. All ambient injections are determined by first passing the peak height response into the calibration curve to determine a predicted mixing ratio. The predicted mixing ratio is corrected by multiplying by a correction ratio that is determined first by passing the predicted mixing ratio into the linear correction ratio equation. A target gas of known concentration is injected every 5th hour to evaluate the accuracy of the system. The analytical precision for the CO measurements is estimated to be 0.5% (0.2-2 ppb) based on replicate analyses of standard gas.

3.3.2. CO STANDARD GASES

The standard CO scale, to which the AES CO measurements are referenced, is based on a set of six 37.5 L aluminum cylinders purchased in 1993 from Scott Marin located in California. The cylinders span the typical range of background CO measurements. Prior to shipment at AES, the cylinders were sent to NOAA/CMDL for calibration. NOAA/CMDL are the WMO assigned holder for the international CO scale. In 1998, three of the cylinders were sent back for re-calibration. The NOAA/CMDL calibration results are summarized in Table 3-13.

Initially, there was concern regarding the mixing ratio change in cylinder CC1864 and whether it was due to a drift in a calibration curve at NOAA or whether it was a drift in the tank. Several tests were done at NOAA that clearly indicated that a drift in the tank was more likely to have occurred rather than a drift in their scale. Further evidence for this was supported when these tanks were run against each other at AES and fits through the calibration results were better when the updated value on CC1864 was used.

The internal consistency of the primary set is checked periodically. The six tanks are run against each other and a quadratic curve is fit through their responses. A predicted result is obtained from the curve. The results are summarized in Table 3-14.

The results in Table 3-14 reveal that the CO calibration program at AES appears to be stable within the analytical precision of the analysis. With a regular scheduled internal calibration check protocol, along with scheduled calibrations at NOAA/CMDL, an apparent drift in one or more of the tanks should be observable.

Table 3-13. Results of the AES assigned Primaries calibrated by NOAA/CMDL. Results are reported in ppb.

Serial Number	Dec. 19, 1993	Jan. 4, 1994	Jan. 10, 1994	Jan. 7 , 1998
CC1864	53.8 ± 0.5	52.1 ± 0.5	54.1 ± 0.5	49.6 ± 0.5
CC1869	111.8 ± 1.2	109.4 ± 1.1	111.1 ± 1.1	----------
CC1875	166.2 ± 1.7	164.9 ± 1.5	164.0 ± 1.7	166.2 ± 1.7
CC1852	214.0 ± 2.1	215.1 ± 2.3	214.3 ± 2.2	----------
CC1860	261.2 ± 0.5	263.1 ± 3.2	263.1 ± 2.6	----------
CC1863	306.7 ± 3.1	310.5 ± 3.3	307.1 ± 3.1	307.8 ± 9.3

Table 3-14. Results of the primary calibration suites. Results are reported in ppb.

Serial Number	Assigned	Feb. 1995	Nov. 1996	May 1997	Feb. 1998
CC1864	49.60	49.54	49.68	49.41	49.76
CC1869	110.80	110.47	109.83	110.65	110.03
CC1875	166.20	166.83	167.84	167.16	167.14
CC1852	214.50	215.21	215.08	214.80	214.96
CC1860	262.49	260.91	260.18	260.69	261.15
CC1863	308.10	308.44	308.80	308.97	308.35

3.4. IN SITU BLACK CARBON MEASUREMENTS

Fred Hopper, Joe Kovalick and Armand Gaudenzi

Aerosol Black Carbon (BC) measurements have been made at Alert (1989-1996) and Fraserdale (1990-1996) using commercially available aethalometers from Magee Scientific. The instruments made hourly measurements of the optical attenuation of aerosol deposits collected on quartz fibre filters. BC concentrations were calculated from the following equation:

$$BC = k * \Delta ATN / (\alpha * V)$$

where ΔATN is the change in optical attenuation over measurement period, V is the volume of air sampled, k is a constant and α is the specific attenuation. Note that this optical attenuation is representative of the aerosol/filter matrix within the aethalometer and is not equivalent to optical attenuation caused by the aerosols in the free atmosphere.

Investigations by others have suggested that the specific attenuation α of aerosols in the atmosphere is not constant but is a function of location, time, aerosol origin, internal/external mixing, etc. Aethalometer sensitivity to these factors is not known. Consistent BC data sets for Alert and Fraserdale have been prepared using a specific attenuation of $\alpha = 19\ m^2\ g^{-1}$ to convert aethalometer optical attenuation to BC concentration, based on the original aethalometer calibrations by the instrument developers. Absolute calibrations of the aethalometers for typical Alert and Fraserdale aerosol samples have not been carried out. There is no consensus regarding an absolute method for determining the BC concentration in aerosols, necessitating a modest research and development program to develop a technique for calibration.

At Alert, two aethalometers were normally operated at each site for redundancy and QA/QC purposes. Instrument flow rates of 5 L min^{-1} were used in order to balance periods of lost data due to lower sensitivity and due to optical saturation (filter over-loading). Filters were normally changed weekly, but in recent years filters were changed twice per week in one aethalometer at each site, permitting use of a higher flow rate (10 L min^{-1}) for 2x increase in sensitivity. Aethalometer sensitivities are on the order of 5 ng m^{-3} to 15 ng m^{-3} (assuming the specific attenuation is 19 m^2 g^{-1}).

Sample air for the Fraserdale aethalometers was drawn from a 10 m tower through dedicated lines of aluminum tubing. Sample air for the initial Alert aethalometer was initially drawn from a 10 m tower through a manifold system supplying other instruments. This Alert system was abandoned in late 1992 because of gross contamination of the original sample lines. It was replaced by a dedicated stainless steel aerosol sampling stack (10 m height) with (approximately) isokinetic sample probes. Size-selective devices have not been used in the Alert and Fraserdale sampling systems due to lack of funds.

3.5. IN SITU OZONE MEASUREMENTS

Kurt Anlauf, Kathy Hayden and Maurice Watt

3.5.1. MEASUREMENT PROTOCOL

At both sites, two TECO Model 49 UV photometric ozone analyzers were used to measure the ambient ozone. The voltage output of each analyzer was monitored by a Campbell Scientific 21X data logger and was recorded as 5-minute averages at Alert (with time recorded as GMT) and 3-minute averages at Fraserdale (with time recorded as EST). The verified data were corrected for the analyzers' zero offsets and calibration factors and then stored as 1-hour averages in units of parts per billion (ppb), i.e., mixing ratios in units of 10^{-9}. A 50% data availability criterion was used for missing data within any one hour.

At Alert, the two analyzers were connected to a glass manifold that contained a continuous flow of ambient air, using separate 0.64 cm o.d. PFA Teflon® lines (each several metres long). Each Teflon® inlet line was fitted with an in-line 5-micron filter housed in a 47 mm PFA Teflon® filter cartridge made by Savillex Corporation; these filters were changed weekly. The intake of the manifold was about 10 m above ground level outside the building.

At Fraserdale, the ambient air inlet was about 5 m above ground level. The air intake was protected by a similar particle filter, which was changed weekly in the summer and every two weeks in the winter; the ambient intake line was 0.64 cm o.d. PFA Teflon® and about 5 m long.

All analyzers were programmed to sample "zero air" for 45 minutes every second day at midnight; the 2-day cycles were staggered so that one analyzer remained on ambient air. Initially, each analyzer was fitted with an MSA gas mask canister for providing zero air from room air. This proved unreliable because of contamination of these canisters by spurious chemicals in the room. These were replaced with KOBY in-line air purifier cartridges, which were connected with separate Teflon® inlet lines to the ambient air intake glass manifold at Alert and directly to the outside at Fraserdale. This change in procedure has resulted in long-term stability of the analyzer zero. The KOBY cartridges continue to be changed every 1-2 years.

3.5.2. CALIBRATION PROTOCOL

At Fraserdale, the analyzers were calibrated every four months using a transfer standard (Dasibi Model 1008 UV photometric analyzer) that was calibrated by the National Institute of Standards and Technology in Gaithersburg, Maryland, U.S.A. At Alert, an on-site Dasibi Model 1008 UV photometric analyzer was used by the local operators to calibrate the two ambient analyzers alternately every second month. Every year, this local Dasibi calibrator was calibrated against the NIST transfer standard. The calibrations included 7-9 points per calibration and a linear least squares regression was used to calculate the equation describing the analyzer's response. The on-site calibrations were usually within 1% of the mean calibration factor.

Presently, it is estimated that the corrected ozone mixing ratios at these sites are accurate within ± 2% or ± 0.5 ppb, whichever is greater. The latter uncertainty is principally due to fluctuations in the measurement of the zero offset and the ozone UV light absorption (detection limit of about 0.5 ppb). Using all data when both analyzers were in operation, a linear regression between analyzers at each site revealed good precision: for Fraserdale (1992-1995), r^2=0.998 and slope=1.006; for Alert (1992-1995), r^2=0.992 and slope=0.993. For the purpose of illustration, Figure 3.13 shows a comparison of analyzer #1 and #2 at Alert for the year 1995.

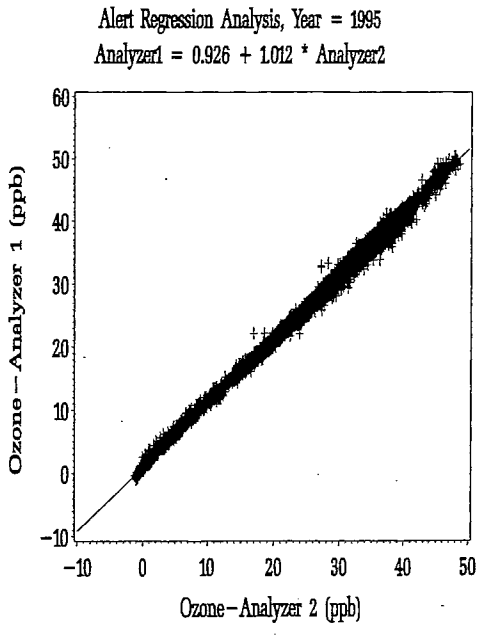

Figure 3.13 A comparison of hourly ozone mixing ratios (ppb) as measured simultaneously by two analyzers (OT1 and OT2) at Alert in 1995.

3.5.3. STRATOSPHERIC OZONE AND UV-B METHODOLOGY

Jim B. Kerr and David I. Wardle

Total ozone measured with the Brewer instrument is described by *Kerr et al.* [1980] and *Evans et al.* [1987]. The principle measurement method uses radiation from the direct sun at five wavelengths in the ultraviolet where ozone has strong and variable absorption features. Comparison of the intensity of radiation at wavelengths with different ozone absorption leads to the determination of the column ozone in the atmosphere. Measurement of total ozone is also carried out using the moon as a light source [*Kerr*, 1989], although this method is less precise than the direct sun method due to reduced radiation intensity and is limited to within five days of the full moon. The direct moon method is important for measurements in the Arctic during polar winter when the sun is not available.

Measurements of the ozone profile are done with electrochemical concentration cell (ECC) ozonesondes that are connected to regular upper air radiosondes. The ozonesondes are routinely flown once per week, but in winter months, when stratospheric ozone is relatively variable and is of maximum interest for depletion studies, ozonesondes are flown two or three times per week. The principle of measurement is the reaction of ozone with potassium iodide to produce free iodine. Ambient air is pumped through a solution containing potassium iodide in an electrochemical reaction cell with a platinum cathode and anode. Each molecule of ozone generates two electrons, which are sensed as output current across the electrodes. The current, which is directly proportional to the number of ozone molecules, is transmitted to the ground as part of the radiosonde signal. Detailed description of the operation of the ozonesonde is given by *Komhyr* [1986] and *Komhyr et al.* [1994].

The Brewer instrument is used to measure UV-B radiation [*Kerr and McElroy*, 1993]. The intensity of global radiation incident on a horizontal diffuser plate on top of the instrument is measured as a function of wavelength in the UV-B spectral range (290-325 nm). The absolute sensitivity of the instrument is determined by measuring the intensity of lamps with known output with calibration traceable to the references of the US National Institute of Standards and Technology. Spectral measurements are made with a resolution of 0.5 nm at intervals of 0.5 nm between 290 and 325 nm. A measurement is comprised of the average of a forward and backward scan, which takes about eight minutes to complete. Measurements are made about twice per hour throughout the day from sunrise to sunset. Erythemal and other biological dose rates are determined by integrating the measured irradiance spectra weighted by an action spectrum that quantifies biological sensitivity to UV-B radiation as a function of wavelength. Daily irradiation values and doses are determined by integrating the irradiance values and dose rates measured throughout the day.

3.5.4. REFERENCES

Evans, W.F.J., H. Fast, A.J. Forester, G.S. Henderson, J.B. Kerr, R.K.R. Vupputuri and D.I. Wardle, Stratospheric ozone science in Canada: An agenda for research and monitoring, *Internal Rep. ARD-87-3,* Environment Canada, 1987.

Kerr, J.B., Observations of Arctic total ozone with the Brewer spectrophotometer during the polar winter using the moon as a light source, In *Ozone in the Atmosphere,* R.D. Bojkov and P. Fabian (Eds), Proc. Quadrennial Int. Ozone Symp., DEEPAK Publ., Hampton, Va., 728-731, 1989.

Kerr, J.B., C.T. McElroy and R.A. Olafson, Measurements of ozone with the Brewer spectrophotometer, Proc., Quadrennial Int. Ozone Symp., Vol. I, J. London (Ed.), Int. Ozone Comm. (IAMAP), 74-79, 1980.

Kerr, J.B. and C.T. McElroy, Evidence for large upward trends of ultraviolet-B radiation linked to ozone depletion, *Science*, **262**, 1032-1034, 1993.

Komhyr, W.D., Operations handbook: Ozone measurements to 40 km altitude with model 4A electrochemical concentration cell (ECC) ozonesondes (used with 1680 MHZ readiosondes), NOAA Tech. Memo. ERL ARL-149, Air Resources Lab., Boulder. Colo., 49pp, 1986.

Komhyr, W.D., J.A. Lathrop, D.P. Opperman, R.A. Barnes and G.B. Brothers, ECC ozonesonde performance evaluation during STOIC, *J. Geophys. Res.*, **100**, 9231-9250, 1995.

3.6. In situ CFC-11 and CFC-12 Measurements

Douglas E.J. Worthy and Michele K. Ernst

3.6.1 Measurement System and Sampling Protocol

The automated measurement of CFC-11 and -12 at Alert are made using a Hewlett Packard (HP) 5890 gas chromatograph (GC), equipped with an electron capture detector. The GC is the same GC that is used for the automated methane measurements (see Figure 3.13 in Section 3.1.4). The automated sampling module is identical to that used with the methane GC system and is therefore not described here (see Section 3.1.4 for further details). An HP 3392A integrator acquires the ECD output, and also controls the automatic operation of the analysis procedure. The automated operation is via programmed external timed events through a connection to a HP 19405A Sampler/Event control module (S/ECM). A Campbell Scientific data logger (Model CR21X) connected to the serial port of the 3392A integrator is used to acquire the integrator report generated by the integrator. The specifications for the GC systems are given in Table 3.15.

At Alert, ambient air is supplied to the GC at approximately 5 L min^{-1} by vacuum pump sampling through a 0.95 cm o.d. sample line (Dekoron®) from a 10 m intake on the platform tower outside the laboratory. Prior to the pump, ambient air passes a pressure relief valve set at 1 atmosphere to release excess pressure. The airflow is split between inlets for the N_2O/SF_6 GC, the flask pump for the NOAA/CMDL flasks sampling programs and the CFC GC. Standard gas is supplied to the GC from a pressurized gas cylinder equipped with a high-purity, single-stage gas regulator. Stainless steel tubing (0.32 cm o.d. x 0.22 cm i.d.) is used for the standard gas sample line and the ambient sample line.

Each GC measurement cycle consists of a standard gas injection followed by one ambient air injection repeated every 90 minutes (16 ambient air measurements per day). The peak area for the standard injection is used to calculate a system response factor for both CFC-11 and -12. The response factors are then used to calculate the CFC-11 and CFC-12 mixing ratios of the subsequent ambient injection and the standard injection of the next cycle.

All CFC measurements at Alert are reported in parts per trillion (ppt). Ambient CFC measurements are only included in the final data set if the re-evaluation of the standard gas was within 5 ppt of its assigned value. Approximately 90% of the data are accepted at both sites using this criterion. The data are also manually inspected and examined using quality control routines before being accepted as valid ambient measurements (refer to Section 4 for data management procedures). The analytical precision for the CFC measurements is estimated to be 0.5% (0.5 ppt to 2 ppt) based on replicate analyses of standard gas.

3.6.2 CFC-11 and CFC-12 Standard Gases

The standard CFC-11 and -12 scale, to which the AES measurements are referenced, is based on the calibration scale maintained at NOAA/CMDL. The standards at Alert are purchased from and calibrated at NOAA. The assigned mixing ratios are at typical background CFC-11 and CFC-12 concentrations. The calibration cylinders utilized at Alert are summarized in Table 3.16.

Table 3.15. GC specifications for automated CFC-11 and CFC-12 measurement system.

COLUMN	10' glass (1/4 inch o.d.)
Packing	Porasil D (Mesh 100-120)
Temperature	40 ± 0.1° C
CARRIER GAS	Ultra high purity Nitrogen (> 99.9995%)
Flow rate	80 ml min^{-1}
DETECTOR	ECD
Temperature	350 ± 0.1° C
SAMPLE SIZE	3 ml

Table 3-16. Standard tanks purchased from and calibrated by NOAA. Results are reported in ppt.

Serial Number	Time On	Time Off	CFC-12	CFC-11
ALM-00809	May 15, 1993	September 4, 95	491.0	265.1
ALM-33810*	September 4, 95	November 6, 95	534.6	273.0
ALM-09299*	November 6, 95	January 15, 96	496.9	267.5
ALM-09287	January 15, 96	May 26, 97	534.5	275.0
ALM-52799	May 26, 97	January 23, 98	544.2	272.8
ALM-60009	January 23, 98	Present	545.2	271.5

* Tanks were shared between the in situ CFC GC and the in situ N_2O/SF_6 GC.

3.7. IN SITU PAN MEASUREMENTS

Jan W. Bottenheim

3.7.1. MEASUREMENT SYSTEM & PROTOCOL

The measurements at Alert have been made continuously since 1986 on a half hourly basis. The first year monitoring was performed with a modified Hewlett Packard model HP5710B Gas Chromatograph. These data are available but are not used in analysis efforts since the instrumental response was unstable due to poor GC oven temperature control. Beginning September 1987 the equipment has consisted of a Hewlett Packard model HP5890 Gas Chromatograph. Outside air is sampled every 30 minutes via 5m (3.2 mm i.d.) stainless steel tubing, outfitted with a 5μ pore size Teflon® filter to a 10 cm^3 stainless steel sampling loop and introduced to the GC employing a motor driven Carle 6-port valve. Separation is performed isothermally (40° C) on a 1 m long, 6.3 mm o.d. silanized Pyrex® glass column filled with 5% Carbowax-400 on Chromosorb G-AW (DMCS, 100-120 mesh) using UHP N_2 as carrier gas, and PAN is detected with an electron capture detector (ECD) held at 60° C. Integration of the chromatogram is obtained using a Hewlett Packard model HP3392 integrator and the GC signal is also continuously recorded on a Philips Model PM8252A chart recorder. Overall instrument control is performed by a Campbell Scientific Model 21X data logger and a Hewlett Packard Model HP19405A Sampler/Event Control Module. The data logger also stores the integrator reports. Until 1996 this information was transferred to tape, which together with the printed integrator reports and the chart records was shipped weekly to AES/HQ in Downsview. Since 1996 the data logger information is polled at regular intervals by a master computer at Alert and stored on disk; a copy of this information is now send on floppy disk to Downsview.

3.7.2. CALIBRATION PROTOCOL

The standard calibration method since late 1986 has been the "Teflon® bag" procedure. Table 3-18 indicates the dates of the calibrations performed since late 1986. It can been seen that on average the system has been calibrated three times per year. A plot of all calibration results obtained between 1987 and 1997 is shown in Figure 3.14. Between 1990-1992 some calibrations were also performed using a "constant flow" procedure, but this was discontinued since the procedure appeared to be unreliable in the field. Both procedures were evaluated at the Centre for Atmospheric Research Experiments (CARE) in 1989 [*Blanchard et al.*, 1990]. A new calibration procedure employing a new calibration system based on acetone photolysis and calibrated NO-in-N_2 has been evaluated since 1996 and promises to be the future method of choice.

The "Teflon® bag" procedure involves diluting high concentration PAN (mixing ratios of 100 - 300 ppmv in UHP N_2) into humidified zero air in Teflon® bags (ca. 50 dm^3 volume) to give mixing ratios of 0.25 – 5 ppbv. The high mixing ratio PAN is synthesized at the laboratory in Downsview from the photolysis of C_2H_5ONO (ethylnitrite) in O_2, purified with prep-GC, and stored in glass sample flasks [*Brice et al.*, 1988]. Its mixing ratio is determined before and after the trip to Alert using a Carle gas chromatograph model C211, using flame ionization detection, by comparison with a reference cylinder of C_6H_6 (benzene) in air. The relative response factor is based on tests with high mixing ratio PAN quantified by IR spectroscopy and ion chromatography. At Alert, the high mixing ratio PAN is calibrated again by injection onto a second (identical) column on the PAN chromatograph and detected by flame ionization detection, and comparison with a calibrated C_6H_6 mixture.

Table 3-18. Dates of calibration of the PAN system at Alert.

Year	Dates of Calibration Trip	Calibration Methods
1987	Sep.	Bags
1988	Jan., Apr., Sep., Nov.	Bags
1989	Apr., Aug., Nov.	Bags
1990	Feb., May, Oct.	Bags, constant flow (M,O)
1991	Jan., Apr., Sep.	Bags, constant flow (J,A,S)
1992	Feb., Apr., Sep.	Bags
1993	Jan., May, Sep.	Bags
1994	Jan., Apr., Oct.	Bags
1995	Jan., Mar., Nov.	Bags
1996	Feb., Nov.	Bags
1997	Feb., May, Oct.	Bags, calibrator (M,O)

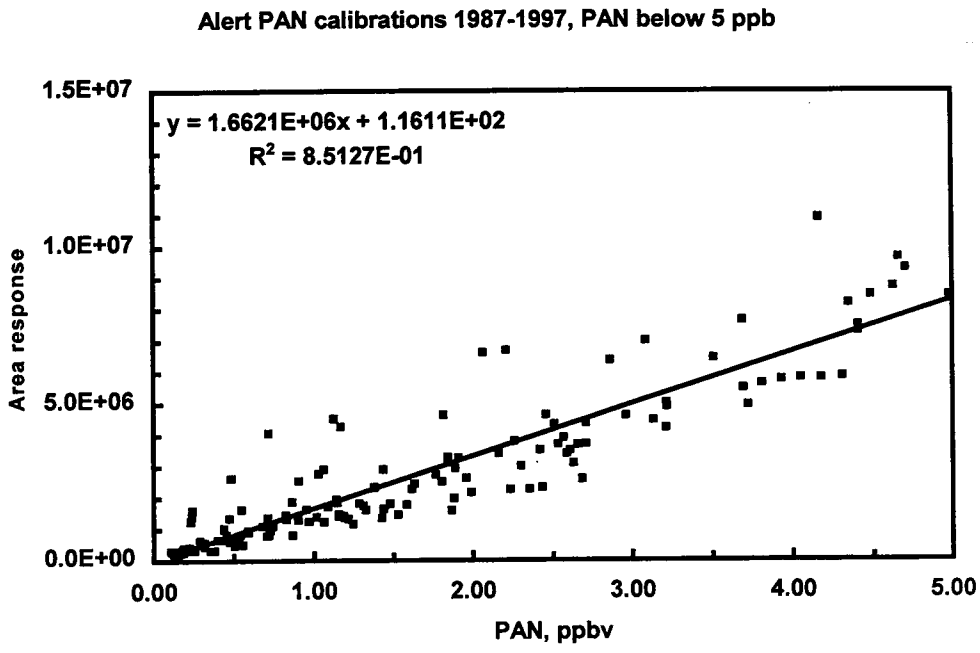

Figure 3.14 Composite graph of calibration data.

The "constant flow" procedure involved bubbling a known flow of ca 10 cm^3 min^{-1} UHP air through a solution of PAN in $C_{12}H_{26}$ (dodecane) synthesized and purified following the procedures of *Nielsen et al.*, [1982]. The solution was held at a temperature of 0 °C, resulting in a mixing ratio of about 1-3 ppmv PAN in air. Subsequent dilution in UHP air then produced a final flow of ppbv mixing ratios of PAN in air. The final mixing ratio was monitored with a TECO Model 42S "NO_x" instrument. The mixing ratio of the initial PAN flow was also occasionally determined by GC/FID following the same procedures outlined above for the "Teflon® bag" method, but this was not very successful due to the very high levels of dodecane, which interfered with the chromatography.

The new calibrator is a Meteorology Consult PAN calibrator. This system is based on mixing a known flow (typically 1 cm^3 min^{-1}) of NO in N_2 from a calibration standard (typically at ca. 1 ppmv) with a second flow of ca 50 cm^3 min^{-1} zero air which has passed through a permeation cell containing pure acetone. The resultant mixture is photolyzed employing a Hg Pen-Ray light source (with UV radiation below 302 nm filtered out) which quantitatively converts the NO into PAN. This mixture is then diluted with a second flow of zero air (0.5 to 5 dm^3 min^{-1}) to obtain a constant, known, flow of PAN in air at 0.2 – 2 ppbv. Until we develop more confidence in this method, we will continue to perform calibrations both using the new calibrator in conjunction with the traditional "Teflon® bag" method.

3.7.3. REFERENCES

Blanchard, P., P.B. Shepson, K.W. So, H.I. Schiff, J.W. Bottenheim, A.J. Gallant, J.W. Drummond, and P. Wong, A comparison of calibration and measurement techniques for gas chromatographic determination of atmospheric peroxyacetyl nitrate (PAN), *Atmospheric Environment, 24A*, 2839-2846, 1990.

Brice, K.A., J.W. Bottenheim, K.G. Anlauf, and H.A. Wiebe, Long-term measurements of atmospheric peroxyacetylnitrate (PAN) at rural sites in Ontario and Nova Scotia; seasonal variations and long-range transport, *Tellus, 40B*, 408-425, 1988.

Nielsen, T., A.M. Hansen, and E.L. Thomsen, A convenient method for the preparation of pure standards of peroxyacetyl nitrate for atmospheric analyses, *Atmospheric Environment, 16*, 2447-2450, 1982.

3.8. AEROSOL CHEMISTRY METHODOLOGY

Leonard A. Barrie

At Alert the sampling site is located 6 km to the south of the main base on an elevated plateau 210 m above sea level. The site is powered from the main base where electricity is produced by a diesel generator. Seven day aerosol samples were collected on 20 by 25 cm Whatman 41 filters using a high volume sampler. The face velocity of sampling (50 cm s^{-1}) and typical filter loadings ensured collection efficiencies better than 95% [*Watts et al.*, 1987]. At the beginning and end of sampling, air flow rates were determined using a critical orifice plate calibrated initially by a primary standard Roots gas meter and checked in the field twice a year using a secondary standard critical orifice. Sample volume at a standard temperature of 0 °C and 1 atm pressure was calculated from the duration of sampling and the mean of the initial and final flow rate. Sampling precision of volume is estimated to be ±5% and accuracy ±5%. Samples were pre-loaded into Teflon®-coated cartridges in an aerosol clean bench in Toronto, wrapped in polyethylene bags, shipped to the field, used to filter approximately 16,000 m3 of air, returned to the polyethylene bags and shipped back to Toronto. Once every four weeks, a field blank sample was taken in which a filter was treated exactly as a sample filter except after being placed briefly on the high volume sampler it was immediately returned to its polyethylene bag.

Once samples were back in the laboratory, they were cut into 8 aliquots using a polyethylene template, stainless steel scalpel, Teflon®-coated tweezers and polyethylene gloves. Each aliquot was sealed in a "Whirlpak" polyethylene bag and stored in the dark at room temperature in the clean room archive. Once per year, 52 samples and 12 field blanks ending in May were taken from each of three aliquot series for chemical analysis. The exception was MSA which was analyzed as a separate series for the period 1980-1991 [*Li et al.*, 1993]. Thereafter, it was analyzed annually.

Samples were analyzed for those constituents listed in Table 3-19. Three analytical methods were used, liquid ion chromatography (IC), instrumental neutron activation analysis (INAA) and inductively coupled plasma emission spectroscopy (ICP). IC analysis was done by extracting 1/8 of a filter in 60 ml of deionized water and subsequently analyzing it with a Dionex ion chromatograph. Over the period of 15 years, different ion chromatographs and columns have been used as the technology changed. Quality control of standards was conducted by an independent laboratory (CAPMoN) that is part of the European Monitoring and Evaluation Program intercalibration project. CAPMoN is also the leader in Canadian air and precipitation monitoring in Canada. In an aliquot of the IC extract, pH and hence the concentration of H^+ was determined.

INAA analysis was performed at the University of Toronto Slowpoke Reactor using short irradiation of 1/8 filters in polyethylene vials followed by counting of the samples in separate non-irradiated vials. Calibration is checked by analysis of NIST fly ash standards.

ICP analysis was done on the residue of 1/8 of a filter. Filters were ashed at 475° C and extracted in a mixture of ultrapure hydrochloric and nitric acid. Final extracts were prepared in 1 ml of concentrated HNO3 and 30 ml distilled deionized water. Several quality control samples based on composite solutions of metals or on Standard Reference Materials such as NBS1648 Urban Particulate matter, NBS1633a Trace Elements in Coal Fly Ash and NRCC MESS-1 Marine Sediment Reference material were carried through the ashing digestion and analysis process on a routine basis. Loss of elements reported in Table 3-19 due to volatilization during ashing of the sample was less than 10%. Extraction efficiency of metals from the ash residue in the acid digestion step was better than 98%. This procedure was not good for metals such as Al with substantial mass in minerals (e.g., silicates) not digested in the acid mixture used.

Field blanks and analytical detection limits (ADL) were used in the determination of an operational detection limit (ODL) for the mass concentration in air. For a particular species the ODL (Table 3-19) varied over the years as sample handling and/or analytical sensitivity improved. The ODL for H^+ (0.60 ng m-3) is defined to correspond to a pH in the solution extract of 4.7. Thus, concentrations of H+ that are >ODL are likely associated with strong acids and not affected by carbonates. No attempt to preserve organic acids in extract solutions was made. Table 3-19 also includes the fraction of data below the ODL for the full 15-year period. The treatment of below detection limit data in the trend analysis is discussed below.

Table 3-19. Summary of constituents analyzed, method of analysis, range of operational detection limits(ODL) and percentage of data below the ODL. INAA - instrumental neutron activation analysis. IC - ion chromatography. ICP - inductively coupled plasma emission spectroscopy.

Constituent	Analytical Method	Operational Detection Limit (ODL) (ng m^{-3})		Percentage Of Data Below Operational Detection Limit
		From	To	
SO_4^{2-}	IC	4	13	0.1
H^+	PH meter	0.60	0.60	36.9
Br	INAA	0.06	1.24	21.3
NH_4^+	IC	5.7	30.8	2.4
NO_3^-	IC	1.4	18.3	0.7
Na	IC	1.4	8.3	5.0
Cl	IC	2.2	14	14.0
K^+	IC	0.8	12	21.2
Pb	ICP	0.07	1.2	40.6
V	INAA	0.01	0.03	3.3
Mg	ICP	0.9	7.4	2.9
Zn	ICP	0.10	3.48	10.3
Cu	ICP	0.03	0.67	13.3
Ca	ICP	6.6	44.6	3.3
Mn	INAA	0.01	0.30	2.6
I	INAA	0.01	0.29	9.8
Al	INAA	0.7	9.3	0.7
MSA	IC	0.26	0.36	1.1

3.8.1. REFERENCES

Li, S.M., L.A. Barrie and A. Sirois, 1993, Biogenic Sulfur Aerosol in the Arctic Troposphere: 2. Trends and Seasonal Variations. *J. Geophys. Res.*, *92*, 20, 623-20, 631.

Watts, S.F., R. Yaaqub, T. Davies, D.H. Lowenthal, K.A. Rahn, R.M. Harrison, B.T. Storr and J.L. Baker, 1997, The use of Whatman 41 filter papers for high volume aerosol sampling, *Atmos. Envir.*, *21*, 2731-2736.

3.9. METHOD FOR LONG-TERM OBSERVATIONS OF TOXIC ORGANIC SUBSTANCES

Leonard A. Barrie and Crsipin Halsall

Sample collection at each site was carried out using a high-volume air sampler consisting of a 10 micrometer-diameter particle size-selective inlet and housing (Wedding and Associates, Fort Collins, CO, USA). Air is drawn through the inlet and then through a 20 cm diameter sample cartridge containing a glass-fiber filter for collection of airborne particles and two 4 cm thick 20 cm diameter polyurethane foam (PUF) plugs for collection of organic vapours. Once every 4 weeks, two filters were used instead of one to check for gaseous adsorption artifacts on the filter matrix. Volumetric flow control at 1.13 m^3 min^{-1} was achieved using a critical flow device. This resulted in nominal air volumes of about 11,400 m^3 over a collection period of seven days. Large air volumes were required to achieve detectable concentrations, as many of the analytes are present in extremely low concentrations in the Arctic atmosphere. Throughout the course of a year, 52 weekly samples were collected from each site. Complete sampling details including sample preparation, have been reported previously by *Fellin et al.*, [1997]. Chemical analysis was done by organic extraction and subsequent analysis by gas chromatography (for details see *Halsall et al.*, 1997; *Stern et al.*, 1997; *Halsall et al.*, 1998).

3.9.1. REFERENCES

Fellin, P. Barrie, L. A.; Dougherty, D.; Toom, D.; Muir, D.; Grift, N.; Lockhart, L.; Billeck, B. (1996) Air monitoring in the arctic: results for selected persistent organic pollutants for 1992. Environmental Toxicology and Chemistry 15, 253-261.

Halsall C. J., R. Bailey, G. A Stern, L. A. Barrie, P. Fellin, D. C. G. Muir, F. Ya. Rovinsky, E. Ya. Kononov, B. Pastukhov, 1998, Organohalogen pesticides in the arctic atmosphere, Environmental Pollution, 102, 51-62.

Halsall, C. J.; Barrie, L. A.; Fellin, P. Muir, D. C. G.; Rovinski, F. Ya.; Kononov, E. Ya. and Pastukhov, B. V. (1997) Spatial and temporal variation of polycyclic aromatic hydrocarbons in the arctic atmosphere. Environmental Science Technology 31, 3593-3599.

Stern, G. A.; Halsall, C. J.; Barrie, L. A.; Muir, D. C. G. Fellin, P.; Rosenberg, B.; Rovinski, F. Ya.; Kononov, E. Ya. and Pastukhov, B. V. (1997) PCBs in the arctic atmosphere 1. Spatial and temporal trends: 1992-1994. Environmental Science Technology 31, 3619-3628.

3.10. MERCURY

William H. Schroeder, Alexandra Steffen and Julia Lu

3.10.1. MEASUREMENT PROTOCOL

The sampling and analytical protocols for the exploratory series of TGM measurements at Alert (from 1992 to 1993) have previously been described in detail [*Schroeder et al.*, 1995a]. Briefly, as can be seen from Figure 3.15, ambient air was filtered through two sequential quartz wool traps to remove atmospheric aerosols, including particulate-phase Hg. The filtered air was then split into two streams (for replication and quality control of measurement results). Each stream passed through two vapour-phase mercury traps arranged in tandem. These retained gas-phase mercury species by sorption (amalgamation) onto the surface of a column of gold-coated silica sand contained in a quartz tube. The exposed traps, along with field travel, and storage blanks, were transported to the AES laboratories for chemical analysis. The analytical procedure involved thermal desorption of Hg from the sample traps/blanks and re-collection onto an analytical trap (similar to a method reported by *Fitzgerald and Gill*, 1979), followed by fast thermal release into a cold vapour atomic fluorescence detector for quantification.

The high-temporal-resolution TGM measurements begun at Alert in 1995, are made with an automated Tekran Inc. (Model 2537A) mercury vapour monitor, usually operated with either a 5-minute or a 30-minute integrated sampling time. This instrument has consistently demonstrated excellent performance in the three international atmospheric mercury measurement methods field intercomparisons conducted so far [*Schroeder et al.*, 1995b & c; *Ebinghaus et al.*, 1996]. A flow schematic for this instrument is shown in Figure 3.16. Airborne particulate matter is removed from the ambient air, before it enters the monitor, by a 47 mm diameter Teflon filter (0.2 μm pore size). The filtered air, normally at a flow rate of 1.5 L min^{-1}, then passes through one of two identical cartridges (arranged in a parallel configuration) in which the gaseous mercury species are amalgamated (retained) on a fine gold mesh. At the end of the pre-determined sampling period the air flow is switched automatically to the other cartridge. While sampling proceeds with this cartridge, the other one is purged with argon gas (to remove any residual air which would otherwise interfere with the subsequent analysis) and is then analyzed for its mercury content by thermally desorbing it into an argon carrier gas stream which transfers the mercury (now existing entirely in the elemental vapour form) into a cold vapour atomic fluorescence spectrophotometric (CVAFS) detector for quantification. The instrument allows for automated calibration at selected intervals programmed into its on-board microprocessor, which then triggers the internal mercury vapour permeation source. This source, however, is not a primary standard and thus requires routine manual calibrations involving injections, with a well-conditioned gas-tight syringe, of saturated (elemental) mercury vapour drawn from an external calibration source maintained at a precisely known temperature. Further details for the conventional (5-minute cycle) automated TGM measurement protocol can be found in the manufacturer's *Instrument Manual* [Tekran Inc., 1994] and in the *Standard Operating Procedures (S.O.P.) Manual* (Atmospheric Environment Service, 1997) for TGM measurements within the Canadian Atmospheric Mercury Measurement Network (CAMNet).

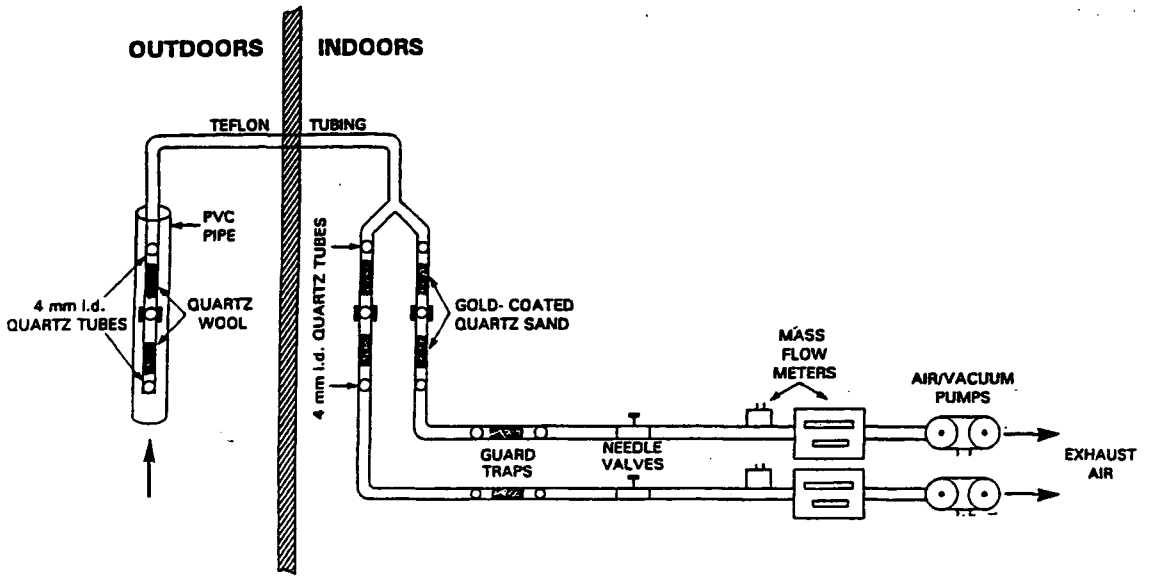

Figure 3.15 Components of atmospheric mercury sampling train used for the 1992-93 exploratory series of TGM measurements at Alert.

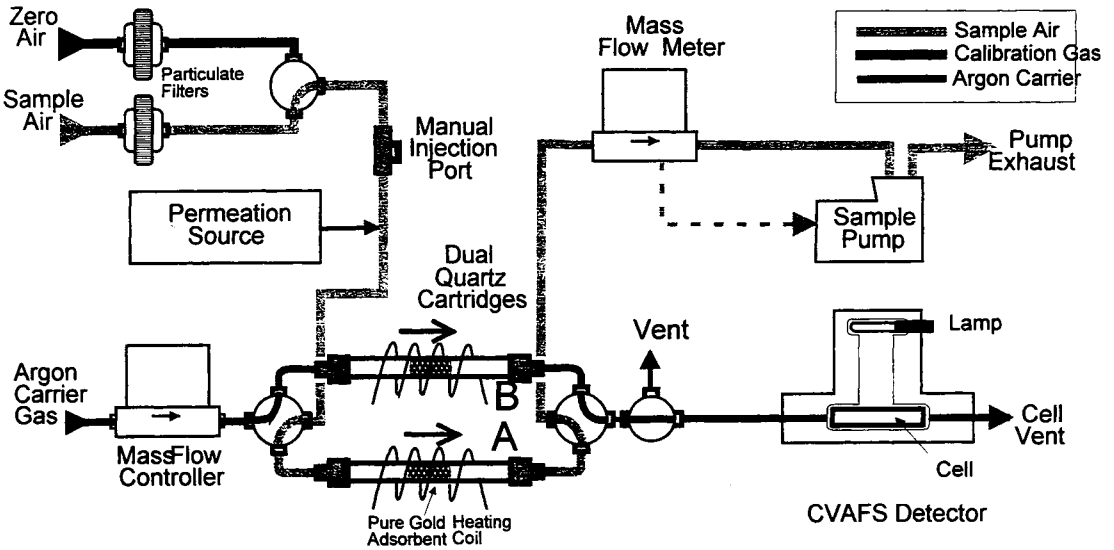

Figure 3.16 Simplified flow schematic for the Tekran Model 2537A atmospheric mercury vapour monitor.

3.10.2. REFERENCES

Atmospheric Environment Service, 1997. *Standard Operating Procedures Manua for Total Gaseous Mercury Measurements.* (October 1997 Draft) Atmospheric Environment Service, Environment Canada, 4905 Dufferin Street, Downsview, Ontario, M3H 5T4.

Ebinghaus R., Jennings S.G., Schroeder W.H., Berg T., Buttermore L., Donaghy T., Ferrara R., Guentzel J., Kenny C., Kock H.H., Kvietkus K., Mazzolai B., Mühleck T., Munthe J., Prestbo E.M., Schneeberger D., Sommar J., Urba A., Wallschläger D. and Xiao Z., 1996. International field intercomparison measurements of atmospheric mercury species at Mace Head, Ireland. Fourth International Conference on Mercury as a Global Pollutant. Hamburg, Germany, August 4-8.

Fitzgerald W.F. and Gill G.A., 1979. Subnanogram determination of mercury by two-stage gold amalgamation and gas phase detection applied to atmospheric analysis. Anal. Chem. 51: 1714-1720.

Schroeder W.H., Ebinghaus R., Shoeib M., Timoschenko K. and Barrie L.A., 1995a. Atmospheric mercury measurements in the northern hemisphere from 56° N to 82.5° N Latitude. Water, Air, Soil Pollut. 80: 1227-1236.

Schroeder W.H., Keeler G., Kock H., Roussel P., Schneeberger D. and Schaedlich F., 1995b. International field intercomparison of atmospheric mercury measurement methods. Water, Air, Soil Pollut. 80: 611-620.

Schroeder W.H., Lamborg C., Schneeberger D., Fitzgerald W.F. and Srivastava B., 1995c. Comparison of a manual method and an automated analyzer for determining total gaseous mercury in ambient air. In: *Proceedings of the International Conference on Heavy Metals in the Environment.* Wilken R.-D., Förstner U. and Knöchel A. (Eds.), CEP Consultants Ltd. (Publisher), Edinburgh, U.K. Vol. 2, pp. 57-60.

Tekran Inc., 1994. *Model 2537A Mercury Vapour Analyzer User Manual.* Rev. 1.52. Tekran Inc., 132 Railside Rd. (Unit 1), Toronto, Ontario.

4. DATA MANAGEMENT

Senen J. Racki

4.1. NETWORK AND CENTRAL DATABASE

4.1.1. HARDWARE FACILITIES, OPERATING SYSTEMS, AND SUPPORT SOFTWARE

The Carbon Cycle Research Laboratory's (CCRL) computer network consists of three primary components:

1. central servers
2. Alert GAW Observatory
3. Fraserdale Observatory

4.1.1.1. CENTRAL SERVERS: "BASELINE" & "CARBON"

The two central CCRL servers are 1) an *IBM Server 320* with 256 megabytes of RAM and about 30 gigabytes of disk storage, and 2) an *HP 9000 Model 777/C100* with 320 megabytes of RAM and about 18 gigabytes of fast-wide SCSI disk storage.

The IBM machine is identified on the network as "Baseline", while the HP machine is identified as "Carbon". Baseline runs Microsoft® Windows NT® 4.0 Server operating system and serves as a central data storage facility, print server and to a limited extent an application server. Its dual Pentium architecture runs at 90 MHz and the disk subsystem is divided among two Adaptec 2940UW SCSI adapters. An Exabyte Mammoth tape subsystem is used to back up the disks.

Carbon runs HPUX on the PA-RISC 7100 at 100MHz. It's primarily intended for model development in Fortran and data visualization and analysis using IDL.

Both Carbon and Baseline participate in a LAN that is protected by a "firewall". Neither of these machines is accessible via the Internet. To facilitate sharing files between cooperative agencies, CCRL uses an unofficial external FTP server called AirQuality (airquality.tor.ec.gc.ca). AirQuality is based on the Intel platform and runs Linux as the host operating system. The current CCRL web site is located at http://airquality.tor.ec.gc.ca/baseline. As demand increases for resources, CCRL will eventually obtain a permanent official external site for World Wide Web and FTP activity.

4.1.1.2. ALERT GAW OBSERVATORY

The computing facilities at the Alert office consist of a pseudo-server called "Alert-Main", a data collection computer "Alert-Op", and a *Lexmark* laser printer. Alert-Main is a *Dell Optiplex GXMT5166* Pentium computer with 96 megabytes of RAM and 2 gigabytes of disk capacity. It runs the Microsoft® Windows NT® 4.0 (workstation) operating system and is the only CCRL computer that has a link to the Internet from Alert. It is also wired with coax cable to a localized workgroup network. Alert-Op is a *Dell 466/M* computer with 32 megabytes of RAM and 1 gigabyte of disk capacity. It runs the Windows® 95 operating system and is primarily used for data and word processing. The *Lexmark* laser printer is served by Alert-Main and shared on the local workgroup so that the Alert-Op computer can print to it. The data collection computer is a *Compaq 286* computer running MS-DOS®. It is not networked and is only used to collect data via an *ATI 2400etc* modem linked to the Alert GAW Observatory.

"Live" Internet connection is possible at the Alert office. A single auxiliary IP address has been assigned to CCRL and may be used for visiting scientists to communicate via e-mail and to transfer small files. Due to technical limitations, the bandwidth of the link to the Internet is limited.

The Alert GAW Observatory has various computer systems to facilitate data collection. The main mode of collection is via the *Campbell Scientific CR21X/MD9* logger network (see Data Collection and Processing, Section 4.1.2.1). In the logger network, a *NEC 386* computer is used to poll each individual data logger for data every 3 hours. The computer stores the data on a local hard disk and the Alert operator routinely copies the data to an *Iomega Zip*™ disk. The data collection computer at the Alert office accesses the logger network via modem in the same way as the *NEC* except it does it 90 minutes later. There are, however, instruments, such as the radon, N_20 and mercury analyzers, that do not use data loggers. Instead, they have dedicated computers and the data are manually copied on a routine basis.

4.1.1.3 FRASERDALE OBSERVATORY

As of June 1998, the data collection system at the observatory in Fraserdale consists of 1) four Campbell Scientific data loggers, 2) a dedicated computer for the radon system, and 3) a data acquisition computer. The data acquisition computer is an *HP 486 Vectra* computer with 64 megabytes of RAM and a 1.2 gigabyte hard disk. The installed operating system is Windows NT® 4.0 (workstation). Campbell Scientific's PC208W is used to retrieve data from the data logger network and Windows NT® Remote Access Service is used for transfer of data and remote administration. NT RAS on the data collection computer is bi-directional. That is, a technician can use RAS to dial into the AES building backbone to check or send e-mail from Fraserdale while on a maintenance trip, and the data acquisition computer can be remotely maintained in a limited way from AES in Downsview.

4.1.2. STORAGE AND ORGANIZATION

Most of the data from the Alert and Fraserdale observatories is stored on Baseline as ASCII files on a disk formatted with Windows NT® native NTFS file system with compression enabled. Each observatory's data is stored on a unique disk in ASCII format so that importing into programs is done more easily and the data can be read with standard ASCII editors.

A specific directory structure has been implemented by CCRL. At the root of each data disk, directory entries are created for each year. Under each year, directory entries for raw, weekly, and monthly data are labelled as TAPES, WEEKPAR, and MONTHPAR, respectively. For the data from Alert, the TAPES directory has two subdirectories called RAW and ALT. Raw data as it comes from the data loggers is stored in the RAW subdirectory, whereas raw data that has been checked for gaps and time discrepancies is stored in the ALT subdirectory. The data from Fraserdale are stored similarly, i.e., in RAW and FRD subdirectories. The WEEKPAR and MONTHPAR directories are identical in structure and each contains subdirectories for the atmospheric component being measured. The name of the directory is reflective of the atmospheric component. For example, the CO_2 data are stored in the \year\MONTHPAR\CO2 directory. Each atmospheric component directory is further divided into three subdirectories – LOG, OP, and PI. The LOG directory contains ASCII log files that contain historical information about changes made to the flagging information within each data file (see Quality Control Flags in Section 4.1.3.4). The OP* directory contains files that the station operator has altered, and the PI directory contains files that the Principal Investigator has altered. The PI directory is not used for weekly (WEEKPAR) files since the PI usually works with the monthly data. For an explanation of how data are processed from raw form to monthly form refer to Section 4.1.2.5 Data Processing. Figure 4.1 shows a Windows® File Manager snapshot of a portion of the directory structure described above for the Alert monthly methane data for 1996.

4.1.2.1. OVERVIEW OF DATA COLLECTION AND PROCESSING

The first step in collecting data is to retrieve it from the measurement instrument. For most instruments that CCRL manages, micro data loggers are used for this purpose. A typical micro data logger is able to read analog and digital voltages, as well as output TTL level voltages. Campbell Scientific makes the micro data loggers that CCRL currently utilizes – specifically, the CR21X model. The CR21X was chosen for its robustness, ease of use, and flexibility. Campbell Scientific makes a number of add-on modules that expand the CR21X functionality. One such module is the MD9 multidrop interface. This device is used to link multiple data loggers over substantial distances using RG59 coax cable, and to retrieve data from any of the data loggers in the chain from a single computer. Figure 4.2 shows a CR21X wired to an instrument and/or sensors, and Figure 4.3 shows multiple CR21X loggers linked via coax cable. With an additional MD9 interface and a modem module called the DC112 (also made by Campbell Scientific), the data logger network can be accessed via standard telephone line. Figure 4.4 shows a typical hookup over a standard telephone line.

* OP is used as a short-form for OPERATOR.

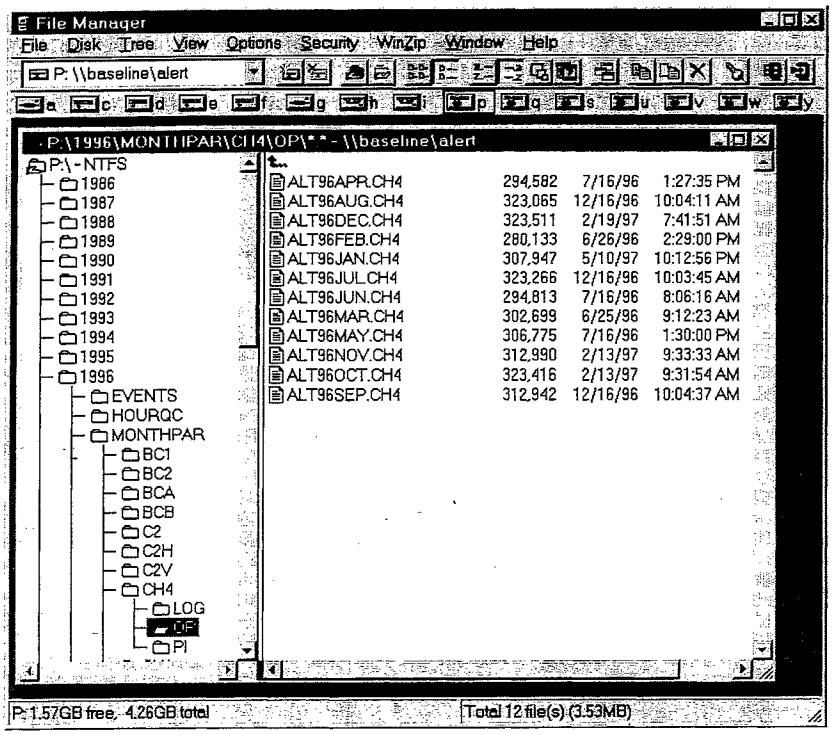

Figure 4.1 Snapshot of a portion of the directory structure on the Baseline server.

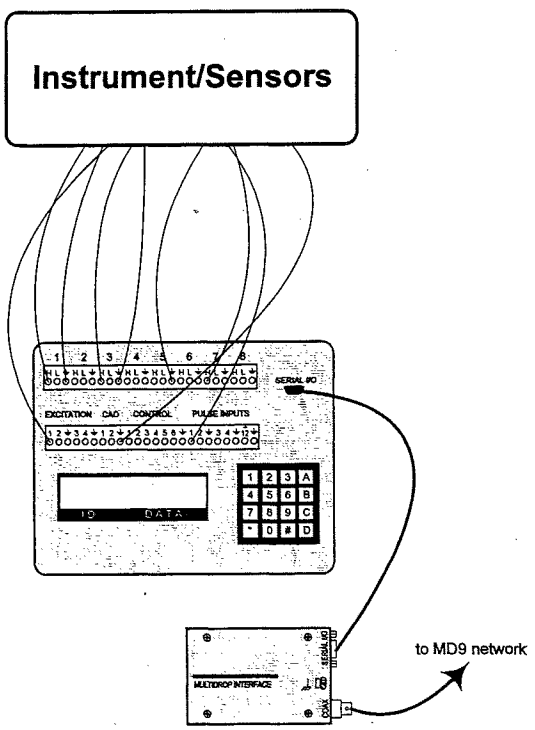

Figure 4.2 CR21X data logger hookup to instrument or sensors.

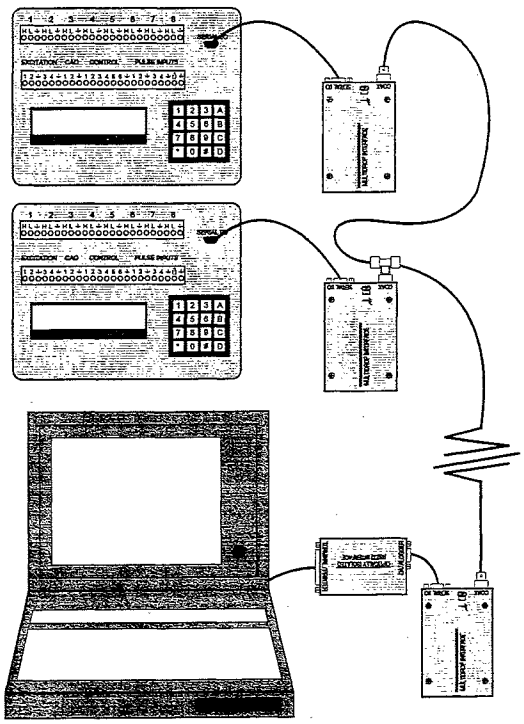

Figure 4.3 Multiple data loggers to computer interface.

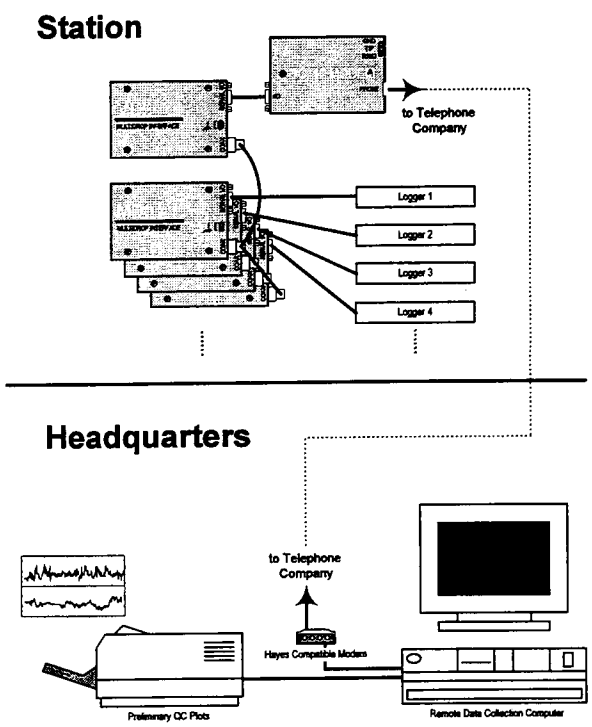

Figure 4.4 Data collection via a standard telephone line into an MD9 network.

4.1.2.2. DATA COLLECTION AT ALERT

Currently, 10 Campbell Scientific CR21X data loggers are used for collecting data at the Alert laboratory. Table 4-1 lists the data loggers, by assigned names, and the monitoring functions of each. Note that the Tekran mercury vapour analyser and radon monitor are not connected to data loggers. The instruments are connected directly to individual computers.

An MD9 network links these loggers as depicted in Figures 4-3 and 4-4. At the office, the Compaq computer retrieves data from the CR21X data loggers at the observatory in sequence via a modem and standard telephone line every three hours. At the observatory, the NEC computer performs the same process as the Compaq 90 minutes later. The version of the data collected by the computer at the observatory is considered "master or primary" while the data collected via modem at the office is considered "backup or secondary". Utilizing these two streams of incoming data minimizes data loss.

Data from the radon and mercury data collection systems are manually copied by the operator to removable media, and then copied to the Alert-Main computer upon returning to the office.

4.1.2.3. DATA PROCESSING AT ALERT

The operator is responsible for processing the weekly raw data, and thus plays a vital role in the quality assurance of the data. The operator records events at the observatory that can affect the quality of the data and flags the data accordingly. The flags aid principal investigators (PIs) in quality assuring the data. In addition to processing data, the operator also forwards weekly data plots to PIs. The PIs use these plots to monitor instrument performance.

Weekly raw data is processed on the Alert-Main computer from all loggers except BL6PAN. Processing includes splitting out instrument parameters in the raw data file; time checking data; filling in missing records; re-splitting data into individual parameter files; plotting the raw weekly data files; and flagging the weekly files. All of this processing is accomplished by using programs supplied by Campbell Scientific (i.e., SPLIT) and others, and by using programs written by CCRL staff specifically for these tasks.

Weekly data files are comprised of data that is collected for one week (from one Monday morning to the next) and are processed as soon as possible (within a week) then mailed to the Alert Operations Coordinator (AOC) as AES headquarters. The AOC copies the data to the CCRL "Baseline" server so that the data is accessible by PIs.

4.1.2.4. DATA COLLECTION AT FRASERDALE

Four Campbell Scientific CR21X data loggers are currently used for collecting data at the Fraserdale observatory. Table 4-2 lists the data loggers by assigned names and their monitoring functions. Note that the radon monitor is not connected to a data logger. The instrument is connected directly to a computer.

An MD9 network links these loggers as depicted in Figures 4.3 and 4.4. The HP computer retrieves data from the CR21X data loggers in sequence every three hours, while a computer at AES headquarters retrieves the same data 1 hour later. The version of the data collected by the computer at Fraserdale is considered "master or primary" while the data collected via modem at AES in Downsview is considered "backup or secondary". A third computer has been recently installed as an additional safeguard. This computer retrieves data in the same way as the HP computer but does so two hours afterwards and runs under the MS-DOS® operating system. CCRL anticipates that, since the HP computer is also given the task of retrieving

data from the radon monitor every half hour, and since it is acting as an Windows NT® Remote Access Server (RAS), the likelihood of system crashes and other problems is increased slightly. Therefore, data from the third computer is accumulated for the entire year and will be used later in the event that the HP computer developed problems and the computer at AES headquarters was unable to retrieve data via modem due to problems such as persistently poor telephone connections.

Besides the obvious benefit of being able to perform limited remote maintenance of the computer, the HP computer runs RAS to allow retrieval of radon data in an automated way. The radon data accumulates on the hard disk of the HP computer every 30 minutes and is "picked up" by a call from the Baseline server at AES headquarters weekly. Using the Remote Console service, TLIST, and KILL utilities (provided by the Windows NT® Resource Kit), remote initialization and software maintenance of the radon-monitoring instrument is possible.

4.1.2.5. DATA PROCESSING

As mentioned in Section 4.1.2.3, the Alert operator processes data to a degree before it reaches AES. The Fraserdale observatory does not have a full-time operator so all data processing must be done at AES. Figure 4.5 shows a flowchart that describes the processing procedures for data from both observatories. In the figure, cylinders depict storage on the Baseline server, squares depict processing programs/routines, and arrows show the sequence of processing. Note that quality control procedures are considered an integral part of processing data. To better understand the processing procedures, refer to Section 4.1.3.

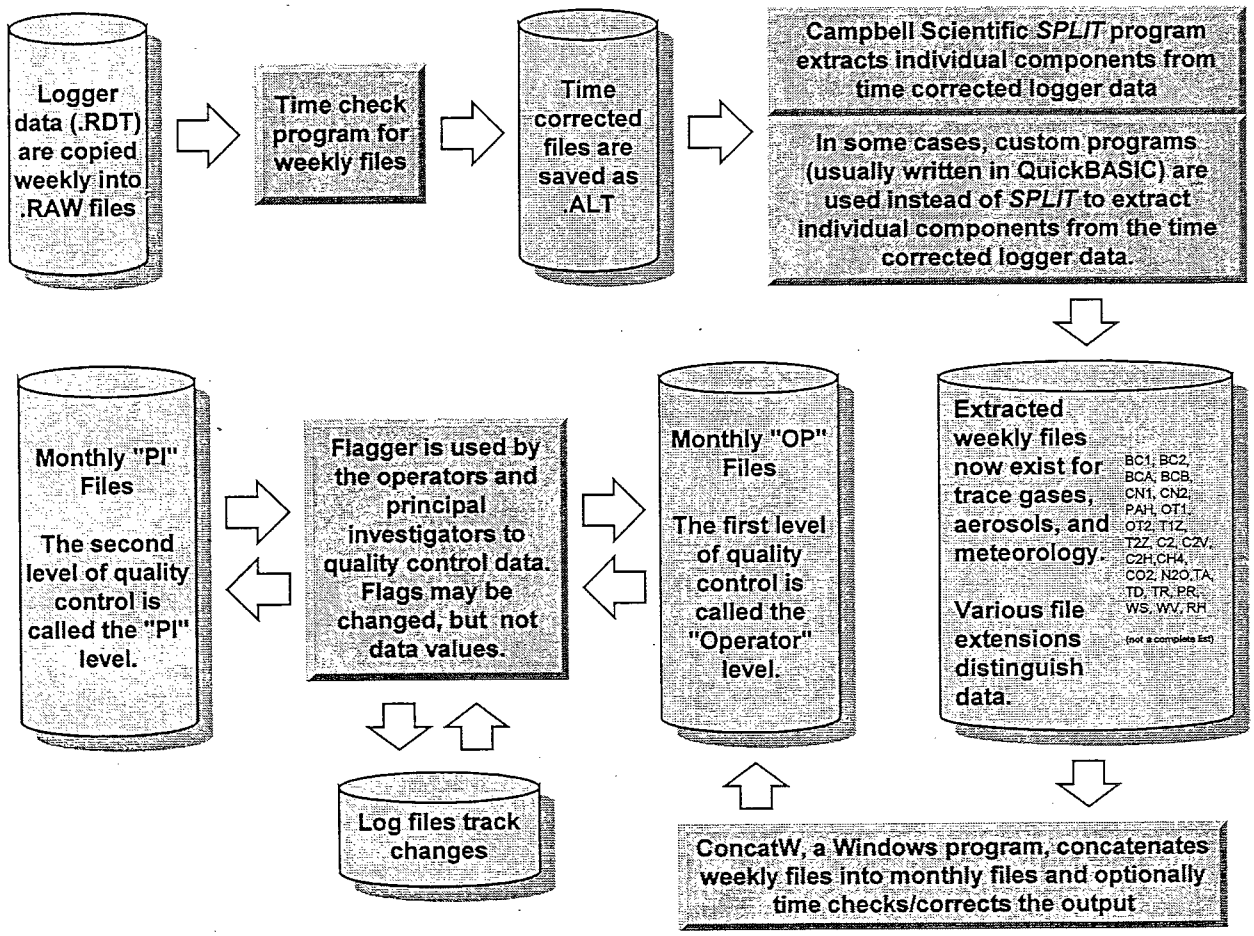

Figure 4.5 Data processing flowchart.

Table 4-1. Data logger names and monitoring functions at Alert.

Logger Name	Monitoring Function
BL1AER	aerosol measurement system
BL3CO2	NDIR measurement system for CO_2 determination, and PAH measurement system
BL4GAS	ozone measurement system
BL5MET	meteorological measurements from the anemometers on the walk-up tower and Stevenson screen
BL6PAN	GC measurement system for PAN determination
BL7CH4	GC measurement system for CH_4 determination
BL8CO	GC measurement system for CO determination.
BL9FRN	GC measurement system for CFCs F-11, F-12 and F-113 determination

Table 4-2. Data logger names and monitoring functions at Fraserdale.

Logger Name	Monitoring Function
FD2MET	meteorological measurements from anemometers located on the tower, solar radiation
FD3NDIR	NDIR measurement system for CO_2 determination
FD4N2O	GC measurement system for N_2O/SF_6 determination
FD5CH4	GC measurement system for CH_4/CO_2 determination

4.1.3. FILE STRUCTURES

4.1.3.1. CCRL STANDARD DATA FORMAT

CCRL data files are ASCII files with comma-separated fields, text surrounded with double-quotes, and conform to any of the following formats:

1. Year, JulDay, Time, Parameter1, Parameter2, Parameter3, Parameter4, Flag1
2. Year, JulDay, Time, Parameter1, Parameter2, Parameter3, Parameter4, Flag1, Flag2
3. Year, JulDay, Time, Parameter1, Parameter2, Parameter3, Parameter4, Flag1, Flag2, Flag3
4. Year, JulDay, Time, Parameter1, Parameter2, Parameter3, Parameter4, Flag1, Flag2, Flag3, Comment
5. Year, JulDay, Time, Parameter1, Parameter2, Parameter3, Parameter4, Flag1, Flag2, Flag3, Comment, ExtraInfo

Type 4 and 5 are the current versions. All existing measurement data has been converted to these standard formats. The following limitations are placed on the above fields. **Note the Julian day and 24 hour time fields, and the use of four digits for the year field. By storing these fields separately the data are not subjected to century rollover problems.**

Field	Limitation
Year	4 digits representing the year (century included)
JulDay	1-3 digits representing the Julian day of the year
Time	1-4 digits representing 24hr time (GMT based)
Parameter 1-4	Single precision numbers usually representing Mean, Max, Min, Std, respectively.
Flag1	1 character as outlined in Quality Control Flags (Primary) in Section 4.1.3.4
Flag2	1 character as outlined in Quality Control Flags (Secondary) in Section 4.1.3.4
Flag3	Principal Investigator's flag. May be a string of up to 30 valid ASCII characters. The "@" symbol is used as a placeholder. May not contain commas.
Comment	General-purpose comment field. May be used as an additional flagging field. May be up to 255 valid ASCII characters in length. May not contain commas or square brackets. The "@" symbol is used as a placeholder.
ExtraInfo	Extra information may be placed at the end of the line. This field can be a maximum of 128 valid ASCII characters in length and it ***may*** include commas.

The following is an example of a portion of CO_2 data in type 4 format:

1996,1,1155,384.51,384.59,384.45,.0326,"C","I","C5++OZOS","@"
1996,1,1200,367.24,367.32,367.16,.0346,"U","U","AR++OZOS","@"
1996,1,1205,342.48,342.55,342.38,.0429,"S","I","W1++OZOS","@"
1996,1,1210,359.65,359.72,359.61,.031,"S","I","W2O+OZOS","@"
1996,1,1215,366.85,366.92,366.76,.0387,"U","U","AR++OZOS","@"
1996,1,1220,366.89,367.02,366.79,.0404,"U","U","AR++OZOS","@"
1996,1,1225,366.89,366.98,366.8,.0353,"U","U","AR++OZOS","@"
1996,1,1230,366.89,366.99,366.81,.0372,"U","U","AR++OZOS","@"
1996,1,1235,366.85,366.95,366.75,.0443,"U","U","AR++OZOS","@"
1996,1,1240,366.74,366.87,366.59,.0562,"U","U","AR++OZOS","@"
1996,1,1245,366.69,366.81,366.6,.0377,"U","U","AR++OZOS","@"
1996,1,1250,366.76,366.87,366.65,.0429,"U","U","AR++OZOS","@"
1996,1,1255,366.83,366.92,366.71,.0389,"U","U","AR++OZOS","@"
1996,1,1300,366.87,367.03,366.77,.0467,"U","U","AR++OZOS","@"
1996,1,1305,342.44,342.49,342.38,.0308,"S","I","W1++OZOS","@"
1996,1,1310,359.39,359.46,359.32,.0335,"S","I","W2++OZOS","@"
1996,1,1315,366.94,367,366.85,.0459,"U","U","AR++OZOS","@"

4.1.3.2. RAW DATA

CCRL defines "raw data" as information that comes directly from the data loggers before any processing occurs. Raw data is stored after missing blocks are identified and filled appropriately. Partial data blocks are discarded and time sequence is verified. Raw data are used to create the weekly data files, which are later used to create monthly data files (see Section 4.1.2.5 Data Processing). The following is an example of raw data that is clipped on the right for ease of presentation.

101,1997,001,0000,103,0,1,1,4.5572,361.89,18.589,62.182,-64.463,-61.466,15.003,298.84,992.7,.30918,4.
201,1997,001,0000,103,13.912,20.257,9702.1,2,1,12,13,3,9,2,3,343.98,364.11,354.81,2.6992,4.7878,9.638
101,1997,1,5,103,0,2,1,2.6883,343.87,18.712,61.899,-64.512,-61.476,15.003,298.8,992.86,.5017,2.6954,3
101,1997,1,10,103,0,3,1,4.7798,364.03,18.582,62.425,-64.492,-61.483,15.004,298.81,992.75,.38899,4.788
101,1997,1,15,103,0,4,1,3.371,350.45,18.584,62.765,-64.303,-61.478,15.003,298.8,992.73,.55475,3.3764,
101,1997,1,20,103,0,5,1,2.7692,344.65,18.673,62.832,-64.813,-61.514,15.003,298.8,992.66,.46193,2.779,
101,1997,1,25,103,0,6,1,4.5473,361.79,18.529,62.69,-64.292,-61.491,15.003,298.8,992.73,.66305,4.5572,
101,1997,1,30,103,0,7,1,.04317,318.38,18.454,62.443,-64.633,-61.472,15.004,298.8,992.72,.38678,.05394
101,1997,1,35,103,0,8,1,.89926,326.63,18.528,62.168,-64.202,-61.499,15.003,298.8,992.7,.24975,.90747,
101,1997,1,40,103,0,9,1,2.3476,340.59,18.625,61.91,-64.256,-61.5,15.004,298.8,992.7,.76251,2.3529,340
101,1997,1,45,103,0,10,1,3.7251,353.87,18.628,61.671,-64.284,-61.502,15.003,298.8,992.73,.55034,3.733
101,1997,1,50,103,0,11,1,5.0378,366.52,18.548,61.625,-64.309,-61.494,15.003,298.8,992.79,.31163,5.047
101,1997,1,55,103,0,12,1,6.2142,377.86,18.717,62.051,-64.424,-61.496,15.003,298.79,992.71,.30942,6.22
101,1997,1,100,103,0,1,2,4.551,361.83,18.688,62.572,-64.566,-61.504,15.003,298.78,993.31,.20333,4.558
201,1997,1,100,103,14.093,20.18,9702.1,2,2,12,13,3,9,2,3,343.98,364.11,354.81,2.6992,4.7878,9.6382
101,1997,1,105,103,0,2,2,2.6855,343.85,18.598,62.818,-64.469,-61.517,15.003,298.8,993.45,.14587,2.692

4.1.3.3. WEEKLY DATA

An intermediate set of weekly data files is created because a weekly parcel of data is convenient to work with (not too large), and flagging events are fresh in the mind of the operator. The weekly files are created from the time-checked raw data files and are stored in type 4 or type 5 format (see Section 4.1.3.1). The operator alters Flag1 and/or the Comment fields of the weekly data files using *Flagger*. The PI does not use this intermediate data file.

4.1.3.4 MONTHLY DATA

Monthly data files are identical to weekly data files but contain a month's worth of data. They are created by concatenating the weekly data files. The PI quality controls monthly data files by using either *Flagger* or his/her own custom program. A final version of the quality-controlled monthly data is stored in the PI directory (see Section 4.1.2).

Quality Control Flags

Flag1, Flag2, and Flag3 in the CCRL data format are used for quality control. The operator modifies Flag1, and the PI modifies Flag2 and Flag3 (optionally). Flag1 is determined by events that occur at or near the sampling site. Since more than one event may occur, the Comment field is used to accommodate "overflowing" flags. A predefined flag priority has been established. Flag1 always carries the highest priority of the Primary flags, while the Comment field carries lower priority, or "overflow" Primary flags. *Flagger* automates the application of priority rules during flagging. The PI may use Flag3 in addition to Flag2 if a more elaborate flagging mechanism is required (see Section 4.1.3.1 CCRL Standard Data Format for an example of CO_2 data in type 4 format, and Table 4-4 for an explanation of the CO_2 Flag3 assignments).

The flags defined by CCRL are given in Table 4-3.

Table 4-3. List of flags defined by CCRL.

Primary – Valid
U, Unchanged
+, Data passes all tests

Primary – Invalid
S, Span check (O_3/CNC/CO_2-NDIR)
Z, Zero check (O_3/CNC/CO_2-NDIR)
C, Instrument calibration
A, Adjusting something caused irregular readings
I, Intake sample line problems
R, Offline due to repair
M, Instrument missing
K, Flask sample taken from intake line
F, Filter change or in line
H, System is flushing
T, Records missing
D, Diagnostic Checks

Primary – Questionable
O, Person outside lab
L, Vehicle at the lab
G, Vehicle at Hi-Vol site
Y, Vehicle at Special studies
X, Vehicle at TX site
B, DND base camp
P, Person inside lab
Q, Unspecified questionable data

Secondary (PI)
V, Data passes all tests
U, Unclassified (no QC performed)
Q, Questionable as defined by PI
I, Invalid as defined by PI

Table 4-4 illustrates the use of Flag3. A custom program called ALTCO2SP inserts Flag3 and splits out the NDIR CO_2 data.

Table 4-4. Flag3 definitions for NDIR CO_2 data.

Flag	Description
++	No system problems
O+	Outlier from daily median analysis of 5 minute means
+V	Outlier from daily median analysis of 5 minute standard deviations
OV	Combined from both above
	The flags below identify calibration gases and are added to the above flags.
W1	1st working gas
W2	2nd working gas
W3	3rd working gas
W4	4th working gas
TT	Target gas
ZZ	Zero gas
LL	Low calibration gas
MM	Mid calibration gas
HH	High calibration gas
QQ	Span calibration gas
	The flags below identify system checks and are added to the above flags.
PR	Pressure variable (probably OK but needs checking)
TR	Room temperature fluctuations (could be a problem for the NDIR)
ZC	Analyser zero chamber temperature fluctuations > 1° C
SC	Analyser sample chamber temperature fluctuations > 1° C
ZT	Zero trap temperature fluctuations > 1° C
ST	Sample trap temperature fluctuations > 1° C
ZF	Zero flow fluctuations > 1 cm^3 min^{-1}
UZ	Unstable Zero regulation (max – min) > 1%
SF	Sample flow fluctuations > 1 cm^3 min^{-1}
US	Unstable Sample regulation (max – min) > 1%
CN	CNC fluctuations > 100 counts

Flag Priorities and Rules

Flagging rules have been established to complement the flag priority assignments. *Flagger* applies the rules as follows:

1. If the existing Flag1 is from the **Primary-Valid** set of flags, the new flag will replace the existing Flag1 and nothing will be carried into the Comment field.
2. If the existing Flag1 is from the **Primary-Invalid** set of flags, then Flag1 remains and the new flag is put into the Comment field.
3. If the existing Flag1 is from the **Primary-Questionable** set of flags, then priorities are compared and if Flag1 is a higher priority flag than the new flag, Flag1 remains and the new flag is put into the Comment field. Conversely, if Flag1 is a lower priority flag than the new flag, Flag1 is placed in the Comment field and the new flag is placed into the Flag1 field.

Priority assignment for the Primary-Questionable set of flags is currently as follows:

"O" = 1 (highest)
"L" = 2
"G" = 3
"Y" = 4
"X" = 5
"B" = 6
"P" = 7
"Q" = 8 (lowest)

As an example, suppose the following line were in a data file and the operator wished to change Flag1 to "X" to indicate a vehicle at the TX site:

1996,4,1340,1.8564,1.9682,1.9689,0,"U","U","@","@",61,11,.01

"U" is from the Primary-Valid set, therefore "X" would replace "U" in Flag1 (using rule 1). The line would then look like this:

1996,4,1340,1.8564,1.9682,1.9689,0,"X","U","@","@",61,11,.01

Suppose the operator then wanted to indicate that a person was outside the lab by applying "O" to Flag1. Both "X" and "O" are from the Primary-Questionable set of flags and "O" has a higher priority than "X", therefore the following would be the result:

1996,4,1340,1.8564,1.9682,1.9689,0,"O","U","@","[X]",61,11,.01

Note that *Flagger* puts "overflow" flags in square brackets so that comment information is not disturbed. The "@" symbol is used as a placeholder. Now, suppose the operator wanted to indicate a filter change by applying flag "F". The following would be the result:

1996,4,1340,1.8564,1.9682,1.9689,0,"F","U","@","[OX]",61,11,.01

4.1.3.5. LOG FILES

Flagger tracks changes using a log file. A log file is created in the LOG directory (see Section 4.1.2) if it does not already exist, otherwise information is appended to the existing log file. Each data file has an associated log file that is used to keep track of changes. Since *Flagger* requires the user to login, the log file can track changes made, when they were made, and who made them.

The following is an example of a typical log file:

Geoff Jones (OPERATOR) created the file on 09-01-96 at 17:58. Machine: Alert Dell
Geoff Jones (OPERATOR) opened the file for batch processing on 09-01-96 at 17:58. Machine: Alert Dell
Range edited in batch: 232 1409 -> 232 1529 - Flag1 and/or Comment field was changed/appended with X.
Geoff Jones (OPERATOR) closed the file on 09-01-96 at 18:08:06
Geoff Jones (OPERATOR) opened the file for batch processing on 09-01-96 at 17:58. Machine: Alert Dell
Range edited in batch: 232 2135 -> 232 2235 - Flag1 and/or Comment field was changed/appended with X.
Geoff Jones (OPERATOR) closed the file on 09-01-96 at 18:21:19
Erika W (OPERATOR) opened the file on 09-01-96 at 22:45. Machine: Alert Dell
Range edited: (1996, 232 1335 -> 232 2030) - Flag1 and/or Comment field was changed/appended with "Q". RANGE REPLACE CRITERION USED: Wildcard, existing flag could be anything.
Erika W (OPERATOR) closed the file on 09-01-96 at 23:00:30. (Modified)
KWhale (OPERATOR) opened the file on 09-03-96 at 15:06. Machine: Alert dell
Line edited: (1996 236 2000) - Flag1 changed from "P" to "A"
Line edited: (1996 236 2010) - Flag1 unchanged, comment field appended with "A"
KWhale (OPERATOR) closed the file on 09-03-96 at 15:09:05. (Modified)
KORB WHALE (OPERATOR) opened the file for batch processing on 09-10-96 at 01:12. Machine: ALERT DELL
Range edited in batch: 239 1243 -> 239 1403 - Flag1 and/or Comment field was changed/appended with X.
KORB WHALE (OPERATOR) closed the file on 09-10-96 at 01:18:59
KORB WHALE (OPERATOR) opened the file for batch processing on 09-10-96 at 01:12. Machine: ALERT DELL
Range edited in batch: 243 1545 -> 243 1552 - Flag1 and/or Comment field was changed/appended with O.
KORB WHALE (OPERATOR) closed the file on 09-10-96 at 01:49:22
Geoff Jones (OPERATOR) opened the file on 09-11-96 at 17:25. Machine: Alert dell
Line edited: (1996 239 2000) - Flag1 changed from "P" to "A"
Line edited: (1996 239 2005) - Flag1 unchanged, comment field appended with "A"
Line edited: (1996 243 1700) - Flag1 unchanged, comment field appended with "Q"
Geoff Jones (OPERATOR) closed the file on 09-11-96 at 17:40:33. (Modified)
Korb Whale (OPERATOR) opened the file on 09-17-96 at 17:48. Machine: Alert dell
Line edited: (1996 246 1410) - Flag1 unchanged, comment field appended with "A"
Line edited: (1996 249 0005) - Flag1 unchanged, comment field appended with "M"
Line edited: (1996 250 1505) - Flag1 unchanged, comment field appended with "A"
Korb Whale (OPERATOR) closed the file on 09-17-96 at 17:59:17. (Modified)

5. COOPERATIVE MEASUREMENT PROGRAMS

5.1. QUASI-CONTINUOUS OBSERVATIONS OF ATMOSPHERIC TRACE SUBSTANCES AND THEIR ISOTOPIC COMPOSITION AT ALERT

Ingeborg Levin, Bernd Kromer, Christian Poß and Thomas Marik
Institut für Umweltphysik (Uni-HD/IUP), University of Heidelberg,
Im Neuenheimer Feld 366, D-69120 Heidelberg, Germany

in collaboration with

Hartmut Sartorius and Wolfgang Weiss
Bundesamt für Strahlenschutzt, Inst. for Atmospheric Radioactivity (BfS-IAR),
D-79098 Freiburg, Germany
and
Manfred Maiss
Uni-HD/IUP, now at MPI for Chemistry, D-55020 Mainz, Germany

MOTIVATION AND SCOPE OF MEASUREMENT PROGRAM

Observation of greenhouse gas concentrations in the global atmosphere is the crucial pre-requisite to investigate their global budgets as the atmosphere effectively integrates the signals from their sources and sinks. Isotope observations, complementing these concentration measurements, provide the information necessary to allow for source apportionment. In addition, atmospheric tracers such as the anthropogenically produced radioactive noble gas ^{85}Krypton or, likewise, the greenhouse gas sulfur hexafluoride (SF_6) are quasi ideal tracers to validate global atmospheric circulation models [*Levin and Hesshaimer*, 1996]. Moreover, the natural radioactive noble gas ^{222}Radon serves as the optimum tracer to distinguish continental from maritime air masses, and select background conditions at a monitoring site.

A global network for quasi-continuous observations of isotopes in atmospheric CO_2 and CH_4 as well as for atmospheric ^{85}Krypton and SF_6 has been established by Uni-HD/IUP and BfS-IAR [*Levin et al.*, 1992; *Weiss et al.*, 1992; *Maiss et al.*, 1996]. The most northern station within this global network is the High Arctic Research Laboratory at Alert where all these trace substances are measured, as well as ^{222}Radon.

The special role of the Alert station in this network is many fold: (1) Alert provides the northern margin of the network defining the background situation neighbouring the most important anthropogenic source areas of mid northern latitudes. (2) Concerning CO_2 exchange with the biosphere, this station experiences the largest seasonal changes and therewith allows best to study isotopic disequilibrium effects. (3) The vicinity of the station to northern wetland areas in Canada and Siberia allows studying hemispheric scale changes of trace gas emissions (i.e., CH_4) from this important natural source. (4) Global and hemispheric scale atmospheric transport models often fail to simulate air mass exchange over the poles: transport tracer observations, are, therefore, most crucial here as an important validation tool for these models as well as for air mass identification.

In addition to our engagement at Alert, several studies have been performed at the continental baseline station Fraserdale at the margins of the Hudson Bay Lowlands wetland area. Here we established continuous atmospheric ^{222}Radon daughter observations to use this tracer for parameterization of vertical transport in the boundary layer, and, thus, as a tool to quantify methane emissions from the regional catchment area of the site. To estimate the respective ^{222}Radon emanation rates from the ground, two campaigns for ^{222}Radon flux measurements were performed together with two diurnal cycle studies to estimate the isotopic signature of the wetland methane emissions [*Kuhlmann et al.*, 1998].

As most of our measurement program demands sophisticated isotope analyses (by mass spectrometry resp. radioactive counting) in most cases, high volume samples are collected at the sites and analysed in Germany. For ^{222}Radon measurements, a special monitor has been developed in Heidelberg with support from AES and installed at the stations for continuous monitoring.

MAIN RESULTS

1. ^{14}C activity in atmospheric CO_2

Individual values of atmospheric $^{14}CO_2$ from 1987 to 1997 at Alert are displayed in Figure 1. The record shows a steady decrease which is due to (1) the ongoing long-term equilibration of nuclear bomb $^{14}CO_2$ with the ocean and with the long-lived biospheric reservoirs, and (2) to an increasing input of ^{14}C free fossil fuel CO_2 added to the atmosphere. The significant seasonal variations with lower values during the winter season and higher values in late summer reflect seasonal variations of $^{14}CO_2$ sources and sinks. These concern the anthropogenic contribution of ^{14}C free fossil fuel CO_2 at the station, a variable input of ^{14}C from the stratosphere where the main natural production occurs, as well as fractionation and disequilibrium effects during the seasonal exchange of CO_2 with the northern hemispheric biosphere. A quantitative deconvolution of the observed signal is actually performed via global compartment and two-dimensional atmospheric $^{14}CO_2$ model simulations [*Hesshaimer*, 1997].

2. Atmospheric CH_4

The CH_4 concentration results from tank samples and from *in situ* GC measurements at Alert agree very well since February 1991 (see Figure 2). Before this time, flushing of the compressor and the tanks for conditioning had not been via the normal sampling line, probably causing some small contamination of the high-volume samples. The good correlation of the two concentration records confirms that our isotope sampling technique using integrated collection in high volume bags and subsequent transfer into aluminium tanks with an oil compressor is reliable.

We observe a seasonal concentration cycle with a peak-to-peak amplitude of about 65 ppb with minimum values occurring in July, and maxima in January/February. This can be explained by the seasonality of methane sources and sinks in combination with a seasonally varying meridional circulation pattern. The atmospheric OH sink (which contributes about 90% to the total sink of atmospheric methane) is stronger during summer. Although the nearby wetland sources of CH_4 are more important during the summer season, the OH sink seems to overcompensate this effect. The high methane concentrations during the winter months are probably caused by a deficiency of the OH sink in combination with transport of stratified polluted air masses from mid latitudes to the Arctic station during this season.

Reliable results for the stable isotopic composition in atmospheric methane could be achieved only from July 1991 onwards, when we modified our enrichment procedure. Almost in phase with the seasonal methane concentration cycle is the seasonality of $\delta^{13}C$ in methane with lowest values during autumn (maximum influence from northern wetland emissions depleted in the rare carbon isotope) and maxima in late winter (possibly due to the influence from anthropogenic emissions from Northern Siberia, enriched in the rare isotope). No significant trend is observed in $\delta^{13}C$- CH_4 from 1991 to 1997.

CONCLUSIONS

Collection and analytical procedures of our high-volume atmospheric samples for isotope analyses proofed to be reliable, leading to overall results consistent with the station climatology. Our isotopic and transport tracer results provide important independent information for the interpretation of the routine observations at the High Arctic Research Station Alert. This is particularly true for investigations connected to the Arctic Haze phenomenon, using ^{85}Krypton and SF_6 as transport tracers and ^{14}C to quantitatively evaluate the fossil fuel CO_2 component. On the other hand, using isotope observations is a promising tool for a better CH_4 source apportionment in this region, which is important in establishing the global methane budget. Finally, Alert appears to be an indispensable position in our global isotope network for CO_2, CH_4, as well as the global transport tracers SF_6 and ^{85}Krypton.

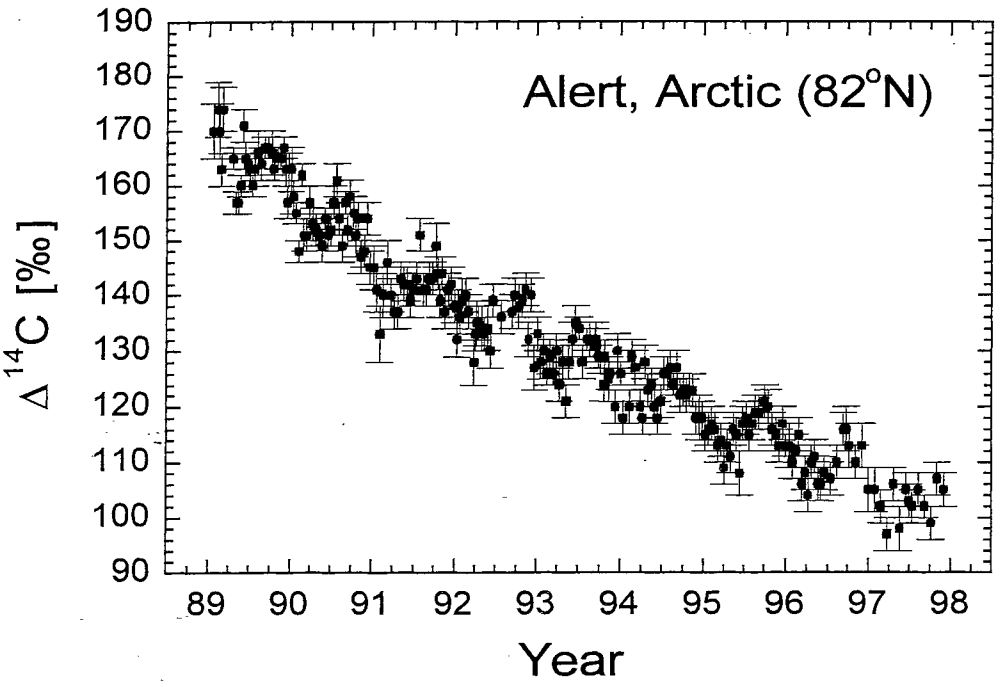

Figure 1. $\Delta^{14}C$ in atmospheric CO_2 at Alert. The amplitude of the seasonal cycle is larger than at mid-to-low latitudes in the northern hemisphere (e.g., Izaña) due to a larger amplitude of seasonal exchange with the biosphere and an enhanced fossil fuel signal in mid-to-late winter at Alert [*Levin et al.*, 1992].

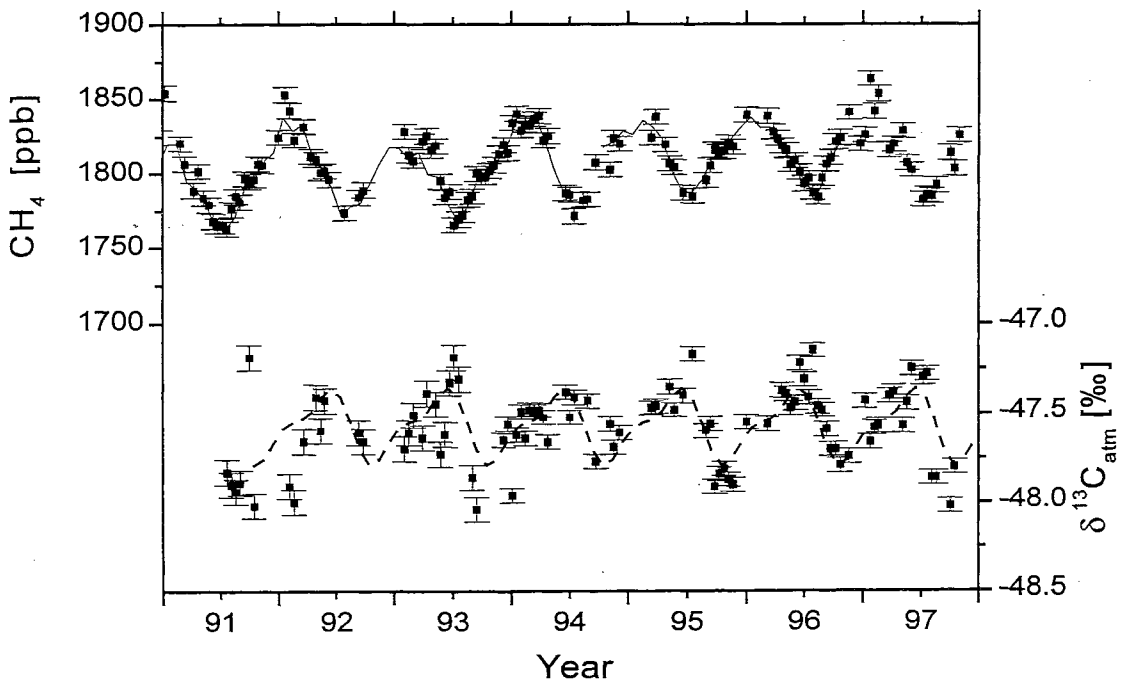

Figure 2. Upper part: Comparison of two-week integrated CH_4 concentrations in the high-volume air samples (individual points with error bars) with continuous in-situ measurements at Alert (monthly means, solid line). Lower part: $\delta^{13}C$-CH_4 from high volume air samples (the dashed line is a harmonic fit curve through the data).

REFERENCES

Hesshaimer, V., 1997. *Tracing the global carbon cycle with bomb radiocarbon.* Ph.D. thesis, University of Heidelberg.

Kuhlmann, A.J., D. Worthy, N.B.A. Trivett and I. Levin, 1998. Methane emissions from a wetland region within the Hudson Bay Lowland: An atmospheric approach. *J. Geophys. Res. 103,* 16 009 - 16 016.

Levin, I., R. Bösinger, G. Bonani, R.J. Francey, B. Kromer, K.O. Münnich, M. Suter, N.B.A. Trivett and W. Wölfli, 1992. Radiocarbon in atmospheric carbon dioxide and methane: global distribution and trends. In: R.E. Taylor, A. Long and R.S. Kra (Eds.) *Radiocarbon After Four Decades: An Interdisciplinary Perspective*, Springer-Verlag, New York, 503-517.

Levin, I. and V. Hesshaimer, 1996. Refining of atmospheric transport model entries by the globally observed passive tracer distributions of ^{85}Krypton and sulfur hexafluoride (SF_6). *J. Geophys. Res. 101, D11*, 16,745-16,755.

Maiss, M., L.P. Steele, R.J. Francey, P.J. Fraser, R.L. Langenfels, N.B.A. Trivett and I. Levin, 1996. Sulfur hexafluoride - a powerful new atmospheric tracer. *Atmosph. Environment, 30,* 1621- 1629.

Weiss, W., H. Sartorius and H. Stockburger, 1992. Global distribution of atmospheric ^{85}Kr - a database for the verification of transport and mixing models. In: *Isotopes of Noble Gases as Tracers in Environmental Studies.* Proceedings of a Consultants Meeting, Vienna, 29 May - 2 June 1989, IAEA, Vienna, 29-62.

AES-IUP JOINT PUBLICATIONS (ONLY REVIEWED ARTICLES)

Kuhlmann, A.J., D. Worthy, N.B.A. Trivett and I. Levin, 1998. Methane emissions from a wetland region within the Hudson Bay Lowland: An atmospheric approach. *J. Geophys. Res. 103,* 16 009 - 16 016.

Levin, I., R. Bösinger, G. Bonani, R.J. Francey, B. Kromer, K.O. Münnich, M. Suter, N.B.A. Trivett and W. Wölfli, 1992. Radiocarbon in atmospheric carbon dioxide and methane: global distribution and trends. In: R.E. Taylor, A. Long and R.S. Kra (Eds.) *Radiocarbon After Four Decades: An Interdisciplinary Perspective*, Springer-Verlag, New York.

Levin, I., R. Graul, and N.B.A. Trivett, 1995. Long term observations of atmospheric CO_2 and carbon isotopes at continental sites in Germany. *Tellus 47B,* 23-34.

Maiss, M., L.P. Steele, R.J. Francey, P.J. Fraser, R.L. Langenfels, N.B.A. Trivett and I. Levin, 1996. Sulfur hexafluoride - a powerful new atmospheric tracer. *Atmosph. Environment, 30,* 1621- 1629.

Worthy, D.E.J., N.B.A. Trivett, J.F. Hopper, J.W. Bottenheim, and I. Levin, 1994. Analysis of long range transport events at Alert, N.W.T., during the Polar Sunrise Experiment. *J. Geophys. Res. 99, D12*, 25 329-25 344.

Worthy D.E.J., I. Levin, N.B.A. Trivett, A.J. Kuhlmann, J.F. Hopper and M.K. Ernst, 1998. Seven years of continuous methane observations at a remote boreal site in Ontario, Canada, *J. Geophys. Res. 103*, D103, 15 995 – 16 007.

ACKNOWLEDGEMENTS

We wish to thank N.B.A. Trivett, his co-workers, and the Alert station staff for their permanent engagement and support to establish and run our sampling equipment at Alert. This fruitful and most friendly cooperation will hopefully continue and lead up in further joint publications. We wish to thank H. Glatzel-Mattheier and M. Schmidt for help with the CH_4 concentration measurements. This work was supported by the German Minister of Education, Science, Research and Technology through the *Internationales Büro* and several research projects as well as by the European Community within the 4th Framework of Environment and Climate.

5.2. CO_2/CO AND $^{13}CO_2$ AT ALERT

Towards consistent global data sets of atmospheric carbon dioxide and its stable isotopes: A tool for carbon cycle modeling.

Ken Masarie[1,2]

1: University of Colorado, Cooperative Institute for Research in Environmental Sciences, Boulder, Colorado 80309, United States
2: NOAA CMDL Carbon Cycle Group, Boulder, Colorado 80303, United States

Systematic observations of atmospheric CO_2 and the stable isotopes of CO_2 are essential to our understanding of the present-day global carbon cycle. Such long-term measurement records have been widely used with atmospheric transport models to derive natural and anthropogenic flux estimates of CO_2. Serious obstacles to this approach are the sparsity of sampling sites, the lack of temporal continuity at some sites, and the fact that not all sites have data covering the same period of time. Transport models can potentially misinterpret these spatial and temporal gaps, resulting in derived source/sink scenarios that are biased by the deficiencies in the sampling network. To reduce these biases, a global trace gas monitoring network of unprecedented spatial resolution and temporal continuity is needed. Since both the costs and the logistics of operating such a network prove too formidable for any one laboratory, a cooperative international effort is required. NOAA CMDL, in cooperation with many other international measurement programs, has released GLOBALVIEW-CO_2, the most extensive globally-consistent atmospheric CO_2 data set yet available for use in carbon cycle modeling studies. The latest release, GLOBALVIEW-CO_2, 1997, includes extended records [*Masarie and Tans*, 1995] derived from actual observations from 15 independent programs representing nine countries. Enhancements include improved techniques used to establish consistency among independent laboratories and the addition of measurement records from tall towers and routine aircraft sampling programs which will likely improve the validation of model-derived concentration fields above the earth's surface.

Integrating trace gas observations made by independent laboratories into data sets that are self-consistent to the demanding tolerances required is a difficult task. Inconsistencies among independent measurements may be caused by differences in calibration scales, as well as subtle differences in methods of sample collection, analysis, and/or data processing. Several laboratories have established ongoing inter-comparison programs that are part of their regular monitoring activities as a way to document differences from actual atmospheric observations. This strategy combined with regular inter-laboratory inter-comparison (round-robin) efforts may be sufficient to properly assess the consistency among atmospheric measurements from independent laboratories.

The unique ongoing flask-air inter-comparison program between NOAA CMDL (Boulder, Colorado) and CSIRO DAR (Aspendale, Victoria), based on air samples collected for both laboratories at Cape Grim, Tasmania serves as a model strategy for assessing consistency among actual observations [*Masarie et al.*, in preparation]. Together, NOAA and CSIRO are attempting to establish and subsequently maintain consistency between their measurement networks by first establishing consistency between independent atmospheric measurements of air sampled at Cape Grim in Tasmania. Cape Grim is well-suited to this effort because of existing ongoing long-term independent sampling efforts and because the Cape Grim Baseline Air Pollution Station (CGBAPS) is the cornerstone of the Australian comprehensive atmospheric measurement program and can provide the necessary resources and expertise to provide consistent and reliable flask sampling. Briefly, a subset of CMDL flask samples is routinely measured in both laboratories for atmospheric CO_2, CH_4, CO, H_2, N_2O, and $\delta^{13}C$ and $\delta^{18}O$ of CO_2. Measurement results are automatically and routinely exchanged between the laboratories and inter-comparison results examined monthly. While results from the NOAA/CSIRO flask inter-comparison experiment confirm the difficulty associated with establishing and maintaining consistency of measurements among independent laboratories, the exercise has proven to be a necessary component in the data extension and integration methodology.

Since 1975, AES of Canada has been making weekly measurements of CO_2 in air samples collected in AES glass flasks at Alert, N.W.T. In 1985, the CMDL Carbon Cycle Group also began making weekly measurements of CO_2 in air samples collected in CMDL glass flasks at Alert. Ambient samples are

collected for each program at approximately the same time using sample containers and collection techniques developed by each laboratory. Flasks are shipped to their respective laboratories where they are analyzed for several trace gas compounds including CO_2.

The NOAA and AES independent flask measurement records have been compared with each other and with NDIR measurements from the Alert continuous CO_2 monitoring program operated by AES as part of the WMO GAW program [*Hudec and Trivett*, 1995]. Results show that agreement among the flask records and the NDIR record is variable and depends, in part, on flask type (e.g., pressurized or evacuated, greased or greaseless). The ongoing flask inter-comparison experiment at Alert documents discrepancies between the NOAA and AES independent measurement programs which may be due to factors within each of the participating laboratories. Documenting these inconsistencies has been valuable and has spawned further investigation into the measurement methods employed by the participating programs. However, it has been difficult to identify, with confidence, the causes of the observed differences because too many of the variables in the measurement process are uncontrolled.

Beginning this year, 1998, NOAA and AES have committed to establishing a flask-air inter-comparison program based on the sampling efforts at Alert. Alert is a logical location to focus this effort; the Alert Observatory is the cornerstone of the Canadian atmospheric research effort and can provide the support that is required to ensure consist and reliable sampling. We are confident that an ongoing NOAA/AES flask-air inter-comparison program modeled after the NOAA/CSIRO program will, in time, enable the two laboratories to identify the causes of the observed measurement discrepancies that up-to-now have been documented but poorly understood.

Canada, France, Germany, Japan, and New Zealand have joined the United States and Australia in establishing more reliable and direct methods for assessing consistency among measurements from independent programs. Canadian participation in this international effort is essential. High-precision measurements of CO_2 and other trace gas species at Estevan Point (west coast Canada), Sable Island (east coast Canada), and Alert (northern-most long-term sampling location) provide valuable constraints on the abundance and distribution of these trace gas constituents in the high-latitudes of North America. For this reason, it is critical that Canadian measurement records be integrated with independent measurement records from other national programs. The NOAA/AES flask-air inter-comparison program at Alert, inter-comparison efforts between AES and CSIRO also at Alert, and periodic round-robin exercises are necessary if we are to integrate with confidence, independent measurement records from NOAA, CSIRO, and AES into cooperative global data sets for use in carbon cycle modeling studies.

REFERENCES

GLOBALVIEW-CO_2: Cooperative Atmospheric Data Integration Project - Carbon Dioxide. CD-ROM, NOAA/CMDL, Boulder, Colorado. [Also available on Internet via anonymous FTP to ftp.cmdl.noaa.gov, Path: ccg/co2/GLOBALVIEW], 1997.

Hudec, V.C. and N.B.A. Trivett, An evaluation of CO_2 flask measurement programs at Alert, N.W.T., in the Report of the Eighth WMO Meeting of Experts on Carbon Dioxide Concentration and Isotopic Measurement Techniques, 1995, edited by T. Conway, pp. 42-57, World Meteorological Organization Global Atmosphere Watch, No. 121, 1997.

Masarie, K.A. and P.P. Tans, "Extension and Integration of Atmospheric Carbon Dioxide Data into a Globally Consistent Measurement Record." Journal of Geophysical Research, Vol. 100, No. D6, p. 11593-11610. June 1995.

Masarie, K.A., P.P. Tans, L.P. Steele, R.J. Francey, R.L. Langenfelds, T.J. Conway, E.J. Dlugokencky, P.C. Novelli, M. Trolier, and J.W.C. White, "A Report on the ongoing Flask-Air Inter-comparison Program between the NOAA CMDL Carbon Cycle Group and the CSIRO DAR Global Atmospheric Sampling Laboratory." In preparation, 1998.

5.3. ATMOSPHERIC CO_2 OBSERVATIONS AT STATION ALERT: A PRELIMINARY REPORT

Report date: March 25, 1998

Observations by:
Neil Trivett and observers

Analysis by:
Timothy Whorf, Alane Carter, and Charles D. Keeling
Scripps Institution of Oceanography
University of California, San Diego
La Jolla, California 92093-0220

This report summarizes CO_2 observations carried out during the 1990's at Alert, N.W.T (82N, 62W) in a continuing cooperative program between Scripps Institution of Oceanography (SIO) and the Atmospheric Environment Service of Canada. In addition to CO_2 measurements, isotopic measurements of the $^{13}C/^{12}C$ ratio of air sampled at Alert are continuing to be made by SIO using a VG Prism II isotope ratio mass spectrometer at SIO.

Since May 1985 air samples have been collected in 5-liter glass flasks, equipped with greased stopcocks and evacuated at SIO prior to use. Approximately 100 such flasks per year have been exposed at Alert in pairs, four times per month on average, and then returned to the Scripps laboratory where they have then been analyzed for their CO_2 concentration with an NDIR gas analyzer of the same design as that installed at Mauna Loa Observatory (MLO).

Calibrations of the system have continued with reference gases similar to those used at Mauna Loa [*Keeling et al.*, 1968; *Keeling et al.*, 1986]. A list of flasks taken since 1991 and their concentrations (in the SIO 1995 calibration scale), as well as flags indicating rejected data and a list of observers, is shown in Table 1. Samples were rejected automatically if pairs did not agree within 0.40 parts per million (ppm) or if later found to be outliers having a residual greater than 3 standard deviations from a smooth curve fit describing the seasonal and interannual variations. Singlets were also rejected.

The function chosen uses a sum of four harmonics to describe the seasonal variations, and a cubic spline [*Reinsch*, 1967] to describe the interannual variations [*Keeling et al.*, 1989]. Pairs of flasks rejected by the 0.40 ppm criterion are identified in the table by asterisks in the first flag column, with 3 sigma rejections flagged in the second.

Results of fitting daily averages of the accepted data from Alert are shown in Figures 1 and 2, with each accepted flask average shown as a solid dot. The data rejected by poor flask agreement are shown as plus signs while data rejected by 3 sigma are shown as asterisks. Nearly all flagged data has been rejected by the criterion of poor flask pair agreement. The curve fit in Figure 1, which has been fit to the entire record back to 1985, uses a linearly increasing seasonal amplitude factor to describe an observed increasing seasonal amplitude. While this works well for stations with records sufficiently long, considerable variability in the linear gain factor may occur in shorter records such as Alert. Table 2a lists the amplitude of the seasonal cycle for each year independently from 1985-1997 with error estimates, along with the linear gain factor. This factor has been reduced in recent years from about 1.4 %/year to 0.43 %/year due to declining amplitudes during the 1993-96 period and to a rather decadal pattern of amplitudes susceptible to large variability when attempting a linear fit (see further discussion below on C13). Comparison with gains measured at other SIO stations with longer records such as Point Barrow, Alaska show a rate of rise averaging from 0.8-1.3 %/year suggesting amplitudes at Alert will likely rise again as they have in 1997. Implications of rising trends and changes in timing of CO_2 seasonal cycles are discussed further in [Keeling et al., 1996].

Shown in Figure 2 is the curve fit with seasonal cycle subtracted from the data and the fit. This plot reveals changes in trend and quality of the data over the length of the record. The trend through 1992 and into 1993 slowed dramatically during the post Pinatubo eruption cooling but then resumed a strong rate of rise of 2.1 ppm/year over 3 years until a brief slowing in mid-1996. This compares very well with similar results from Point Barrow. Monthly values of the fitted trend are shown in Table 2a for the entire 13-year record along with monthly averages of the data adjusted to the

15th of each month. Also listed is the fitted seasonal cycle for the mid-year of the record at which time the gain factor is unity, so that the fitted function can be computed for any time by multiplying the seasonal cycle by the gain factor and then adding this to the corresponding monthly trend value.

In addition to CO_2 measurements, SIO has been making its own isotopic measurements of the $^{13}C/^{12}C$ ratio of the air sampled at Alert using a VG Prism II isotope ratio mass spectrometer since 1991 with very good results. Listed in Table 2b are the monthly averages of the ^{13}C isotopic data adjusted to the 15th of each month along with isotopic values of the fitted trend. Also listed is the fitted seasonal cycle for ^{13}C. Monthly averages of these isotopic data are shown from 1991-1997 in Figures 3 and 4, which show respectively the seasonal variation and seasonally adjusted trend. The plots are made with a vertical scale of 0.05 per mil for the same distance on the plot as 1.0 ppm on Figures 1 and 2, so that the seasonal amplitudes of isotopic ratio, expressed as a per mil variation from a standard, and CO_2 concentration are approximately equal. Also we plot negative variation upward to reveal similarities in patterns with CO_2 concentration. The presence of a similar interannual signal in both the CO_2 concentrations and the isotopic data is apparent and is of particular interest with regard to continuing El Niño studies.

Recent adjustments of the values of our reference standards during our recent NBS calibration have changed ^{13}C values previously reported for Alert and our other stations by +0.095 per mil. The sigma for the curve fit which is of the same type as used to fit the CO_2 data is 0.065 per mil and the linear gain factor yields a 1.08 %/year increase in the ^{13}C seasonal cycle over the time period 1985-1997. The difference from the gain factor for CO_2 (given above) is partly due to sparse ^{13}C data in 1988-1990 yielding lower seasonal amplitudes in a couple of these early years and therefore a larger linear gain factor for ^{13}C as well. Amplitudes for both CO_2 and ^{13}C are plotted in Figure 5 (for comparisons with other stations see [*Whorf et al.*, 1996]). The importance of continuing quality measurements for CO_2 and ^{13}C at Alert is certainly heightened if we are to maintain accurate records of amplitude change at high latitudes based on the measurements already made. Also differences in patterns of seasonal cycle amplitudes between Alert and sites such as Point Barrow as well as differences in their rate of rise are both of great importance in the continuing search to help identify specific sources and sinks of CO_2.

As for the overall quality of the data at Alert, a comparison of the standard error of the fit during 1985-1997 of 0.958 ppm with the results of a previous fit to Alert made in 1992 having a standard error of 0.975 ppm, shows the last 5 years of data from Alert to be very similar in quality to earlier data. A closer look at the statistics of the Alert data from one year to the next (see Table 3) shows that overall flask rejection rates have been reduced during 1991-97 to nearly half of what they were during the period 1985-92 and among the lowest at any of our other sites. Only Mauna Loa has had fewer flasks rejected (based on the 1985-92 period). The lower rates during 1991-97 may be due to improved techniques of sampling in extremely cold weather. A slight increase in the annual sigma of accepted pairs and in the percentage rejected is noticeable in 1996-97, however.

ACKNOWLEDGEMENTS

We thank Dr. Neil Trivett for his assistance in all phases of this collaborative study with the Atmospheric Environment Service of Canada. His encouragement to include us in his Carbon Dioxide Program at Alert Station was crucial to our long term success in obtaining reliable data. His interest in the scientific results and advocacy of the continuance of this important chemical and climatic field station deserves the appreciation of all of us involved in studies of global environmental change related to the impacts of human activities on the environment, in general, especially to high latitudes which are unusually susceptible to climatic change. This work was supported by the Atmospheric Environment Service of Canada and by NSF Grant ATM-91-21986 and DOE Grants DEFGO390ER60940 & DEFGO395ER62075.

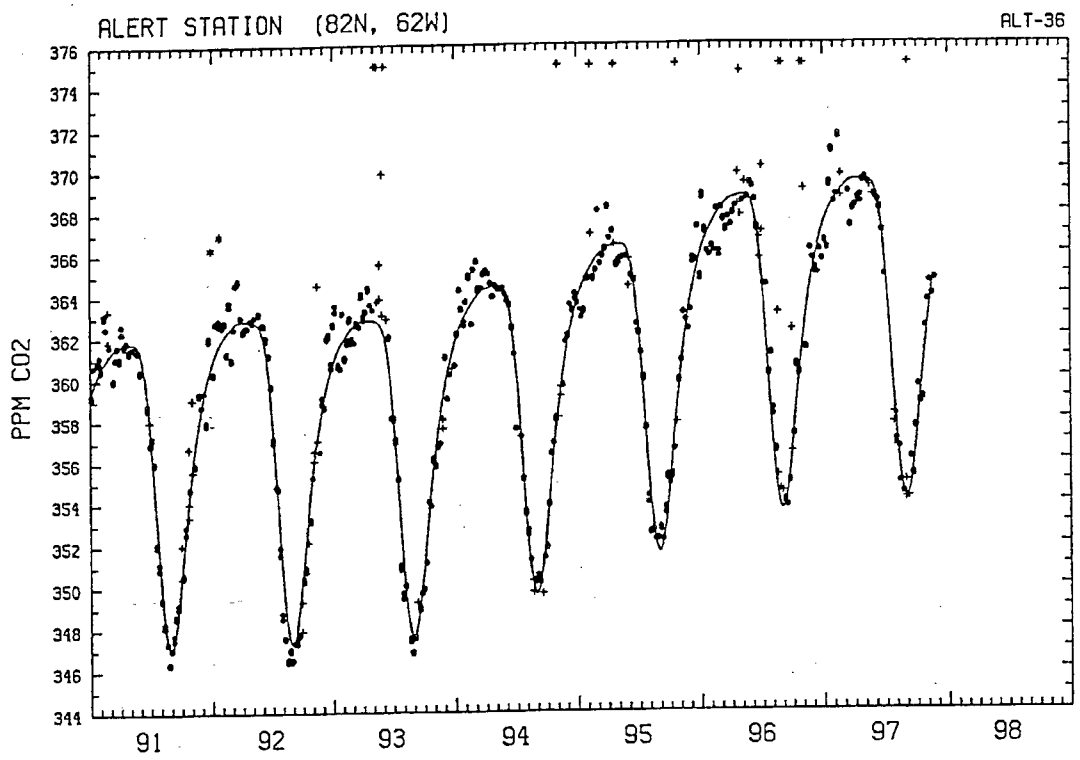

Figure 1. Results of fitting daily averages of the accepted data from Alert.

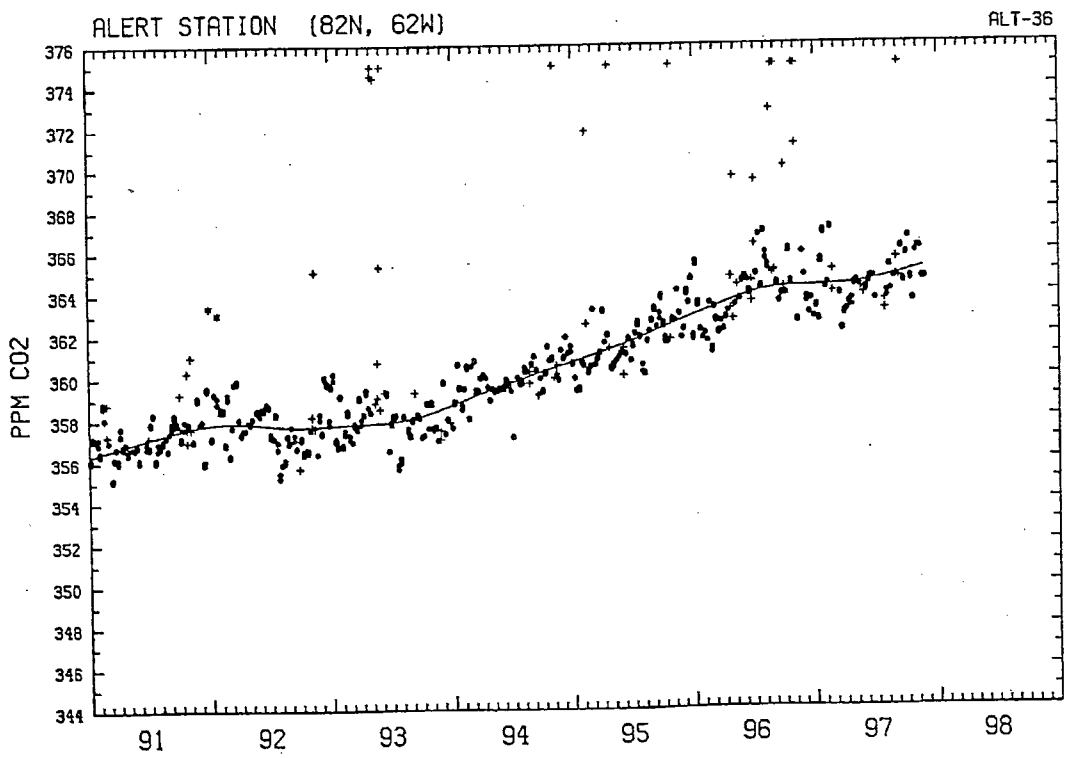

Figure 2. Results of fitting daily averages of the accepted data from Alert.

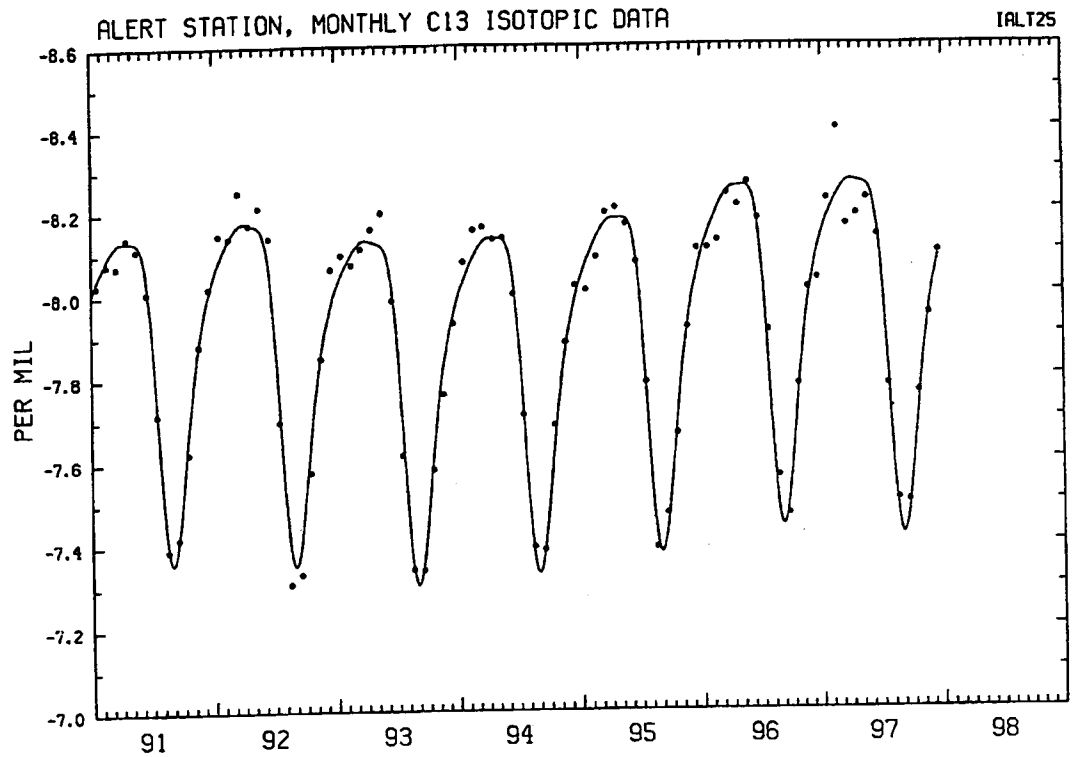

Figure 3. Monthly averages of ^{13}C isotopic data from 1991-1997.

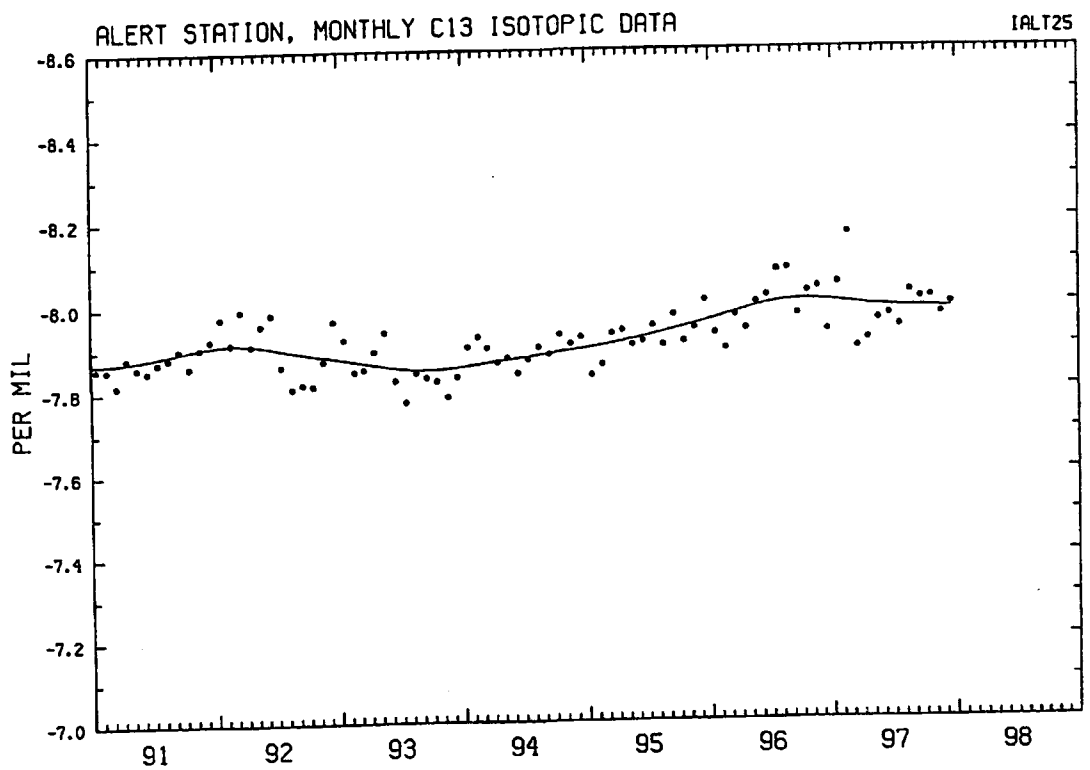

Figure 4. Monthly averages of ^{13}C isotopic data from 1991-1997.

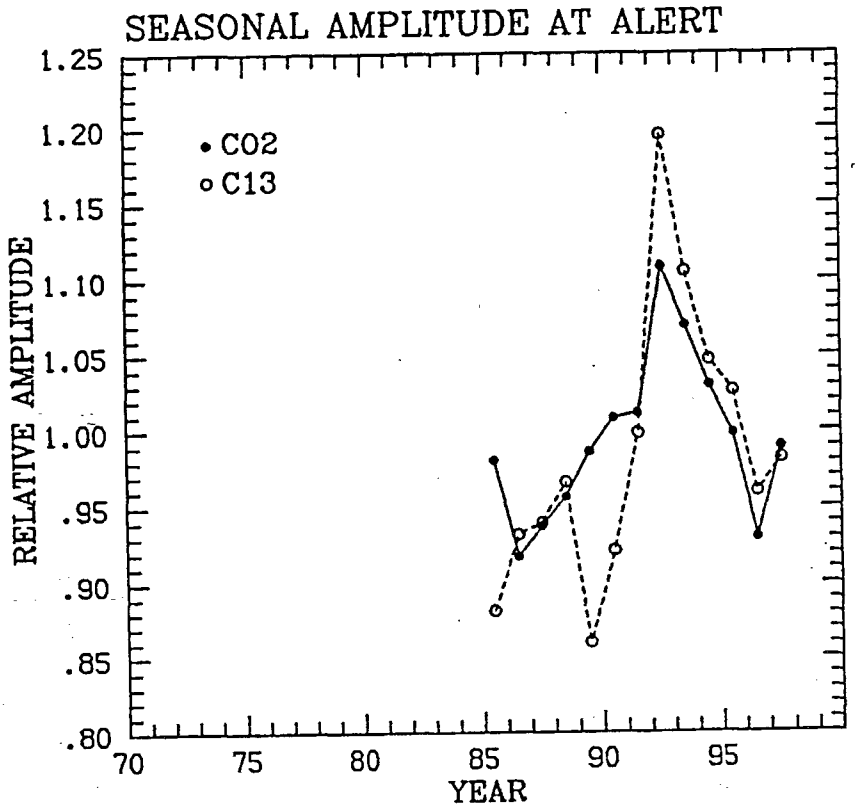

Figure 5. Amplitudes for both CO_2 and ^{13}C.

Table 1. CO2 Concentrations of Individual Flasks at Alert.

Flask No.	Vol	Date and Time (Local)	Obsr	Flask Av (ppm)	Flask No.	Vol	Date and Time (Local)	Obsr	Flask Av (ppm)
M5025	5	91 1 4 1611	VC	359.29	M5035	5	91 726 1331	DW	350.89
M5026	5	91 1 4 1620	VC	359.15	M5036	5	91 726 1331	DW	351.18
M5027	5	91 111 1203	DW	360.65	M5033	5	91 8 2 1602	VC	349.40
M5028	5	91 111 1203	DW	360.65	M5034	5	91 8 2 1606	VC	349.49
M5022	5	91 121 1743	DW	360.80	M5025	5	91 810 1150	VC	348.31
M5021	5	91 121 1744	DW	360.84	M5026	5	91 810 1155	VC	348.12
M5023	5	91 128 1638	DW	360.84	M5027	5	91 819 1102	VC	347.32
M5024	5	91 128 1638	DW	361.13	M5028	5	91 819 1108	VC	347.37
M5011	5	91 2 1 2021	DAE	360.60	M5001	5	91 824 1605	VC	346.39
M5012	5	91 2 1 2027	DAE	360.43	M5002	5	91 824 1612	VC	346.34
M5035	5	91 212 1700	DAE	363.17	M5003	5	91 830 1142	VC	347.06
M5036	5	91 212 1705	DAE	363.01	M5004	5	91 830 1147	VC	347.05
M5033	5	91 216 1653	DAE	362.51	M5021	5	91 9 7 1253	VC	347.74
M5034	5	91 216 1656	DAE	362.51	M5022	5	91 9 7 1301	VC	347.51
M5009	5	91 223 1543	VC	361.84*	M5023	5	91 914 1151	VC	348.55
M5010	5	91 223 1548	VC	363.34*	M5024	5	91 914 1157	VC	348.70
M5037	5	91 227 1615	VC	361.65	M5041	5	91 920 1226	VC	349.04
M5038	5	91 227 1620	VC	361.65	M5042	5	91 920 1231	VC	349.22
M5039	5	91 312 2000	VC	360.05	M5043	5	91 930 1332	MR	350.46*
M5040	5	91 312 2006	VC	359.96	M5044	5	91 930 1339	MR	352.04*
M5005	5	91 317 1323	VC	361.07	M5013	5	9110 4 1450	MR	350.65
M5006	5	91 317 1328	VC	361.02	M5014	5	9110 4 1457	MR	350.50
M5007	5	91 322 1732	VC	361.62	M5016	5	911013 1415	VC	352.59
M5008	5	91 322 1739	VC	361.58	M5017	5	911013 1423	VC	352.93
M5001	5	91 329 1628	VC	360.92	M5018	5	911022 0049	VC	356.72*@
M5002	5	91 329 1637	VC	361.10	M5019	5	911022 0056	VC	353.40*
M5003	5	91 4 5 1303	VC	362.27	M5020	5	911022 0101	VC	354.04*
M5004	5	91 4 5 1312	VC	362.61	M5029	5	911025 1635	VC	354.71
M5041	5	91 412 1331	VC	361.74	M5030	5	911025 1642	VC	354.77
M5042	5	91 412 1337	VC	361.60	M5031	5	9111 2 1322	VC	355.59*
M5043	5	91 419 1528	VC	361.77	M5032	5	9111 2 1325	VC	359.04*#
M5044	5	91 419 1533	VC	361.85	M5005	5	9111 9 1746	VC	355.84
M5013	5	91 427 1352	VC	361.32	M5006	5	9111 9 1752	VC	355.94
M5014	5	91 427 1359	VC	361.43	M5009	5	911122 1514	VC	359.35
M5015	5	91 5 3 1111	VC	361.55	M5010	5	911122 1518	VC	359.21
M5016	5	91 5 3 1116	VC	361.55	M5011	5	911129 1304	VC	358.72
M5017	5	91 511 1220	VC	361.56	M5012	5	911129 1310	VC	358.72
M5018	5	91 511 1224	VC	361.56	M5033	5	9112 6 1438	VC	359.39
M5019	5	91 517 1334	VC	361.40	M5034	5	9112 6 1444	VC	359.39
M5020	5	91 517 1341	VC	361.40	M5035	5	911213 1720	VC	357.83
M5029	5	91 525 1045	VC	361.32	M5036	5	911213 1730	VC	357.99
M5030	5	91 525 1051	VC	361.40	M5038	5	911221 1752	PC	361.88
M5031	5	91 531 1049	VC	360.34	M5037	5	911221 1757	PC	362.01
M5032	5	91 531 1054	VC	360.46	M5039	5	911229 1424	PC	366.13&#
M5005	5	91 622 1127	VC	358.80	M5040	5	911229 1431	PC	366.13&#
M5006	5	91 622 1133	VC	358.60	M5025	5	92 1 3 1853	PC	360.31
M5007	5	91 628 1213	VC	358.01*	M5026	5	92 1 3 1859	PC	360.21
M5009	5	91 7 1 1252	VC	356.87	M5027	5	92 110 1857	PC	362.67
M5010	5	91 7 1 1256	VC	356.97	M5028	5	92 110 1904	PC	362.72
M5011	5	91 7 5 1331	VC	357.25	M5001	5	92 120 1640	DW	362.57
M5012	5	91 7 5 1338	VC	357.16	M5002	5	92 120 1640	DW	362.86
M5037	5	91 712 1157	VC	356.03	M5003	5	92 123 1529	PC	366.74&#
M5038	5	91 712 1203	VC	355.93	M5004	5	92 123 1534	PC	366.79&#
M5039	5	91 719 1416	DW	352.13	M5021	5	92 130 1839	PC	362.49
M5040	5	91 719 1416	DW	351.98	M5022	5	92 130 1844	PC	362.65

Table 1 (continued)

Flask No.	Vol	Date and Time (Local)	Obsr	Flask Av (ppm)	Flask No.	Vol	Date and Time (Local)	Obsr	Flask Av (ppm)
M5023	5	92 2 6 1645	PC	362.65	M5030	5	92 823 1337	VC	347.05
M5024	5	92 2 6 1651	PC	362.79	M5031	5	92 828 1426	LL	346.56
M5013	5	92 213 1437	PC	361.19	M5032	5	92 828 1428	LL	346.47
M5014	5	92 213 1442	PC	361.29	M5005	5	92 9 3 1326	VC	347.35
M5015	5	92 220 1744	PC	363.75	M5006	5	92 9 3 1328	VC	347.35
M5016	5	92 220 1749	PC	363.55	M5007	5	92 912 1047	LL	347.55
M5017	5	92 227 1547	PC	361.00	M5008	5	92 912 1049	LL	347.31
M5018	5	92 227 1553	PC	360.90	M5009	5	92 919 1624	SI	347.70
M5019	5	92 3 5 1755	PC	362.43	M5010	5	92 919 1626	SI	347.75
M5020	5	92 3 5 1800	PC	362.43	M5011	5	92 927 1108	SI	347.93*
M5041	5	92 312 1508	PC	364.63	M5012	5	92 927 1110	SI	349.32*
M5042	5	92 312 1513	PC	364.58	M5036	5	9210 3 1332	NS	350.42
M5043	5	92 319 1723	PC	364.68	M5035	5	9210 3 1334	NS	350.28
M5044	5	92 319 1729	PC	364.82	M5033	5	921010 1154	NS	350.76
M5005	5	92 326 1906	PC	363.01	M5034	5	921010 1156	NS	350.95
M5006	5	92 326 1911	PC	363.01	M5037	5	921017 1024	NS	352.17*
M5009	5	92 4 3 1225	PC	362.36	M5039	5	921024 1302	NS	353.27
M5010	5	92 4 3 1229	PC	362.26	M5040	5	921024 1303	NS	353.14
M5011	5	92 4 9 1544	PC	362.46	M5025	5	921031 1323	NS	355.27
M5012	5	92 4 9 1549	PC	362.51	M5026	5	921031 1324	NS	355.27
M5029	5	92 416 1614	PC	362.51	M5027	5	9211 5 1554	NS	356.06*
M5030	5	92 416 1619	PC	362.46	M5028	5	9211 5 1554	NS	356.54*
M5007	5	92 423 1709	PC	362.85	M5041	5	921114 1818	NS	357.05*
M5008	5	92 423 1715	PC	362.85	M5042	5	921114 1843	NS	364.52*#
M5031	5	92 430 1706	PC	362.81	M5044	5	921121 1343	NS	356.51
M5032	5	92 430 1711	PC	362.71	M5043	5	921121 1345	NS	356.51
M5033	5	92 5 7 1617	VC	362.96	M5021	5	921128 1150	NS	359.07
M5034	5	92 5 7 1623	VC	363.00	M5022	5	921128 1151	NS	358.81
M5035	5	92 521 1810	PC	363.20	M5023	5	9212 4 1602	NS	358.70
M5036	5	92 521 1814	PC	363.10	M5024	5	9212 4 1605	NS	358.60
M5037	5	92 529 1511	U	362.63	M5019	5	921213 1644	NS	361.90
M5038	5	92 529 1512	U	362.63	M5020	5	921213 1645	NS	362.01
M5039	5	92 6 4 1702	VC	362.63	M5017	5	921219 1918	NS	362.00
M5040	5	92 6 4 1704	VC	362.53	M5018	5	921219 1919	NS	362.15
M5025	5	92 611 1503	VC	362.02	M5001	5	921226 1244	NS	360.52
M5026	5	92 611 1508	VC	361.87	M5002	5	921226 1245	NS	360.74
M5027	5	92 619 1209	VC	361.18	M5003	5	921231 1331	VC	362.54
M5028	5	92 619 1211	VC	361.09	M5004	5	921231 1332	VC	362.64
M5001	5	92 627 2133	VC	359.60	M5005	5	93 1 7 1800	VC	363.23
M5002	5	92 627 2134	VC	359.69	M5006	5	93 1 7 1803	VC	363.52
M5003	5	92 7 3 1141	VC	356.96	M5007	5	93 115 1844	VC	360.71
M5004	5	92 7 3 1144	VC	357.15	M5008	5	93 115 1901	VC	360.56
M5013	5	92 712 1334	VC	354.81	M5009	5	93 121 1525	VC	360.48
M5014	5	92 712 1336	VC	354.86	M5010	5	93 121 1527	VC	360.55
M5015	5	92 717 1639	VC	354.77	M5011	5	93 128 1537	VC	363.14
M5016	5	92 717 1640	VC	354.67	M5012	5	93 128 1539	VC	363.18
M5019	5	92 723 1703	VC	351.91	M5013	5	93 2 4 1533	VC	361.02
M5020	5	92 723 1705	VC	351.58	M5014	5	93 2 4 1535	VC	360.89
M5017	5	92 730 1341	VC	348.77	M5015	5	93 211 1316	VC	361.88
M5018	5	92 730 1343	VC	348.53	M5016	5	93 211 1319	VC	361.68
M5021	5	92 8 7 1519	VC	347.60	M5029	5	93 218 1454	VC	362.96
M5022	5	92 8 7 1521	VC	347.55	M5030	5	93 218 1456	VC	362.79
M5023	5	92 815 1421	VC	346.43	M5031	5	93 225 1200	VC	361.93
M5024	5	92 815 1425	VC	346.58	M5032	5	93 225 1200	VC	361.71
M5029	5	92 823 1335	VC	346.94	M5033	5	93 3 5 1547	VC	361.74

Table 1 (continued)

Flask No.	Vol	Date and Time (Local)	Obsr	Flask Av (ppm)	Flask No.	Vol	Date and Time (Local)	Obsr	Flask Av (ppm)
M5034	5	93 3 5 1549	VC	361.73	M5005	5	93 923 1148	LO	349.72
M5035	5	93 311 1208	VC	362.55	M5004	5	93 930 1013	LO	349.91
M5036	5	93 311 1210	VC	362.71	M5003	5	93 930 1015	LO	349.92
M5042	5	93 319 1615	VC	362.47	M5001	5	9310 7 1041	LO	351.17
M5043	5	93 319 1620	VC	362.53	M5002	5	9310 7 1045	LO	351.20
M5044	5	93 319 1623	VC	362.55	M5039	5	931015 1116	LO	354.03
M5037	5	93 326 1312	VC	363.97	M5040	5	931015 1118	LO	354.07
M5038	5	93 326 1315	VC	364.10	M5037	5	931021 0944	LO	353.86
M5039	5	93 4 1 1256	VC	363.02	M5038	5	931021 1000	LO	353.86
M5040	5	93 4 1 1258	VC	362.80	M5024	5	931028 1105	LO	356.17
M5021	5	93 4 8 1201	VC	363.27	M5023	5	931028 1106	LO	356.02
M5022	5	93 4 8 1203	VC	363.21	M5021	5	9311 4 1147	LO	355.88
M5023	5	93 415 1624	VC	364.24	M5022	5	9311 4 1148	LO	355.78
M5024	5	93 415 1628	VC	364.42	M5020	5	931111 1114	LO	356.80
M5025	5	93 422 1647	VC	363.58	M5019	5	931111 1115	LO	356.70
M5026	5	93 422 1648	VC	363.58	M5017	5	931118 1119	LO	356.87
M5027	5	93 429 1453	VC	363.34	M5018	5	931118 1121	LO	356.89
M5028	5	93 429 1457	VC	363.33	M5014	5	931125 1143	LO	358.04*
M5002	5	93 5 6 1200	MM	387.50*#	M5013	5	931125 1145	LO	357.61*
M5001	5	93 5 6 1201	MM	379.49*#	M5016	5	9312 3 1112	LO	360.98
M5004	5	93 513 1427	MM	379.33*#	M5015	5	9312 3 1114	LO	361.03
M5003	5	93 513 1430	MM	363.71*	M5009	5	9312 9 1117	LO	359.02
M5005	5	93 520 1405	MM	363.85*	M5010	5	9312 9 1119	LO	359.03
M5006	5	93 520 1407	MM	365.52*@	M5012	5	931216 1125	LO	360.18
M5007	5	93 527 1133	MM	363.07*	M5011	5	931216 1127	LO	360.20
M5008	5	93 527 1135	MM	369.87*#	M5026	5	931223 1130	LO	360.47*
M5017	5	93 6 3 1312	MM	386.06*#	M5027	5	931230 1219	SO	360.61
M5018	5	93 6 3 1314	MM	390.46*#	M5028	5	931230 1220	SO	360.58
M5019	5	93 610 1719	MM	362.88*	M5033	5	94 1 6 1215	MM	362.05
M5013	5	93 617 1421	MM	361.92	M5034	5	94 1 6 1216	MM	362.16
M5014	5	93 617 1422	MM	362.03	M5035	5	94 114 1231	MM	364.27
M5015	5	93 624 1131	MM	358.13	M5036	5	94 114 1232	MM	364.23
M5016	5	93 624 1132	MM	358.11	M5031	5	94 119 1757	MM	363.35
M5009	5	93 7 1 1128	MM	358.15	M5032	5	94 119 1758	MM	363.27
M5010	5	93 7 1 1129	MM	358.01	M5029	5	94 127 1238	MM	362.52
M5011	5	93 7 7 1623	MM	356.93	M5030	5	94 127 1239	MM	362.72
M5012	5	93 7 7 1625	MM	357.10	M5001	5	94 2 2 1558	MM	363.69
M5029	5	93 715 1608	MM	355.20	M5002	5	94 2 2 1559	MM	363.65
M5030	5	93 715 1609	MM	355.12	M5003	5	94 210 1227	MM	364.96
M5031	5	93 722 1621	MM	351.05	M5004	5	94 210 1228	MM	364.82
M5032	5	93 722 1622	MM	350.85	M5037	5	94 217 1504	MM	362.57
M5033	5	93 729 1434	MM	349.47	M5038	5	94 217 1504	MM	362.61
M5034	5	93 729 1435	MM	349.71	M5039	5	94 223 1617	MM	365.23
M5035	5	93 8 6 0716	MM	350.09	M5040	5	94 223 1623	MM	365.20
M5036	5	93 8 6 0717	MM	350.04	M5041	5	94 3 4 1156	MM	365.57
M5042	5	93 820 0810	SO	347.42	M5042	5	94 3 4 1157	MM	365.64
M5041	5	93 820 0812	SO	347.57	M5043	5	94 310 1113	MM	364.32
M5043	5	93 826 1031	MM	346.90	M5044	5	94 310 1114	MM	364.17
M5044	5	93 826 1034	MM	346.85	M5005	5	94 317 1238	MM	364.35
M5025	5	93 9 2 1117	SO	347.66	M5006	5	94 317 1242	MM	364.34
M5026	5	93 9 2 1119	SO	347.54	M5007	5	94 324 0000	VC	365.03
M5028	5	93 9 9 1041	SO	349.29*	M5008	5	94 324 0000	VC	364.98
M5007	5	93 917 1031	LO	349.07	M5021	5	94 331 1035	MM	365.16
M5008	5	93 917 1033	LO	348.93	M5022	5	94 331 1036	MM	365.17
M5006	5	93 923 1146	LO	349.73	M5023	5	94 4 7 1443	MM	365.03

Table 1 (continued)

Flask No.	Vol	Date and Time (Local)	Obsr	Flask Av (ppm)	Flask No.	Vol	Date and Time (Local)	Obsr	Flask Av (ppm)
M5024	5	94 4 7 1444	MM	365.04	M5016	5	941027 1165	PSG	357.95
M5011	5	94 414 1103	MM	364.55	M5041	5	9411 3 1848	PSG	426.26*#
M5012	5	94 414 1105	MM	364.59	M5042	5	9411 3 1848	PSG	358.10*
M5009	5	94 421 1048	MM	363.96	M5043	5	941110 1744	PSG	359.55*
M5010	5	94 421 1050	MM	363.90	M5044	5	941110 1744	PSG	359.13*
M5013	5	94 428 1053	MM	364.43	M5021	5	941117 1815	PSG	359.67
M5014	5	94 428 1054	MM	364.49	M5022	5	941117 1815	PSG	359.61
M5015	5	94 5 5 1044	SO	364.32	M5023	5	941124 1758	PSG	361.72
M5016	5	94 5 5 1045	SO	364.29	M5024	5	941124 1758	PSG	361.72
M5017	5	94 512 1022	LO	364.27	M5033	5	9412 1 1912	PSG	362.04
M5018	5	94 512 1024	LO	364.27	M5034	5	9412 1 1913	PSG	361.91
M5019	5	94 519 0954	LO	364.36	M5036	5	9412 8 1749	PSG	363.51
M5020	5	94 519 0955	LO	364.28	M5035	5	9412 8 1750	PSG	363.52
M5025	5	94 526 1041	LO	364.08	M5002	5	941215 1720	PSG	363.29
M5026	5	94 526 1042	LO	364.05	M5001	5	941215 1722	PSG	363.19
M5027	5	94 6 2 0947	LO	363.85	M5003	5	941223 1835	PSG	363.79
M5028	5	94 6 2 0948	LO	363.71	M5004	5	941223 1836	PSG	364.05
M5030	5	94 6 9 0951	LO	363.48	M5005	5	941229 1615	WEB	363.53
M5029	5	94 6 9 0952	LO	363.58	M5006	5	941229 1617	WEB	363.63
M5032	5	94 617 1027	LO	362.33	M5007	5	95 1 6 1628	TB	363.25
M5031	5	94 617 1028	LO	362.46	M5008	5	95 1 6 1629	TB	363.27
M5035	5	94 623 1315	LO	361.14	M5039	5	95 112 1611	TB	362.89
M5036	5	94 623 1317	LO	361.15	M5040	5	95 112 1612	TB	362.96
M5033	5	94 630 1029	LO	357.60	M5037	5	95 119 1618	TB	363.29
M5034	5	94 630 1030	LO	357.58	M5038	5	95 119 1619	TB	363.15
M5039	5	94 714 1020	LO	357.20	M5015	5	95 128 2053	TB	364.71
M5040	5	94 714 1021	LO	357.19	M5016	5	95 128 2054	TB	364.82
M5037	5	94 721 1019	LO	355.20	M5013	5	95 2 2 1940	TB	364.81
M5038	5	94 721 1021	LO	355.12	M5014	5	95 2 2 1942	TB	364.74
M5001	5	94 728 1022	LO	353.62	M5011	5	95 2 9 1904	TB	376.21*#
M5002	5	94 728 1023	LO	353.46	M5012	5	95 2 9 1905	TB	366.90*
M5003	5	94 8 4 1104	LO	352.48	M5009	5	95 216 1729	TB	364.86
M5004	5	94 8 4 1105	LO	352.70	M5010	5	95 216 1730	TB	364.70
M5005	5	94 811 1020	LO	351.27	M5017	5	95 223 1615	TB	365.13
M5006	5	94 811 1021	LO	351.29	M5018	5	95 223 1616	TB	365.21
M5007	5	94 819 0940	SO	350.28*	M5019	5	95 3 2 1526	TB	368.01
M5008	5	94 819 0941	SO	349.74*	M5020	5	95 3 2 1527	TB	368.02
M5017	5	94 825 0936	LO	350.28	M5025	5	95 3 9 1323	EW	365.52
M5018	5	94 825 0937	LO	350.20	M5026	5	95 3 9 1324	EW	365.45
M5020	5	94 9 1 1001	LO	350.52	M5027	5	95 316 1423	TB	365.80
M5019	5	94 9 1 1002	LO	350.54	M5028	5	95 316 1423	TB	365.87
M5009	5	94 9 8 0903	PSG	350.24	M5029	5	95 323 1137	TB	366.21
M5010	5	94 9 8 0905	PSG	350.18	M5030	5	95 323 1137	TB	366.14
M5012	5	94 915 1101	PSG	349.67*	M5031	5	95 331 1414	TB	368.24
M5029	5	94 922 1027	PSG	351.40	M5032	5	95 331 1414	TB	368.16
M5030	5	94 922 1030	PSG	351.41	M5035	5	95 4 6 0958	TB	366.69
M5027	5	94 929 1159	PSG	351.91	M5036	5	95 4 6 0958	TB	366.70
M5028	5	94 929 1201	PSG	351.83	M5039	5	95 414 1106	TB	367.06
M5031	5	9410 6 1110	PSG	353.86	M5040	5	95 414 1106	TB	367.00
M5032	5	9410 6 1111	PSG	353.98	M5037	5	95 420 1149	BS	396.95*#
M5025	5	941013 1056	PSG	356.36	M5038	5	95 420 1150	BS	366.40*
M5026	5	941013 1057	PSG	356.41	M5033	5	95 427 1016	GP	365.50
M5013	5	941020 1348	PSG	356.88	M5034	5	95 427 1017	GP	365.35
M5014	5	941020 1349	PSG	356.89	M5023	5	95 5 4 1137	GP	365.47
M5015	5	941027 1161	PSG	358.09	M5024	5	95 5 4 1138	GP	365.65

Table 1 (continued)

Flask No.	Vol	Date and Time (Local)	Obsr	Flask Av (ppm)	Flask No.	Vol	Date and Time (Local)	Obsr	Flask Av (ppm)
M5021	5	95 511 1125	BS	365.74	M5014	5	951117 1317	CH	362.74
M5022	5	95 511 1126	BS	365.71	M5010	5	951124 1325	CH	362.31
M5005	5	95 518 1105	GP	365.80	M5009	5	951124 1327	CH	362.29
M5006	5	95 518 1106	GP	365.80	M5012	5	951130 1227	CH	363.26
M5007	5	95 525 1054	GP	365.83	M5011	5	951130 1230	CH	363.21
M5008	5	95 525 1055	GP	365.77	M5015	5	9512 8 1323	CH	365.52
M5041	5	95 6 1 1110	GP	365.70*	M5016	5	9512 8 1325	CH	365.71
M5042	5	95 6 1 1111	GP	364.40*	M5017	5	951215 1324	CH	365.61
M5043	5	95 6 8 1109	KMG	364.91	M5018	5	951215 1327	CH	365.65
M5044	5	95 6 8 1110	KMG	364.84	M5019	5	951222 1203	CH	367.24
M5015	5	95 616 1044	GP	364.71	M5020	5	951222 1205	CH	367.19
M5016	5	95 616 1045	GP	364.61	M5026	5	951229 1507	AP	364.90
M5013	5	95 623 1014	KMG	362.55	M5025	5	951229 1511	AP	364.71
M5014	5	95 623 1015	KMG	362.57	M5027	5	96 1 5 1533	AP	368.77
M5009	5	95 629 1055	GP	362.07	M5028	5	96 1 5 1546	AP	368.58
M5010	5	95 629 1056	GP	362.19	M5029	5	96 112 1617	TS	367.11
M5011	5	95 7 6 1045	KMG	361.15	M5030	5	96 112 1619	TS	366.93
M5012	5	95 7 6 1046	KMG	361.20	M5041	5	96 119 1516	AP	366.01
M5001	5	95 713 1102	BS	359.85	M5042	5	96 119 1519	AP	366.05
M5002	5	95 713 1104	BS	360.02	M5043	5	96 126 1232	TS	365.85
M5003	5	95 720 1007	KMG	357.52	M5044	5	96 126 1233	TS	365.88
M5004	5	95 720 1008	KMG	357.61	M5021	5	96 2 2 1329	WEB	366.26
M5017	5	95 728 1418	WEB	353.96	M5022	5	96 2 2 1330	WEB	366.30
M5018	5	95 728 1421	WEB	354.29	M5023	5	96 2 9 1240	TS	366.06
M5019	5	95 8 3 1033	KMG	352.58	M5024	5	96 2 9 1243	TS	366.08
M5020	5	95 8 3 1034	KMG	352.52	M5033	5	96 216 1250	TS	368.05
M5026	5	95 811 1057	AP	352.68	M5034	5	96 216 1251	TS	368.04
M5025	5	95 811 1100	AP	352.62	M5035	5	96 223 1246	TS	366.03
M5028	5	95 818 1115	AP	352.20	M5036	5	96 223 1247	TS	365.83
M5027	5	95 818 1118	AP	352.22	M5005	5	96 3 1 1214	TS	368.14
M5029	5	95 825 1212	AP	352.27	M5006	5	96 3 1 1215	TS	368.07
M5030	5	95 825 1215	AP	352.20	M5007	5	96 3 7 1236	TS	367.62
M5031	5	95 9 1 1210	CH	352.79	M5008	5	96 3 7 1238	TS	367.50
M5032	5	95 9 1 1217	CH	352.65	M5009	5	96 315 1241	TS	367.02
M5006	5	95 9 8 1106	CH	352.23	M5010	5	96 315 1242	TS	367.15
M5005	5	95 9 8 1113	CH	352.18	M5013	5	96 322 1255	TS	367.64
M5007	5	95 917 1129	CH	353.74	M5014	5	96 322 1256	TS	367.67
M5008	5	95 917 1131	CH	353.46	M5011	5	96 329 1441	TS	367.26
M5022	5	95 922 1207	CH	355.14	M5012	5	96 329 1442	TS	367.34
M5021	5	95 922 1210	CH	355.28	M5015	5	96 4 5 1438	TS	367.91
M5023	5	95 929 1133	CH	354.90	M5016	5	96 4 5 1439	TS	367.81
M5024	5	95 929 1136	CH	355.07	M5017	5	96 412 1324	TS	368.18
M5033	5	9510 5 1121	CH	355.18	M5018	5	96 412 1325	TS	368.19
M5034	5	9510 5 1125	CH	355.38	M5019	5	96 419 1715	TS	368.29*
M5035	5	951013 1302	CH	356.58	M5020	5	96 419 1716	TS	369.79*
M5036	5	951013 1304	CH	356.54	M5025	5	96 426 1525	TS	367.77*
M5039	5	951020 1056	CH	388.59*#	M5026	5	96 426 1526	TS	374.65*#
M5040	5	951020 1059	CH	357.84*	M5027	5	96 5 3 1524	TS	368.48
M5037	5	951027 1152	CH	359.89	M5028	5	96 5 3 1525	TS	368.42
M5038	5	951027 1154	CH	359.77	M5031	5	96 5 9 1421	TS	368.57*
M5001	5	9511 3 1354	CH	360.80	M5032	5	96 5 9 1422	TS	369.35*
M5002	5	9511 3 1356	CH	360.78	M5029	5	96 517 1356	TS	368.63
M5003	5	951110 1308	CH	363.08	M5030	5	96 517 1357	TS	368.57
M5004	5	951110 1310	CH	363.11	M5039	5	96 524 1535	TS	369.26
M5013	5	951117 1315	CH	362.78	M5040	5	96 524 1536	TS	369.33

Table 1 (continued)

Flask No.	Vol	Date and Time (Local)	Obsr	Flask Av (ppm)	Flask No.	Vol	Date and Time (Local)	Obsr	Flask Av (ppm)
M5037	5	96 531 1853	TS	369.18	M5005	5	961213 1643	GJ	364.96
M5038	5	96 531 1854	TS	369.12	M5006	5	961213 1645	GJ	364.96
M5042	5	96 6 7 1322	TS	368.51	M5034	5	961220 1248	GJ	366.07
M5041	5	96 6 7 1324	TS	368.47	M5033	5	961220 1250	GJ	366.11
M5043	5	96 614 1636	AP	367.05	M5020	5	961227 1826	KW	365.60
M5044	5	96 614 1638	AP	367.21	M5019	5	961227 1828	KW	365.64
M5021	5	96 621 1511	AP	365.71*	M5018	5	97 1 3 1803	KW	366.44
M5022	5	96 621 1513	AP	366.69*	M5017	5	97 1 3 1806	KW	366.54
M5023	5	96 629 1420	TS	370.08*#	M5002	5	97 110 1627	SM	366.12
M5024	5	96 629 1421	TS	366.98*	M5001	5	97 110 1632	SM	366.20
M5033	5	96 7 4 1048	AP	364.45	M5037	5	97 117 1706	SM	369.30
M5034	5	96 7 4 1050	AP	364.41	M5038	5	97 117 1711	SM	369.13
M5035	5	96 712 1538	TS	364.41	M5039	5	97 124 1346	SM	370.91
M5036	5	96 712 1540	TS	364.43	M5040	5	97 124 1348	SM	370.77
M5001	5	96 719 1109	TS	360.20	M5027	5	97 131 1451	SM	368.36
M5002	5	96 719 1111	TS	360.10	M5028	5	97 131 1457	SM	368.38
M5003	5	96 726 1355	TS	361.05	M5030	5	97 2 6 1255	SM	368.71*
M5004	5	96 726 1357	TS	361.13	M5031	5	97 213 1406	SM	371.49
M5005	5	96 8 2 1205	TS	358.47	M5032	5	97 213 1411	SM	371.60
M5006	5	96 8 2 1206	TS	358.17	M5025	5	97 220 1224	SM	368.64*
M5008	5	96 8 9 1201	KW	356.39	M5026	5	97 220 1226	SM	369.67*
M5007	5	96 8 9 1203	KW	356.55	M5021	5	97 313 1636	SM	368.89
M5009	5	96 816 1111	TS	355.27*	M5022	5	97 313 1637	SM	368.83
M5010	5	96 816 1113	TS	363.08*#	M5023	5	97 320 1053	SM	367.18
M5013	5	96 823 1212	VH	354.57*	M5024	5	97 320 1055	SM	367.25
M5014	5	96 823 1212	VH	382.90*#	M5011	5	97 327 1353	SM	368.08
M5018	5	96 830 1229	GJ	354.46*	M5012	5	97 327 1354	SM	367.98
M5017	5	96 830 1231	GJ	389.03*#	M5009	5	97 4 3 1903	SM	368.21
M5019	5	96 9 6 1454	GJ	354.09	M5010	5	97 4 3 1905	SM	368.17
M5020	5	96 9 6 1457	GJ	353.96	M5017	5	97 410 1606	SM	368.55
M5025	5	96 913 1126	GJ	353.76	M5018	5	97 410 1608	SM	368.50
M5026	5	96 913 1128	GJ	353.80	M5019	5	97 417 1533	SM	368.36
M5040	5	96 920 1254	GJ	354.94	M5020	5	97 417 1535	SM	368.67
M5039	5	96 920 1257	GJ	355.02	M5034	5	97 425 2000	SM	369.35
M5037	5	96 927 1242	GJ	356.40*	M5033	5	97 425 2002	SM	369.43
M5038	5	96 927 1244	GJ	362.25*#	M5035	5	97 5 1 1739	SM	369.52
M5027	5	9610 4 1608	GJ	357.28	M5036	5	97 5 1 1742	SM	369.49
M5028	5	9610 4 1611	GJ	357.22	M5003	5	97 5 9 1427	PA	369.29
M5029	5	961011 1501	GJ	360.45	M5004	5	97 5 9 1430	PA	369.32
M5030	5	961011 1503	GJ	360.60	M5008	5	97 515 1416	PA	369.12*
M5031	5	961018 1021	GJ	360.08	M5005	5	97 522 1341	PA	368.68*
M5032	5	961018 1023	GJ	360.22	M5001	5	97 529 1313	PA	368.73
M5011	5	961025 1334	GJ	398.92*#	M5002	5	97 529 1315	PA	368.58
M5012	5	961025 1336	GJ	375.23*#	M5037	5	97 6 6 1527	PA	368.47
M5015	5	9611 1 1136	GJ	379.18*#	M5038	5	97 6 6 1528	PA	368.38
M5016	5	9611 1 1139	GJ	369.01*#	M5039	5	97 612 1229	PA	368.09
M5024	5	9611 8 1200	GJ	361.32	M5040	5	97 612 1230	PA	367.99
M5021	5	9611 8 1347	GJ	361.40	M5029	5	97 620 0922	PA	366.99
M5022	5	9611 8 1357	GJ	361.32	M5030	5	97 620 0923	PA	366.96
M5008	5	961122 1302	GJ	366.13	M5027	5	97 626 1625	PA	364.86
M5007	5	961122 1305	GJ	366.16	M5028	5	97 626 1627	PA	364.86
M5036	5	961129 1400	GJ	365.68	M5011	5	97 724 1321	PA	358.21*
M5035	5	961129 1403	GJ	365.68	M5012	5	97 724 1324	JM	357.76*
M5003	5	9612 6 1306	GJ	364.98	M5009	5	97 731 1350	PA	356.70
M5004	5	9612 6 1309	GJ	365.21	M5010	5	97 731 1353	PA	356.93

Table 1 (continued)

Flask No.	Vol	Date and Time (Local)	Obsr	Flask Av (ppm)	Flask No.	Vol	Date and Time (Local)	Obsr	Flask Av (ppm)
M5019	5	97 8 8 1614	PA	356.55	M5031	5	9710 2 1652	CP	359.51
M5020	5	97 8 8 1625	PA	356.60	M5032	5	9710 2 1655	CP	359.55
M5017	5	97 811 1904	PA	354.91	M5029	5	9710 9 1649	CP	358.68
M5018	5	97 811 1906	PA	354.91	M5030	5	9710 9 1651	CP	358.82
M5013	5	97 821 1851	PA	354.35	M5035	5	971016 1422	CP	358.89
M5014	5	97 821 1853	PA	354.40	M5036	5	971016 1424	CP	358.95
M5021	5	97 828 1726	PA	354.12*	M5025	5	971023 1559	CP	362.35
M5022	5	97 828 1728	PA	354.97*	M5026	5	971023 1602	CP	362.37
M5023	5	97 9 4 1705	PA	354.16*	M5003	5	971030 1518	CP	363.65
M5024	5	97 9 4 1707	PA	431.71*#	M5004	5	971030 1520	CP	363.64
M5015	5	97 911 1641	CP	356.10	M5001	5	9711 6 1507	CP	364.58
M5016	5	97 911 1644	CP	356.03	M5002	5	9711 6 1509	CP	364.54
M5033	5	97 918 1521	CP	355.19	M5007	5	971113 1717	CP	363.91
M5034	5	97 918 1524	CP	355.30	M5008	5	971113 1719	CP	363.93
M5027	5	97 925 1657	CP	357.60	M5039	5	971120 1622	CP	364.70
M5028	5	97 925 1659	CP	357.52	M5040	5	971120 1624	CP	364.65

Flag symbols:

- `*` rejected because there do not exist a flask pair that agree within 0.40 ppm.
- `&` rejected because flask is greater than 3.0 sigma from fit and was not rejected by previous criterion
- `@` flask lies outside 2.5 sigma of fit
- `#` flask lies outside 3.0 sigma of fit

Alert Station List of Observers:

VC	- Valerie Chorney	DW	- Doug Worthy
DAE	- Darrell Ernst	MR	- Michele Rauh
PC	- P. Chomik	LL	- Lori Leeder
SI	- Syed Iqbak	NS	- Neman Syed
MM	- Mitch Marszel	SO	- Shawn Ogston
LO	- L. Oatway	PSG	- Paul Gerla
WEB	- Webster	TB	- T. Biesenthal
EW	- Erika Wallgren	BS	- B. Sargent
GP	- G. Pelland	KMG	- K. M. Gaider
AP	- A. Platt	CH	- Craig Hawthorne
TS	- Tina Scherz	KW	- Korb Whale
VH	- Victoria Hudec	GJ	- G. James
SM	- S. Mercer	PA	- Peter Ayranto
JM	- J. McNairn	CP	- C. Piller
U	- Unknown		

Table 2a. Summary of fit to Concentration Data at ALERT.

Spline Stiffness Parameter (Sigma) : 0.9575 ppm

Seasonal Amplitude (Gain) for Each Year ;					Linear Gain Factor (by least squares)
YEAR	PTS	DEL	GAIN	ERROR	
1985	18	0.95	0.9809	0.0401	0.4322 %/year
1986	32	0.98	0.9177	0.0387	error: 0.2599 %/year
1987	38	0.86	0.9378	0.0258	
1988	29	0.90	0.9566	0.0361	
1989	25	0.92	0.9865	0.0434	
1990	41	0.73	1.0082	0.0231	
1991	44	0.80	1.0115	0.0222	
1992	46	0.91	1.1083	0.0253	
1993	43	0.98	1.0694	0.0291	
1994	47	0.79	1.0299	0.0226	
1995	48	0.91	0.9981	0.0250	
1996	40	1.14	0.9301	0.0367	
1997	36	1.08	0.9895	0.0337	

Fitted Seasonal Cycle (4 Harmonics) :

JAN	FEB	MAR	APR	MAY	JUN	JUL	AUG	SEP	OCT	NOV	DEC
3.58	4.40	4.86	4.93	4.81	2.93	-3.06	-9.48	-9.39	-4.71	-0.48	2.04

Station: ALERT
Concentration of Atmospheric CO2 (ppm)
Averages of Data Adjusted to the 15th of Each Month :

MONTH	YEAR							
	1985	1986	1987	1988	1989	1990	1991	1992
JAN	0.00	350.94	351.44	354.02	356.22	359.20	360.41	362.07
FEB	0.00	351.48	352.08	355.38	358.78	360.02	361.98	362.12
MAR	0.00	352.67	353.87	356.11	360.00	360.69	360.86	363.71
APR	0.00	352.93	353.50	357.12	359.45	360.51	361.82	362.59
MAY	352.56	353.54	354.46	356.82	359.44	360.09	361.37	363.09
JUN	348.07	351.57	352.76	355.97	357.58	357.65	359.70	361.56
JUL	343.22	346.86	348.21	348.38	351.51	351.22	354.11	353.90
AUG	0.00	340.23	341.03	343.97	345.58	346.24	347.52	346.99
SEP	338.44	339.20	340.36	0.00	346.04	346.96	348.59	347.76
OCT	342.59	344.10	346.03	349.42	349.73	350.72	352.90	352.17
NOV	346.90	348.51	349.22	354.74	354.61	355.67	357.50	356.80
DEC	349.25	349.33	352.47	357.30	358.18	358.33	359.89	361.00
AVE	0.00	348.45	349.62	0.00	354.76	355.61	357.22	357.81

MONTH	YEAR				
	1993	1994	1995	1996	1997
JAN	361.85	363.03	363.52	366.90	368.18
FEB	361.88	364.16	364.95	366.66	370.26
MAR	362.72	364.87	366.76	367.57	368.00
APR	363.48	364.49	366.38	368.05	368.66
MAY	0.00	364.30	365.77	369.03	369.25
JUN	360.87	362.10	364.26	367.32	367.37
JUL	354.14	356.75	358.63	362.60	360.68
AUG	348.13	350.87	352.07	355.90	354.96
SEP	348.42	350.68	353.44	354.39	355.83
OCT	353.37	356.09	357.27	360.00	360.53
NOV	356.98	360.10	362.32	363.71	364.65
DEC	360.30	363.29	365.60	365.38	0.00
AVE	0.00	360.06	361.75	363.96	0.00

Table 2a continued:

Concentration of Atmospheric CO2 (ppm)
Trend (Exponential + Spline) at 15th of Month :
(JAN0 Refers to Value at Beginning of Year)

MONTH	YEAR							
	1985	1986	1987	1988	1989	1990	1991	1992
JAN	0.00	347.71	348.73	351.01	354.12	355.41	356.39	357.86
FEB	0.00	347.83	348.87	351.27	354.30	355.44	356.54	357.89
MAR	0.00	347.95	349.02	351.53	354.45	355.46	356.67	357.89
APR	0.00	348.07	349.21	351.81	354.60	355.48	356.81	357.88
MAY	346.86	348.18	349.40	352.09	354.74	355.51	356.95	357.84
JUN	346.94	348.27	349.61	352.39	354.86	355.55	357.09	357.80
JUL	347.03	348.35	349.80	352.67	354.97	355.62	357.23	357.75
AUG	347.13	348.41	350.00	352.95	355.08	355.71	357.37	357.71
SEP	347.24	348.46	350.18	353.23	355.17	355.82	357.50	357.69
OCT	347.35	348.50	350.37	353.47	355.25	355.95	357.62	357.70
NOV	347.46	348.56	350.57	353.71	355.32	356.09	357.72	357.72
DEC	347.58	348.63	350.78	353.92	355.37	356.24	357.80	357.74
AVE	0.00	348.24	349.71	352.50	354.85	355.69	357.14	357.79
JAN0	0.00	347.65	348.68	350.90	354.02	355.39	356.32	357.83

MONTH	YEAR				
	1993	1994	1995	1996	1997
JAN	357.77	358.85	360.84	363.06	364.32
FEB	357.80	359.05	361.00	363.25	364.33
MAR	357.82	359.22	361.15	363.43	364.35
APR	357.85	359.40	361.31	363.62	364.39
MAY	357.87	359.57	361.48	363.80	364.46
JUN	357.91	359.74	361.67	363.97	364.54
JUL	357.97	359.91	361.86	364.10	364.64
AUG	358.05	360.08	362.06	364.20	364.76
SEP	358.16	360.24	362.27	364.25	364.89
OCT	358.30	360.39	362.47	364.29	365.01
NOV	358.47	360.55	362.68	364.30	365.14
DEC	358.65	360.69	362.87	364.31	0.00
AVE	358.05	359.81	361.81	363.88	0.00
JAN0	357.76	358.75	360.77	362.97	364.31

Table 2b. Summary of fit to C13 Isotopic Data at ALERT.

Isotopic Spline Stiffness Parameter (Sigma) : 0.0650 per mil
Linear Gain Factor: 1.0812 %/year
error: 0.3818 %/year

Fitted Seasonal Cycle (4 Harmonics) :

JAN	FEB	MAR	APR	MAY	JUN	JUL	AUG	SEP	OCT	NOV	DEC
-0.17	-0.22	-0.25	-0.26	-0.25	-0.16	0.16	0.49	0.48	0.24	0.02	-0.09

Station: ALERT
C13 Isotopic Data of Atmospheric CO2 (per mil)
Averages of Data Adjusted to the 15th of Each Month :

MONTH	YEAR							
	1985	1986	1987	1988	1989	1990	1991	1992
JAN	0.000	-7.957	-7.821	-7.939	-8.042	-8.027	-8.027	-8.145
FEB	0.000	-7.978	-7.899	-8.000	-8.173	-8.100	-8.076	-8.137
MAR	0.000	-8.043	-8.033	-8.004	-8.260	-8.123	-8.071	-8.249
APR	0.000	-7.968	-7.966	-8.169	-8.075	-8.128	-8.140	-8.170
MAY	-7.998	-7.969	-7.999	-8.101	-8.090	-8.125	-8.111	-8.211
JUN	-7.867	-7.820	-7.942	-8.130	-8.076	-7.979	-8.008	-8.137
JUL	-7.567	-7.611	-7.699	-7.636	-7.736	-7.586	-7.715	-7.696

Table 2b continued:

AUG	0.000	-7.256	-7.326	-7.420	-7.557	-7.437	-7.390	-7.308
SEP	-7.339	-7.270	-7.268	0.000	-7.509	-7.464	-7.419	-7.332
OCT	-7.577	-7.500	-7.555	-7.656	-7.703	-7.654	-7.623	-7.575
NOV	-7.863	-7.667	-7.722	0.000	-7.904	-7.887	-7.880	-7.847
DEC	-7.846	-7.723	-7.828	0.000	-7.998	-7.967	-8.018	-8.061
AVE	0.000	-7.730	-7.755	0.000	-7.927	-7.873	-7.873	-7.906

MONTH	YEAR				
	1993	1994	1995	1996	1997
JAN	-8.094	-8.076	-8.007	-8.106	-8.223
FEB	-8.071	-8.153	-8.086	-8.124	-8.396
MAR	-8.109	-8.160	-8.193	-8.238	-8.161
APR	-8.156	-8.131	-8.205	-8.210	-8.187
MAY	-8.196	-8.135	-8.165	-8.264	-8.225
JUN	-7.984	-7.999	-8.073	-8.177	-8.135
JUL	-7.614	-7.710	-7.785	-7.907	-7.777
AUG	-7.341	-7.394	-7.391	-7.561	-7.503
SEP	-7.340	-7.387	-7.472	-7.468	-7.497
OCT	-7.581	-7.685	-7.663	-7.779	-7.759
NOV	-7.760	-7.881	-7.916	-8.010	-7.945
DEC	-7.928	-8.019	-8.104	-8.032	-8.095
AVE	-7.848	-7.894	-7.922	-7.990	-7.992

C13 Isotopic Data of Atmospheric CO2 (per mil)
Trend (Exponential + Spline) at 15th of Month :
(JAN0 Refers to Value at Beginning of Year)

MONTH	YEAR							
	1985	1986	1987	1988	1989	1990	1991	1992
JAN	0.000	-7.754	-7.723	-7.802	-7.895	-7.888	-7.869	-7.911
FEB	0.000	-7.749	-7.728	-7.810	-7.899	-7.884	-7.870	-7.913
MAR	0.000	-7.744	-7.734	-7.819	-7.902	-7.880	-7.872	-7.913
APR	0.000	-7.739	-7.741	-7.829	-7.904	-7.876	-7.874	-7.911
MAY	-7.775	-7.733	-7.748	-7.838	-7.905	-7.873	-7.877	-7.908
JUN	-7.773	-7.728	-7.755	-7.848	-7.906	-7.871	-7.881	-7.904
JUL	-7.772	-7.724	-7.761	-7.856	-7.905	-7.870	-7.885	-7.899
AUG	-7.771	-7.721	-7.768	-7.865	-7.905	-7.869	-7.890	-7.894
SEP	-7.769	-7.718	-7.774	-7.872	-7.903	-7.868	-7.895	-7.889
OCT	-7.766	-7.717	-7.780	-7.879	-7.900	-7.868	-7.900	-7.885
NOV	-7.763	-7.717	-7.786	-7.885	-7.896	-7.868	-7.904	-7.882
DEC	-7.759	-7.719	-7.793	-7.890	-7.892	-7.868	-7.908	-7.878
AVE	0.000	-7.730	-7.758	-7.849	-7.901	-7.874	-7.885	-7.899
JAN0	0.000	-7.757	-7.721	-7.798	-7.893	-7.890	-7.869	-7.910

MONTH	YEAR				
	1993	1994	1995	1996	1997
JAN	-7.874	-7.857	-7.898	-7.963	-8.001
FEB	-7.870	-7.861	-7.902	-7.970	-7.998
MAR	-7.866	-7.864	-7.906	-7.977	-7.995
APR	-7.862	-7.867	-7.911	-7.984	-7.992
MAY	-7.858	-7.870	-7.916	-7.990	-7.990
JUN	-7.854	-7.874	-7.921	-7.996	-7.989
JUL	-7.851	-7.877	-7.926	-8.000	-7.987
AUG	-7.850	-7.880	-7.932	-8.004	-7.987
SEP	-7.849	-7.884	-7.938	-8.005	-7.986
OCT	-7.850	-7.887	-7.944	-8.006	-7.985
NOV	-7.851	-7.891	-7.951	-8.005	-7.984
DEC	-7.854	-7.894	-7.957	-8.003	-7.984
AVE	-7.857	-7.876	-7.925	-7.992	-7.990
JAN0	-7.876	-7.856	-7.896	-7.960	-8.002

Table 3. Summary of Flask Rejections at Alert Due to Poor Agreement: (flasks rejected if do not agree that day within 0.40 ppm)

Date	Total # Flasks	# Rejctd flsks	% Rejctd	# Accptd flasks	# 3 Sig Rejctd	Sigma Acc flsks
1991	100	10	10 %	88	2	0.81
1992	103	7	7 %	94	2	1.10
1993	100	15	15 %	85	0	0.99
1994	101	7	7 %	94	0	0.80
1995	104	8	8 %	96	0	0.92
1996	103	22	21 %	81	0	1.21
1997	81	11	14 %	70	0	1.11
1/91-11/97	692	80	11.6 %	608	4	0.98
previously reported period:						
5/85-2/92	603	131	21.7 %	462	6	0.87

Summary of Flask Rejections at Other Sites Due to Poor Agreement:
(From previous reported data)

Station	Date	% Rejctd
Point Barrow	5/85-2/92	21.3 %
	1/82-2/92	17.5 %
Cape Kumukahi	3/79-2/92	13.8 %
Mauna Loa	1/70-2/92	8.2 %
Christmas Is.	1/84-1/92	26.4 %

REFERENCES

Keeling, C.D., Harris, T.B., and Wilkins, E.M., Concentration of atmospheric carbon dioxide at 500 and 700 millibars, \flJournal of Geophysical Research,\fR v 3, p 4511-4528, (1968).

Keeling, C.D., Guenther, P.R., and Moss, D.J., Scripps reference gas calibration system for carbon dioxide-in-air standards: Revision of 1985. Report No. 4 of the Environmental Monitoring Programme of the World Meteorological Organization, Geneva, 34 p. and Addendum, 43 p., (1986).

Keeling, C.D., Bacastow, R.B., Carter, A.F., Piper, S.C., Whorf, T.P., Heimann, M., Mook, W.G., and Roeloffzen, H., A three-dimensional model of atmospheric CO2 transport based on observed winds: 1. Analysis of observational data, in Aspects of Climate Variability in the Pacific and the Western Americas, edited by D. H. Peterson, Geophysical Monograph American Geophysical Union, v 55, Washington, D.C., p 165-236, (1989).

Reinsch, C.H., Smoothing by spline functions, Numerische Mathematik, v 10, p 177-183, (1967).

Whorf, T.P., Keeling, C.D. and Wahlen, M., A Comparison of CO2 and 13C/12C seasonal amplitudes in the Northern Hemisphere, \flClimate Monitoring and Diagnostics Laboratory B23, Summary Report 1994-95, NOAA, Boulder, CO, p 153-156, (1996).

Keeling, C.D., Chin, J.F.S., and Whorf, T.P., Increased activity of northern vegetation inferred from atmospheric CO2 measurements, Nature, v 382, p 146-149, (1996).

5.4. COOPERATIVE REPORT: NOAA/CMDL MEASUREMENTS OF TRACE HALOCOMPOUNDS AND NITROUS OXIDE FROM FLASK SAMPLES AND IN SITU INSTRUMENT AT ALERT.

James W. Elkins[1], James H. Butler[1], Stephen A. Montzka[1], Thayne M. Thompson[1], Debra J. Mondeel[1,2], Loreen T. Lock[1,2], Geoffrey S. Dutton[1,2], and Matthew R. Pender[1,2]

[1]NOAA/CMDL, N_2O and Halocompounds Group, Mail Stop R/E/CG1, 325 Broadway, Boulder, Colorado 80303 USA

[2]CIRES, University of Colorado, Campus Box 216, Boulder, Colorado 80309 USA

Abstract: We report the measurements of atmospheric N_2O, CFC-11, CFC-12, CFC-113, halon-1211, halon-1301, halon-2402, SF_6, HCFC-22, HCFC-141b, HCFC-142b, and HFC-134a collected from flask samples at Alert. These observations are compared to values measured from other sites in the NOAA/CMDL N_2O and halocompound flask network. We also describe our measurement system for monitoring atmospheric N_2O and SF_6 from an in situ instrument operated at Alert.

INTRODUCTION

Alert is the most northern station in our flask network (see map insert in Figure 1). Typically, Alert has the highest concentration for these trace gases at any one time, because most of their emissions are located in the middle and high latitudes and tropospheric circulation forces the trace gases towards the highest latitudes. We began our measurements for nitrous oxide (N_2O), CFC-11 (CCl_3F), CFC-12 (CCl_2F_2) and halon-1211 ($CBrClF_2$) and –1301 ($CBrF_3$) from flask pair samples collected at Alert in 1988. By 1992, we added CFC-113 (CCl_2F-$CClF_2$), hydrochlorofluorocarbon-22 or HCFC-22 ($CHClF_2$), -141b (CH_3CCl_2F), -142b (CH_3CClF_2) to our program. Other molecules were added to program as new techniques were developed. We installed the in situ gas chromatograph (GC) for measuring N_2O and SF_6 in late 1995. The first report of the reduction in the growth rates for halon-1211 and -1301 in the atmosphere included Alert data [*Butler et al.*, 1992]. Measurements of the CFCs at Alert were reported in first publication showing the slowdown in the global growth rates of CFC-11 and CFC-12 [*Elkins et al.*, 1993]. The Montreal Protocol and its amendments appear to be working and in fact, ahead of schedule. The first report on the reduction of global total effective chlorine sometime between 1993 and 1994 also included Alert data [*Montzka et al.*, 1996]. While total chlorine has decreased, total organic bromine is still increasing because of the large amount of halon stored in banked cylinders by developed countries and legal production of halons in developing countries [*Butler et al.*, 1998]. The continued growth of halon-1211 will be a concern for policy makers in the near future.

CFC MEASUREMENTS FROM FLASKS

Almost all production of these major CFCs and chlorinated solvents ended on January 1, 1996 in the developed countries. The growth rates of the CFCs, methyl chloroform (CH_3CCl_3), and carbon tetrachloride (CCl_4) are decreasing with time (Figure 1). The atmospheric growth rate of CFC-12 while still positive is decreasing with time as a result of voluntary and mandated emission reductions under the Montreal Protocol. CFC-12 was used in pre-1993 auto air conditioners, as an aerosol propellant, and in refrigerators. The accumulation of CFC-11 in the atmosphere peaked during 1993-1994. CFC-11 was used as a cell-blowing agent for manufacture of foams, in large building air conditioning, and refrigeration. CH_3CCl_3 has decreased in mixing ratios (about -14 parts-per-trillion (ppt) yr^{-1}) between 1995 and 1996. CH_3CCl_3 was used as a metal degreaser in manufacturing. CFC-113 has leveled off and is slowly dropping in mixing ratio with time. It was used as a solvent degreaser in the manufacture of circuit boards. CCl_4 is decreasing in mixing ratio at an almost constant rate of 0.8% yr^{-1}. It was used in dry cleaning and as a feedstock to produce the CFCs.

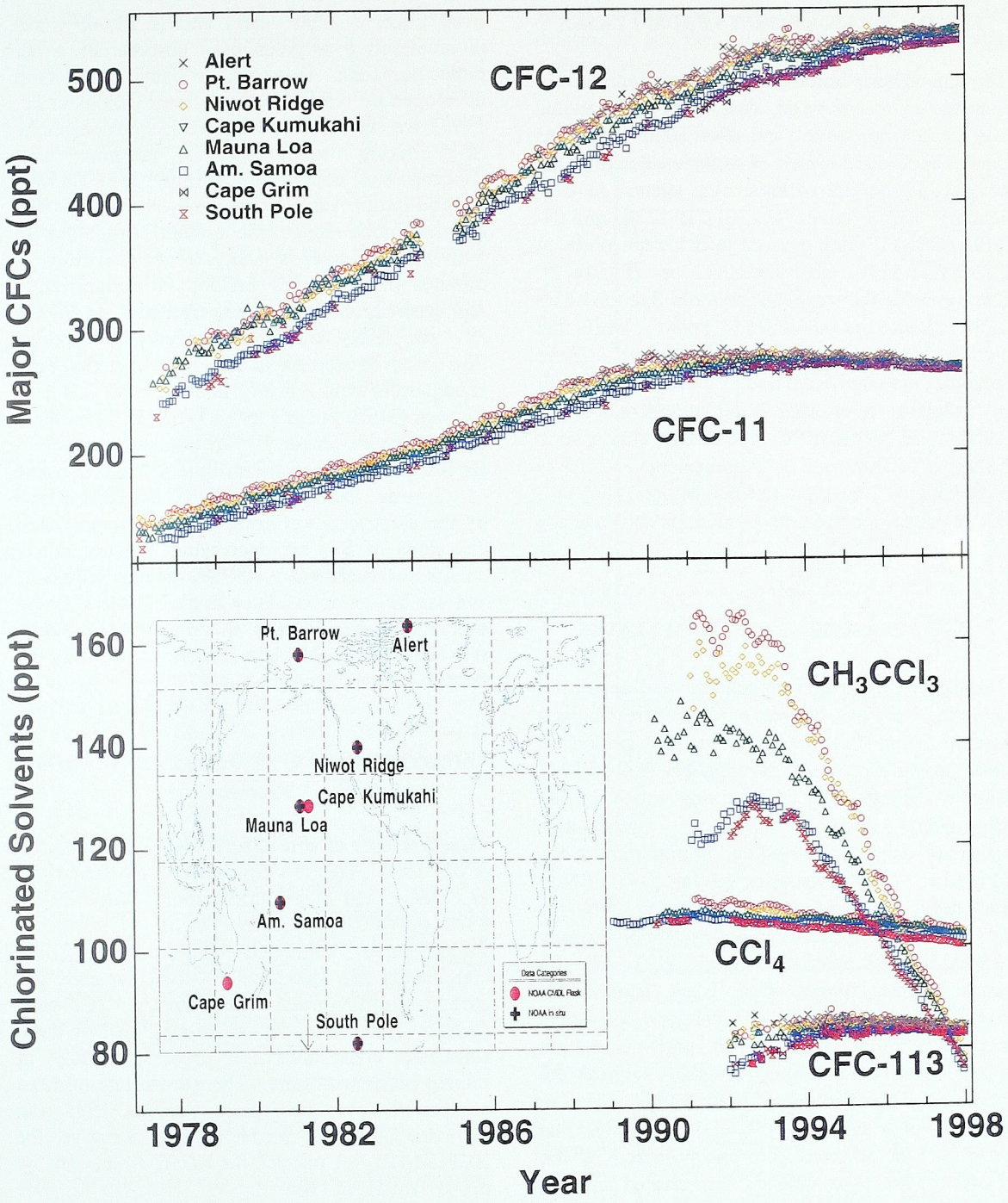

Figure 1. Atmospheric trends of chemicals, chlorofluorocarbons (CFCs) and chlorinated solvents, controlled under the Montreal Protocol to Reduce Substances that Deplete the Ozone Layer. All mixing ratios are reported as parts-per-trillion (ppt) in dry air. *Upper panel:* The mixing ratios from weekly flask pairs that started in 1977 are reported as monthly means for these major CFCs, CFC-11 and CFC-12. *Lower panel:* Atmospheric trends reported as monthly means (ppt) of the chlorinated solvents of methyl chloroform (CH_3CCl_3) and carbon tetrachloride (CCl_4) measured by *in situ* gas chromatography, and flask pair means reported for CFC-113 ($CCl_2F\text{-}CClF_2$) collected from weekly flask pairs measured by gas chromatography and mass spectrometry.

HALON MEASUREMENTS FROM FLASKS

The atmospheric burden of halons has continued to increase in recent years, despite an international ban on their production and sales. Halon emissions persist because of a lack of suitable substitutes for critical uses as fire extinguishing agents. As of 1 January 1997, halons H-1301, H-1211, and H-2402 (CBr_2F_4) were present in the troposphere at 2.3±0.1, 3.5±0.1, and 0.45±0.03 ppt (Figure 2). During 1996, the tropospheric mole fraction of H-1301 increased at 0.044±0.011 ppt yr^{-1}, while that for H-1211 grew at 0.16±0.016 ppt yr^{-1}. These increases are significant and of concern because of the efficiency of bromine in depleting stratospheric ozone and because of the long atmospheric lifetimes of these gases. Atmospheric H-2402 is increasing at 9 ±1 parts-per-quadrillion (ppq) yr^{-1}, but historical data on its production and use are lacking.

N_2O MEASUREMENTS FROM FLASKS

Atmospheric N_2O is a greenhouse and an ozone-depleting trace gas. Nitrous oxide is increasing at a rate of about 0.8 ppt yr^{-1} over the period of observations from 1977 through the end of 1997 (Figure 3). Because CH_4 mixing ratios in the atmosphere are reaching steady-state [*Dlugokencky et al.*, 1998] and is important in the formation of HCl, increasing mixing ratios of N_2O may delay the recovery of the ozone layer by 10-20 years. The US Environment Protection Agency (EPA) believes that atmospheric N_2O will rise more in the future since most automobiles worldwide are equipped with catalytic converters that emit more N_2O (20-50 parts-per-million (ppm)) from the tailpipe than autos without the converters (near 0 ppm). Ironically, it is an example of a technology intended to solve one problem, the problem of urban pollution by the oxides of nitrogen (NOx), but created another problem that adds to global warming and stratospheric ozone depletion.

SF_6 MEASUREMENTS FROM FLASKS

We reported recent trends from baseline stations, tower sites, flask sampling, and oceanic cruises based on an independent calibration scale developed at NOAA/CMDL [*Geller et al.*, 1997]. The significance of this work is that SF_6 is long-lived tracer (~3200 years) and is 22,000 times more effective as greenhouse absorber on a per molecule basis than CO_2. Using a method developed on our airborne platform [Elkins *et al.*, 1996], we can measure very precisely tropospheric SF_6 mixing ratios (<±1%) without pre-concentration of the air sample. We use this method in our Alert N_2O and SF_6 in situ GC. This new technique reduces the amount of time that an individual sample is analyzed to less than 6 minutes (n.b. the new balloon GC, Lightweight Airborne Chromatograph Experiment (LACE), can now sample N_2O and SF_6 once every 70 seconds). The observed increase in atmospheric mixing ratio is consistent with a nearly linear growth of 6.5 % per year (~0.23 ppt yr^{-1} for early 1996). From these data we derive an early 1996 emission rate of 5.9 Gg SF_6 yr^{-1} and an interhemispheric exchange time of 1.3 years. Our results directly contradict claims by the electric power companies that report their emissions of SF_6 are decreasing. Electric power companies represent ~80-90% of the emissions and use SF_6 as an insulator in transformers. Based on our results and others, the US EPA is pressing forward with voluntary reductions for SF_6 by electric power industry.

SUBSTITUTE CFC MEASUREMENTS FROM FLASKS

Measurements of atmospheric HCFC-22 [*Montzka et al.*, 1993], HCFC-141b and -142b [*Montzka et al.*, 1994], and hydrofluorocarbon-134a or HFC-134a (CH_2FCF_3) [*Montzka et al.*, 1996] from flasks have continued (Figure 5). These compounds are measured by two separate gas chromatography-mass spectrometry (GC-MS) systems in our Boulder laboratory. All of these substitute compounds are growing rapidly in mixing ratios with time. The growth rate of these compounds over two years between 1995 and 1996 are 5.0 ppt yr^{-1} for HCFC-22, 1.9 ppt yr^{-1} for HCFC-141b, 1.1 ppt yr^{-1} for HCFC-142b, and 1.4 ppt yr^{-1} for HFC-134a.

TOTAL EQUIVALENT CHLORINE

Montzka et al., [1996] showed that total equivalent chlorine including both organic chlorine and bromine peaked sometime between 1993 and 1994 and continue to decline in 1997 (Figure 6). While HCFC and HFC use has increased, their use has not made up for the rapid decline of CH_3CCl_3. If you add in the increasing levels of bromine and the

fact that bromine is 40-60 times more effective than chlorine in destroying stratospheric ozone, the decline in mixing ratios of CH_3CCl_3, total equivalent chlorine is still decreasing with time. The decrease in measured mixing ratios for total organic chlorine is consistent with estimated emissions by industry. The improvement in the halogen loading of the atmosphere may be somewhat short-lived once most of the CH_3CCl_3 is destroyed (lifetime ~5 yr.) if developing countries produce legally more CFCs and halons and developed countries maintain their huge halon banks. This work is extremely important for scientific modelers by providing new data to calibrate lifetimes and emission histories, and for public policy-makers who are interested in the progress underway with the restrictions on the use and manufacture of the Class I compounds banned by the Montreal Protocol.

In situ N_2O and SF_6 Measurements

A one channel GC, similar to our tower GCs [*Hurst et al.*, 1997] and designed after the Airborne Chromatograph for Atmospheric Trace Species (ACATS-IV) instrument [*Elkins et al.*, 1996] on the NASA ER-2 aircraft, was installed at Alert in late 1995 to measure N_2O and SF_6 once every hour. The purpose of this GC was to quantify the seasonal cycle of N_2O in the Arctic and examine potential sources of N_2O from the former Soviet Union. While this new project has had some start-up problems including gaps of missing data, we plan to fix a number of minor problems and upgrade the software to QNX, an UNIX-like operating system for IBM-type computers. The precision for N_2O is about 0.2-0.3% and will be improved in the future with a new detector and electrometer.

Conclusions

Alert provides us with the most northern data for our global flask network. The challenges of the future for our field will be whether the drop in the equivalent chlorine will continue. The concern is that the large halon bank in developed countries and new production of halons permitted by developing countries will delay the improvement of the ozone layer. If N_2O's growth rate in the near future increases because of automobile emissions and CH_4 reaches steady state, then N_2O also may delay the recovery of the ozone layer. We will be adding more molecules to our list of measured species in the future. We also plan to update the existing in situ GC for better precision and faster data analysis.

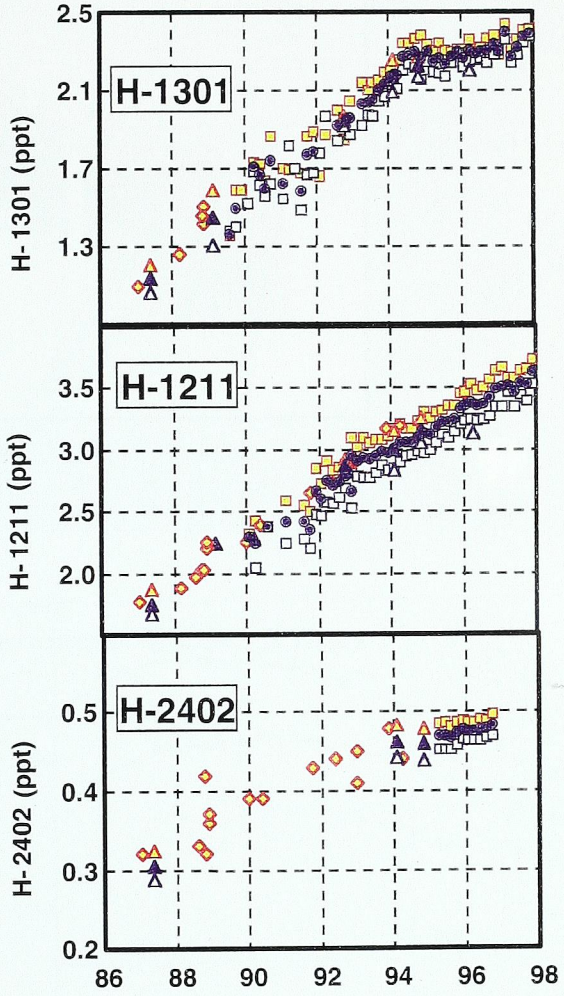

Figure 2. Hemispheric and global bi-monthly averages of tropospheric mole fractions of (a) H-1301, (b) H-1211, and (c) H-2402. Data are taken from the NOAA/CMDL flask network (squares), research cruises (triangles), and cylinders of archived air (diamonds). Northern hemispheric results are shown as shaded symbols, southern hemispheric results as open symbols, and global means as solid symbols. Bimonthly, hemispheric averages are calculated by weighting measurements by the cosine of the sampling latitude within each hemisphere. Global averages are computed as means of the hemispheric averages.

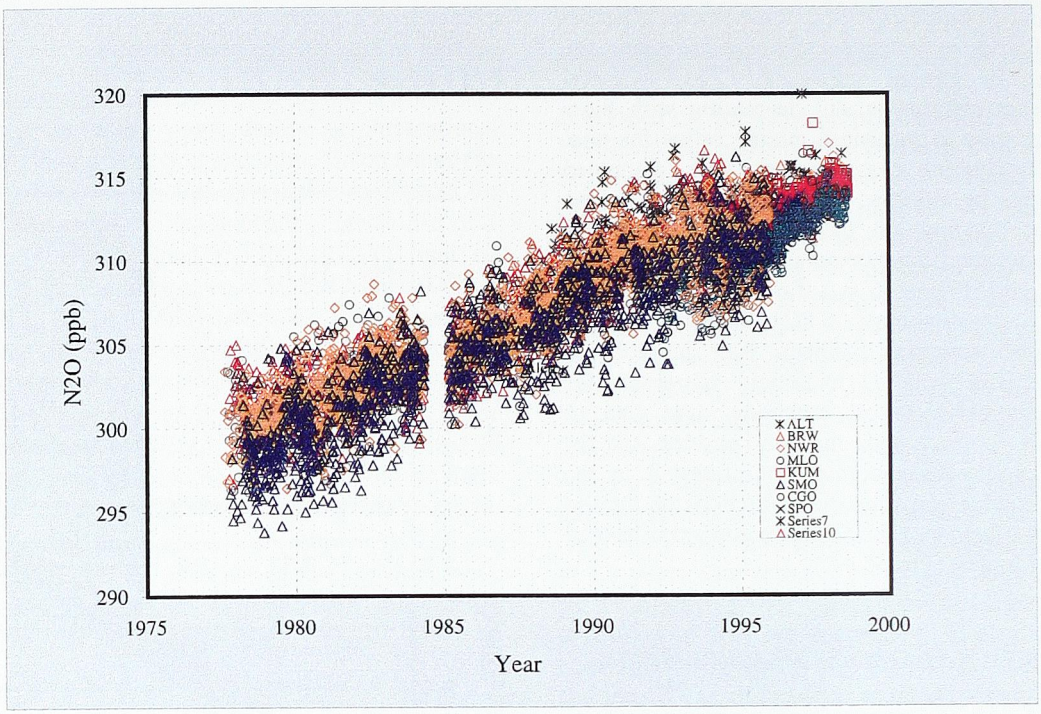

Figure 3. Flask N_2O measurements from the NOAA/CMDL network.

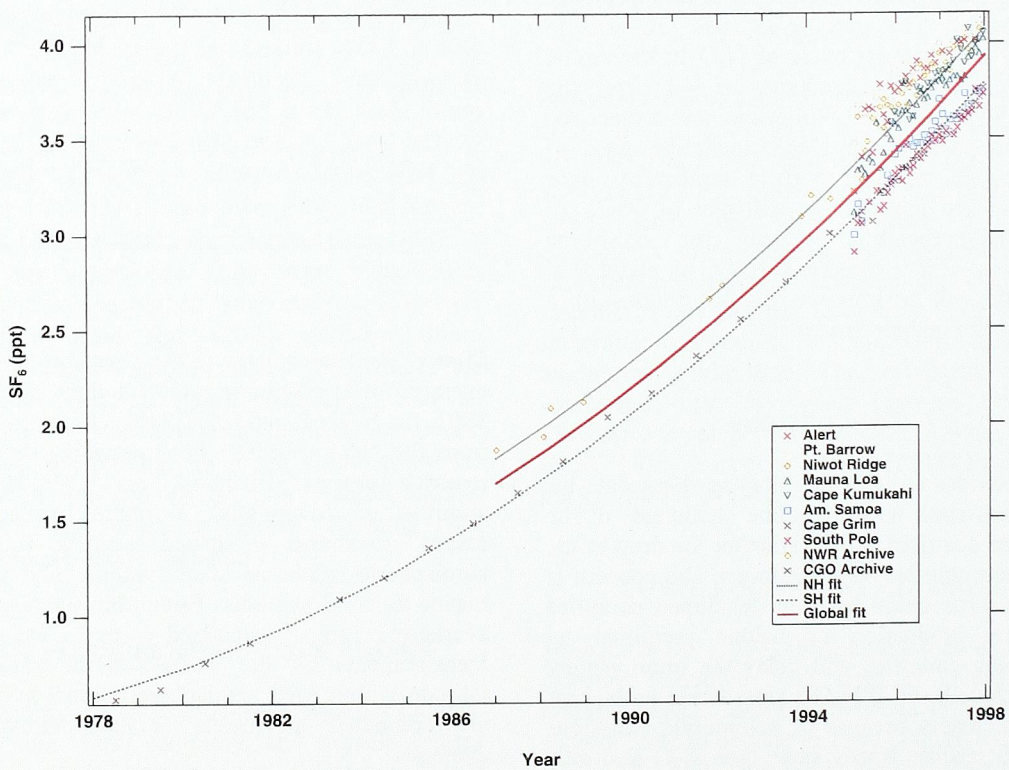

Figure 4. Flask SF_6 measurements from the NOAA/CMDL network.

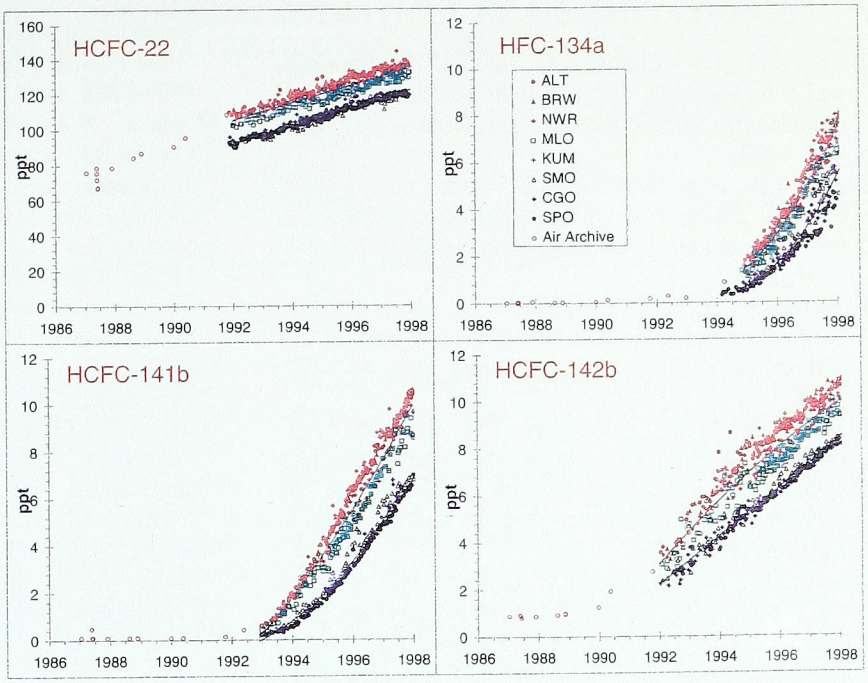

Figure 5. Atmospheric dry mole fractions (ppt) of the most abundant HCFCs and HFC-134a. Each point represents the mean of 2 simultaneously filled flasks from one of eight stations: ALT, filled circle; BRW, filled triangle; NWR, filled diamond; KUM, plusses; MLO, open square; SMO, open triangle; CGO, filled diamond; SPO, filled circle. Also plotted are results from analysis of archived air samples (open circles) filled at NWR and in past cruises from both hemispheres.

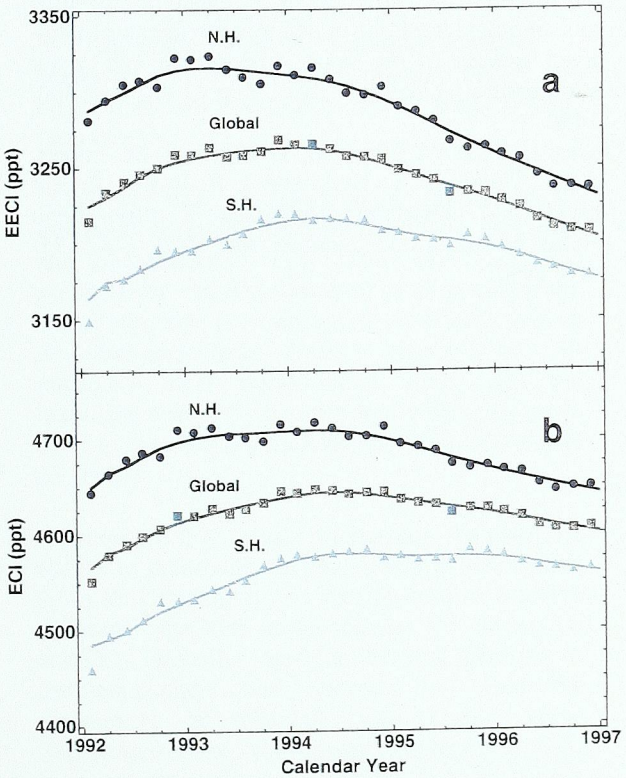

Figure 6. (a) Amount of Cl and Br (as effective equivalent chlorine or EECl) in the troposphere as mean mixing ratios (ppt) of the Northern Hemisphere (circles), global (squares), and Southern Hemisphere (triangles) that are predicted to be released as inorganic halogen in the lower mid-latitude stratosphere at some future time from the halocarbons. (b) Amount of Cl and Br (as equivalent chlorine or ECl) in the troposphere as mean mixing ratios (ppt) of the Northern Hemisphere (circles), global (squares), and Southern Hemisphere (triangles) that are predicted to be released as inorganic halogen in the springtime polar stratospheric vortex at some future time from the halocarbons shown in Figure 5. Curves through data points represent a non-parametric least-squares fit where the fraction of the number of points that will be used to compute each fitted value is 30%. Data represented here are updated for slight calibration changes in CFC-12, CCl_4, and CH_3CCl_3 from *Montzka et al.* [1996].

REFERENCES

Butler, J.H., J.W. Elkins, B.D. Hall, S.O. Cummings, and S.A. Montzka, A decrease in the growth rates of atmospheric halon concentrations, *Nature, 359*, 403-405, 1992.

Butler, J.H., S.A. Montzka, A.D. Clarke, J.M. Lobert, and J.W. Elkins, Growth and distribution of halons in the atmosphere. *J. Geophys. Res., 103*, (D1),1503-1511, 1998.

Dlugokencky, E.J., K.A. Masarie, P.M. Lang, and P.P. Tans, Continuing decline in the growth rate of the atmosphere methane burden, *Nature, 393*, 447-450, 1998.

Elkins, J.W., T.M. Thompson, T.H. Swanson, J.H. Butler, B.D. Hall, S.O. Cummings, D.A. Fisher, and A.G. Raffo, Decrease in the growth rates of atmospheric chlorofluorocarbons 11 and 12, *Nature, 364*, 780-783, 1993.

Elkins, J.W., D.W. Fahey, J.M. Gilligan, G.S. Dutton, T.J. Baring, C.M. Volk, R.E. Dunn, R.C. Myers, S.A. Montzka, P.R. Wamsley, A.H. Hayden, J.H. Butler, T.M. Thompson, T.H. Swanson, E.J. Dlugokencky, P.C. Novelli, D.F.Hurst, J.M. Lobert, S.J. Ciciora, R.J. McLaughlin, T. L. Thompson, R.H. Winkler, P.J. Fraser, L.P. Steele, and M.P. Lucarelli. Airborne gas chromatograph for in situ measurements of long-lived species in the upper troposphere and lower stratosphere. *Geophys. Res. Lett.23(4),* 347-350, 1996.

Geller, L. S., J. W. Elkins, R. C. Myers, J. M. Lobert, A. D. Clarke, D. F. Hurst and J. H. Butler, Recent trends and latitudinal distribution of tropospheric sulfur hexafluoride, *Geophys. Res. Lett., 24, 675-678,* 1997.

Hurst, D.F., P.S. Bakwin, R.C. Myers, and J.W. Elkins, Behavior of trace gas mixing ratios on a very tall tower in North Carolina, *J. Geophys. Res., 102* (D7), 8825-8835, 1997.

Montzka, S.A., R.C. Myers, J.H. Butler, S.C. Cummings, and J.W. Elkins, Global tropospheric distribution and calibration scale of HCFC-22, *Geophys. Res. Lett., 20* (8), 703-706, 1993.

Montzka, S.A., R.C. Myers, J.H. Butler, and J.W. Elkins, Early trends in the global tropospheric abundance of hydrochlorofluorocarbons -141b and 142b, *Geophys. Res. Lett., 21* (23), 2483-2486, 1994.

Montzka, S.A., J.H. Butler, R.C. Myers, T.M. Thompson, T.H. Swanson, A.D. Clarke, L.T. Lock, and J.W. Elkins. A decline in the tropospheric abundance of halogen from halocarbons: Implications for stratospheric ozone depletion. *Science 272*, 1318-1322, 1996.

Montzka, S.A., R.C. Myers, J.H. Butler, and J.W. Elkins. Observations of HFC-134a in the remote troposphere. *Geophys. Res. Lett.23(2),* 169-172, 1996.

Acknowledgements: We would like to acknowledge the assistance of Doug Worthy of Atmospheric Environment Service (AES) for all of his help with our program throughout the years. We also thank the Alert staff for their efforts in collecting our flasks and running our GC. Support for our work has been graciously provided by the AES of Environment Canada. This Alert cooperative project is supported by the Atmospheric Chemistry Project of the NOAA Global and Climate Change Program. Our data are available at our anonymous ftp site, ftp://ftp.cmdl.noaa.gov/noah.

5.5. ATMOSPHERIC OXYGEN CONCENTRATIONS AT ALERT STATION IN RELATION TO THE GLOBAL CARBON CYCLE

Ralph F. Keeling
Elizabeth M. McEvoy
Andrew C. Manning

Scripps Institution of Oceanography, La Jolla, CA 92037

With the development of the interferometric oxygen analyzer [*Keeling*, 1988a, 1988b] in the late 1980's, it became possible to measure atmospheric O_2 concentrations with sufficient precision to detect changes in the background atmosphere. At that time, a flask air-sampling program was initiated under the direction of one of us (R.K.) to sample air globally and document spatial and temporal trends in O_2 concentration. Among the primary goals was to use measurements of atmospheric O_2 in conjunction with measurements of atmospheric CO_2 to better determine the magnitude of ocean and land biotic sinks for CO_2 at the global and hemispheric scales and to improve our understanding of the rates of biological productivity in the oceans [*Keeling and Shertz*, 1992; *Keeling et al.*, 1993, *Bender et al.*, 1996].

Alert station was selected as the first remote baseline site in that program, and a cooperative program was initiated with Atmospheric Environment Service of Environment Canada to collect flask air samples at regular bi-weekly intervals and to ship the samples to the O_2 analysis laboratory (then at the National Center for Atmospheric Research, in Boulder, Colorado but which moved to Scripps in Jan., 1993) for analysis of O_2 and CO_2 concentrations. Air sampling procedures used at Alert and the laboratory analysis procedures for O_2 and CO_2 have been described previously in *Keeling* (1988a) and *Keeling et al.* (1998). The Alert collaborative program has continued up to the present, and the O_2 record from this site is now more than seven years in length. The Alert data, shown in Figure 1, reveal a pronounced seasonal cycle superimposed on an irregular interannual decrease. These features, as well as differences between Alert and other stations, have been discussed in four publications [*Keeling and Shertz*, 1992, *Keeling et al.*, 1996; *Keeling et al.*, 1998; *Stephens et al.*, 1998], as described further below.

As background, the geochemistry of atmospheric O_2 is closely tied to that of CO_2 through chemical reactions that create or destroy organic carbon, such as photosynthesis, respiration, and combustion. Typical O_2:C ratios vary between 1.0 and 1.2 for photosynthesis and respiration of land biota [*Severinghaus*, 1995], ~1.1 to 1.2 for coal combustion, 1.4 to 1.5 for liquid fuels, and 1.9 to 2.0 for natural gas combustion [*Keeling*, 1988b]. If only these processes were operating, atmospheric CO_2 increases would always be coupled with O_2 decreases and vice versa. Complicating this simple coupling are exchanges of O_2 and CO_2 with the oceans. Dissolved O_2 and CO_2 are both influenced by temperature-induced solubility changes in seawater and by marine photosynthesis and respiration, which typically occurs with an O_2:C ratio of ~1.4.

Dissolved CO_2 is additionally influenced by inorganic chemical reactions involving carbonate and bicarbonate ions and involving the precipitation and dissolution of calcium carbonate. These inorganic reactions cause the oceans to have an unusually large storage capacity and an unusually slow equilibration time with the atmosphere for CO_2 as compared with other gases such as O_2 [*Keeling and Shertz*, 1992; *Keeling et al.*, 1993].

Atmospheric O_2 measurements can improve our ability to determine the magnitude of land biotic sinks for CO_2 largely as a consequence of the very different capacities of the oceans for storing O_2 and CO_2. Globally, fossil fuel burning adds CO_2 to the atmosphere and removes O_2 from the atmosphere at relatively well known rates. Superimposed on the global atmospheric CO_2 increase are changes caused by CO_2 exchanges with land biota and the oceans. The oceans take up excess CO_2 largely by inorganic reactions in seawater, which have no influence on O_2. An estimate of the influence of land biota on atmospheric O_2 can thus be derived from the

residual year-to-year change in atmospheric O_2 not accounted for by fossil-fuel combustion. This effectively determines the net land biotic effect on CO_2 because of the close O_2:C coupling in land biotic exchanges, and also determines the net oceanic effect on CO_2 from the residual changes in atmospheric CO_2 content that are not accounted for by fossil-fuel burning or land biota. One complication with this method, however, is the possibility that O_2 may be exchanged with the oceans on interannual time scales by processes unrelated to inorganic reactions, such as changes subsurface O_2 concentrations caused by variations in ocean mixing [*Bender et al.*, 1996; *Keeling et al.*, 1993, 1996]. Interannual air-sea O_2 exchanges must be independently determined in order to use the O_2 budget to provide rigorous estimates of land and ocean carbon fluxes.

Atmospheric O_2 provides a new window for studying marine photosynthesis, respiration, and vertical watermass exchanges largely as a result of the rapid equilibration rate of O_2 between the upper ocean and the atmosphere. The seasonal spring and summer growth of phytoplankton in surface waters produces O_2 which is largely degassed into the overlying air. Comparable amounts of O_2 are removed from the air in the fall and winter when phytoplankton growth rates are slower and when O_2-depleted deeper waters are mixed to the surface. These O_2 exchanges are closely linked to the rates at which organic carbon is produced and exported seasonally from surface waters into the ocean interior. The plankton growth/mixing cycle also produces changes in dissolved CO_2 in the water, but the buffering effect of the inorganic carbon reactions effectively suppresses the air-sea gas exchange of CO_2 on seasonal and shorter time scales [*Keeling and Shertz*, 1992; Keeling et al., 1993].

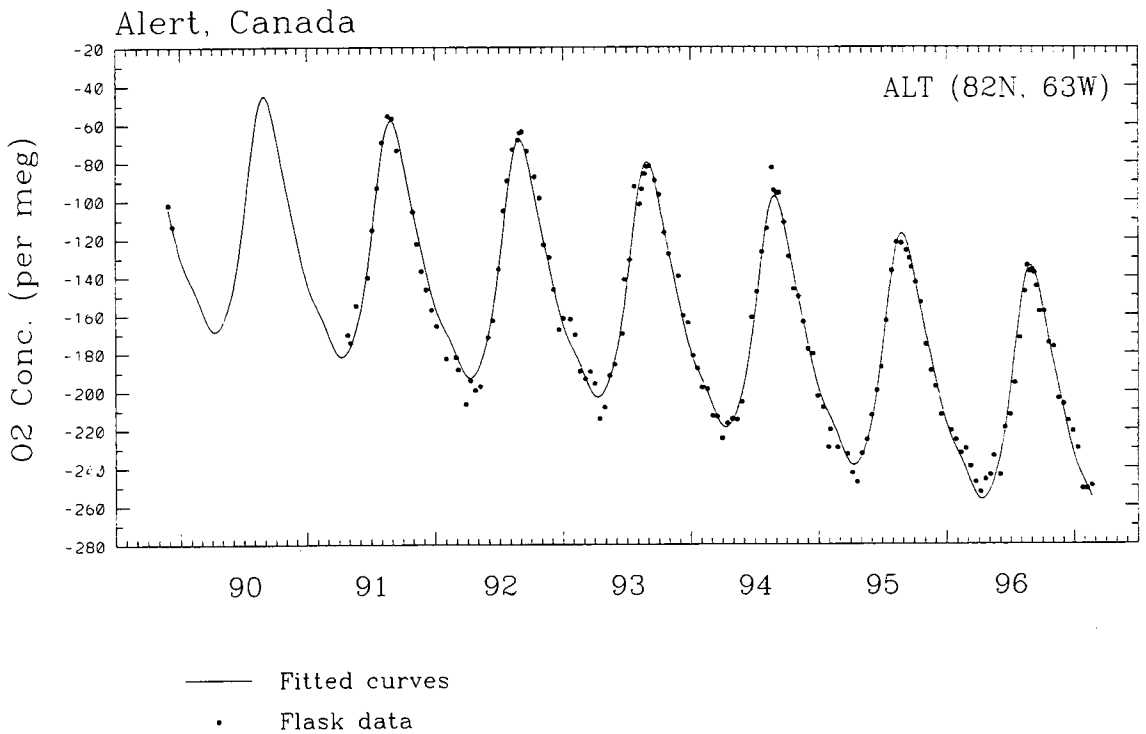

Figure 1. Time series from 1989 to 1997 of atmospheric oxygen concentration measured in flask samples collected at Alert Station. Points are averages of flask replicates collected on a given date. The curve is a least-squares fit consisting of a four-harmonic fit to the seasonal cycle plus a stiff spline fit to the interannual trend. Note that small interannual variations in the shape and amplitude of the seasonal cycle are not captured by the fit. Concentrations are expressed as changes in the O_2/N_2 ratio, such that a change of 1 per meg is defined to equal a change of 10^{-6} in the normalized ratio $(O_2/N_2)_{sample}/(O_2/N_2)_{reference}$ (see also *Keeling et al.*, 1998). In these units, adding 1 mole of O_2 to a mole of dry air would induce a change of +4.8 per meg.

The first full year of the Alert O_2 record was presented in *Keeling and Shertz* [1992], where the data were used along with data from La Jolla, California and Cape Grim, Tasmania, to derive global estimates of the rates of photosynthetic organic carbon production in surface oceans based on the amplitude of the seasonal O_2 cycles. These cycles are caused partly by exchanges with land biota, and partly by O_2 exchanges with the oceans. The land biotic contribution can be estimated from concurrent observations of the seasonal CO_2 cycle, which is predominately caused by land biotic exchanges due to the slow exchange with the oceans, and which therefore can be related to the land biotic component of the O_2 cycle based on the known O_2:C exchange ratio with land biota. At Alert, for example, about half of the O_2 cycle is caused by land biota, and the other half of the cycle is caused by oceanic exchanges. Of this oceanic component, about 15% is caused by thermal degassing and ingassing of O_2 and N_2 due to solubility changes, and the remainder is caused by the oceanic cycle of biological production and vertical mixing. Keeling and Shertz concluded that the non-thermal oceanic component to the cycle required that global organic carbon production (i.e., "new" production) in the oceans must be around 19 Pg C/yr, which was considerably higher than most earlier estimates.

Four years (1991-1994) of the concurrent O_2 and CO_2 records from Alert were presented in *Keeling et al.*, [1996] along with results from La Jolla and Cape Grim. These data were used to estimate global interannual O_2 and CO_2 trends and to resolve gradients in annually averaged O_2 and CO_2 concentrations between the northern and southern hemispheres. The interannual trends showed that, from 1991 through 1994, the oceans and land biota each removed from the air an amount of CO_2 comparable to roughly 30% of fossil-fuel emission. The gradients provided evidence that the land biotic CO_2 uptake was concentrated in the northern middle or high latitudes, as opposed to the tropics. The Alert data was critical for this analysis by defining trends in the northern hemisphere and the differences in average concentration from the Southern Hemisphere.

The interpretation of the combined O_2 and CO_2 gradients was explored in more detail in *Stephens et al.* [1998], where more than six years of Alert data were combined with records from eight additional stations. The emphasis in this study was on the average differences in concentration between stations along a north-south transect and their relation to exchanges of O_2 and CO_2 with the oceans. The O_2 and CO_2 data were combined to derive a novel tracer, "potential oxygen", which is effectively equal to the sum of O_2 and CO_2 and which is in principle is not changed by photosynthesis and respiration of land biota. The observations show a large deficit in potential oxygen in the northern hemisphere relative to the southern hemisphere, with Alert station showing the lowest concentrations globally. The observed north-south gradients in annual-average potential oxygen were compared with model simulations incorporating O_2 and CO_2 fluxes across the air-sea interface derived from three different ocean carbon cycle models and incorporating O_2 and CO_2 fluxes from fossil fuel burning. These fluxes were imposed at the surface of an atmospheric transport model to produce simulated atmospheric concentration fields. A striking result of this study was that the model simulations failed to account for the full magnitude of the northern deficit in potential oxygen. Stephens et al argued that a likely cause for at least part of the discrepancy is difficulties in the ocean models' representation of large-scale water-mass transports, particularly as they relate to meridional heat transports. Evidently all three ocean models tested may share similar deficiencies. The inability of the simulations to account for the low potential oxygen concentrations at Alert, for example, may imply that the ocean models underestimate the transport of heat to high northern latitudes.

Finally, another application for O_2 measurements, involving placing constraints on the kinetics of air-sea gas exchange, was explored in *Keeling et al.*, [1998]. Here, the oceanic components of the seasonal cycles in O_2 were examined at nine stations, including Alert. The observed cycles were compared with model simulations using an atmospheric tracer transport model with seasonal air-sea O_2 fluxes derived from a climatology of O_2 saturation anomalies in the oceans [*Najjar and Keeling*, 1997] and N_2 fluxes computed indirectly from the net air-sea heat flux. Effectively, the only free parameter in the model is the air-sea gas exchange velocity, which relates the saturation anomaly to the air-sea flux. This parameter is tightly constrained by the ocean and atmospheric observations. The results showed that the constraint on large-scale average gas exchange velocity required by the seasonal cycles in O_2 agrees well with the constraints on gas exchange velocity derived some years ago based on mass balance of radiocarbon in the oceans [*Broecker and Peng*, 1974; *Broecker et al.*, 1985, 1986).

Such constraints are important because they suggest the appropriate transfer velocities for computing large-scale air-sea fluxes, such as uptake of anthropogenic CO_2 by the oceans or sources of other trace gases by the oceans.

In summary, the O_2 data from Alert have played an important role in improving our understanding of several aspects of the global carbon cycle, including constraining rates of uptake of CO_2 by land biota and the oceans, and constraining the natural processes affecting carbon cycling in the oceans, including rates of photosynthesis, rates of gas exchange, and rates of watermass exchange. The Alert O_2 record is the longest from a clean baseline site in the northern hemisphere, and the length of this time series makes the record pivotal for documenting long-term trends in O_2 globally. Relative to stations further south, Alert is also a key station for constraining O_2 and CO_2 exchanges throughout the northern high latitudes because of its strategic location for sampling arctic air masses free of local influences.

REFERENCES

Bender, M., J.T. Ellis, P.P. Tans, R.J. Francey and D.Lowe, 1996, Variability in the O_2/N_2 ratio of southern hemisphere air, 1991-1994: Implications for the carbon cycle, *Global Biogeochemical. Cycles,* **10**, 9-21.

Broecker, W.S., T.-H. Peng, 1974, Gas exchange rates between air and sea, *Tellus*, **26**, 21-25.

Broecker, W.S., T.-H. Peng, G. Ostlund and M. Stuiver, The distribution of bomb radiocarbon in the ocean, *J. Geophys. Res.*, **90**, 6953-6970, 1985.

Broecker, W.S., J.R. Ledwell, T. Takahashi, R. Weiss, L. Merlivat, L. Memery, T.-H. Peng, B. Jähne and K.O. Münnich, 1986, Isotopic versus micrometeorological ocean CO_2 fluxes: A serious conflict. *J. Geophys. Res.*, **91**, 10517-10527.

Keeling, R.F., 1988a, Measuring correlations between atmospheric oxygen carbon dioxide mole ractions: a preliminary study in urban air. *Journal of Atmospheric Chemistry*, **7**, 153-176.

Keeling, R.F., 1988b, Development of an interferometric oxygen analyzer for precise measurement of the atmospheric O_2 mole fraction, Ph.D. thesis, 178pp., Harvard University, Cambridge, Mass.

Keeling, R.F. & S.R. Shertz, 1992, Seasonal and interannual variations in atmospheric oxygen and implications for the global carbon cycle. *Nature*, **358**, 723-727.

Keeling, R.F., R.P. Najjar, M.L. Bender, P.P. Tans, 1993, What atmospheric oxygen measurements can tell us about the global carbon cycle. *Global Biogeochemical Cycles,* **7**, 37-67, 1993.

Keeling, R.F., S.C. Piper, M. Heimann, 1996, Global and hemispheric CO_2 sinks deduced from changes in atmospheric O_2 concentration. *Nature* **381**, 218-221.

Keeling, R.F., B.B. Stephens, R.G. Najjar, S.C. Doney, D. Archer, M. Heimann, 1998, Seasonal variations in the atmospheric O_2/N_2 ratio in relation to the kinetics of air-sea gas exchange of O_2, *Global Biogeochemical Cycles*, 12, 141-163.

Najjar, R.G., R.F. Keeling, 1997, Analysis of the mean annual cycle of the dissolved oxygen anomaly in the world ocean. *J. Marine Res.,* **55**, 117-151.

Severinghaus, J.P., 1995, Studies of the terrestrial O_2 and carbon cycles in sand dune gases and in Biosphere 2, Ph.D. thesis, 148 pp., Columbia University, New York.

Stephens, B.B., R. F. Keeling, M. Heimann, K.D. Six, R. Murnane, K. Caldeira, 1998, Testing global ocean carbon cycle models using measurements of atmospheric O_2 and CO_2 concentration, *Global Biogeochemical Cycles*, **12**, 213-230.

Acknowledgements: We thank Neil Trivett of AES for his able and optimistic leadership, and whose vision made the O_2 sampling at Alert possible, and also for the efforts of the many observers who collected samples at Alert over the years. We also thank Steve Shertz, Bill Paplawsky, and Chris Atwood, all of whom played key roles in the O_2 analysis laboratory. The O_2 program has been supported by the U.S. National Science Foundation under grants ATM-8720377, ATM-9309765, and ATM-9612518, and by the U.S. Environmental Protection Agency under IAG DW49935603-01-2.

5.6. CSIRO TRACE GAS MEASUREMENTS FROM CANADIAN SITES

R J Francey[1,2], L P Steele[1,2], R L Langenfelds[1], L N Cooper[1] and C E Allison[1]

[1]CSIRO Division of Atmospheric Research, Aspendale, Victoria 3195, AUSTRALIA
[2]Cooperative Research Centre for Southern, Hemisphere Meteorology, Monash University, Clayton, Vic 3168

N.B.A. Trivett and V. Hudec
RAGS Research Section, Canadian Baseline Program, Atmospheric Environment Service, 4905 Dufferin St, Downsview, Ontario, CANADA M3H5T4

INTRODUCTION

The collaboration between CSIRO and AES to measure atmospheric trace gases from Canadian baseline sampling sites commenced in 1990, with the initial emphasis placed on $\delta^{13}C$ of CO_2. The early methodology and results from 1990 and into 1991 are described by *Francey et al.* [1997].

A prime application of the measurements is in inversion studies aimed at locating and quantifying global surface sources and sinks of a trace gas. Inversion studies have evolved from earlier "forward" modelling in which atmospheric transport representations were applied to prescribed sources (strength and distribution) of CO_2 and CO_2 isotopes for comparison with observations (e.g., *Pearman and Hyson*, 1986). Typically, the inversion process involves a deconvolution of measurements of the spatial differences in the species, specified distributions of sources (e.g. fossil fuel releases, oceans and terrestrial biomass distributions) plus a 2- or 3-dimensional representation of atmospheric transport (e.g., *Tans et al.*, 1989; *Enting and Mansbridge*, 1989; *Heimann and Keeling*, 1989; *Ciais et al.*, 1995a,b; *Enting et al.*, 1995) to determine source strengths. Recently, *Rayner et al.* [1998] have developed a method for a time-dependent 3-dimensional inversion providing information on regional inter-annual variability in carbon fluxes, and highlighting the need for coherent globally distributed data sets. In the inversion process, precision of the measurements becomes a critical limiting factor. Generally, data from different trace gas measuring networks have not been merged for inversion studies. The failure to merge the data reflects analytical uncertainties in the inter-calibration between measurement laboratories. The calibration problems are highlighted in the case of $\delta^{13}C$ of CO_2, by two recent conflicting papers (*Keeling et al.*, 1995 and *Francey et al.*, 1995) on interannual variability of the global carbon budget.

Thus a key motivation for the AES-CSIRO collaboration was to establish a very high latitude northern site for the CSIRO global sampling network at Alert, (ALC, 82.450°N, 62.517°W) completing a pole-to-pole network of sites, with the CSIRO network being unusually well-represented in the Southern Hemisphere. Note that in this paper 3-letter site abbreviations for CSIRO sites are in capital letters, with the last letter indicating the country of collection). An implicit assumption at the time of establishing the network was that marine boundary layer measurements at each site represented a zonal average in that latitude band. A secondary objective focussed on excluding the possibility of "anomalously fractionated" isotopic influences arising from the tundra regions, by including sampling at the continental site, Fraserdale (FRC: 49.900°N, 81.600°W).

In this report, we describe the changes in methodology and sampling strategy for the CSIRO-AES collaboration which have occurred since 1991. Data for the range of trace gases now routinely measured at CSIRO are presented graphically, along with instructions for electronic access to the data. Exploratory analyses of some of the data are briefly presented so that their biogeochemical significance can be gauged. Finally, in light of the evolution of the scientific requirements, and the measurements so far obtained from the collaboration, the rationale for continuing the collaboration is assessed.

METHODS AND STRATEGY CHANGES

Since the last report, the CSIRO GASLAB (Global Atmospheric Sampling Laboratory) has reached full operational status. All flasks collected routinely from the global network of sampling sites (currently 11 sites, plus regular aircraft profiling above Cape Grim, Tasmania and ship cruises between Tasmania and Antarctica) are routinely analysed for CO_2, CO_2 stable isotopes, CH_4, CO, H_2 and N_2O. Full details are given by *Francey et al.* [1996].

Measurements are established relative to standards which are high pressure cylinders of dry natural air, or gravimetrically prepared mixtures, spanning a full range of anticipated atmospheric values for trace gas mixing ratios. For all species except H_2, accurate mixing ratios have been initially determined by NOAA (National Oceanic and Atmosphere Administration, USA)/CMDL (Climate Monitoring and Diagnostics Laboratory), and confirmed at regular (typically 2-year) intervals. Despite excellent reproducibility and precise agreement in the high pressure cylinder intercomparisons, significant differences have been detected between flasks collected at overlapping sites. This has led to the development of a multi-species "operational intercalibration" between CSIRO and the NOAA program in which both laboratories have routinely analysed, since 1991, air from the same flasks collected at Cape Grim (*Francey et al.*, 1994; *Steele et al.*, 1996; *Masarie et al.*, 1997 and in preparation). A key element in the comparison is automated, routine reporting of laboratory differences on a monthly basis. The operational intercalibration significantly improves the prospect for merging data sets for inversion studies and has been used for such (*Ciais et al.*, 1995a, 1995b). Difficulties remain when the cause for a discovered discrepancy remains obscure, and protocols for dealing with network data when this occurs are still under development. Analyses by the AES of flasks filled at Cape Grim and analysed in GASLAB has recently commenced for carbon isotopes (A. Norman, Environment Canada, private communication).

In mid-1993, collaborative AES-CSIRO sampling was discontinued at the continental tundra site of Fraserdale, reflecting an absence of evidence for any unusual isotopic labelling of CO_2 (including and particularly during the periods of tundra refreeze and thaw involving enhanced release of stored trace gases from fresh water areas). Instead, sampling was transferred to the AES marine boundary layer site at Estevan Point (EPC: 49.383°N, 126.533°W). Around the same time, CSIRO sampling was commenced in the Shetland Islands in collaboration with the UK TIGER (Terrestrial Initiative in Global Environmental Research) program (SIS: 60.170°N, 1.170°W, Francey et al., 1998) and was discontinued at the NOAA site of Barrow, Alaska (BWU: 71.323°N, 156.609°W). Barrow sampling was discontinued because, compared to Alert, measurements generally exhibited larger scatter but very similar seasonal variation and mean level; thus zonal differences between the sites were not well-defined by the sampling. Instead focus was switched to address the emerging realisation of the inadequacy of the "zonally-representative" assumption. The modified sampling strategy was an attempt to verify and quantify Pacific-Atlantic differences in CO_2 and to explore possible differences in the CO_2 isotopes.

DATA

Figure 1 shows data for CO_2, CH_4, CO, N_2O, H_2 and $\delta^{13}C$, $\delta^{18}O$ of CO_2 measured at Alert, Fraserdale and Estevan Point. The trace-gas results are superposed on a curve for Alert only, obtained using a fitting procedure described by *Thoning et al.* [1989], see also http://www.cmdl.noaa.gov. The curve fit incorporates harmonic and quadratic functions, and 80-day smoothing is applied to the residuals. A 3-sigma filter is iteratively applied in the smoothing process to obtain a best-fit curve, excluding statistical outliers.

These data are scheduled to be available by the second half of 1998 in digital form via anonymous ftp to:

> ftp.atmos.dar.csiro.au; login: *anonymous*;
> password: *your e-mail address*;
> cdGASLAB/*species*.

SPATIAL VARIATION IN CO_2

A preliminary examination of the spatial variations in the data illustrates the potential impact of the measurements in the context of large-scale inversion modelling, and in a way in which the precision requirements and statistical uncertainties can be assessed visually. To facilitate a comparison of CO_2 between the high latitude

northern sites, for each site we subtract a curve representing the mean zonal behaviour of CO_2 at a latitude of 60°N, constructed from only those NOAA sites representing the marine boundary layer [*Masarie and Tans*, 1995].

The difference plots for the collaborative sites of Estevan Point and Alert, compared to the 60°N marine boundary layer (MBL) are shown in Figure 2 (note that the large CO_2 variability from the continental Fraserdale site make it unsuitable for this type of detailed comparison). Also shown are the CSIRO data for Shetland Islands. Much of the variability in this presentation is likely to arise from differences in the wave form and phasing of the seasonal cycle in CO_2 with latitude, particularly at high latitudes where the CO_2 exchange with terrestrial biota is limited by temperature to a small part of the year. This is under further investigation. Here we are most interested in mean levels. The mean CO_2 at Shetlands Is. at 60°N (westerly winds only), is generally below the values for Alert 82.45°N and Estevan Pt., at 49.38°N, by an average of around 1 ppm.

To further explore the nature of the large-scale spatial variation, similar differences from the 60°N MBL curve have been determined from NOAA sampling sites nearby to Estevan Pt. and Shetland Is. (Note that NOAA 3-letter site codes are distinguished from CSIRO site codes by small letters). In the Pacific region we use NOAA data from Shemya Is., Alaska (shm: 52.71°N, 174.1°E), Cold Bay, Alaska (cba: 55.20°N, 174.1E), Barrow, Alaska (brw: 71.32°N, 156.60°W), and Mould Bay, N.W.T. (mbc: 76.25°N, 119.35°W). In the Atlantic region we use NOAA data from Station M (stm: 66.000°N, 2.000°E), Iceland (ice: 63.250°N, 20.150°W) and Mace Head, Ireland (mht: 53.333°N, 9.900°W). Two year average deviations from the 60°N MBL curve are plotted in Figure 3. (Note, depending on data availability, the two years span 1993.0 to 1995.0, or 1993.5 to 1995.5; where data are available for both periods, no significant difference is obtained). For convenience, Alert is plotted as a "Pacific" station for NOAA data (alt), and as an "Atlantic" station for CSIRO data (ALC). Note also, that an operational intercalibration difference of 0.40±0.21 ppm (CSIRO minus NOAA) has been applied to the CSIRO data to obtain compatibility with the NOAA data, including the 60°N MBL curve. (While most of this difference has a well-understood explanation, corrections had not been applied to either of the data sets used in this analysis). The most striking feature in Figure 3 is the large zonal gradient of order 1 ppm evident at 50-60°N, between the Pacific (EPC, shm, cba) and Atlantic marine boundary layer, possibly associated with enhanced oceanic uptake near the region of North Atlantic deep water formation (Keeling et al., 1989).

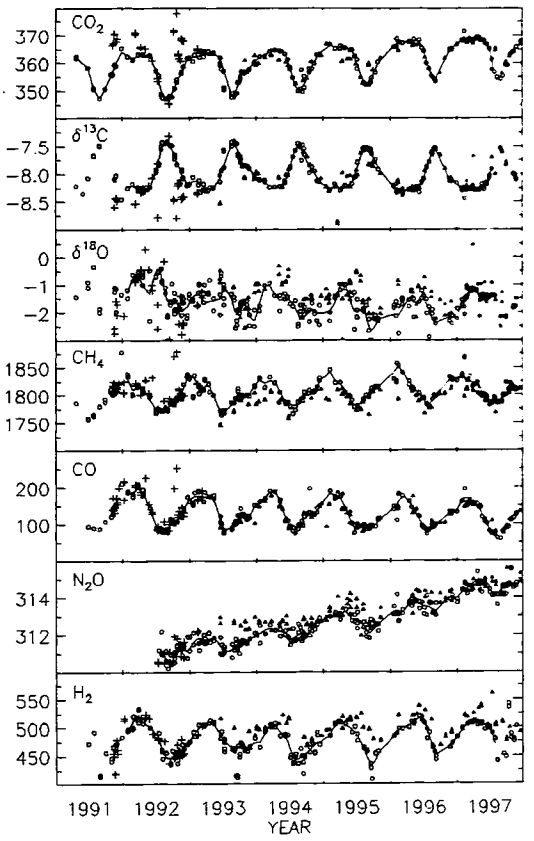

Figure 1. Measurements of CO_2 (ppm), $\delta^{13}C$ (‰), $\delta^{18}O$ (‰), CH_4 (ppb), CO (ppb), N_2O (ppb) and H_2 (ppb), from the AES-CSIRO flask program for Fraserdale (+), Alert (o) and Estevan Point (▲). A curve fit through the Alert data involves iterative fitting of a harmonic and quadratic function, with a 3 sigma rejection of outliers (*Thoning et al.*, 1989).

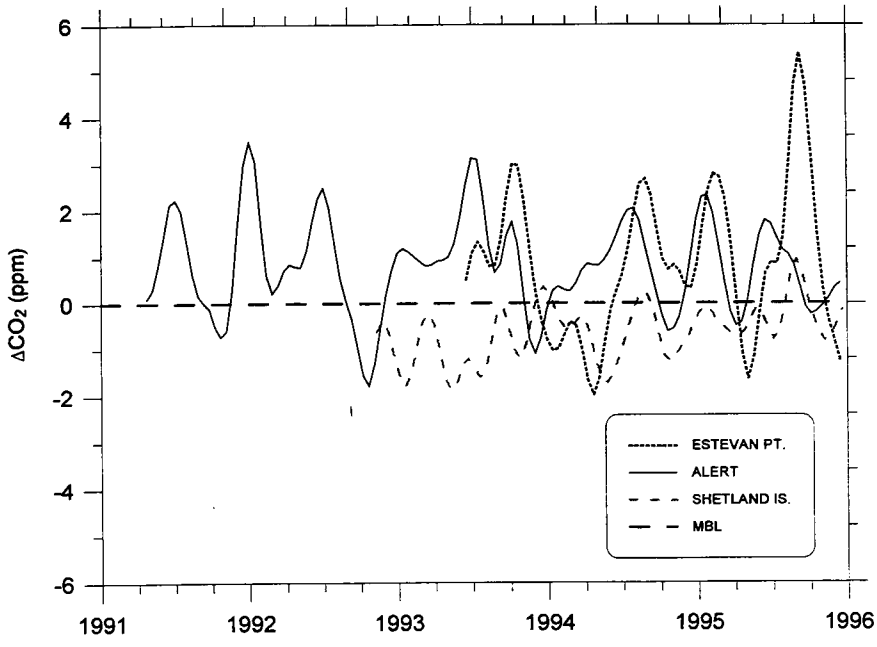

Figure 2. CO_2 differences from the 60°N marine boundary layer mean curve of *Masarie and Tans* [1995] for function fits to the measurements at Alert, Estevan Point and the Shetland Islands.

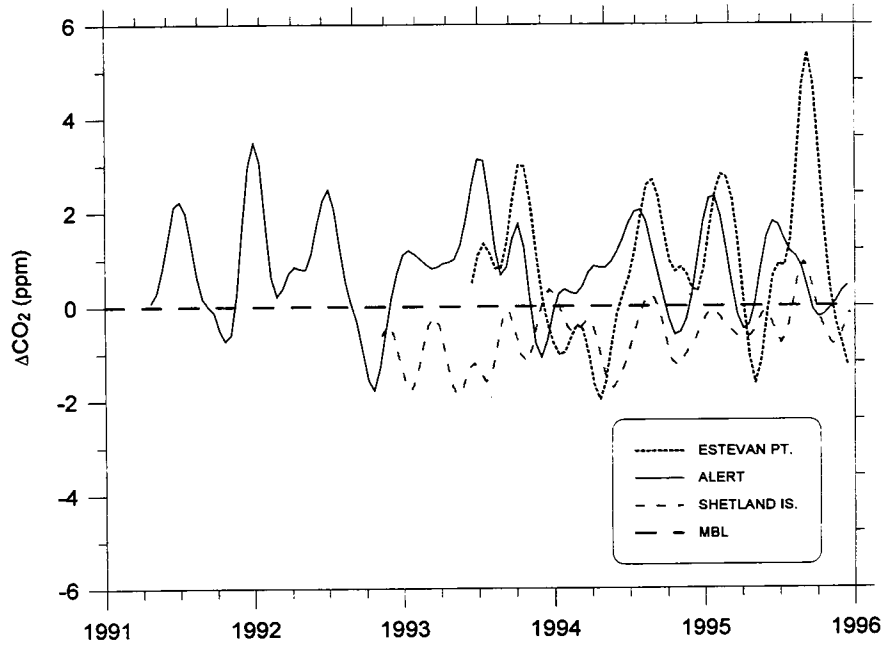

Figure 3. Two-year average CO_2 differences from the 60°N marine boundary layer mean curve for CSIRO (capital letters) and NOAA (small letters) sites at mid-to-high northern latitudes. Stations are separated into Pacific and Atlantic groupings.

For each site, $\delta^{13}C$ measurements are regressed against the inverse of CO_2 concentration for each available set of flask data (typically 2-4 years). The intercept of the regression line with the $\delta^{13}C$ axis, has been used historically to identify an isotopic signature of source CO_2 which is mixed with ambient CO_2 [*Keeling*, 1961]. Values of the intercept are plotted against latitude for CSIRO sites in Figure 4. Because of the short time-span involved, the data here predominantly reflect the isotopic signature of the large seasonal variation observed at each site. Also included are data from the University of Colorado [*Trolier et al.*, 1996] measured on the NOAA/CMDL flasks from Mace Head. The Mace Head and Shetland Is. data are adapted from *Francey et al.*, 1998. It is clear from this plot that there are additional influences on the $\delta^{13}C$ data, with Shetland (West) showing the largest CO_2 depletion compared to EPC and ALC, but with an isotopic signature not significantly different from EPC or ALC. However, significantly depleted carbon isotope ratio is indicated for Mace Head (with some caution required in introducing selected isotopic measurements from a different laboratory). As pointed out by *Francey et al.* [1998] the mht isotopic signature is similar to that measured by CSIRO from the Shetland East (winds directly from Europe, with enhanced terrestrial and fossil CO_2), shown in Figure 4. The reason for the less-depleted isotopic values at EPC, ALC and SIS is thought to lie in the generally long ocean fetches, permitting greater isotopic equilibration of any terrestrial isotopic signals with the large oceanic CO_2 reservoir.

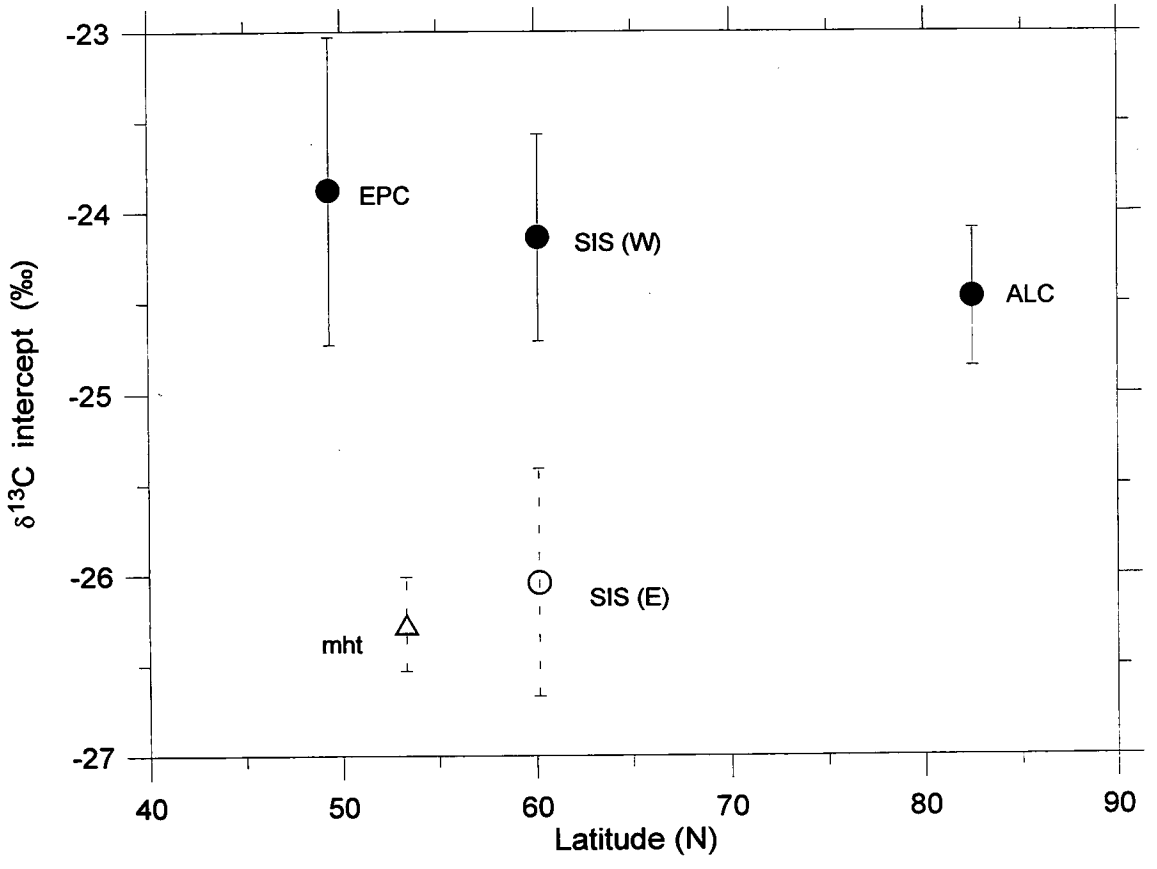

Figure 4. $\delta^{13}C$ intercepts (obtained from linear regressions of $\delta^{13}C$ versus inverse CO_2 mixing ratio) for CSIRO sites, plus the NOAA Mace Head site (mht) at mid-to-high northern latitudes. The Shetland (SIS) data are shown for both Westerly (long oceanic fetches) and Easterly (European fetches).

The preliminary scrutiny of data of the sort illustrated here for CO_2, is an important step in the process of inverting global data to determine and understand surface exchanges. For the experimentalist, it provides a valuable perspective on the role that an individual site plays in the process and, in concert with model inversion output, on the precision requirements to identify fluxes of a specified magnitude. For the modeller, it can often provide insight into the sensitivity of inversions to individual stations and to network inter-calibration factors, and provide guidance in designing an optimum global observing network.

FUTURE PLANS

A shadow over every program involved in global monitoring of atmospheric trace gas composition with current techniques is the escalating cost of operation of a sampling network. This is offset to some degree by major improvements underway in the automation of laboratory analyses. A more fundamental problem is that the spatial resolution and representation of sampling networks (both on the earth's surface and vertically) is insufficient to advance the inversion technique to a level where, for example, national emissions might be quantified and monitored with precision sufficient for guidance in global regulation activities. Yet, the high-precision aspects of flask sampling (for multi-species), compared to emerging remote sensing techniques for example, are likely to retain flask sampling as a leading relevant technology for many years to come.

Our focus on the ability to merge data with the most comprehensive NOAA/CMDL network via the operational intercalibration is one response to such problems. Many systematic errors have been revealed and corrected (in both laboratories) by such intimate comparisons, however there are still unresolved problems for some species (e.g. H_2, CO and $\delta^{13}CO_2$), which urge caution for all species, in claiming that success has been achieved in merging data. When merging is routinely possible, it would make sense for a network like CSIRO to focus most resources on the Australasian/Antarctic regions; and for Canada and USA, for example, to implement a similar arrangements in the North America/Arctic region. However, until this happens, there is an argument to retain essential elements of the individual smaller networks. Thus, in general terms we see considerable value in maintaining sampling at Alert and Estevan point via the existing collaboration for several years. However, we can anticipate a substantially rationalised global network in the future. If Canadian programs in this network carry a major responsibility for comprehensive and precise trace gas monitoring in its region, close "operational" intercomparisons between the Australian and Canadian programs would certainly contribute to a valuable long-term, precise, multi-species time-series for the region.

REFERENCES

Ciais, P., P. Tans, J.W. White, R. Francey, M. Trolier, J. Berry, D. Randall, P. Sellers, J. Collatz and D. Schimel. The global carbon budget inferred from a new worldwide data set of $\delta^{13}C$ measurements in atmospheric CO_2. *J. Geophys. Res.*, 100 D3, 5051-5070. 1995a.

Ciais, P., P.P. Tans, M. Trolier, J.W.C. White and R.J. Francey. A large northern hemisphere terrestrial CO_2 sink indicated by $^{13}C/^{12}C$ of atmospheric CO_2. *Science*, 269 (5227), 1098-1102, 1995b.

Enting, I.G. and J.V. Mansbridge. Seasonal sources and sinks of atmospheric CO_2 :I. Direct inversion of filtered data. *Tellus*, 41B, 111-126, 1989.

Enting, I.G., C.M. Trudinger and R.J. Francey. A synthesis inversion of the concentration and $\delta^{13}C$ of atmospheric CO_2. *Tellus*, 47B, 35-52, 1995.

Francey, R.J., C.E. Allison, L.P. Steele, R.L. Langenfelds, E.D. Welch, J.D. White, M. Trolier, P.P. Tans and K.A. Masarie. Intercomparison of stable isotope measurements of CO_2, in *Climate Monitoring and Diagnostics Laboratory CMDL No.22 Summary Report 1993*, eds. Peterson, J.T. and Rosson, R.M., pp. 106-110, US Department of Commerce, NOAA, Boulder Co., 1994.

Francey, R.J., P.P. Tans, C.E. Allison, I.G. Enting, J.W.C. White and M. Trolier, Changes in the oceanic and terrestrial carbon uptake since 1982. *Nature*, 373(6512), 326-330, 1995.

Francey, R.J., L.P. Steele, R.L. Langenfelds, M.P. Lucarelli, C.E. Allison, D.J. Beardsmore, S.A. Coram, N. Derek, F. de Silva, D.M. Etheridge, P.J. Fraser, R.J. Henry, B. Turner and E.D. Welch, Global Atmospheric Sampling Laboratory (GASLAB): supporting and extending the Cape Grim trace gas programs, in *Baseline Atmospheric Program*

(Australia) 1993, eds. R.J.Francey, A.L.Dick and N.Derek, pp. 8-29, Bureau of Meteorology and CSIRO Division of Atmospheric Research, Melbourne, 1996.

Francey, R.J., C.E. Allison, E.D. Welch, N.B.A. Trivett and V.C. Hudec. Seasonality in $\delta^{13}C$ of CO_2 at mid-to-high northern latitudes, *Canadian Baseline Program Annual Report 1992*, Environment Canada, Toronto, pp. A48-A52, 1997.

Francey, R.J., L.P. Steele, R.L. Langenfelds, C.E. Allison, L.N. Cooper, B.L. Dunse, B.G. Bell, T.D. Murray, H.S.Tait, L. Thompson and K.A. Masarie. Atmospheric carbon dioxide and its stable isotope ratios, methane, carbon monoxide, nitrous oxide and hydrogen from Shetland, *Atmospheric Environment* (1998, in press).

Heimann, M. and C.D. Keeling. A three-dimensional model of atmospheric CO_2 transport based on observed winds: 2. Model description and simulated tracer experiments. *Geophysical Monograph 55, Aspects of Climate Variability in the Pacific and the Western Americas* (Ed. David H. Peterson) American Geophysical Union, pp. 237-275, 1989.

Keeling, C.D. The concentration and isotopic abundance of carbon dioxide in rural and marine air. *Geochim. et Cosmochim. Acta*, 24, 277-298, 1961.

Keeling, C.D., S.C. Piper, and M. Heimann. A three-dimensional model of atmospheric CO_2 transport based on observed winds: 4. Mean annual gradients and interannual variations. *Geophysical Monograph 55, Aspects of Climate Variability in the Pacific and the Western Americas* (Ed. David H. Peterson) American Geophysical Union, pp 305-363, 1989.

Keeling, C.D., T.P. Whorf, M. Wahlen and J. van der Plicht, Interannual extremes in the rate of rise of atmospheric carbon dioxide since 1980. *Nature*, 375, 666-670, 1995.

Masarie K.A. and P.P. Tans. Extension and integration of atmospheric carbon dioxide data into a globally consistent measurement record. *J. Geophys. Res.* 100, 11,593-11,610, 1995.

Masarie, K.A., P.P. Tans, L.P. Steele, R.J. Francey, R.L. Langenfelds, T.J. Conway, E.J. Dlugokencky, P.C. Novelli, M. Trolier, and J.W.C. White. An ongoing flask inter-comparison between CMDL and CSIRO: a new level of cooperation and improvement of quality control. In: *Fifth International Carbon Dioxide Conference: extended abstracts, 1997: [Australia]*. Cairns, Qld.: Fifth International Carbon Dioxide Conference Committee. p. 18 (AB0069), 1997.

Pearman, G.I. and P. Hyson. Global transport and inter-reservoir exchange of carbon dioxide with particular reference to stable carbon isotopic distributions. *J. Atmos. Chem.*, 4, 81-124, 1986.

Rayner, P.J., I.G. Enting, R.J. Francey and R.L. Langenfelds, Reconstructing the recent carbon cycle from trace gas observations. *Tellus* (submitted).

Steele, L.P., R.J. Francey, R.L. Langenfelds, C.E. Allison, M.P. Lucarelli, P.P. Tans, E.J. Dlugokencky, T.J. Conway, P.C. Novelli, K.A. Masarie, J.W.C. White and M. Trolier. An operational intercalibration experiment between CMDL and CSIRO to measure several atmospheric trace species. In: *Climate Monitoring and Diagnostics Laboratory no.23 summary report 1994-95*. D.J. Hofmann, J.T. Peterson, and R.M. Rosson (editors). Boulder, Colo.: Environmental Research Laboratories. pp. 148-149, 1996.

Tans, P.P., T.J. Conway and T. Nakazawa. Latitudinal distribution of the sources and sinks of atmospheric carbon dioxide derived from surface observations and an atmospheric transport model. *J. Geophys. Res.*, 94D, 5151-5172, 1989.

Thoning K.W., P.P. Tans and W.D. Komhyr. Atmospheric carbon dioxide at Mauna Loa Observatory, 2, Analysis of NOAA/GMCC data, 1974-1985. *J. Geophys. Res.*, 94, 8549-8565, 1989.

Acknowledgements: The supply of flasks, sampling site collection and logistic management by staff of the Atmospheric Environment Service makes this program possible.

5.7. VERTICAL DISTRIBUTIONS OF CO_2 AND CH_4 AT ALERT

Stefan Grosch

INTRODUCTION

Besides the ground based monitoring of CO_2 and CH_4, measurements aboard an aircraft can provide some additional and useful information on the abundance and the characteristic behaviour of these gases in the atmosphere.

One basic prerequisite for every baseline station (like Alert) must be its representative character for a large area. Data derived from aircraft experiments can be used to check this representative quality of the routine ground based measurements. Furthermore vertical profiles of gases and aerosols are an excellent tool to examine the occurrence and the intensity of episodes of arctic haze in detail (e.g., *Herbert et al.*, 1987; *Khalil and Rasmussen*, 1984).

The main aim of the experiment as described below was to build and to test a prototype flask sampling system to be used on an aircraft.

EXPERIMENTAL

Sixteen flask samples were collected during one flight of a Twin Otter on April 14, 1991. Samples were collected during two descents, one over Alert between the camp and the Alert GAW Observatory and one over the open ice field, approximately 6-8 km NNW of the first sampling location. Sampling took place in well-defined heights between 3000 m a.s.l. and close to the ground (<50 m a.s.l.). The samples were collected in evacuated (~10^{-4} hPa) 1 L (one stopcock) cylindrical glass flasks (i.e., the same type of flasks that are used in the Canadian Baseline Program). The sampling line consisted of a stainless steel line as intake nozzle followed by a Teflon®-coated flexible aluminum line. The intake nozzle extended about 0.40 m through a window in the cockpit of the aircraft and therefore forward of the engine exhaust. The line and the intake of the flask were purged sufficiently before each sample collection. The pump in use was a powerful GAST diaphragm pump providing a constant flow rate between 28-29 $L \cdot min^{-1}$ up to the maximum sampling height of 3000 m a.s.l.. The flasks were filled to ~17 psi controlled by a pressure relief valve. The filling procedure took about 10-15 sec.. The sampling heights were based on the pressure starting at 700 hPa (3010 metres a.s.l. standard atmosphere) and increasing stepwise by 50 hPa. The last sample of each descent was taken as close as possible to the ground. (<50 m a.s.l.).

The air samples were analyzed for CO_2 by NDIR analysis and for CH_4 by GC analysis within a time period of four weeks after sampling. Analytical details are described within this report elsewhere (refer to: Ernst, Hudec, Trivett, Worthy) and need not to be repeated.

RESULTS AND DISCUSSION

The CO_2 and CH_4 concentrations measured in the flask air samples are plotted versus altitude and pressure respectively (Figures 1 and 2). The results obtained from the first descent over Alert (Figure 1) show a similar behaviour for both gases. Generally the concentration is slightly decreasing with height. In the second but highest sampling level there is a distinct maximum. The profiles derived from the second descent (i.e., over the ocean) (Figure 2) show the same maximum in ~2500 metres a.s.l. for CO_2 but not for CH_4. An increase in concentration within the first 100 m to the ground is obvious over the ocean and also slightly indicated over Alert (Figure 1).

The CO_2 concentration ranged from 361.36 ppm to 361.73 ppm over Alert and 361.51 ppm to 361.73 ppm over the ocean. For CH_4, the concentration ranged between 1.821 and 1.834 ppm over Alert and 1.827 to 1.837 ppm over the ocean.

Additional information on the vertical structure of the atmosphere was available from the routine airsonde measurements provided by the Alert weather station. The airsonde was started at the same time the air samples were collected (around 19:00 p.m. local time). In Figure 3, both CO_2 profiles are plotted along with the vertical temperature profile. The temperature profile shows a distinct and typical inversion layer with increasing temperatures between about 700 and 1300 m a.s.l. A second very shallow inversion was apparent close to the ground (~70-110 m). First of

all this figure shows the comparability of the two CO_2 profiles to be excellent. The CO_2 maximum in 2500 m altitude is not however, correlated with the actual height of the inversion layer. Also the CH_4 concentration is not increasing within this layer of restricted vertical transport (Fig. 4).

Because of the preliminary character of this experiment no additional physical or chemical parameters of the atmosphere were measured. Therefore the interpretation of the profiles presented here must be very limited and cannot be proceeded in detail. It is possible but however speculative that the marked increase in concentration between 2000 and 3000 m a.s.l. was caused by a haze layer in this altitude.

The concentration variation for CO_2 and CH_4 along the vertical profiles however is considered to be rather small. It shows that the atmospheric boundary layer of the high arctic region generally is already well mixed at this time of the year. The results of this flight can be taken as an additional proof that CO_2 and CH_4 measurements at the ground are in good agreement with the concentrations in 1000-2000 m altitude. This is an important prerequisite for the use of Alert as a representative station for baseline monitoring.

The most recent investigation on vertical profiles at Alert was carried out exactly five years earlier. During the second "Arctic Gas and Aerosol Sampling Program" (AGASP II) flasks air samples were collected during two descents on April 14 and 15, 1986 (flights 205 and 206). The results were reported by *Conway and Steele* [1989]. The spatial resolution with height was poorer, only two samples were collected within 3000 m a.s.l. Figures 5 and 6 compare the profiles of CO_2 and CH_4 derived from AGASP II with the results from this paper. It demonstrates most striking the change of background CO_2 concentrations during these five years. Based on the results within the lowest 200 m one can calculate a concentration difference of 9 ppm for CO_2 and 77 ppb for CH_4 respectively between the two sampling periods. It would be equivalent to an increase of 1.8 ppm CO_2 and 15.4 ppb CH_4 per year. This is in rather good agreement with the average yearly increase of of ~1.5 ppm CO_2 [*Trivett*, 1990] and ~16.5 ppb CH_4 [*Khalil and Rasmussen*, 1990] taking into account that the comparison is based only on two individual experiments, not representing necessary long-term concentration measurements.

To summarize, a rather simple and inexpensive experimental setup was positively tested to be useful for aircraft measurements. Because of the prototype character, the database of this experiment is not sufficient to allow a more detailed discussion on typical or average vertical distributions. More frequent sampling aboard the routine supply flights to Alert might be useful to extent the database sufficiently. It would include the possibility to gain some information on the horizontal distribution as well by collecting air samples on the way to Alert. However, it would be very useful to run a CN counter on the flight continuously. The CN concentration will be a valuable parameter indicating, for example, arctic haze layers but also artificial results caused by contamination effects (e.g., from the aircraft itself).

REFERENCES

Conway, T.J. and L.P. Steele (1989) Carbon Dioxide and Methane in the Arctic Atmosphere Journal of Atm. Chem. 9, 81-99.

Herbert, G.A., H.A. Bridgeman, R.C. Schnell, B.A. Bodhane and S.J. Oltsman (1987). The analysis of meteorological conditions and haze distribution for the second Arctic Gas and Aerosol Sampling Program (AGASP-II), March-April 1986. NOAA Tech. Memo., ERL ARL-158, Air Resources Laboratory, Silver Spring, Md., 67.

Khalil, M.A. and R.A. Rasmussen (1984). Statistical analysis of trace gases in Arctic haze. Geophys. Res. Lett. 11, 437-440.

Khalil, M.A. and R.A. Rasmussen (1990). Constraints on the global sources of methane and an analysis of recent budgets. Tellus 42B, 229-236.

Trivett, N.B.A. (1990). A comparison of seasonal cycles and trends in atmospheric CO_2 concentration as determined from robust and classical regression techniques. Atmospheric Environment Service, Toronto, Ontario.

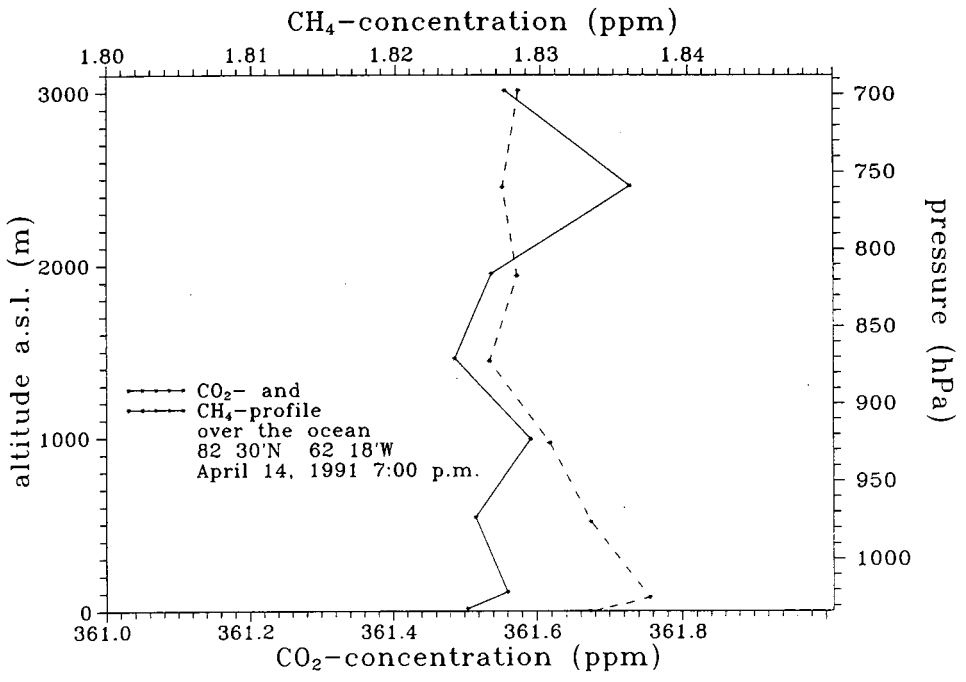

Figure 1. Flask sample concentration of CO_2 and CH_4 over the ocean (6-8 km NNW of Alert) versus altitude and pressure.

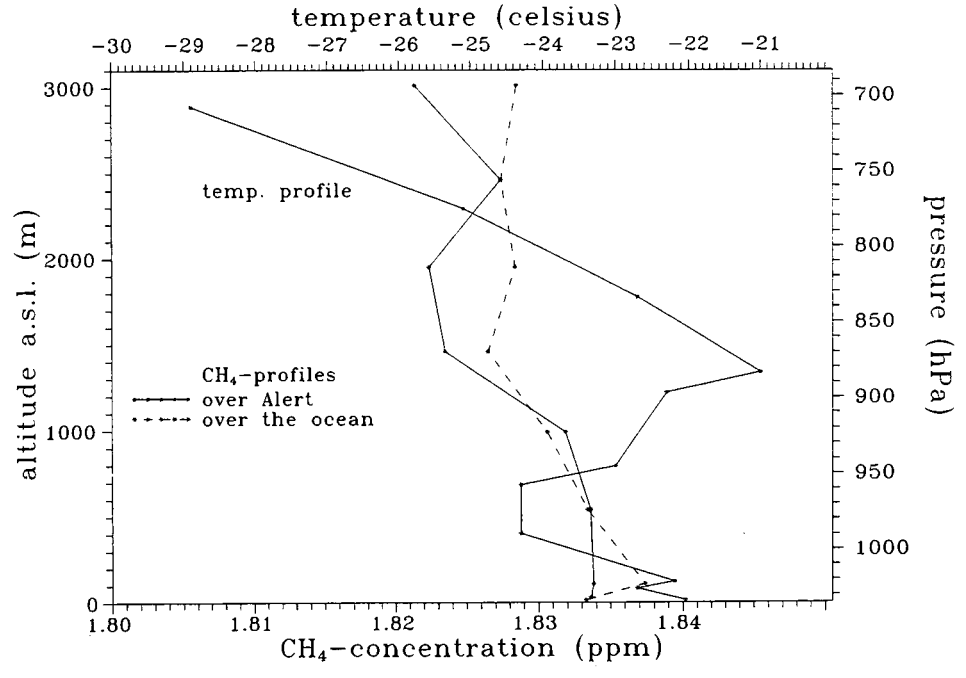

Figure 2. Vertical distribution of CH_4 derived from flask sampling at two locations compared with the temperature profile measured at the same time.

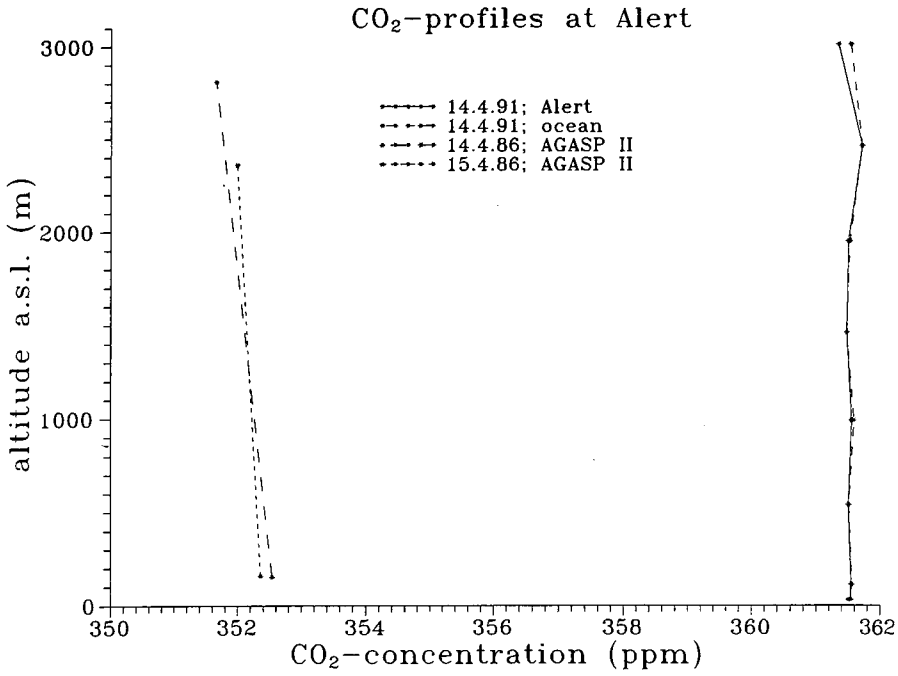

Figure 3. CO_2 profiles in April 1991 (this paper) compared to CO_2 profiles in April 1986 [*Conway and Steele*, 1989].

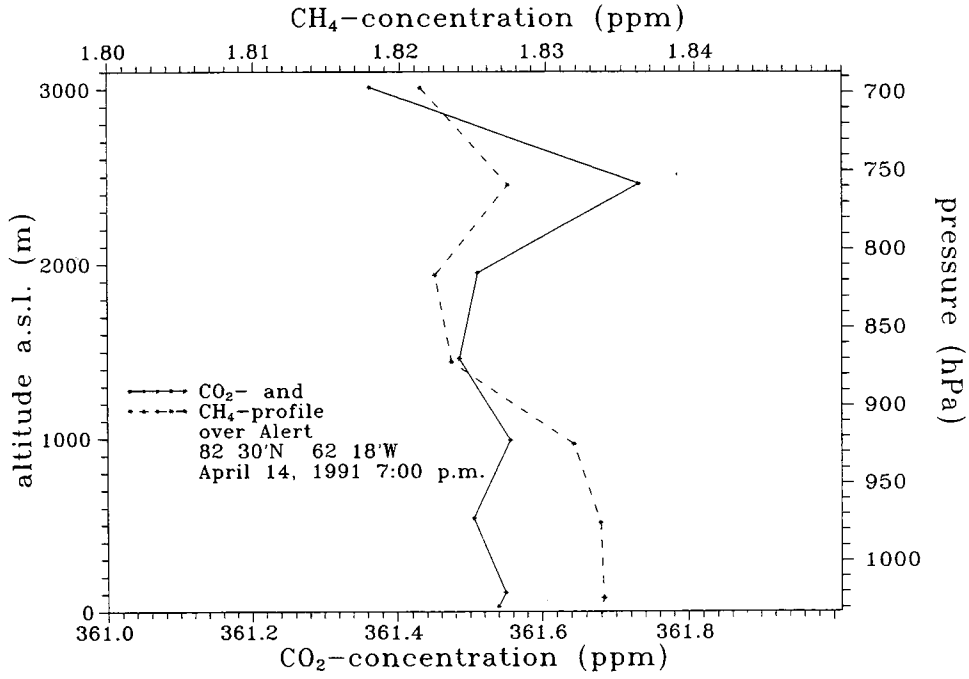

Figure 4. Flask sample concentration of CO_2 and CH_4 over Alert versus altitude and pressure.

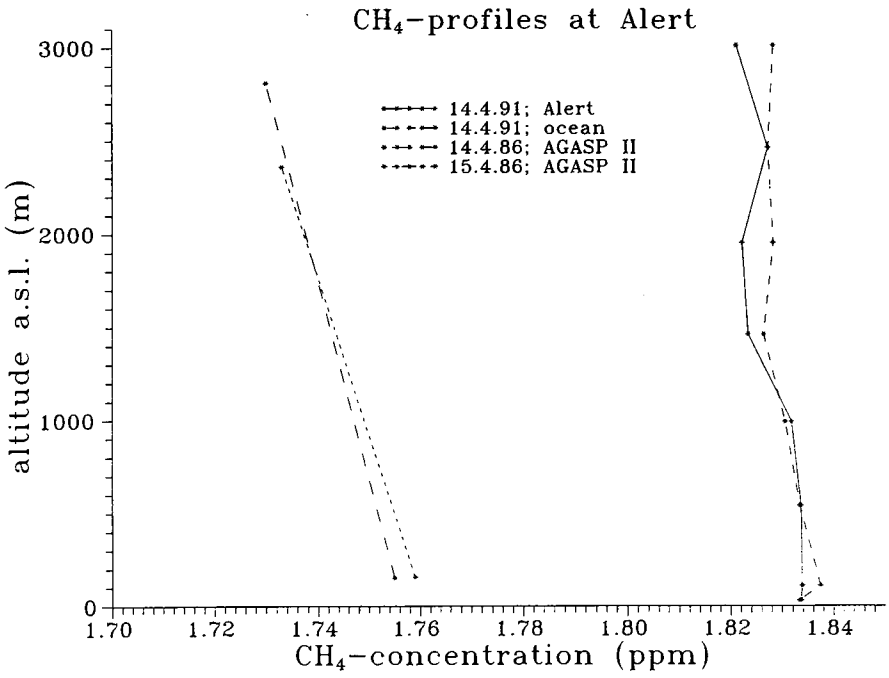

Figure 5. CH_4 profiles in April 1991 (this paper) compared to CH_4 profiles in April 1986 [*Conway and Steele*, 1989].

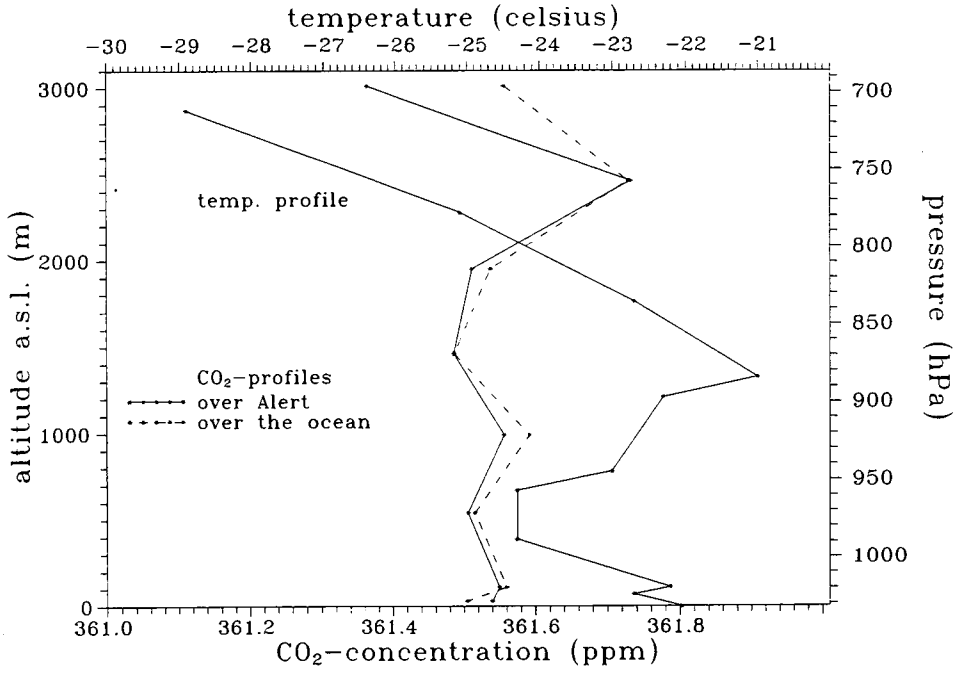

Figure 6. Vertical distribution of CO_2 derived from flask sampling at two locations compared with the temperature profile measured at the same time.

5.8. HYDROCARBONS IN THE POLAR ATMOSPHERE

Jochen Rudolph
Centre for Atmospheric Chemistry and Department of Chemistry
York University
4700 Keele St., North York Ontario, Canada M3J 1P3

Former address: Institut für atmosphärische Chemie, Forschungszentrum Jülich GmbH, Jülich, Germany

INTRODUCTION

Measurements of volatile organic compounds (VOC) in the polar troposphere can serve different purposes. Although at remote polar stations CO and methane dominate the photochemical turnover of carbon, there are certain pathways of chemical reactions that are only accessible via reactions of nonmethane volatile organic compounds. Examples are the formation of peroxyacetyl nitrate (PAN), aldehydes other than formaldehyde, or alkyl nitrates.

Measurements at stations such as Alert are also valuable to establish the temporal and spatial distribution of organic trace gases on a large scale. Such distributions are the basis for studies of budgets, source and sink distributions, and large scale transport processes. Large scale distributions of ethane and terachloroethene which are partly based on measurements from the northern high latitude station in Alert have been extremely useful to improve our understanding of the atmospheric chemistry of these substances [*Koppmann et al.*, 1994, 1996, 1998; *Rudolph et al.*, 1995]. It is important to notice that an improved understanding of the processes governing the tropospheric distribution of selected VOC will also be beneficial for the general understanding of important atmospheric processes. E.g., the analysis of the budgets of ethane and tetrachloroethene allowed to deduce useful upper limits for the global and hemispheric average concentrations of Cl-atoms in the troposphere [*Rudolph et al.*, 1996].

The concentrations as well as the relative patterns of VOC are closely connected to the trajectories of the studied air mass. Valuable information about sources that impacted on the airmass can be deduced from measurements of VOC concentrations. Such information is valuable supplement to all studies of atmospheric chemical and transport processes. Since the atmospheric residence times of individual VOC range from a few hours to several months, such information can be obtained on spatial scales ranging from a few hundred to many thousand kilometers.

Very important insight into atmospheric processes relevant for tropospheric ozone depletion events in the Arctic has been obtained from measurements of hydrocarbon concentrations. From changes in the hydrocarbon patterns the concentrations of Cl- and Br-atoms can be derived. In view of the extreme difficulties associated with direct measurements of halogen atom concentrations in the troposphere such information is essential for the quantitative understanding of low ozone events in the Arctic troposphere. Indeed, halogen atom concentrations derived from hydrocarbon measurements quantitatively explain the observed ozone loss.

In this paper results from long term measurements of hydrocarbons at Alert are presented. Sampling started in January 1989 and continued till 1996. Samples were collected on average biweekly. Detailed data validation, analysis and interpretation is still continuing, but a number of features of the seasonal variability of the hydrocarbon concentrations are already evident from the presently validated and evaluated measurements.

The measurements were generally made outside the "low ozone episodes" that occur during Arctic spring. Thus they represent more or less the typical average situation. The group of Prof. Niki at York University studied the behavior of hydrocarbon concentrations in more detail. These activities centered on the ozone depletion episodes and the inferences that can be drawn from the change of the hydrocarbon concentrations during Arctic, tropospheric ozone depletion episodes. Most of these results are published; a brief overview will be included in this paper.

EXPERIMENT

The air samples were collected in evacuated stainless steel canisters with metal bellows valves. The Canadian Environment Service collected the samples at Alert, on average one sample every second week. They were transferred to the laboratory in Jülich and analyzed by gas chromatography in combination with a cryogenic preconcentration procedure. As part of our program various types of tests were made to verify that storage did not affect the composition of the sampled air. Some sample containers were returned empty and then filled with clean synthetic air. They showed no detectable amounts of the substances investigated in this work. Repeat analyses of some air samples several months after the first measurement showed no indication of a significant change, except for light alkenes. Here the measurements showed an enhanced variability and there are strong indications of an increase with storage time for the concentrations of light alkenes in the canisters. For this reason no results for light alkenes will be presented in this paper.

The samples were analyzed with a combination of packed and capillary columns [*Rudolph et al.*, 1986, 1989]. In order to improve the detection limit and for the sake of a more reliable peak identification a combination of different detectors (flame ionization, photo ionization and electron capture) is used [cf. *Rudolph and Jebson*, 1983]. The detection limit for hydrocarbons is between 1 and 10 ppt, depending on the type of compound and the sample volume. For most halocarbons the theoretical detection limits are below 0.1 ppt. The reproducibility for mixing ratios exceeding the detection limit by a factor of more than 5 was between 5% and 10%. The linearity of the measuring procedure was checked by dilution series. No deviations from linearity were detected for the relevant range of concentrations. In general the blank values were below the detection limit. However, occasionally detectable blank levels were found as a result of leaking valves, contamination of the inlet system or carrier gas impurities. Since our system was operated automatically, some samples were analyzed before such problems were noticed and solved. In these cases, the measurements were corrected for the blank values if the blank contributed less than 20% to the measurement. If the blank exceeded 20% of the peak area for a given substance, the measurement was eliminated from the data set.

GLOBAL DISTRIBUTIONS

Measurements of time series at remote stations play an important role in determining representative space/time variability of trace gas concentrations. As an example the longitudinally averaged seasonal variability of the tropospheric ethane mixing ratio is shown in Figure 1 (for details see *Rudolph*, 1995). The measurements at Alert played an important role for the construction of the dependence since these are the only systematic measurements of non-methane hydrocarbons at high northern latitudes available before 1995. These measurements were crucial in determining the shape of the latitudinal gradient and its seasonal variability north of 60 N. Reliable knowledge of the gradient is essential to derive latitudinally resolved budgets from the distribution. Analysis of the ethane distribution and budget shows that the latitude belt around 50-70 N is a substantial net source of ethane, i.e. the emissions are higher than the atmospheric removal rates. This is compatible with the concept that natural gas loss is a major source of atmospheric ethane. Details of the budget analysis etc. are given in *Rudolph et al.* [1995]. Other examples of the use of global hydrocarbon concentration data, including results from Alert, can be found in *Koppmann et al.* [1994, 1996, 1998] and *Rudolph et al.* [1996].

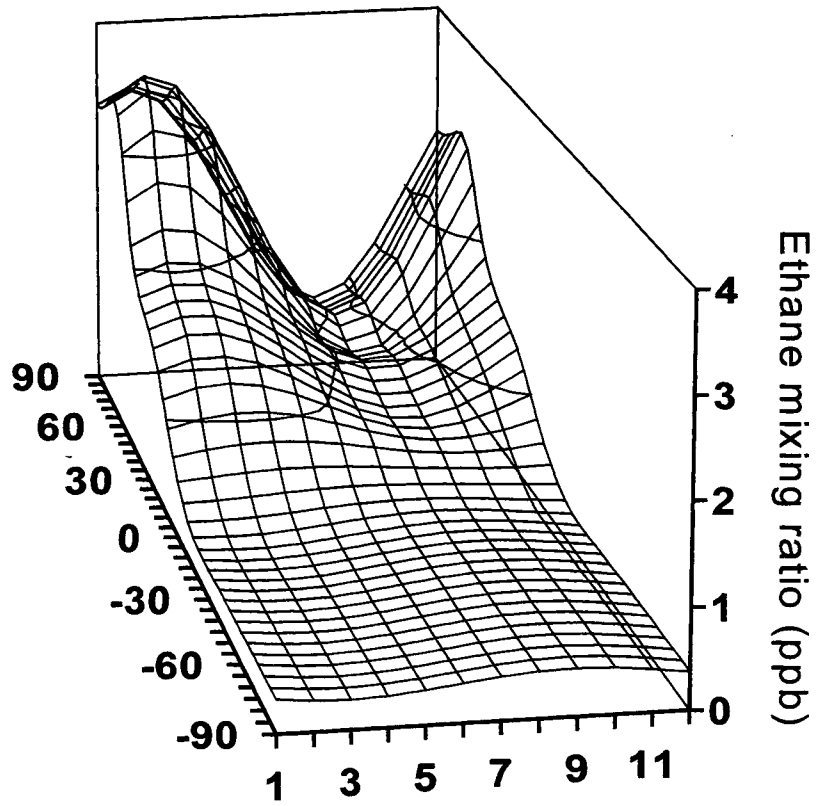

Figure 1. Zonally and vertically averaged seasonal and latitudinal distribution of ethane.

SEASONAL CYCLES

Examples for average seasonal variations of some non-methane hydrocarbons are shown in Figure 2. The available data allow the construction of reasonably defined average seasonalities. All alkanes, acetylene and benzene mixing ratios typically have maxima in late winter and minima in late summer or early fall. One of the main driving forces for the seasonal variability of hydrocarbons is the seasonal cycle of the OH-radical concentration that has its maximum in summer. Since removal by OH-radicals is generally the dominant loss process for most hydrocarbons, it is not surprising that the hydrocarbon concentrations as a first approximation follow the seasonal variation of the OH-radical concentration. The winter to summer concentration ratio is plotted in Figure 3 versus the rate constants for the reaction of the hydrocarbons with the OH-radical. Although there is some scatter, on average the summer/winter ratio increases with increasing reactivity. Again, this is compatible with OH-radical reactions being the main sink for hydrocarbons in the troposphere.

It is frequently found that the relative variability of a trace gas concentration increases with decreasing atmospheric residence time or increasing reactivity. Consistent with this concept it can be seen that the relative variability of the hydrocarbon concentration increases with increasing reactivity (Figure 4). It should be noted that the relative variability exceeds the measurement precision by nearly an order of magnitude. It is also interesting that the variability is generally higher in summer than in winter, consistent with higher OH-radical concentrations and thus shorter atmospheric residence times in summer. However, it should be noted that this does not imply that the hydrocarbon removal by reaction with OH-radicals is predominantly occurring at high latitudes. On the contrary, due to higher OH-radical concentrations at mid and low latitudes and the various exchange processes between the Arctic troposphere and mid latitude air masses, the hydrocarbon concentrations and their seasonal variability are the result of a complex interplay between transport and removal mechanisms.

Figure 2a:

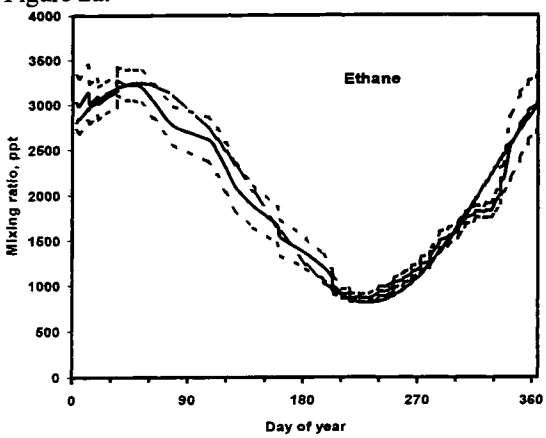

Figure 2b:

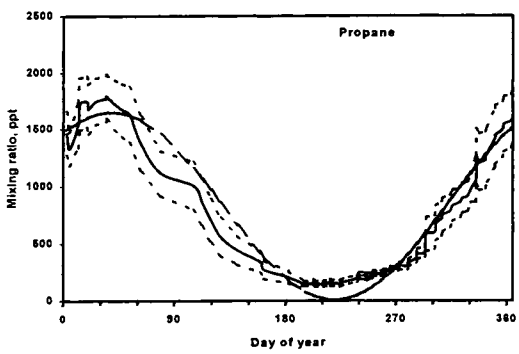

Figure 2c:

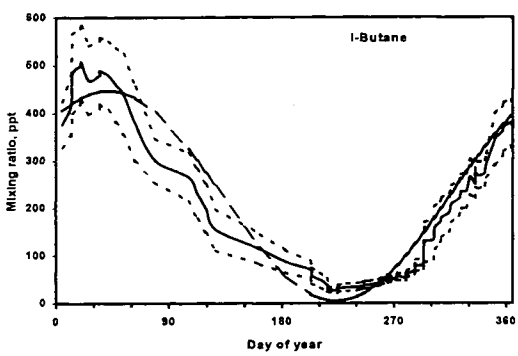

Figure 2d:

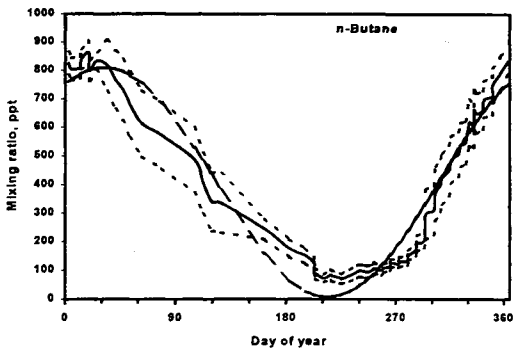

Figure 2e:

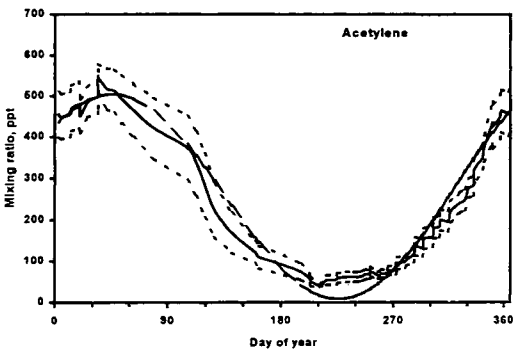

Figure 2f:

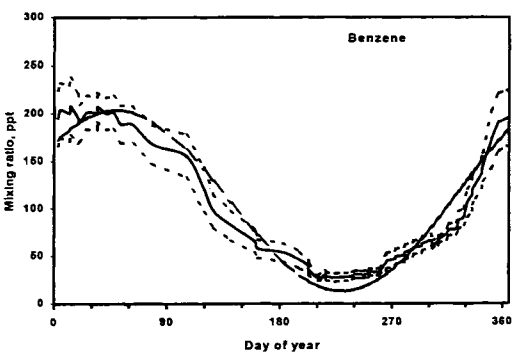

Figure 2. Seasonal cycle of several hydrocarbons at Alert. Shown is the one month running average of the measurements (solid line), the range of error of the running mean (short dashed line), and a sine fit to the data (long dashed line).

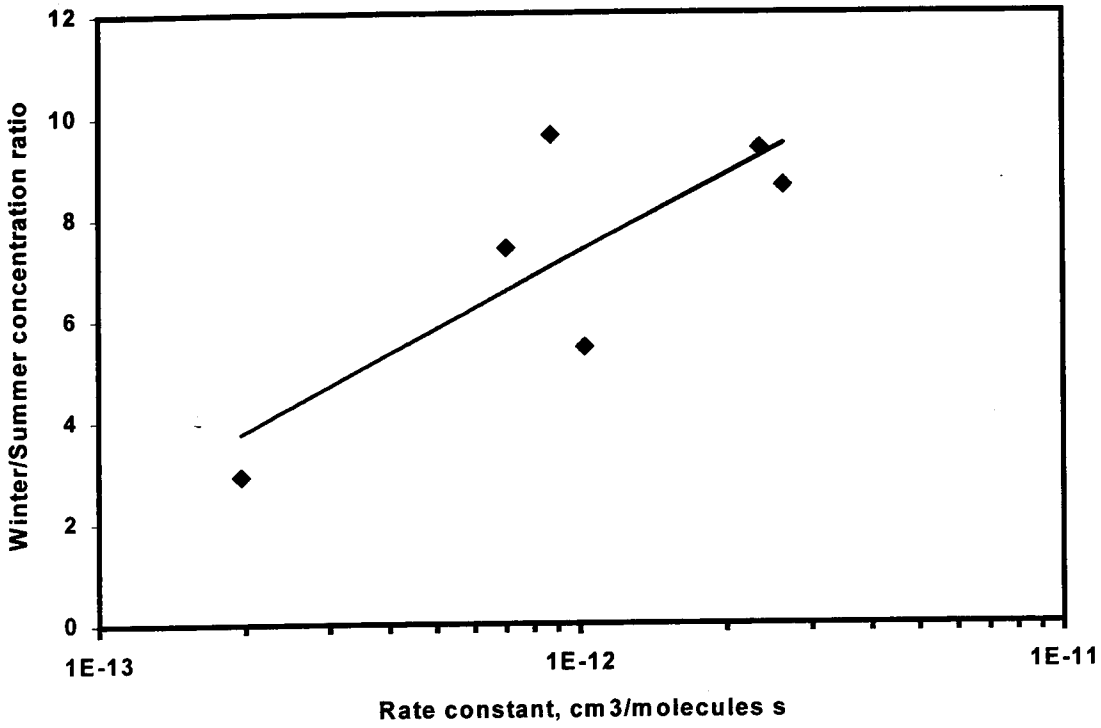

Figure 3. Winter to summer concentration ratio for hydrocarbons observed at alert as function of the rate constant for the reaction of the hydrocarbon with OH-radicals. The solid line shows a least square fit to the data points (R2=0.628).

ARCTIC TROPOSPHERIC OZONE DEPLETION, HALOGEN CHEMISTRY, AND HYDROCARBON CONCENTRATIONS

In the lower Arctic troposphere during polar sunrise episodes characterized by substantially reduced ozone levels occur. From our current understanding this is caused by the presence of high levels of reactive halogen compounds, including Cl- and Br- atoms. Since different hydrocarbons react with Br- and Cl- atoms at different rates, changes in hydrocarbon patterns can be used to deduce concentrations of Cl- and Br- atom concentrations during ozone depletion episodes. As mentioned above, the measurements of the seasonal cycles and the long-term observations did not include studies of the ozone depletion episodes. However, the group of Hiromi Niki at York University has made extensive investigations of hydrocarbon concentrations during ozone depletion. The results have already been published [*Ariya et al.*, 1997a and b; *Catoire et al.*, 1997; *Hooshitar et al.*, 1995; *Hopper et al.*, 1994; *Jobson et al.*, 1994; *Kieser et al.*, 1993; *Niki et al.*, 1995], a brief summary is given here.

Field Studies

During several field studies air samples were collected in the Canadian Arctic and analyzed in the laboratory at York University for several light hydrocarbons. Extensive data sets were obtained during Polar Sunrise Experiment 1992 (measurements at Alert, 150 km north of Alert on Swan Ice Floe, and one aerial survey over the Arctic archipelago), Polar Sunrise Experiment-ICEFLOE 1994 (measurements at Alert, Narwhal Ice Floe north of Alert, and sampling during two airplane flights) and Polar Sunrise Experiment 1995 (measurements at Alert). Acetylene, which reacts with Br-atoms, showed a clear correlation with ozone whereas benzene that does not react with Br-atoms does not vary with the ozone concentration. This agrees with the concept that the depletion of ozone is due to the presence of Br-atoms. Surprisingly, concentrations of ethane and propane, although they do not react with Br-atoms, are to some extent correlated with ozone

concentration. Similar observations were also made for the aircraft studies. Ozone, acetylene, ethane and propane are significantly depleted in the boundary layer (0-600 m altitude) compared to higher altitudes whereas the concentration of benzene remains constant.

The most likely explanation is the presence of not only Br-atoms but also of substantial amounts of Cl-atoms. Indeed, on a logarithmic scale the relative change in the concentrations of hydrocarbons is proportional to their rate constants for the reaction with Cl-atoms. This is exactly the behavior expected if reaction with Cl-atoms is the dominant loss mechanism. The required time integrated Cl-atom concentration is in the range of $5\text{-}10*10^{9}$ cm^{-3} s. Ozone, acetylene, and trichloroethene significantly deviate. This can be explained by their reaction with Br-atoms. From the change of the acetylene and trichloroethene concentrations (after correction for the effect of Cl-atoms) time integrated Br-atom concentrations around 10^{13} cm^{-3} s can be derived. This is sufficient to explain the observed depletion of ozone.

Laboratory Studies

The deduction of halogen atom concentrations from changes in the hydrocarbon concentrations requires the knowledge of the relevant reaction rate constants. As part of the program the reaction rate constants of several C_2-C_8 alkanes with Cl-atoms and of tetra- and trichloroethene with Cl- and Br-atoms were determined.

From the field studies during Arctic spring, it is evident that a substantial part of the organic compounds present in the Arctic troposphere reacts with halogen atoms. The reaction mechanisms and products of the halogen-initiated oxidation of several organic substances were studied.

Model Calculations

The situation during an ozone depletion episode could be simulated in model calculations. The model includes both gas phase and solid phase chemistry. The time dependence of ClO, BrO, OH-radicals, formaldehyde, hydrocarbons and ozone agree very well with the observations during Polar Sunrise Experiment 95. However, it should be noted that the mechanisms that initiate or terminate the ozone depletion episodes are not yet understood.

SUMMARY AND CONCLUSIONS

Measurements of hydrocarbons at an Arctic station provide important information about many processes relevant for the chemistry of the Arctic troposphere, as well as for sources and sinks of hydrocarbons at high latitudes. The observations made at Alert allow determining representative seasonal cycles for a number of light hydrocarbons and halocarbons. Furthermore, these data represent important contributions to the construction of representative global time/space distributions of atmospheric trace constituents. These global distributions then can be used to deduce global and regional budgets of the trace gases.

On a regional scale the hydrocarbon measurements allow to infer the impact of different types of removal processes, specifically the effect of halogen atoms. Thus hydrocarbon measurements are an important tool to better understand the chemistry of tropospheric ozone depletion during polar sunrise.

Presently intensive hydrocarbon measurements are made at Alert as part of the 1998 Polar Sunrise Experiment. It is planned to continue with the hydrocarbon measurements after the end of this campaign in order to extend the existing record and to improve our understanding of the seasonal cycles of hydrocarbon concentrations in the Arctic and the factors determining these concentrations.

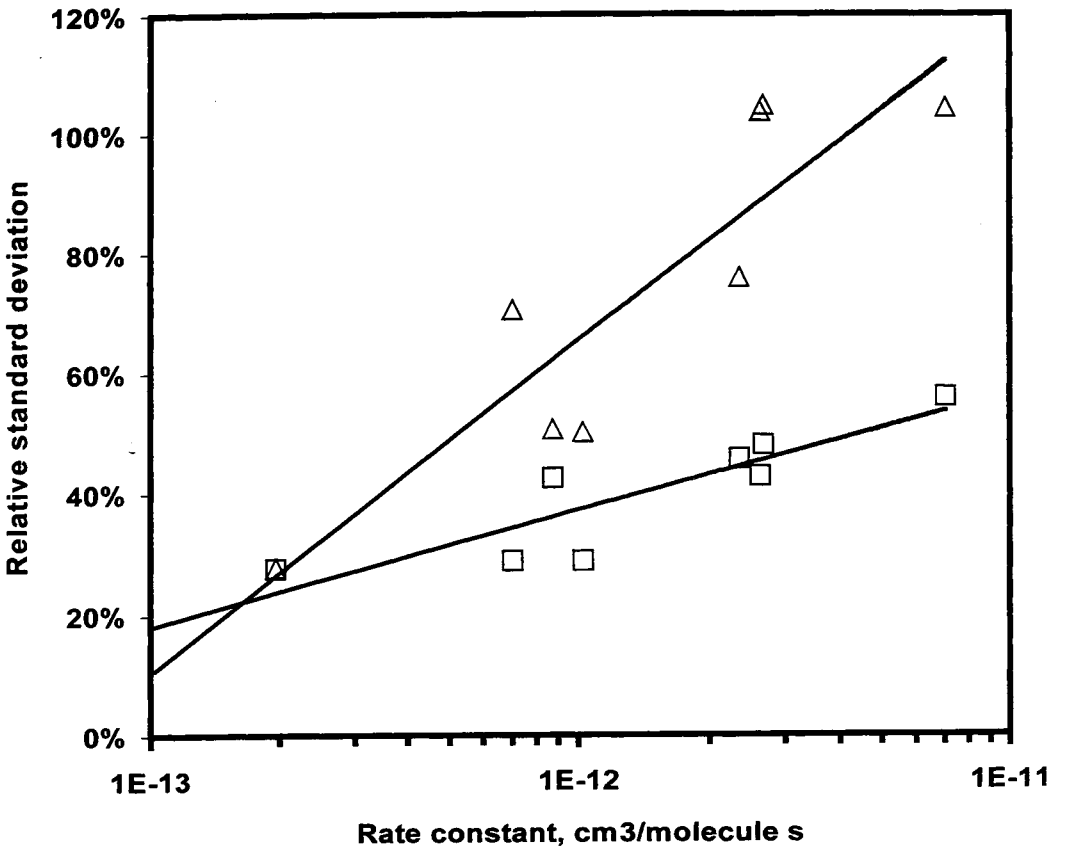

Figure 4. Plot of relative standard deviation for hydrocarbons observed at alert as function of the rate constant for the reaction of the hydrocarbon with OH-radicals. The data are shown separately for summer (triangles) and winter (squares). The solid lines show least square fits to the data points (R2=0.799 and 0.766, respectively).

REFERENCES

Ariya, P.A., B.T. Jobson, R. Sander, H. Niki, G.W. Harris, K.G. Anlauf and J.F. Hopper, Measurements of C_2-C_7 hydrocarbons during the polar sunrise experiment 1994: Further evidence for halogen chemistry in the troposphere, J. Geophysical Research, Accepted 1997.

Ariya, P.A., V. Catoire, R. Sander, H. Niki & G.W. Harris, Trichloroethene and tetrachloroethene: Tropospheric probes for Cl- and Br-atom reactions during the polar sunrise, Tellus, 49B, 583-591, 1997.

Catoire, V., P.A. Ariya, H. Niki, and G.W. Harris, FTIR study of the Cl- and Br-atom initiated oxidation of trichloroethylene, Chemical Kinetics, 29, 695-704, 1997.

Hooshiyar, Parisa A., and Hiromi Niki, Rate constants for the gas-phase reactions of Cl-atoms with C_2-C_8 alkanes at T = 296 ± 2K, Chemical Kinetics, 27, 1197-1206, 1995.

Hopper, J.F., B. Peters, Y. Yokouchi, H. Niki, B.T. Jobson, P.B. Shepson, K. Muthuramu, Chemical and meteorological observations at Ice Camp SWAN during Polar Sunrise Experiment 1992, J. Geophy. Res., 99, No. D12, 25,489-25,498, 1994.

Jobson, B.T., H. Niki, Y. Yokouchi, J. Bottenheim, F. Hopper, and R. Leaitch, Measurements C_2-C_6 hydrocarbons during the Polar Sunrise 1992 Experiment: Evidence for Cl and Br chemistry, J. Geophys. Res. - Atmospheres, Section D12., 99, 25,355-25, 2368, 1994.

Kieser, B.N., T. Sideris, J.W. Bottenheim, and H. Niki, Spring 1989 Observations of

Tropospheric Chemistry in the Canadian High Arctic, Atmos. Environ., 27A, 2979-2988, 1993.

Koppmann, R., B. Ramacher, and J. Rudolph, Hydrocarbon measurements in the ARCTIC troposphere: A probe for tropospheric ozone depletion, Proceedings of the Scientific Seminar, "Atmospheric Research in Ny-Ålesund", Kjeller, Norway, April 9-11, 1997, 147-150.

Koppmann, R., F.J. Johnen, C. Plass-Dülmer, and J. Rudolph, The Distribution of Dichloromethane, Trichloroethene and Tetrachloroethene over the Atlantic. in: Proc. 6th European Symposium on the Physico - Chemical Behaviour of Atmospheric Pollutants, Varese/Italy, 18.-22 October 1993, ed. by G. Restelli and G. Angeletti, pp. 417-423, Report EUR 15609/1 EN, Brussels-Luxemburg, 1994.

Koppmann, R., J. Rudolph, R. Hein, P.J. Crutzen, The distribution of light chlorocarbons in the troposphere. European Commission, The oxidizing capacity of the troposphere, Proceedings of the 7th European Symposium on Physico-Chemical Behaviour of Atmospheric Pollutants, Venice, Italy, October 2-4, 1996, Edited by B. Larson, B. Versino and G. Angeletti, Report 60, air pollution research reports series of the environmental research programme, 446-450, 1997.

Koppmann, R., J. Rudolph, R. Hein and P.J. Crutzen, The distribution of light chlorinated hydrocarbons in the troposphere: Evidence for oceanic sources, Submitted to Geophysical Research Letters, April 1998.

Niki, H., Depletion of Tropospheric Ozone During Arctic Spring: Field and laboratory studies of the role of hydrocarbons. Progress and Problems in Atmospheric Chemistry. Advanced Series in Physical Chemistry, Vol. 3, ed. John R. Barker, University of Michigan, World Scientific Publishing Company, 1995.

Ramacher, B., J. Rudolph, and R. Koppmann, Hydrocarbon measurements in the spring Arctic troposphere during the ARCTOC 95 campaign. European Commission, The oxidizing capacity of the troposphere, Proceedings of the 7th European Symposium on Physico-Chemical Behaviour of Atmospheric Pollutants, Venice, Italy, October 2-4, 1996, Edited by B. Larson, B. Versino and G. Angeletti, Report 60, air pollution research reports series of the environmental research program, 304-308, 1997.

Ramacher, B., J. Rudolph, R. Koppmann, Hydrocarbon measurements in the spring Arctic troposphere during the ARCTOC 95 campaign, Tellus 49B, 466-485, 1997.

Rudolph, J., C. Jebsen, The Use of Photo Ionisation, Flame Ionisation and Electron Capture Detectors in Series for the Determination of Low Molecular Weight Trace Components in the Non-Urban Atmosphere, Intern. J. Environ. Anal. Chem. 13, 129-139, 1983.

J. Rudolph, F.J. Johnen, A. Khedim, Problems connected with the analysis of hydrocarbons and halocarbons in the non - urban atmosphere. Int. J. Environ. Anal. Chem. 27, 97, 1986.

J. Rudolph, F. J. Johnen, A. Khedim, G. Pilwat, The use of automated "on line" gaschromatography for the monitoring of organic trace gases in the atmosphere at low levels, Int. J. Environ. Anal. Chem. 38, 143, 1989.

Rudolph, J., R. Koppmann, and Ch. Plass Dülmer, The budgets of ethane and tetrachlorethene: Is there Evidence for an Impact of reactions with Chlorine Atoms in the Troposphere?, Atmos. Environ., 30, 1887-1894, 1996.

Rudolph, J., The Tropospheric Distribution and Budget of Ethane. J. Geophys. Res., 100, 11 383-11 391, 1995.

5.9. MEASUREMENTS OF METHYL HALIDES (CH_3Cl, CH_3Br AND CH_3I) AT ALERT

Y. Yokouchi
National Insititute for Environmental Studies (NIES)
16-2, Onogawa, Tsukuba, Ibaraki 305-0053 JAPAN
D. Toom-Sauntry and L.A.Barrie
Atmospheric Environmental Service (AES)
4905 Dufferin Street, Downsview, Ontario M3H5T4 CANADA

INTRODUCTION

A variety of halocarbons, such as methyl iodide (CH_3I) and bromoform (CH_3Br), are known to be emitted from the ocean. Among these marine halocarbons, CH_3I is likely to play an important role in the budget of tropospheric ozone, through production of iodine atoms by photolysis. CH_3Cl and CH_3Br are also of great concern, since some of them are transported into the stratosphere and contribute to ozone destruction there. However their temporal variation (both short- and long-period) and spatial variation other than over the ocean is not well understood. Measurements of these methyl halides have been done at Alert as a collaborative study between NIES and AES since April of 1996.

METHOD

Air samples were collected on a bi-weekly basis at the Alert Observatory Lab using evacuated 6 L stainless steel canisters (Silico-can, Restek Co. Ltd.) with a ball valve. Prior to use, the canisters were cleaned by repeating evacuation and filling with humidified pure nitrogen.

Chemical analysis was done at NIES, Japan. Methyl halides in the air samples were analyzed with pre-concentration (ENTECH 7000) / capillary gas chromatography (GC) / mass spectrometry (MS) (HP 5980 / HP5972) as well as some other volatile organic compounds. The MS was used in the selected ion monitoring (SIM) mode, and the target ions were 50 and 52 for CH_3Cl, 94 and 96 for CH_3Br, and 142 and 129 for CH_3I. Detection limits (S/N=3) for these 3 compounds were 0.4 pptv, 0.2 pptv and 0.1 pptv, respectively in case of 500 ml air sampling. Relative standard deviation calculated from duplicate samples collected at Alert was 1.2% for CH_3Cl, 2.3% for CH_3Br, and 7.2% for CH_3I. Rather poor reproducibility for CH_3I is due to low concentration (sub pptv) of CH_3I at Alert.

DATA

Figure 1 shows data for CH_3Cl, CH_3Br and CH_3I measured at Alert (July 1996 – June 1998).

Methyl chloride: The concentration of CH_3Cl measured at Alert ranged from 407 pptv to 577 pptv with an average of 501 pptv. These values are lower than those observed over NW-Pacific or those at Hateruma Island (subtropical). Such a low concentration might be related to undersaturation of CH_3Cl in the cold water, although no latitudinal distribution of atmospheric CH_3Cl had been reported in the high latitude and CH_3Cl had been believed to be well mixed globally. The 2-year data sets have shown the seasonal variation of this compound, highest in spring and lowest in late summer. Such a seasonal trend is consistent with the reactive loss of CH_3Cl with OH radicals, which are more abundant in summer than in winter.

Methyl bromide: The concentration of CH_3Br from Alert was in the range of 8.2 – 12.9 pptv with an average of 10.2 pptv. Its seasonal variation was not so significant, and was slightly different for the first year and the second. This might be due to that so many factors (major sources – ocean, fumigation, biomass burning; major sinks – atmospheric reaction (OH), biological sink in the ocean, soil uptake) re controlling variability of CH_3Br.

CH_3I: The concentration of CH_3I from Alert was in the range of 0.1 – 0.6 pptv with an average of 0.3 pptv, which is much lower than those from the other areas (NW Pacific and Hateruma Island). Its concentration was lower in spring/summer than in winter at Alert, in contrast to highest in summer maximum observed over NW-Pacific and at Hateruma. Considering rather short lifetime of CH_3I in the atmosphere, a possible explanation for this is that CH_3I is mainly emitted in low- and mid-latitudes and it could be carried to Alert only in winter when the photolytic decomposition during transport was suppressed.

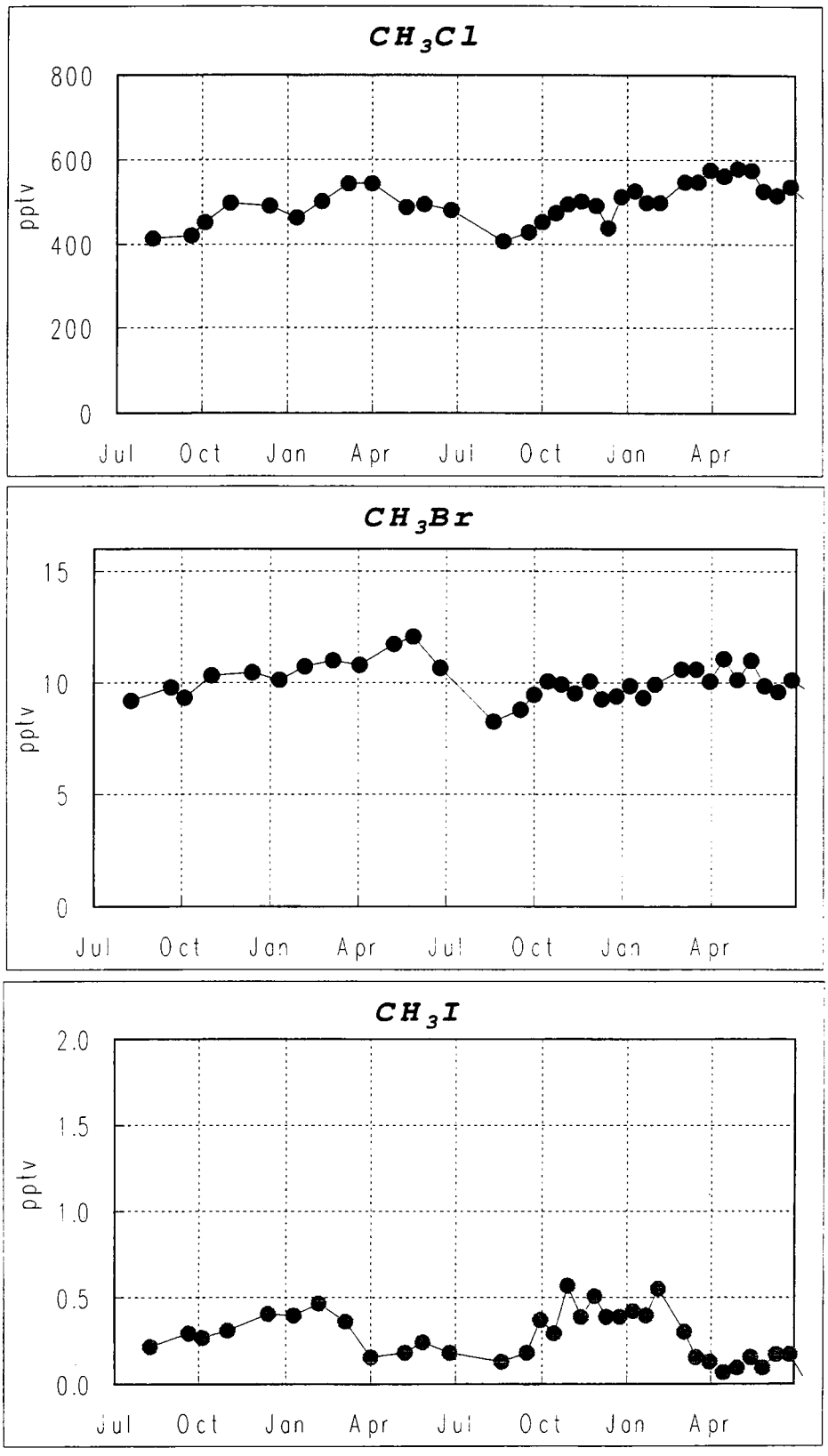

Figure 1. Methyl halides in the atmosphere measured at Alert (July 1996 – June 1998).

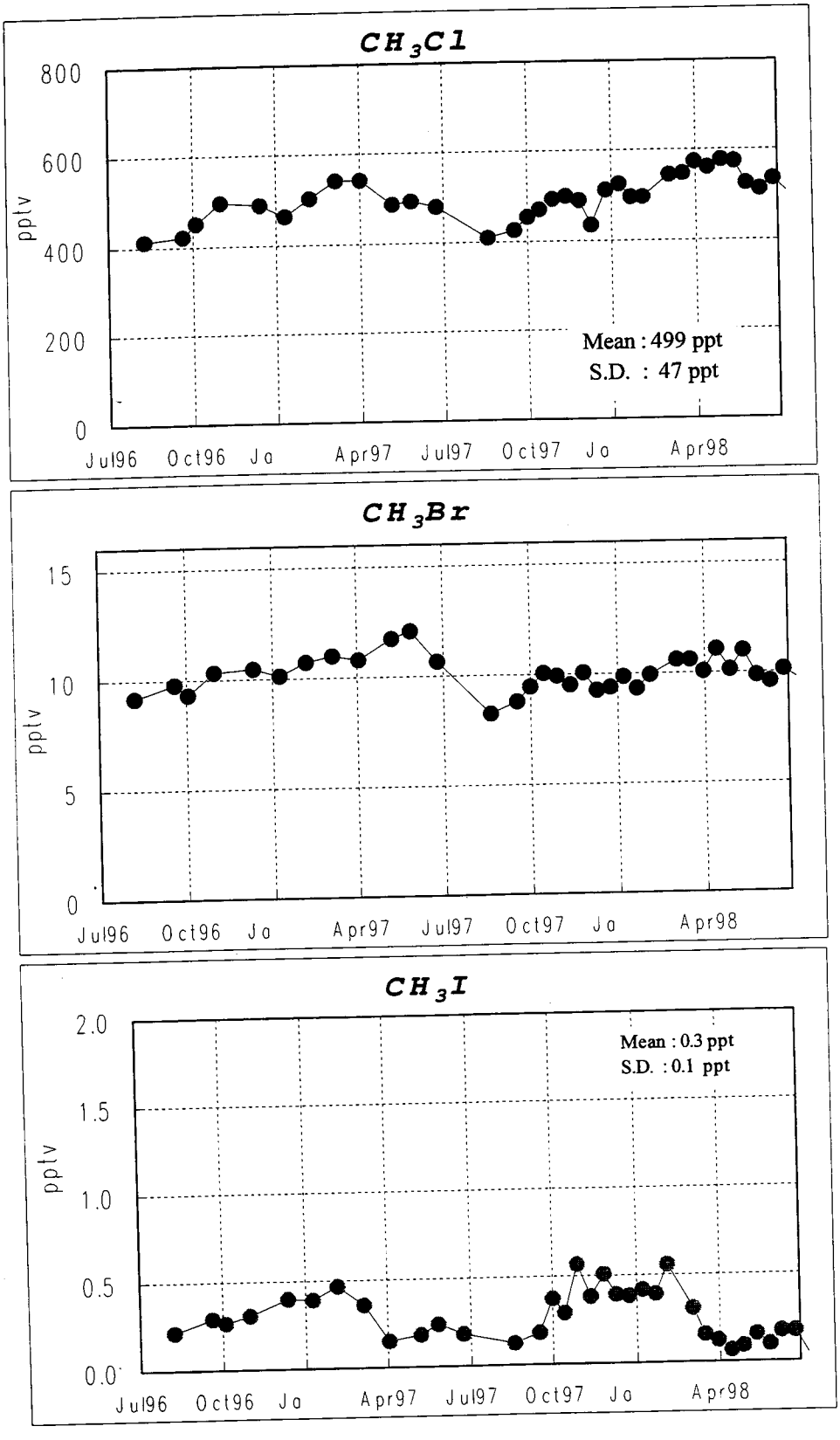

Figure 1. continued:
Methyl halides in the atmosphere measured at Alert (July 1996 – June 1998).

APPENDIX: TRADEMARKS IN THE REPORT

- Swagelok is a registered trademark of Swagelok Corporation
- Teflon is a registered trademark of Dupont
- Viton is a registered trademark of Viton
- Thermo Pad is a registered trademark of Hood Thermopad Canada
- Dekoron is a registered trademark of Furon Company
- Pyrex is a registered trademark of Corning Inc.
- Microsoft, Windows and MS-DOS are registered trademarks of Microsoft Corporation
- NT is a trademark of Northern Telecom Limited
- Zip™ is an unregistered Trademark of Iomega Corporation.